DOE/NASA/0107-1
NASA CR-159690

ENGINEERING SUPPORT FOR MAGNETOHYDRODYNAMIC POWER PLANT ANALYSIS AND DESIGN STUDIES

A.W. Carlson, I.L. Chait, G. Marchmont,
R. Rogali, D. Shikar
Burns and Roe, Inc.
August 1980

Prepared for
National Aeronautics and Space Administration
Lewis Research Center
Under Contract DEN 3-107

For
U.S. DEPARTMENT OF ENERGY
Fossil Energy
Office of Magnetohydrodynamics

DOE/NASA/0107-1
NASA CR-159690

ENGINEERING SUPPORT FOR MAGNETOHYDRODYNAMIC POWER PLANT ANALYSIS AND DESIGN STUDIES

A.W. Carlson, I.L. Chait, G. Marchmont, R. Rogali, D. Shikar
Burns and Roe, Inc.
Woodbury, New York 11797

August 1980

Prepared for
National Aeronautics and Space Administration
Lewis Research Center
Cleveland, Ohio 44135
Under Contract DEN3-107

for
U.S. DEPARTMENT OF ENERGY
Fossil Energy
Office of Magnetohydrodynamics
Washington, D.C. 20545
Under Interagency Agreement EC-77-A-01-2674

CONTENTS

1. ECONOMIC ENGINEERING SELECTION OF STACK INLET TEMPERATURE IN AN MHD POWER PLANT

WORK DEFINITION AND SCOPE

The objective of this work is to identify the major factors which influence the economic engineering selection of stack inlet temperatures for a combined cycle magnetohydrodynamic (MHD) coal-fired power plant of commercial size and to determine the range of suitable stack inlet temperatures under typical operating conditions. The coals considered as fuel for the plant are Illinois No. 6 coal, dried to a moisture content of 2 percent, and Montana Rosebud coal dried to a moisture content of 5 percent. The stack emissions are required to meet the EPA New Source Performance Standards of June 1979.

SUMMARY

The selection of the stack gas temperature is based upon several factors related to the economic design and operation of the power plant. The major factors which are influenced by the stack gas temperature are power plant efficiency, corrosion and deposits on surfaces in contact with the gas, plume dispersion and plume visibility, and investment and operating costs. Table I lists such factors and indicates, qualitatively, how each factor is affected by the stack gas temperature.

Typical stack gas temperatures found in the electric power industry today are in the range of 350° to 420° K (165° to 300° F). The design temperature selected is usually the lowest practical temperature (1) at which the materials of the economizer fans, duct work and stack will not corrode or deteriorate inordinately as the result of the condensation of acid solutions at temperatures below their dewpoints and (2) which provides the velocity required to avoid downwash and the buoyancy to enhance the exhaust gas plume rise for ambient dispersion to meet pollutant regulations.

TABLE I. - FACTORS AFFECTING STACK GAS TEMPERATURE (T_{SG}) SELECTION

Powerplant efficiency	Increases as T_{SG} decreases
Heat exchanger surface area	Increases as T_{SG} decreases
Draft fan power	Net effects of T_{SG} depend on + and - effects on power requirements.
Cost of materials selected for reducing corrosion damage	Increases as T_{SG} decreases ($T_{SG} < T'$)[a]
Operating and maintenance cost (including labor and materials)	Increases as T_{SG} decreases ($T_{SG} < T'$)[a]
Loss or replacement of generating capacity and energy due to down-time for maintenance	Increases as T_{SG} decreases ($T_{SG} < T'$)[a] (unless maintenance, is performed during scheduled outages)
Stack height required for adequate plume dispersion	Increases as T_{SG} decreases ($T_{SG} < T''$)[b]
Stack diameter required for adequate plume rise	Decreases as T_{SG} decreases ($T_{SG} < T''$)[b]

a T' is the critical temperature below which corrosion effects are significant.

b T" is the critical temperature below which standard stack height design practices are inadequate for achieving acceptable plume dispersion (T" is site dependent).

The most important variable in determining the gas temperature for the onset of corrosion is the sulfur trioxide content of the gas. This, in turn, is dependent upon the sulfur content of the fuel, the combustion process and the chemical reactions which occur in the gas upstream of the stack. The chemical reactions depend upon the presence of other chemical species which react with sulfur (such as potassium) or which serve as catalysts (such as Fe_2O_3 and V_2O_5) for the conversion of sulfur dioxide to sulfur trioxide. The overall sulfur content of the flue gas stream is the result of the relative amount of potassium injected for enhancing the conductivity of the gas in the magnetohydrodynamic channel. The moisture content of the gas also has an effect upon the temperature at which corrosion becomes significant.

The influence of plume rise, atmospheric dispersion and plume visibility on the stack gas temperature selection depend upon the local meteorology, regional classification for pollutants, contributions to ground level concentrations from other nearby sources, and therefore, the location of the plant. Since the plume dispersion, plume visibility factors and ground level concentrations are site specific and since the onset of serious corrosion due to condensation is usually the over-riding factor, the emphasis in this report is on the latter factor. However, pollutant dispersion analyses should be performed and plume visibility effects should be determined when the MHD plant is considered for a specific site.

The most important factor in the selection of a stack gas temperature is the acid dew point temperature, which depends primarily on the sulfur trioxide (SO_3) and moisture content of the gas. However, there is a considerable degree of uncertainty as to what the SO_3 content will be in an MHD power plant configuration, leading to considerable uncertainty in the acid dew point. The range of possible dewpoint temperatures in an MHD plant appears to extend from 375° to 446° K (216° to 343° F).

Further investigations are required to be able to predict acid dewpoint temperatures with satisfactory precision and confidence. Predictions will be valid only to the extent that they can be supported by test data under conditions which are very close to those anticipated in an MHD plant. It is recommended that measurements of SO_3 content and acid dewpoints be included as a part of the test program for the U.S. Department of Energy's Heat Recovery Seed Recovery System, which is presently undergoing design, or another equivalent test facility.

Some of the economic factors which are required to determine the feasibility of selecting a stack gas temperature which is lower than that at which acid condensation occurs on material surfaces in contact with the gas are included in this report. It is recommended that further investigation of the relevant economic factors be pursued at a time when satisfactory data become available on acid dewpoint temperatures under MHD conditions and that a comprehensive economic study be conducted for a specific well-defined MHD plant configuration at that time.

The report is arranged as follows

- An introduction which presents the problems of stack gas temperature selection in general terms
- The factors affecting the selection of stack gas temperature including

  Exhaust gas system configurations

  Exhaust gases operating without acid condensation

  Exhaust gases operating under reduced stack gas temperatures with and without acid condensation

  Factors which determine acid dewpoint temperature

  Formation of sulfur oxides in an MHD power plant

  Range of dewpoint temperatures in an MHD power plant
- The economic and technical considerations in selecting stack gas temperature

- A discussion of the selection of stack gas temperature and its limitations
- Conclusions and recommendations

In addition, appendixes are located at the end of the report which include sections on

- The effect of reduction of stack gas temperature on plant efficiency
- Determination of induced draft fan power requirements
- Corrosion-resistant metals for economizer tubing and I.D. fan parts
- Stack lining materials
- Gas-stream additives
- Plume dispersion and visibility considerations
- Economic factors related to changes in design stack gas temperatures

INTRODUCTION

The temperature of the gas stream entering the stack in a power plant is an important factor in determining the economics of the plant. The more thermal energy extracted from the gas and utilized in the thermal cycle (and hence the lower the stack gas temperature), the higher the plant efficiency. However, at temperatures below the dewpoint temperature of the constituents of the gas, condensation will occur. The lower the operating temperature, the greater the condensation of vapor in the flue gas. These vapors in a coal-fired power plant are usually acidic due to the SO_2 and SO_3 carried in the gases. A stack gas inlet temperature which can result in condensation in the stack will introduce several potential problems which may be eliminated or minimized by steps which will reduce or prevent the condensation or resist corrosion. The potential problems include

(1) Corrosion and deposits on surfaces exposed to the gas at the colder end of the flue gas path

(2) Inadequate plume dispersion

(3) Plume visibility

The extent of these problems and the temperatures required to minimize them depend upon a number of factors including

(1) Gas composition, which, in turn, depends upon fuel composition, seed injection rate, and gas chemical reactions

(2) Materials of construction of flue gas ducting, fan, economizer and stack

(3) Temperatures of surfaces in contact with the gas

(4) Ambient conditions

(5) Meteorological conditions

(6) Stack height and exit diameter

The selection of the optimum stack gas temperature usually entails a tradeoff between the lower fuel cost due to improved plant heat rate and the economic penalty of corrosion resistant materials or increased maintenance costs (including lower unit availability and/or cost of replacement capacity and energy) and other measures taken to avoid reduced pollutant dispersion, and increased opacity of emitted gases.

FACTORS AFFECTING SELECTION OF STACK GAS TEMPERATURES

Exhaust Gas Stream Configuration

Figure 1 is a schematic diagram of one possible configuration of the exhaust gas streams of an MHD power plant in the region of the stack. One gas stream consists of the products of combustion in the main MHD combustor and comes from convective sections of

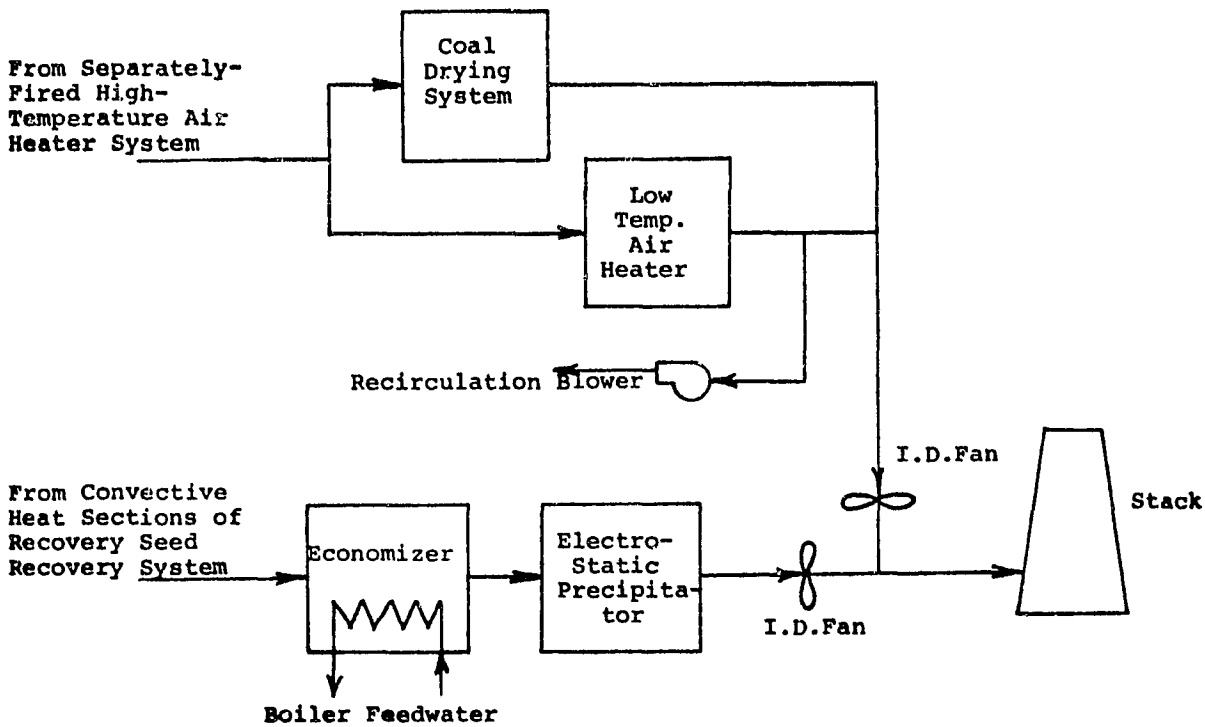

Figure 1. - Schematic diagram of exhaust gas streams in an MHD power plant with a separately-fired high temperature air heater system (ref. 1-1).

the heat recovery-seed recovery system and contains flyash and potassium compounds. The other gas stream consists of the products of combustion of a coal-derived gas and comes from the separately fired high temperature air heater system, part of which is utilized for coal drying. This arrangement corresponds to the one proposed in the Avco ETF Conceptual Design Study (ref. 1-1). The components which are exposed to the seed-laden gas prior to entering the stack are the economizer, electrostatic precipitator and an induced draft fan. The components which are exposed to the second gas stream are the coal drying equipment, a low temperature air heater and an induced draft fan. These six components and the stack are exposed to the gas stream when the gas is at the lower end of its temperature range.

The seed-laden exhaust gas stream is unique to MHD and is therefore emphasized in this investigation. Attention is therefore focused on the simpler schematic diagrams shown in figures 2 and 3 which include only one exhaust gas stream, which would be the case in an MHD power plant utilizing direct fired air preheating or oxygen enrichment. In the arrangement shown in figure 3 the electrostatic precipitator and the I.D. fan are located in higher temperature regions of the gas streams than in figure 2 and the particulate grain loading in the downstream section of the economizer is very low. The gas specific volumes in the electrostatic precipitator and the I.D. fan are slightly larger in this arrangement due to the higher gas temperatures upstream of the cold-end economizer.

Normal Operation (Without Acid Condensation)

As an example of the impact of the gas temperature on the plant design and performance, consider a plant designed to operate at full load with the stack gas temperature in the range in which acid condensation does not occur. The factors which determine the acid dewpoint temperature will be described subsequently.

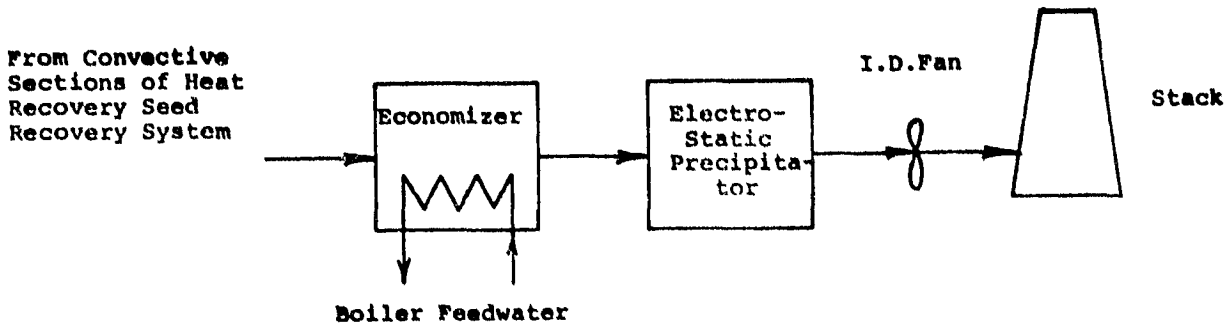

Figure 2. - Schematic diagram of seed-laden exhaust gas stream in an MHD power plant.

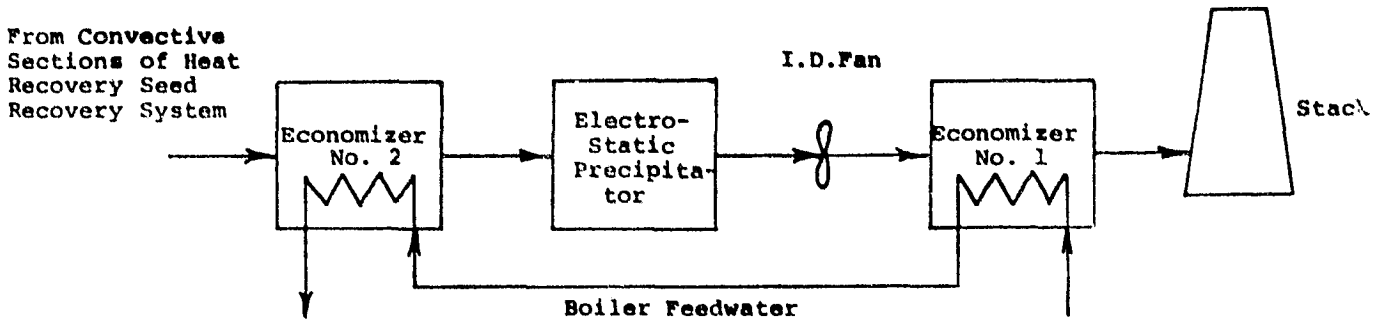

Figure 3. - Schematic diagram of alternate arrangement of seed-laden exhaust gas stream in an MHD power plant.

The temperatures of any surfaces in contact with the gas are lower than the bulk mean gas temperature since heat is being transferred from the gas through the surfaces to either the boiler feedwater or to the surrounding atmosphere. The bulk gas temperature also decreases as the gas flows through the components and up the stack because of this transfer of heat. Condensation of acid occurs on surfaces in contact with the gas if the surface temperature is at or below the dewpoint even when the bulk gas temperature is above the dewpoint temperature.

The ecoromizer is a case in point. The heat transfer coefficient on the water side of the tubing is much greater than the heat transfer coefficient on the gas side so that the tube-metal temperature is typically only a few degrees above the temperature of the water. Thus the lowest surface temperature of the economizer will occur at the boiler feedwater inlet end and will be very close to the feedwater inlet temperature.

During transient or part-load operating conditions, excursions from design-point temperatures can occur in which surface temperatures may fall below the acid dewpoint, leading to acid condensation and hence corrosion. The frequency and duration of such occurrences may or may not be tolerable in any given case. There are practices which can be employed to minimize such problems. One practice, which is employed in industrial boiler applications, is to install a system which preheats the feedwater during upset conditions to maintain the feedwater temperature at the economizer inlet sufficiently high to avoid acid condensation on the economizer surface. This technique can also be employed to maintain an elevated stack gas temperature during upset conditions to avoid acid condensation on stack lining surfaces. This particular technique has not been employed in the electric power industry because modern coal-fired power plants are usually designed with an air preheater situated between the economizer and the stack.

Reduction of Stack Gas Temperature (Without Acid Condensation)

Consideration is given to lowering the stack gas temperature because additional useful thermal energy is thereby extracted from the gas, resulting in an increase in power plant efficiency. As a simplification, consider the implications of designing the plant with a reduced stack gas temperature (relative to the previous case) without lowering it below the point at which acid condensation occurs. For the configurations shown in figures 2 and 3, the stack gas temperature is reduced by (a) lowering the feedwater inlet temperature, (b) reducing the difference between the gas temperature leaving the economizer and the feedwater inlet temperature, or a combination of (a) and (b).

This change, which results in a change in plant performance, is achieved by physical modifications in the plant equipment and, hence a change in plant capital cost. The additional thermal energy recovered from the gas is converted to additional electric power output at a very low efficiency because of the low temperature of the gas. The plant efficiency also may change as a result of a change in I.D. fan power consumption. An estimate of the improvement in plant efficiency and its associated cost impact is indicated in Appendix 1A.

The plant physical modifications include changes in the feedwater heating system, increase in the size of the economizer and possible modifications in the electrostatic precipitator, induced draft fan and stack because of (a) an increase of gas density resulting from the lower gas temperature and (b) an increase in flow resistance due to increased surface area of the economizer.

Modifications to the feedwater system may include changes in the number or size of the feedwater heaters and changes in the feedwater heater operating conditions. The size of the economizer would be increased (as the design stack gas temperature is decreased) to provide the increase in surface area required to extract additional thermal energy from the gas stream. This would also increase

the flow resistance, leading to a slightly larger pressure drop across the economizer. If the electrostatic precipitator (ESP) is situated downstream of the economizer, as shown in figure 2, the gas density will be higher in the ESP for lower gas temperatures, allowing a smaller flow cross-sectional area to achieve the same velocity. In certain regimes of operating conditions, the ESP performance may be effected by the gas temperature. If the ESP is situated upstream of the final economizer section, as in figure 3, the ESP may be unaffected by the stack gas temperature.

A lower temperature and, hence, a higher gas density in the stack reduces the natural draft effect in the stack which must be compensated for by additional fan pressure rise for a given size stack. The stack also serves to disperse the stack gas to the surrounding atmosphere. Environmental regulations require that an analysis be conducted to verify that a given stack design adequately disperses the stack gas. Lowering the stack gas temperature reduces the dispersion capability by virtue of the lower buoyancy of the gas emerging from the stack exit. The extent of reduction in dispersion capability depends on many factors related to the location of the plant. Depending upon local conditions, a given decrease in stack gas temperature may or may not dictate a plant or stack design modification to meet environmental regulations.

If the induced draft fan is situated downstream of the economizer, a decrease in the stack gas temperature results in an increase in the density of the gas handled by the fan. In addition, the fan pressure rise must be increased to compensate for the increased flow resistance of a larger economizer and the reduced natural draft of the stack. For a given mass flow rate, the required fan-drive power is proportional to the pressure rise across the fan and inversely proportional to the gas density. Therefore, depending upon the relative changes in gas density and additional fan pressure rise associated with a given change in

stack gas temperature, the fan power requirement may decrease or increase. Changes in fan size and fan motor size may result in changes in their capital cost as well as in the required auxiliary power. Further discussion of fan-drive power consumption and fan and drive-motor capital cost is given in Appendix 1B.

Reduction of Stack Gas Temperature (With Acid Condensation)

The third case considers a plant which is designed to operate at full load, with the stack gas temperature sufficiently low so that acid condensation may occur on material surfaces which have temperatures below the acid dewpoint temperature. If the surfaces exposed to the gas are made of the customary materials of construction in power plants (primarily carbon steel), corrosion will lead to severe deterioration of such materials. Accommodation to this situation can be made by selecting corrosion-resistant materials for the equipment in the low temperature section of the plant - specifically, economizer tubing in the colder sections of the economizer, ductwork, stack liners, and the I.D. fan. However, the extent to which the additional costs of these materials offsets the gain in plant performance because of the lower stack gas temperature would have to be ascertained to determine the feasibility of this approach. Relocation of the fan and the electrostatic precipitators to a warmer region of the exhaust stream (as in figure 3) may be more economical than building them with corrosion-resistant materials.

Many corrosion-resistant metals may be considered for use in place of carbon steel for economizer tubing and fan parts. Several of these are identified in Appendix 1C which also gives approximate costs per pound of material relative to the cost per pound of carbon steel. The net cost of replacement of carbon steel with corrosion-resistant materials depends upon the amounts of material required and upon the anticipated durability of the selected materials in the particular corrosive environment anticipated. Data do not presently appear to be available on material wastage rates

for the specific conditions of temperatures and gaseous compositions comparable to those anticipated in an MHD power plant. Data on material wastage rates are required in order to select the materials, determine the required metal wall thicknesses and, possibly, the frequency of replacement of parts. It is also necessary to consider the relative strengths of the candidate materials to determine tube wall and fan blading thicknesses to withstand imposed stresses.

When gas temperatures in the stack are high enough to avoid acid condensation, the stack may have a carbon steel liner which would not require maintenance or replacement. If the stack gas temperature is expected to be below the acid dewpoint temperature, the carbon steel liner would have to be replaced with an acid resistant material such as an exotic metal, an acid-brick liner or a fiberglass reinforced plastic (FRP) liner. In addition, the annulus between the lining and the concrete may have to be pressurized to prevent the stack gas from contacting the stack concrete. Appendix 1D gives a discussion of stack gas lining approaches and includes information on stack liner costs.

Another approach which has been proposed for reducing cold-end corrosion problems is to employ additives which would either reduce the tendency for acid condensation to occur or would neutralize the acid which does condense. However, this approach is usually considered as a possible remedy for unanticipated corrosion problems which arise after initial plant start-up. It is not normally considered as a viable approach in the design of a power plant. Appendix 1E includes further information on additives.

Factors Determining Acid Dewpoint Temperature

The source of the acid, which is normally responsible for the corrosion when the stack gas temperature is lowered to the acid dewpoint temperature, is the sulfur in the fuel. Sulfur reacts with oxygen to form sulfur dioxide (SO_2) and sulfur trioxide (SO_3). Sulfur dioxide will dissolve in free moisture in the flue gas and

will form sulfurous acid (H_2SO_3) when the water vapor condenses at the water dewpoint temperature. This typically ranges between 317^{o} and 339^{o} K (110^{o} and 150^{o} F) in stack gases. At higher temperatures, a gas phase reaction produces H_2SO_4 when SO_3 combines with water vapor. Condensation of H_2SO_4 occurs at the acid dewpoint temperature which is higher than the water dewpoint temperature. The acid dewpoint temperature depends upon the concentrations of water vapor and SO_3 in the gas.

A considerable amount of data, on the acid dewpoint as a function of SO_3 and H_2O concentration, has been published based upon experiments and theoretical predictions. There is a wide variation in published data. However, two correlations are in common use in industry today (ref. 1-2, ref. 1-3). One of these, shown in figure 4 (ref. 1-2), relates acid dewpoint to SO_3 concentration (ppm-by-volume) and moisture concentration (percent-by-volume). The other, shown in figure 5 (ref. 1-3), relates the acid dewpoint to H_2SO_4 concentration (ppm-by-volume) and moisture content (percent-by-volume). These correlations are in close agreement with one another on the basis that the volume concentration of H_2SO_4 is equivalent to the volume concentration of SO_3. This implies that each mole of SO_3 present in the gas is converted to one mole of H_2SO_4 and that the concentrations of H_2SO_4 and SO_3 can be used interchangeably in the correlations. The following equation (ref. 1-3) represents the correlation corresponding to figure 5.

$$1/T_{DP} = 2.276 \times 10^{-3} - 2.943 \times 10^{-5} \ln (P_{H_2O}) - 8.58 \times 10^{-5} \ln (P_{H_2SO_4}) + 6.20 \times 10^{-6} \ln (P_{H_2O}) \ln (P_{H_2SO_4}) \quad (1\text{-}1)$$

where

T_{DP} is the acid dewpoint (^{o} K)

P_{H_2O} is the partial pressure of H_2O (mm Hg)

$P_{H_2SO_4}$ is the partial pressure of H_2SO_4 (mm Hg)

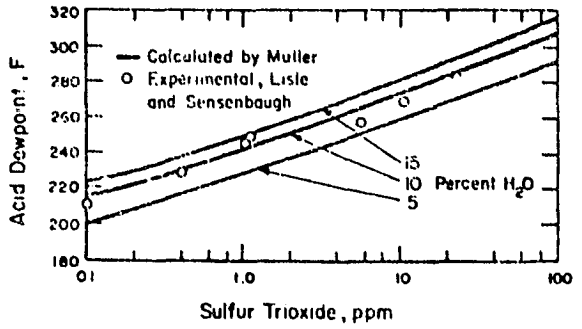

Figure 4. - Sulfuric acid dewpoint temperature as a function of sulfur trioxide concentration for three values of water vapor concentration at a total system pressure of 1 atmosphere (ref. 1-2).

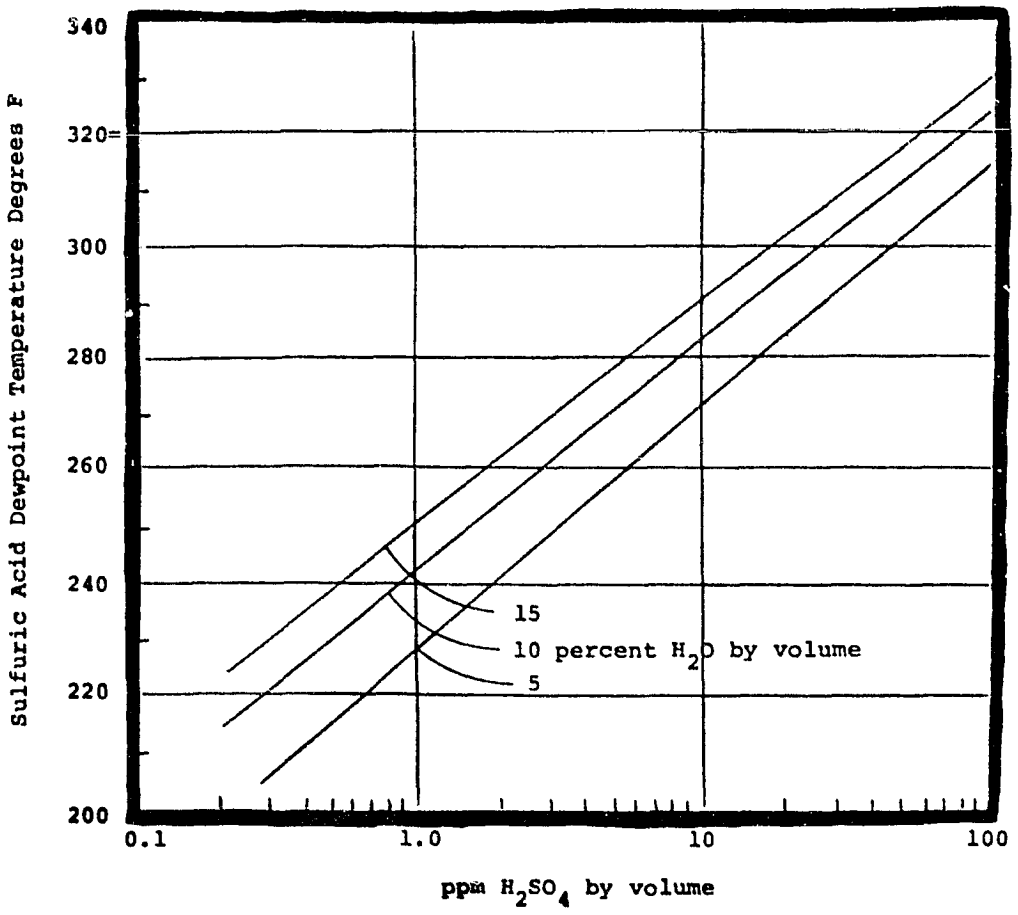

Figure 5. - Sulfuric acid dewpoint temperature as a function of sulfuric acid vapor concentration for three values of water vapor concentration at a total system pressure of 1 atmosphere based on equation (1-1).

It is evident from these correlations that the key to determining the acid dewpoint in an MHD plant is to determine the concentrations of sulfur trioxide and water vapor. The water vapor concentration is readily determined from combustion reactions. Determination of SO_3 concentration is much more difficult and is subject to considerable uncertainty.

Under the combustion conditions with excess air experienced in conventional power plants, the major portion of the sulfur in the fuel is converted into SO_2, no matter what the initial form of the sulfur in the fuel. The main occurrence of SO_3 in flue gas is from flame reactions and by oxidation of SO_2. Formation of SO_3 by dissociation of complex sulfates is not found to be a significant source in conventional power plants.

Two possible reactions occurring in flames which could lead to the production of SO_3 are

$$SO_2 + 1/2\ O_2 \rightleftarrows SO_3$$

which can occur by a homogeneous gas-phase reaction or a heterogeneous catalyzed reaction on active surfaces, and

$$SO_2 + O \rightleftarrows SO_3$$

which depends upon the availability of oxygen atoms. The latter reaction is believed to be the primary source of that portion of the SO_3 which is produced under combustion conditions.

In the flue gas downstream of the furnace of a conventional power plant, the production of SO_3 is governed by the interplay of the chemical equilibrium of the SO_2-SO_3 system and the reaction kinetics. Figure 6 shows the percent conversion of SO_2 to SO_3 under equilibrium conditions as a function of temperature and oxygen partial pressure (ref. 1-2). Depending upon the oxygen partial pressure, the figure shows that the conversion varies from a very small percentage at temperatures above 1367° K (2000° F) to nearly complete conversion to SO_3 at temperatures below 644° K (700° F), which is well above typical stack gas temperatures. However, such high levels of SO_3 are not observed in practice. It is

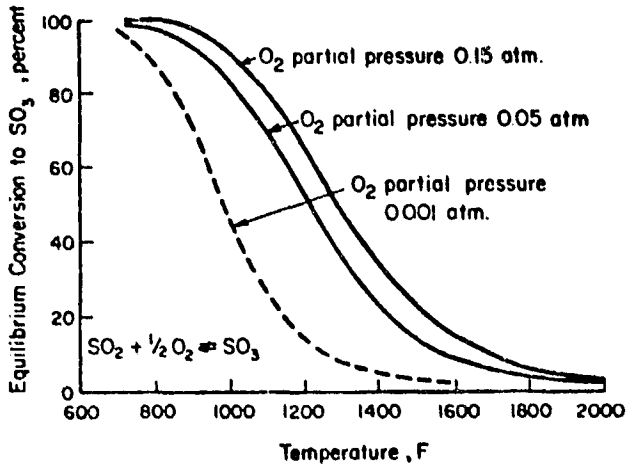

Figure 6. - Equilibrium conversion of SO_2 to SO_3 (ref. 1-2).

found that only about 1 to 2 percent of the SO_2 is converted to SO_3 in conventional power plants due to the low reaction rates in relation to the residence time of the gas in a power plant.

Catalytic reactions play a major role in determining how much SO_3 is produced in the flue gas. Although nitrogen oxide is known to accelerate the production of SO_3 by means of homogeneous catalytic reaction, it is primarily the heterogeneous catalytic reactions with vanadium and iron oxides which are responsible for accelerating the SO_3 production in flue gases. Vanadium may be present in the fuel and iron oxides are formed by corrosion of steel tubing.

SO_3 Formation in MHD Power Plants

There does not appear to be an experimental data base from which to determine levels of SO_3 concentration under conditions appropriate to MHD power generation. Therefore, predictions of acid dewpoint temperatures in an MHD power plant are unreliable. Several factors may contribute to making the percent conversion of SO_2 to SO_3 different from what is found in conventional plants. These factors include

(1) Higher combustion temperatures

(2) Substoichiometric combustion (initially) followed by oxidizer addition at lower temperature

(3) Possible differences in presence and activity of vanadium and iron oxides (depending upon fuel composition and upon steel-tubing corrosion)

(4) Reactions involving sulfur and potassium

The last item may be quite significant in determining the level of SO_3 production. Potassium is depended upon to remove SO_2 from the gas stream by the formation of potassium sulfate (K_2SO_4) to meet environmental regulations. The effect of the formation of K_2SO_4 on the conversion of SO_2 to SO_3 is unknown at the present time.

Figure 7 shows a typical set of equilibrium pressure curves for the major potassium-containing species in a residual fuel-oil fired system in which potassium is introduced to the gas stream in the form of potassium sulfate (ref. 1-4). It is representative of the type of behavior anticipated in a coal-fired system in which potassium is introduced in the form of potassium carbonate. Potassium sulfate begins to form as the gas cools down to temperatures below 1950° K (3050° F). The potassium sulfate will begin condensing when the vapor pressure curve intersects the saturated vapor pressure curve at approximately 1500° K (2240° F). As the K_2SO_4 partial pressure (and hence, concentration) increases, the concentration of SO_2 in the gas decreases.

The concentration of SO_3 in the gas depends upon how much SO_2 is converted to SO_3 at high temperatures where considerable SO_2 is available and to what extent conversion to SO_3 takes place at lower temperatures from the SO_2 remaining after the formation of K_2SO_4. Another factor which complicates the matter is the possibility of SO_3 combining with K_2SO_4 to form $K_2S_2O_7$.

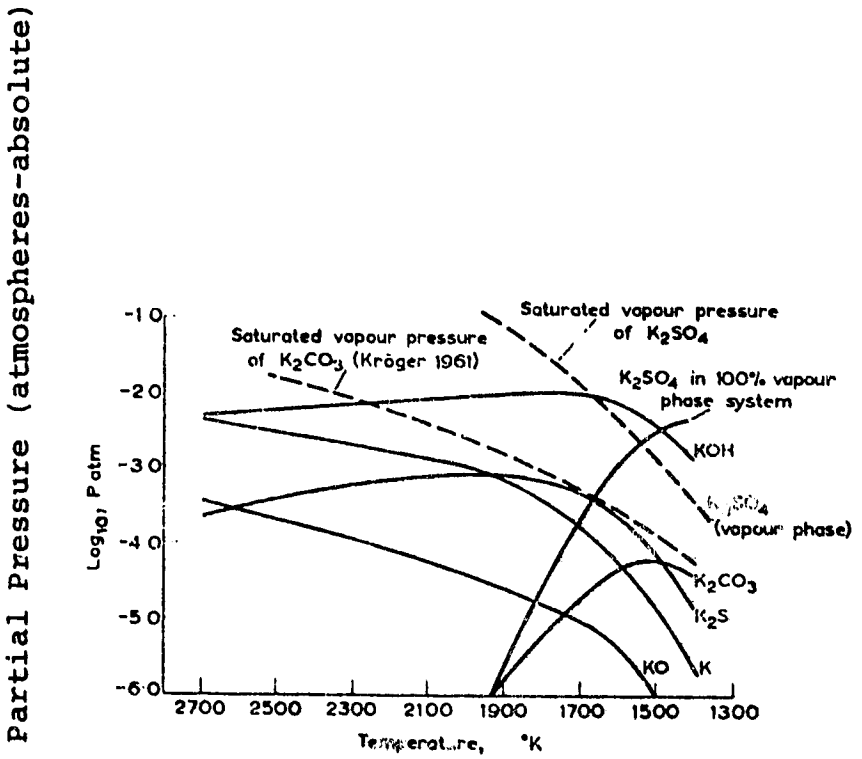

Figure 7. - Variation with temperature of the pressures of the principal K-containing species in an oil-fired MHD exhaust containing 1·0 atom percent K and stoichiometric O_2 (ref. 1-4).

It would require an extensive investigation to determine the SO_3 concentration (and, thereby, the acid dewpoint) under MHD conditions. Tests should be conducted under a variety of plant operating conditions. Since the SO_3 content of the stack gas depends upon the temperature-chemistry-residence-time history of the gas stream from the combustor to the stack, valid test data can be obtained only if the entire flow train is simulated, as in the Heat Recovery Seed Recovery System which is presently being designed. Another factor which makes the conditions in an MHD plant different from those in a conventional plant is the possible occurrence of seed deposits on surfaces in contact with the stack gas. Such deposits could even occur downstream of the electrostatic precipitator. The role which such deposits would play in the corrosion phenomena associated with acid condensation would also require investigation.

Range of Possible Acid Dewpoint Temperatures in an MHD Plant

In view of the difficulties cited before in determining the SO_3 concentration in the stack gas in an MHD plant, upper and lower limits on the SO_3 concentration must be selected by various sets of assumptions. Table II gives data on expected SO_2 concentration levels (in parts per million by volume) in an MHD plant for two types of coal: Illinois No. 6 dried to 2 percent moisture and Montana Rosebud dried to 5 percent moisture. These data are derived from MHD exhaust gas conditions corresponding to those reported in the Avco Engineering Test Facility Conceptual Design Study (ref. 1-1).

For Illinois No. 6 coal, the maximum possible SO_2 concentration by volume is 3107 ppm prior to formation of K_2SO_4 (or the ultimate concentration if potassium were not present). To meet EPA emission standards (NSPS-1979), the allowable sulfur emission level is limited to 0.60 pounds (as SO_2) per million Btu plant thermal input requiring a minimum of 89.7 percent sulfur removal. This is equivalent to an SO_2 concentration in the stack gas of 320 ppm by volume. The moisture content of the gas stream is 7.84 percent by volume.

For Montana Rosebud coal the maximum possible SO_2 concentration by volume is 1017 ppm prior to formation of K_2SO_4 (or the ultimate concentration if potassium were not present). To meet NSPS-1979 EPA emission standards, a minimum of 70 percent sulfur removal is required so that the resulting sulfur emission level will be 0.57 pounds (as SO_2) per million Btu plant thermal input. This is equivalent to an SO_2 concentration in the stack gas of 305 ppm by volume. The moisture content of the gas stream is 7.61 percent by volume.

The maximum uncontrolled emission of SO_3 in the stack gas, which would occur if no potassium were present, would be 3107 ppm by volume for the Illinois No. 6 coal case and 1017 ppm by

TABLE II. - MAXIMUM ALLOWABLE SULFUR CONCENTRATION (as SO_2) IN MHD PLANT STACK GAS ACCORDING TO NEW SOURCE PERFORMANCE STANDARDS (F.R. JUNE 11, 1979)

Parameters	Type of Coal	
	Illinois No. 6	Montana Rosebud
Coal sulfur content, percent	3.3	0.85
Higher heating value, Btu/lb	11265	8920
Potential emissions (as SO_2), $lb/10^6$ Btu	5.853	1.904
EPA emission limit (as SO_2) $lb/10^6$ Btu	[a]0.60	0.57
SO_2 concentration in stack gas by volume corresponding to EPA emission limit, ppm	320	305
Percent reduction of SO_2 emissions required to meet limits	89.7	[a]70

[a] Parameters set by NSPS-79 requirements

volume for the Montana Rosebud coal case. However, it is known that such concentrations cannot occur in an MHD plant because of the formation of potassium sulfate and the necessity to meet environmental regulations. The maximum possible concentration of SO_3 in the presence of sufficient potassium to ensure that environmental regulations are met is that which would occur if 100 percent of the remaining sulfur had formed SO_3. From table II, the maximum SO_3 concentrations (by volume) for Illinois No. 6 coal and Montana Rosebud coal would be 320 and 305 ppm, respectively. The corresponding acid dewpoints found by employing equation (1-1) are 446° and 445° K (343° and 342° F), respectively. These temperatures are virtually the same for the two types of coal because the moisture concentrations in the gas streams are nearly the same and environmental regulations require comparable sulfur emission levels. This does not mean that both coals necessarily result in the same acid dewpoint, because the conversion percentage of SO_2 to SO_3 may differ for the two coals.

In a conventional plant, only 1 to 2 percent of the SO_2 is converted into SO_3. Although there is no firm basis for assuming that the same percentage of conversion will occur in an MHD plant, neither is there a firm basis for stating that the percentage conversion will be greater or less than that which occurs in conventional plants. Unfortunately, there is no adequate data on the extent to which deviations from this 1 to 2 percent guideline occurs in conventional plants.

There are two ways to apply this 1 to 2 percent conversion factor. One is to assume that the conversion occurs primarily before K_2SO_4 is formed, in which case the conversion rate is applied to the maximum possible SO_2 concentrations as indicated in table II. For Illinois No. 6 coal, 1 to 2 percent of 3107 ppm is 31.07 to 62.14 ppm by volume which yields acid dewpoints of 420° and 427° K (296° and 307° F), respectively by equation (1-1). For Montana Rosebud coal, 1 to 2 percent of 1017 ppm is 10.17 to 20.34 ppm by volume which yields acid dewpoints of 408° and 415° K (274° and 287° F), respectively.

The other method is to assume that the conversion occurs primarily after K_2SO_4 is formed, in which case the conversion rate is applied to the maximum SO_2 concentrations allowable under EPA regulations, as indicated in table II. For Illinois No. 6 coal, 1 to 2 percent of 320 ppm is 3.2 to 6.4 ppm by volume, which yields acid dewpoints of 397° and 404° K (254° and 267° F), respectively by equation (1-1). For Montana Rosebud coal, 1 to 2 percent of 305 ppm is 3.05 to 6.1 ppm by volume, which yields acid dewpoints of 396° and 403° K (253° and 265° F), respectively.

These acid dewpoints do not necessarily represent the lower limits since there is a possibility that less than one percent conversion of SO_2 to SO_3 may occur due to special conditions in an MHD plant. Table III summarizes the above calculations of SO_3 concentrations and the corresponding acid dewpoints. It also shows SO_3 concentrations based upon much lower conversion rates of SO_2 to SO_3 - specifically 0.5 and 0.1 percent. It is uncertain how realistic these values are. The corresponding acid dewpoints for Illinois No. 6 coal are 390° and 376° K (242° and 217° F), respectively. The corresponding acid dewpoints for Montana Rosebud coal are 390° and 375° K (242° and 216° F), respectively. Figure 8 is a curve of acid dewpoint as a function of SO_3 concentration for the two coals considered in this investigation. A single curve is shown because the difference between the dewpoints for the two coals is less than the uncertainty of available data.

ECONOMICAL AND TECHNICAL CONSIDERATIONS IN STACK GAS TEMPERATURE SELECTION

Technical considerations in selecting stack gas temperatures and estimates of the range of possible acid dewpoint temperature were indicated in previous sections of the report. The selection of a stack gas temperature upon which to base an MHD plant design requires an investigation of the economic factors involved, as well as the technical considerations. The following steps are recommended for selecting a stack gas temperature

TABLE III. - SULFUR TRIOXIDE CONCENTRATIONS AND ACID DEWPOINT TEMPERATURES IN MHD STACK GAS UNDER VARIOUS ASSUMPTIONS REGARDING CONVERSION OF SULFUR DIOXIDE TO SULFUR TRIOXIDE

Type of Coal	Stack Gas Moisture Content, percent by Vol.	Assumed Basis for Conversion of SO_2 to SO_3	Sulfur Trioxide Concentration, ppm by Vol.	Acid Dewpoint Temperature*, °K (°F)
Illinois No. 6	7.84	100 percent of 320	320	446 (343)
"	"	2 " " 3107	62.14	427 (307)
"	"	1 " " 3107	31.07	420 (296)
"	"	2 " " 320	6.4	404 (267)
"	"	1 " " 320	3.2	397 (254)
"	"	0.5 " " 320	1.6	390 (242)
"	"	0.1 " " 320	0.32	376 (217)
Montana Rosebud	7.61	100 percent of 305	305	445 (342)
"	"	2 " " 1017	20.34	415 (287)
"	"	1 " " 1017	10.17	408 (274)
"	"	2 " " 305	6.1	403 (265)
"	"	1 " " 305	3.05	396 (253)
"	"	0.5 " " 305	1.525	390 (242)
"	"	0.1 " " 305	0.305	375 (216)

*Based upon Equation (1-1)

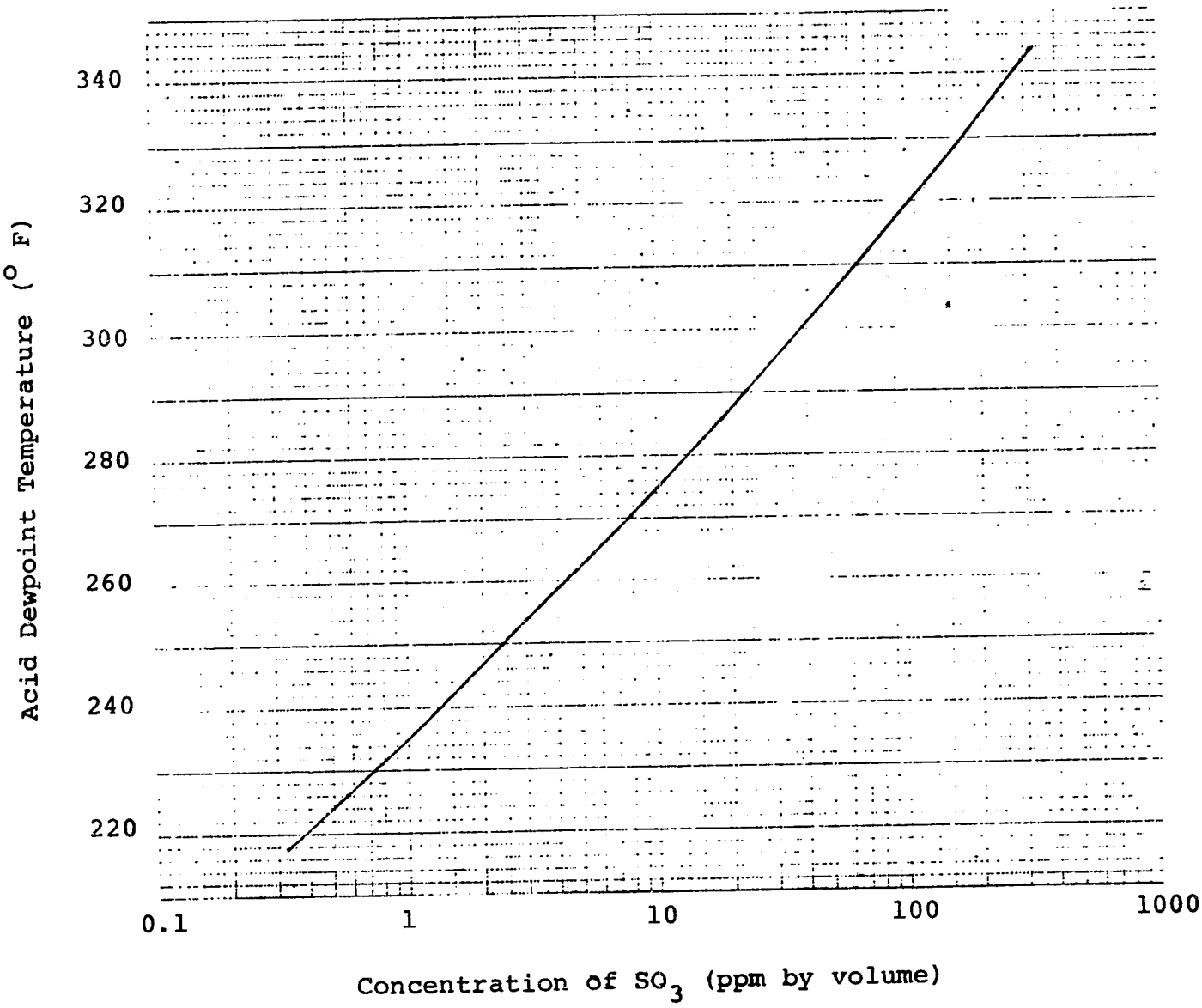

Figure 8. - Acid Dewpoint Temperature as a Function of Concentration of Sulfur Trioxide for Combustion Products of Illinois No. 6 Coal and Montana Rosebud Coal in an MHD Power Plant Based on Equation (1-1).

1. Determine the acid dewpoint temperature for the specified plant conditions. At present, there is insufficient data available for determining the acid dewpoint temperature in an MHD plant. A specific temperature or a specific set of conditions would have to be assumed.

2. Determine by heat transfer analysis, the differential ΔT between the bulk stack gas temperature T_{SG1} at the exit of the economizer and the lowest wall surface temperature T_{Smin} to which the stack gas is exposed

$$\Delta T = T_{SG1} - T_{Smin} \qquad (1\text{-}2)$$

The minimum surface temperature may be found to occur at the economizer tubing walls, the walls of the ducting or on the stack liner surface. The temperature of the gas in contact with the surface can be assumed to be the same as the wall surface temperature.

3. For a stack gas temperature at the economizer exit which is equal to the sum of the acid dewpoint temperature and the differential temperature (as determined in steps 1 and 2), determine whether adequate plume rise and plume clarity is achieved with the stack as designed. This will depend upon site conditions and cannot be determined unless a site location is specified. Further discussion of plume rise and plume visibility considerations appears in Appendix 1F.

4. If the stack gas temperature so determined does result in adequate plume dispersion and clarity, this temperature is selected as a reference stack gas temperature.

$$T_{SG/ref} = T_{ADP} + \Delta T \qquad (1\text{-}3)$$

where

$T_{SG/ref}$ is the reference stack gas temperature at the economizer exit

T_{ADP} is the acid dewpoint temperature as determined in step 1

5. Determine the technical feasibility of designing the plant to operate with a feedwater temperature (at the economizer inlet) which would result in a stack gas temperature equal to or less than $T_{SG/ref}$. Consideration must be given to the effect of using boiler feedwater (directly or indirectly) for cooling the MHD flow train components.

6. If it is not technically feasible to design the feedwater system so that the stack gas temperature is below $T_{SG/ref}$, determine the stack gas temperature $T_{SG/fw}$ (where $T_{SG/fw}$ is greater than $T_{SG/ref}$) which results from the minimum feasible feedwater temperature (at the economizer inlet). Select $T_{SG/fw}$ as the stack gas temperature (unless there are unusual circumstances which result in an optimum stack gas temperature which is greater than $T_{SG/fw}$).

7. If it is technically feasible to design the feedwater system so that the stack gas temperature is below $T_{SG/ref}$, an economic tradeoff analysis must be conducted to determine whether the additional capital investment and additional operating and maintenance costs (due to the plant modifications dictated by the condensation of acid vapors) are warranted by the improvement in plant efficiency due to the reduction in stack gas temperature. The quantitative relations between capital investment, fuel savings and operating and maintenance costs are given in Appendix 1G. The steps to be taken in the economic tradeoff analysis are as follows

a. Select a stack gas temperature, T_{SG} which is less than $T_{SG/ref}$

b. Estimate the increase in plant efficiency due to the reduction in stack gas temperature from $T_{SG/ref}$ to T_{SG} employing the guidelines presented in Appendices 1A and 1B

c. Estimate the fuel cost savings due to the plant efficiency improvement, employing equation (1G-2)

d. Estimate the capital investment cost, CCE_f, which is equivalent to the fuel cost savings, employing equations (1G-3) and (1G-4)

e. Estimate the capital investment, CC required to modify the plant design to allow it to withstand acid corrosion. Consideration must be given to the various alternative modifications (e.g., materials)

f. Estimate the change in plant operating and maintenance costs associated with the various modifications and with plant operation below $T_{SG/ref}$. Determine the capital investment cost, $CCE_{O\&M}$ which is equivalent to the change in O&M cost, employing equation (1G-8)

g. Compare the Capital-Cost-Equivalent savings, CCE_f with the minimum additional capital costs, CC and Capital-Cost-Equivalent, $CCE_{O\&M}$

h. If the comparison results in the relation

$$CCE_f > CC + CCE_{O\&M} \qquad (1\text{-}4)$$

the plant design modifications which yield this result may be considered for adoption and the corresponding stack gas temperature may be selected. However, because of the large number of uncertainties involved in determining the acid dewpoint temperature and in estimating capital and O&M costs, it is not practical to operate with $T_{SG} < T_{SG/ref}$ unless the economic benefit is substantial

i. If the comparison results in the relation

$$CCE_f < CC + CCE_{O\&M} \qquad (1\text{-}5)$$

the stack gas temperature should not be selected to be less than $T_{SG/ref}$

STACK GAS TEMPERATURE SELECTION

Selection of a stack gas temperature at this time is difficult because

a. There is a wide margin of uncertainty in acid dewpoint temperatures under MHD plant conditions

b. Although economic data are presented in Appendixes 1B through 1E, additional data such as the cost of modifying the feedwater system, incremental O&M costs and the additional economizer surface area required, are necessary for a comprehensive economic tradeoff investigation. Determination of such additional economic data is beyond the scope of this investigation and would be of limited usefulness in the absence of greater certainty on acid dewpoint data

If it should be necessary to select a stack gas temperature for the purpose of preparing a conceptual design of an MHD plant, or for conducting parametric studies, it would have to be done with the understanding that there is no firm basis for such a selection at this time and that confirmation of the selected temperature would have to await verification by rigorous testing on large scale apparatus such as the Heat Recovery Seed Recovery System which is currently in the design stage. A reasonable assumption at this time would be that the most economic stack gas temperature is that which occurs when the temperatures of surfaces exposed to the stack gas are above the acid dewpoint temperature of the gas. As indicated by table III, the possible acid dewpoint temperatures range from 375° to 446° K (216° to 343° F). A plausible assumption might be that the concentration of SO_3 in the stack gas is one percent of the maximum SO_2 concentration as indicated previously. This would result in a concentration of 3.2 ppm (by volume) of SO_3 for Illinois No. 6 coal or 3.05 ppm (by volume) of SO_3 for Montana Rosebud Coal. The resulting acid dewpoint is approximately 397° K (254° F) for both types of coal.

The temperature differential between the bulk gas and material surfaces depends upon heat transfer rates and flow condition along the gas flow path. The tube metal temperature in an economizer is typically only a few degrees above the inlet feedwater temperature. In such a case, the temperature differential would

be a few degrees less than the difference between the economizer water inlet temperature and the economizer outlet gas temperature. This differential is normally sufficiently large that the reduction in stack gas temperature between the economizer outlet and the top of the stack would not result in acid condensation near the top of the stack. In the Avco ETF Conceptual Design Study (ref. 1-1), the difference between the economizer water inlet temperature and the economizer gas outlet temperature is 24.2° K (43.5° F). If it is assumed that heat transfer calculations indicate that the gas side metal surface temperature is 1.4° K (2.5° F) above the water temperature, the minimum metal surface temperature exposed to the gas in the economizer is 22.8° K (41° F) below the stack gas bulk temperature at the economizer exit. Under these circumstances, and for an acid dewpoint temperature of 397° K (254° F), the economizer inlet water temperature should be at least 395.6° K (251.5° F) and the stack gas temperature should be at least 419.8° K (295° F). This determination was made for the purpose of illustrating lines of reasoning rather than for the purpose of making a recommendation.

CONCLUSIONS AND RECOMMENDATIONS

The most important factor in the selection of a stack gas temperature is determining the acid dewpoint temperature. The acid dewpoint temperature depends primarily on the sulfur trioxide (SO_3) and moisture content of the gas. Correlations exist, and are widely accepted in the industry, which relate the acid dewpoint to the SO_3 and H_2O content of the gas. However, there is a considerable degree of uncertainty in the determination of the SO_3 content, leading to considerable uncertainty in the acid dewpoint. The range of possible dewpoint temperatures appears to extend from 375° to 446° K (216° to 343° F).

Further investigations are required in order to be able to predict acid dewpoint temperatures with satisfactory precision and confidence. Predictions will be valid only to the extent that they can be supported by test data under conditions which

are very close to those anticipated in an MHD plant. Since the SO_3 content of the gas depends upon temperatures, reactions and residence times all along the gas flow path from the combustor to the stack, test data must be obtained on equipment which simulates the entire MHD gas flow train. It is therefore recommended that measurements of SO_3 content and acid dewpoints be included as a part of the test program for the U.S. Department of Energy's Heat Recovery Seed Recovery System which is presently undergoing design or another equivalent test program.

The economic factors which determine the feasibility of selecting a stack gas temperature such that acid condensation occurs on material surfaces include materials costs for economizer tubing, ducting, stack liners and fans as well as technical data such as material strengths and corrosion resistance. Data on some of these economic factors are included in this report. It is recommended that further investigation of the economic factors be pursued at a time when satisfactory data become available on acid dewpoint temperatures under MHD conditions. Since the results of an economic tradeoff study to determine the stack gas temperature depend heavily upon the MHD plant configuration, data of a general nature may be of limited value. Therefore, it is recommended that a comprehensive economic study be conducted for a specific well-defined MHD plant configuration - but not until better data on acid dewpoint temperatures in an MHD plant become available.

REFERENCES

1-1. Avco-Everett Research Laboratory, Inc.: Engineering Test Facility Conceptual Design - Final Report, Part 1. U.S. Department of Energy Report FE-2614-2, June, 1978.

1-2. Reid, W. T.: External Corrosion and Deposits - Boilers and Gas Turbines. American Elsevier Publishing Co., New York, 1971.

1-3. Verhoff, F. H. and Banchero, J. T.: "Predicting Dew Points of Flue Gases", Chemical Engineering Progress. Vol. 70, No. 8, pp. 71-72, August, 1974.

1-4. Heywood, J. B. and Womack, G. J.: Open-Cycle MHD Power Generation. Pergamon Press, Oxford, 1969.

Appendix 1A

Effect of Reduction of Stack Gas Temperature On Plant Efficiency

The total amount of thermal energy which is extracted from the stack gas increases as the temperature of the stack gas decreases. In a MHD plant with an economizer as the final heat exchanger in the exhaust gas stream, the additional thermal energy made available by lowering the stack gas temperature results in an increase in heat input to the steam bottoming plant, and hence, an increase in the total plant efficiency. A precise calculation of the increase in net plant efficiency is obtained by a complete plant cycle heat balance analysis. However, an estimate can be made by applying thermodynamic principles. Since the temperature at which this additional energy recovery occurs is very low, the net effect on the overall plant efficiency is quite small. If the additional energy recovery occurred over the full temperature range of heat input to the bottoming plant, the increase in electric power generated would be approximately equal to the additional energy recovered times the efficiency of the bottoming plant. However, the additional energy recovery occurs at the tail end of the temperature range and the efficiency of its utilization can be no greater than the Carnot efficiency of a reversible heat engine operating between the temperature of additional energy recovery and the temperature of the surroundings.

For a reversible heat engine with heat input from a gas stream (of constant specific heat capacity) whose temperature changes from T_1 to T_2 and which rejects heat to surroundings at T_o, the maximum efficiency is

$$\eta_{max} = 1 - \frac{T_o \ln (T_1/T_2)}{T_1 - T_2} \qquad (1A\text{-}1)$$

where the temperatures are absolute temperatures. If T_2 is very nearly equal to T_1, an approximation to the maximum efficiency is

$$\eta_{max} = 1 - \frac{T_o}{T_1} \qquad (1A\text{-}2)$$

For heat recovery from a gas stream in which the temperature drops by 28° K (50° F) from 422° to 394° K (300° to 250° F), and the temperature of heat rejection is 289° K (60° F), the maximum energy conversion efficiency by equation (1A-1) is 29.2 percent. If the temperature drops by 28° K (50° F) from 394° to 366° K (250° to 200° F), the maximum conversion efficiency is 24.1 percent.

The impact of this energy recovery on the overall plant efficiency depends upon the magnitude of the recovered energy relative to the total plant power output and total thermal energy input. The procedure for determining the increase in plant efficiency is illustrated by a sample calculation based upon the Avco ETF Conceptual Design Study (ref. 1-1). Since the cycle in that study includes a separately-fired high temperature air heater, the magnitude of the results may differ from those which would apply to an oxygen-enrichment cycle or a direct-fired high-temperature air heater cycle. For the 1644° K (2500° F) air preheat temperature case, the mass flow rate of flue gas in the economizer is 70.5 kg/sec (559,900 lbm/hr). The mean specific heat capacity of the gas is approximately 1075 J/kg ° K (0.257 Btu/lbm ° F) and its temperature is 408° K (275° F). If the temperature at the exit of the economizer is reduced by 28° K (50° F) down to 380° K (225° F), the additional thermal energy which can be recovered is given by

$$mc_p\ (T_1 - T_2) = 2.1\ \text{MW}\ (7.195 \times 10^6\ \text{Btu/hr})$$

where m is the mass flow rate and c_p is the specific heat capacity. The maximum efficiency of conversion of this thermal energy into electric power is 26.7 percent by equation (1A-1), resulting in a maximum increase in electric power output from the steam bottoming plant of 0.56 MW. The initial net electric power generated by the plant was 78.6 MW at an overall plant efficiency of 29.8 percent. The modified plant would generate 79.16 MW. If the thermal energy input is the same in both cases (263.8 MW_t), the overall efficiency of the modified plant would be 30.0 percent, representing an increase in plant efficiency

of 0.2 percent. An additional improvement in plant efficiency could be obtained by lowering the temperature of the separately fired high temperature air heater flue gas.

Appendix 1B

Induced-Draft Fan Power Requirements

The power requirement of the I.D. fan drive-motor is given by

$$P_f = 2.626 \times 10^6 \frac{m}{\rho} \frac{\Delta p}{\eta_f} \qquad (1B\text{-}1)$$

where

P_f is the fan power requirement (brake-horsepower)
m is the gas flow rate (lbm/hr)
ρ is the gas density (lbm/feet^3)
Δp is the pressure rise across the fan (in.-H_2O)
η_f is the fan efficiency (decimal fraction)

Reducing the temperature of the stack gas is achieved by increasing the economizer surface area, thus increasing the gas-path flow resistance. The temperature reduction also increases the gas density and reduces stack buoyancy. This further increases the pressure rise which the fan must produce. If the fan is situated downstream of the economizer, the density of the gas at the fan inlet decreases. The net result is a change in the fan power requirement, as determined by equation (1B-1) due to changes in the density and the required pressure rise.

For a specific fan, however, changes in density and pressure-rise for a given mass flow rate result in a shift in the operating point on the fan performance curve. This can result in either an increase or a decrease in the fan efficiency, depending upon the direction of the shift as well as upon the location of the operating point relative to the point of maximum efficiency. Equation (1B-1) is applicable to determining nominal power requirements prior to selecting a fan. To determine the effect of stack gas temperature on fan power requirements for a specific fan, it is necessary to examine the fan operating characteristics in relation to the flow characteristics (pressure drop vs. flow rate relationships) of the exhaust gas flow path.

A change in power consumption of an I.D. fan has a direct effect on plant efficiency. A reduction in drive power contributes to an increase in net plant electric power output. For a constant plant thermal input, the change in plant efficiency due to a change in auxiliary power requirement is

$$\Delta\eta = \frac{\Delta P}{P} \qquad \text{(1B-2)}$$

where

$\Delta\eta$ is the increase in net plant efficiency
ΔP is the reduction in auxiliary power requirement
P is the original plant output
η is the original plant efficiency

A change in stack gas temperature from 408° to 380° K (275° to 225° F) results in approximately a 7 percent increase in gas density. Neglecting changes in pressure rise and fan efficiency in order to obtain an order-of-magnitude estimate of the possible improvement in plant efficiency, such a change in temperature would result in a 7 percent decrease in fan power. A full-scale commercial plant with a flow rate of 882 kg/sec (7×10^6 lbm/hr), a pressure-rise of 1.047×10^{-4} Pa (20 in.-H_2O) and a fan efficiency of 85 percent would require 6 MW (8000 hp) to drive the fan. A 7 percent reduction in fan power would amount to a savings of 0.42 MW. If the net plant power output is 1000 MW at 45 percent overall efficiency, the maximum plant efficiency improvement associated with the fan would be 0.019 percent. This is an order-of-magnitude smaller than the maximum efficiency gain associated with the thermal energy recovery estimate indicated in Appendix 1A. A simultaneous pressure-rise (previously neglected) would result in a smaller increase or possibly even a decrease in overall plant efficiency.

If the changes in flow conditions (gas density and fan pressure rise) are substantial, a change in selected equipment may be required. Because of the variation in fan efficiency with operating conditions and because equipment is available in discrete sizes, it is difficult to establish a general relationship between capital cost and flow conditions. Table IV presents data obtained

TABLE IV. - INDUCED DRAFT FAN PERFORMANCE PARAMETERS AND COST ESTIMATES FOR TYPICAL FLOW CONDITIONS

Mass Flow Rate, lbm/hr	[a] Gas Temperature, °F	[b] Pressure Rise, in. H_2O	[a] Gas Density, lbm/ft^3	Volumetric Flow Rate, acfm	[c] Fan Efficiency, percent	[d] Fan Speed, rpm	[d] Fan Power Bhp	[e] Fan w/Motor Cost, dollars
870,000	250	20	.0534	271,536	89.43	894	955	172,000
"	"	"	"	"	87.36	1169	978	152,000
"	"	21	.0532	272,556	88.77	1171	1014	152,000
"	"	19	.054	268,519	89.11	883	901	141,000
"	200	20	.057	254,386	89.5	881	894	141,000
"	300	"	.0499	290,581	87.98	1160	1039	159,000
6,960,000	250	"	.0534	2,172,285	79.88	510	8557	1,298,000
"	"	21	.0532	2,180,451	82.13	497	8772	1,423,000
"	"	19	.054	2,148,148	83.25	438	7714	1,307,000
"	200	20	.057	2,035,088	83.46	437	7673	1,307,000
"	300	"	.0499	2,324,649	78.91	502	9270	1,352,000

a. Temperature of gas at fan inlet
b. Pressure of gas at fan exit is 1.0 in.-H_2O in all cases
c. Maximum static efficiency
d. Fan speed and fan power at point of maximum fan efficiency
e. Cost estimates do not include installation costs

from a fan manufacturer which indicates fan power, efficiency and capital costs for a range of conditions to illustrate how these parameters vary with flue gas temperature and fan pressure rise for two different mass flow rates. The larger mass flow rate is typical of a full scale powerplant. The lower mass flow rate is typical of a pilot-scale plant. For the first set of conditions in table IV, two alternate equipment selections are indicated - one being based upon minimum power requirement and the other being based upon minimum equipment cost.

Appendix 1C

Corrosion-Resistant Metals for Economizer Tubing, I.D. Fan Parts and Ductwork

Table V is a listing of several metals with corrosion resistant properties which can be substituted for carbon steel to reduce the impact of corrosion due to acid condensation on economizer tubing, I.D. fan parts and on duct surfaces. The table gives approximate costs per pound for each material. Also included in the table is the cost of carbon steel (per pound) as a base of reference. Several other factors must be considered in selecting a metal for any given application. These considerations include the strength of each material, the degree to which it resists corrosion, its ease of fabrication and assembly (e.g. weldability) and its availability. The availability of a material affects the delivery schedule as well as the cost.

TABLE V. - COST ESTIMATES FOR SEVERAL CORROSION RESISTANT METALS AND CARBON STEEL

Type of Metal	Estimated Cost $/kg ($/lbm)	
	Tubing	Plate
Carbon Steel [a]	1.10 (0.50)	0.53 (0.24)
304 Stainless Steel [b]	3.75 (1.70)	2.43 (1.10)
316 Stainless Steel [c]	6.61 (3.00)	4.19 (1.90)
316L Stainless Steel [c]	6.83 (3.10)	4.30 (1.95)
317 Stainless Steel [c]	9.70 (4.40)	-
317L Stainless Steel [c]	10.36 (4.70)	5.84 (2.65)
Carpenter 20-Cb-3 Stainless Steel	16.98 (7.70)	-

a. not considered to be corrosion resistant

b. minimally resistant to H_2SO_4 corrosion

c. corrosion resistance diminishes at temperatures above 339° K (150° F)

Appendix 1D

Stack Lining Materials

To reduce the problems associated with condensation in the stack, stacks are built with corrosion- and erosion-resistant liners. The outside structural stack is usually of reinforced concrete construction. Liners have been made of acid-resistant brick with acid-resistant mortars, protected steel, fiberglass reinforced plastic (FRP) and metal alloys. The liner should be impervious to the flue gases, chemically inert to sulfuric acid, designed to expand over any possible operating temperature range, withstand temperature excursions, and accept upset operation without developing leaks or cracks. Liners are usually insulated so that surfaces remain close to gas temperatures. Inside surfaces are smooth to avoid pockets and preclude absorption of acid. The top of the chimney often has special protection and 15 to 30 meters (50 to 100 feet) of the outside shell is often made of stainless steel to avoid the corrosive effects of acid downwash.

Table VI is a listing of several of the materials available for stack linings, including estimates of their capital costs (installed) on the basis of cost per unit surface area. As a point of reference, a 229-meter (750-foot) tall stack with a 8.53-meter (28-foot) diameter liner running the entire length of the stack has a surface area of 6132 m^2 (66,000 $feet^2$). The total liner cost for such a stack, based upon the data presented in table VI can therefore range from $2,000,000 to $8,600,000.

Cor-Ten steel would be the recommended lining material for stack gas temperatures above the acid dewpoint. The other materials listed in table VI would be suitable for stack gas temperatures below the acid dewpoint, subject to certain restrictions. The acid-brick lining would not be suitable for stacks requiring liners greater than 150 meters (500 feet) in height or for stacks in high seismic areas. The fiberglass reinforced plastic liners

TABLE VI. - STACK LINING MATERIAL ESTIMATED COSTS (INSTALLED)

Stack Lining Materials	Restrictions	Installed Cost $/m^2 ($/ft^2)
Cor-Ten Steel (A242)		431-484 (40-45)
Acid Brick Lining Type H (ASTM 279) w/Acid-Resistant Mortar	Height < 150 m (500 ft) (also low seismic zone)	323-377 (30-35)
Fiberglass Reinforced Plastic	Gas Temp. < 422° K (300° F)	538-592 (50-55)
316L Stainless Steel	Availability	753-807 (70-75)
317LM Stainless Steel	Availability	1076 (100)
Incoloy 825	Availability	1400 (130)
Inconel 625	Availability	1400 (130)

would not be suitable unless the stack gas temperature can be maintained at temperatures below 394 to 422^{o} K (250 to 300^{o} F) at all times, such as by spray cooling under off-design conditions. Although prices can be quoted on the more exotic metals, the availability and delivery scheduling of these materials, including stainless steels in large quantities, is questionable under today's market conditions.

Appendix 1E

Gas Stream Additives

Injecting additives into the gas stream to inhibit corrosion from condensed acid is not a measure which is commonly employed in electric power plants. The plant is usually designed to take care of the cold-end corrosion problem by other means such as maintaining a sufficiently high stack gas temperature to avoid acid condensation. However, this measure has been employed in several electric power plants which were originally designed to be fired with natural gas, but subsequently required to convert to oil firing.

Additives are available in liquid or powder form. When injected into the gas stream, they form a mono-molecular layer on metal surfaces and act as a physical barrier against corrosive substances. The required feed rate of the additive depends upon the surface area which must be coated as well as the gas composition and flow rate. To make a cost estimate of the additive and the injection equipment would require specific information on the plant configuration and additional knowledge of the gas composition. Typical costs for additives for conventional power plants are in the range of 1.1×10^{-4} to 5.5×10^{-4} dollars per kg ($0.10 to $0.50 per ton) of coal, depending upon the sulfur content of the coal.

Appendix 1F

Plume Dispersion and Visibility Considerations

The NSPS-79 sets visibility standards for particulate matter. Particulate matter means any finely divided solid or liquid material, other than uncombined water, as measured by EPA method 5. The opacity limit for a steam generating plant is 20 percent (6 minute average) except for one 6-minute period per hour of not more than 27 percent opacity. There is no standard for sulfuric acid mist for steam generating plants; there is a 10 percent opacity standard for acid mist from sulfuric acid plants. Plume visibility is normally set by the particulate emissions but any significant smog, smut or mist formed in the exhaust will be included in the opacity determinations and, if the limit is exceeded, proof will be required that the particulate emission limits, using the approved test methods, are being met. Since best available control technology must be applied, it can be expected that the regulatory agencies will insist on a 10 percent opacity (clear stack) if it is at all achievable.

Stack plume dispersion factors depend upon conditions at the site external to the power plant such as mean wind speed at stack height, density of the ambient air at the top of the stack, variation of ambient pressure and temperature with height above the stack as well as plant design factors such as stack height, stack diameter and gas exit velocity. In addition, the increment which any plant may add to the pollutants depends on the allowable limit for the region, the baseline concentration and contributions from all significant sources. The permissable addition from a new source, after applying the best available control technology for removal of the pollutant, is determined by an approved dispersion analysis.

Since these factors are site specific, it is not possible to develop general criteria for selection of stack gas temperature which are applicable to a general site. It is recommended that

the minimum allowable stack temperature be selected on the basis of acid corrosion considerations. When a particular plant site is established, the investigation of allowable ambient ground level concentrations and increments for pollutants should be determined to ascertain whether the selected temperature is suitable for that site.

Appendix 1G

Economic Factors Related to Changes in Design Stack Gas Temperature

The economic impact of an improvement in plant efficiency arises from the fuel savings per kilowatt hour of electricity generated. The amount of fuel Btu value saved per year due to an increase in plant efficiency is

$$F_a = (3413)\ (8760)\ (P)\ (CF)\ \left[-\Delta(1/\eta)\right] \qquad (1G\text{-}1)$$

where

F_a is the number of Btu of fuel saved annually (Btu/yr)
P is the plant electric power output (kW)
CF is the plant capacity factor (decimal)
η is the net plant efficiency (decimal)

The corresponding cost savings for fuel in the first year of plant operation is

$$C_f = (3.413)\ (8.76)\ (f_c)\ (P)\ (CF)\ \left[-\Delta(1/\eta)\right] \qquad (1G\text{-}2)$$

where

C_f is the dollars saved per year in fuel cost
f_c is the fuel price ($/million Btu) during the first year of plant operation

In order to obtain the efficiency improvement which leads to the fuel savings, it is necessary to make initial investments in capital equipment. The investments will occur during the period of plant construction. By the time the plant begins operation, the capital investments for efficiency improvement will include taxes, interest, and other charges in addition to the original equipment purchase prices and installation costs. The capital investment required to achieve an investment improvement in plant efficiency can be justified only if the associated capital investment is less than an amount which is equivalent (at the time

the investment occurs) to the series of payments for fuel which are avoided because of the savings in fuel costs. An estimate of this amount can be obtained by making the simplifying assumption of zero construction time ("overnight construction"). In this case, the capital investment cost which is equivalent to the fuel cost savings over the plant life is given by

$$CCE = \frac{(CPWC_f)(CRF)}{FCR} \qquad (1G\text{-}3)$$

where

CCE is the equivalent capital cost ($)

$CPWC_f$ is the cumulative present worth of the fuel cost savings over the life of the plant ($)

CRF is the capital recovery factor (per year)

FCR is the fixed charge rate (per year)

The actual capital investment which can be justified is less than CCE because of interest and other charges during construction.

The cumulative present worth of the fuel cost savings over the plant life, assuming constant annual fuel consumption, is

$$CPWC_f = \frac{C_f}{e-I}\left[\left(\frac{1+e}{1+I}\right)^N - 1\right] \qquad (1G\text{-}4)$$

where

e is the annual rate of fuel price escalation (assumed to be constant)

I is the annual interest rate (assumed to be constant)

N is the plant life (years)

The capital recovery factor is

$$CRF = \sum_{i=1}^{N} \frac{1}{(1+I)^i} = \frac{I(1+I)^N}{(1+I)^N - 1}$$

The fixed charge rate is equal to the sum of the capital recovery factor, allowance for retirement dispersion, levelized annual income tax, property taxes and insurance.

As an example to illustrate the determination of these economic factors, the following assumptions are made, based upon the sample calculation of plant efficiency improvement cited in Appendix 1A.

N = 30 years
I = 0.1
e = 0.06
FCR = 0.18 per year
f_c = \$1.00 per 10^6 Btu
P = 78,600 kW
CF = 0.6
η = 29.8 percent
$\Delta\eta$ = 0.2 percent

Under these assumptions, the annual fuel savings from equation (1G-1) is 3.154×10^{10} Btu per year, resulting in a first-year cost savings, from equation (1G-2), of \$31,540. The cumulative present worth of the fuel cost savings over the plant life is \$528,900 and the capital recovery factor is 10.61 percent. The resulting equivalent capital investment cost, from equation (1G-3) is \$312,000. This implies that the plant owner can afford to spend up to \$312,000 at the time the plant begins operation in order to achieve a 0.2 percent improvement in plant efficiency. The actual amount available for expenditure during the time of plant construction would be less than this amount because of interest charges during construction.

A plant design modification which is made for the purpose of improving the plant efficiency may also result in a change in the non-fuel operating and maintenance (O&M) costs of the plant. Changes in O&M costs are difficult to estimate - especially for a plant with no long term operating experience. If such data were available, it would be necessary to express the incremental O&M

costs on the same basis as the fuel cost savings and capital investment cost by determining the cumulative present worth of the net change in O&M costs over the plant life.

$$CPWC_{O\&M} = \sum_{i=1}^{N} \frac{\Delta(OMC)_i}{(1+I)^i} \qquad (1G\text{-}6)$$

where

CPWC is the cumulative present worth of the net change in operating and maintenance costs over the life of the plant ($)

$\Delta(OMC)_i$ is the increment in operating and maintenance cost for the ith year ($)

For the case in which the incremental expenditures for O&M are the same each year (in constant dollars), the cumulative present worth at the beginning of the first year of plant operation is

$$CPWC_{O\&M} = \frac{C_1}{I-e}\left[\left(\frac{1+I}{1+e}\right)^N - 1\right] \qquad (1G\text{-}7)$$

where

C_1 is the increment in operating and maintenance cost for the first year of operation ($/yr)

Considering changes in operating and maintenance cost, resulting from a plant design modification improvement, the reduction in capital investment which can be justified ("overnight construction") is

$$CCE_{O\&M} = \frac{CRF}{FCR}\left(CPWC_{O\&M}\right) \qquad (1G\text{-}8)$$

It may also be desired to express increments of the operating cost factors (fuel and non-fuel O&M) in terms of the levelized cost of electricity increment. This can be determined from the cumulative present worth of a series of expenditures by

$$\Delta COE = \frac{CPW\ (CRF)}{8.76\ P\ (CF)} \qquad (1G\text{-}9)$$

where

ΔCOE is the increment in levelized cost of electricity associated with a series of future incremental expenditures (mills/kW-hr)

CPW is the cumulative present worth of such a series of future incremental payments ($)

The levelized cost of electricity increment associated with a capital expenditure increment at the beginning of the plant's first year of operation is

$$\Delta COE = \frac{FCR(CE)}{8.76\ (P)(CF)} \qquad (1G\text{-}10)$$

where

CE is a capital expenditure increment at the beginning of the first year of plant operation ($)

2. MHD POWER PLANT HIGH TEMPERATURE AIR HEATER (HTAH) SYSTEM ENGINEERING DESIGN SURVEY AND COST ESTIMATES

WORK DEFINITION AND SCOPE

The objective of this investigation is to provide engineering data and cost estimates for four indirectly-fired high temperature air heater (HTAH) system designs based upon specified HTAH system conceptual designs. The specified designs are: (A) an oil-fired 1756° K (2700° F) air preheat temperature HTAH system, (B) an oil-fired 1922° K (3000° F) air preheat temperature HTAH system, (C) a low Btu gas-fired 1922° K (3000° F) air preheat temperature HTAH system with atmospheric combustion and (D) a low Btu gas-fired 1922° K (3000° F) air preheat temperature HTAH system with pressurized combustion. A rationale for scale up is to be developed and cost estimates are to be prepared for HTAH systems for each design for system thermal capacities of 100, 250, 500 and 1000 MW_t.

SUMMARY

Cost estimates were developed in this investigation for four indirectly-fired high temperature air heater (HTAH) concepts specified by NASA. The four concepts are based upon conceptual designs which were developed for the U.S. Department of Energy MHD Engineering Test Facility (ETF) program as reported in references 2-1 and 2-2. The four conceptual designs are referred to in this investigation as "ETF reference designs." The specifications which were provided by NASA included fuel type, inlet and exit flow conditions of MHD air, combustion air and recirculation flue gas and system thermal capacity, defined as the rate of thermal energy transferred to the MHD air by the HTAH system. The system thermal capacities specified for each of the HTAH system concepts are 100, 250, 500 and 1000 MW_t.

The flow conditions specified by NASA for each concept are slightly different from the flow conditions specified for the

ETF reference designs and the system thermal capacities specified by NASA are larger than those of the ETF reference designs. It was therefore necessary to develop a rationale for modifying the dimensions of the ETF reference designs to account for the differences in flow conditions as well as for scaling up to the specified system thermal capacities. The phases of this investigation included the following items:

1. Development of rationale for adjustment of dimensions for variations in flow condition specifications
2. Development of rationale for scaling dimensions and selection of number of vessels
3. Determination of modified system dimensions in accordance with items 1 and 2 for each HTAH system concept and for each system thermal capacity
4. Determination of quantities of each type of material comprising the HTAH system excluding auxiliary systems and accessories
5. Obtaining estimated prices from materials manufacturers to determine materials costs on a dollars per unit weight or volume basis
6. Estimating the costs of auxiliary systems and accessories by extrapolation of cost data on ETF reference designs from references 2-1 and 2-2
7. Determining HTAH system total estimated costs on the basis of items 4, 5 and 6 for each HTAH system concept for each specified HTAH system thermal capacity

A computer program was developed for determining the HTAH system costs (excluding auxiliary systems and accessories) because of the large amount of data handling required. The computer program carries out step 4, multiplies the material quantities by the unit costs and performs the summations to determine total costs.

Scaling the high temperature air heater systems to the specified system thermal capacities was achieved by increasing

the numbers of vessels as well as by increasing the sizes of the vessels and ducting. Developing the rationale for scaling and determining the optimum number of vessels involved consideration of several factors in addition to minimizing the capital cost of the HTAH system. These factors include changes in system efficiency due to changes in relative heat loss upon scale-up, system reliability achieved by incorporating additional vessels, fluctuations in delivered air temperature, matrix material and valve lifetimes, as well as practical limitations on vessel and valve sizes. A quantitative analysis incorporating all of these additional factors was not performed in this investigation because much of the analysis would be beyond the scope of this investigation and much of the required data is not available.

The cost estimates developed in this investigation do not necessarily represent the costs of optimized HTAH systems because the detailed matrix design procedures employed for optimizing the ETF reference designs were not available for use in this investigation. The rationale developed in this investigation for scale-up ensures that the local conditions of temperature, heat transfer and stress are nearly the same for the scaled-up systems as for the corresponding locations within the matrices of the ETF reference designs. However, if the original detailed design procedures were to be employed for each HTAH system concept at each of the specified system thermal capacities, the amount of matrix material required is likely to be less than that determined by means of the procedures employed in this investigation and the resulting HTAH system costs would be less than the costs reported herein. The cost estimates given in this report may therefore be considered to represent the upper limit on HTAH system costs within the accuracy of the cost estimates.

Auxiliary systems and accessories include valves, burners, instruments and controls, equipment for pressurization/depressurization, fuel supply systems, a turbocompressor system for

one of the concepts and a HTAH building including foundations and the system support structure. A comprehensive investigation of auxiliary system and accessory cost estimates is beyond the scope of this investigation. Therefore the cost estimates for auxiliary systems and accessories are determined to a large extent by extrapolation of cost data presented in references 2-1 and 2-2. Cost estimates on coal gasification plants were obtained from an industrial firm which possesses licensing rights in the U.S. to the type of gasification system specified in reference 2-2. An investigation to determine whether other types of coal gasifiers would be more economical in the sizes specified by NASA was not conducted. Estimates for the foundations, support structures or buildings for the HTAH systems were not developed in this investigation, although their costs may be substantial.

Figures 9, 10, 11 and 12 present the cost estimates developed in this investigation for each of the four HTAH system concepts. The data are shown in the form of bar charts, since a smooth curve connecting the points on the graph would not be realistic because of discrete rather than continuous increments in costs due to changes in numbers of vessels and to the selection of standard vessel and ducting steel wall thicknesses. As anticipated, the estimated costs of the HTAH systems per MW_t of system thermal capacity decrease as the system thermal capacity increases. It may be noted that the reduction in cost per MW_t is more substantial for Cases B and C than it is for Cases A and D. This occurs primarily because the overall system thermal capacity increases with an increase in the number of vessels to a much greater extent for Cases B and C than for Cases A and D.

In addition to the reduction in capital cost per MW_t as the system thermal capacity increases, the heat loss per MW_t generally decreases as the system thermal capacity increases. There is thus a potential credit for fuel savings which increases as the system thermal capacity increases. The potential credit was not determined in this investigation. However, equations are developed in the Appendixes of this report for conducting such an analysis.

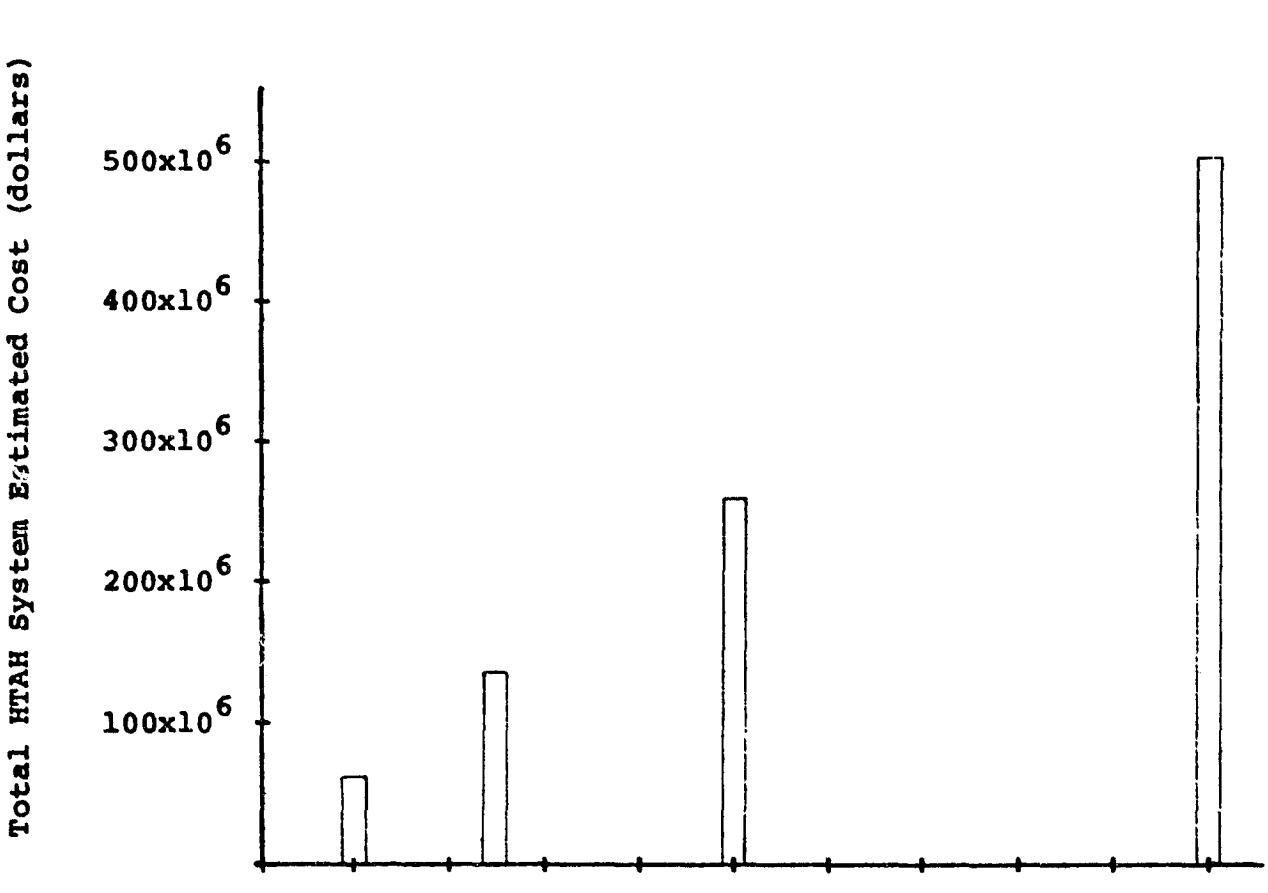

Figure 9. - Total estimated cost for HTAH system for Case A - oil-fired, 1756° K (2700° F) air preheat.

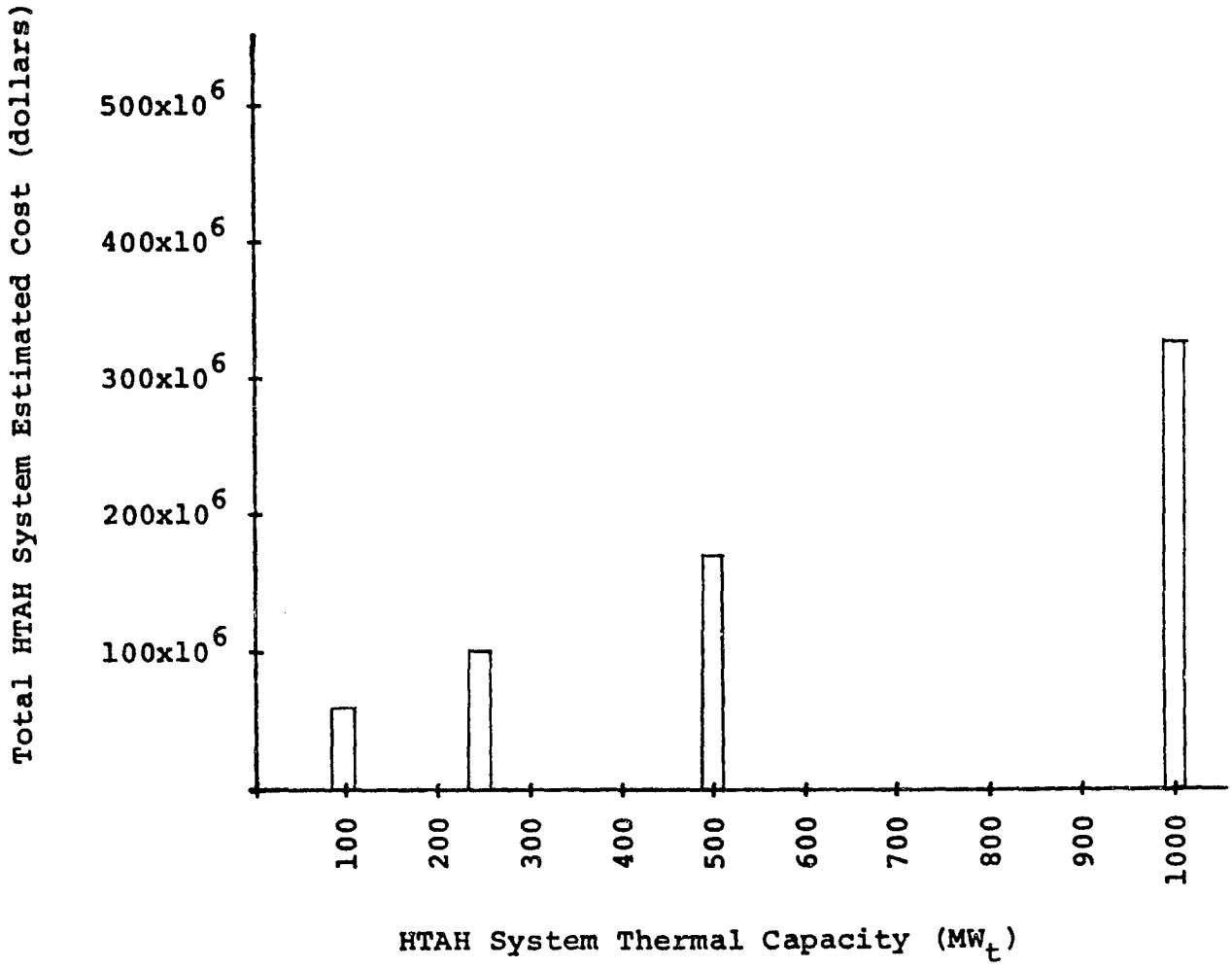

Figure 10. - Total estimated cost for HTAH system for Case B - oil-fired, 1922° K (3000° F) air preheat.

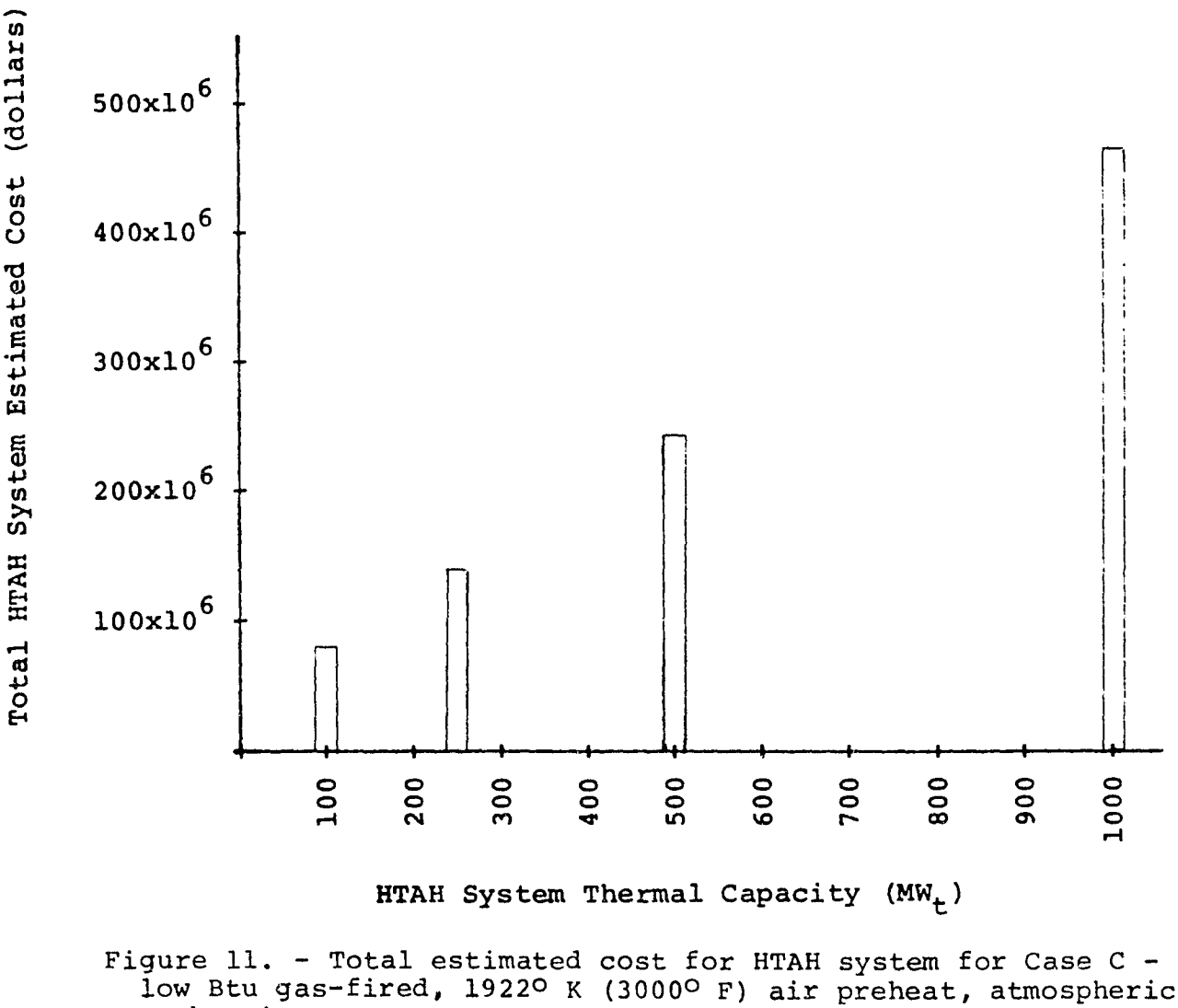

Figure 11. - Total estimated cost for HTAH system for Case C - low Btu gas-fired, 1922° K (3000° F) air preheat, atmospheric combustion.

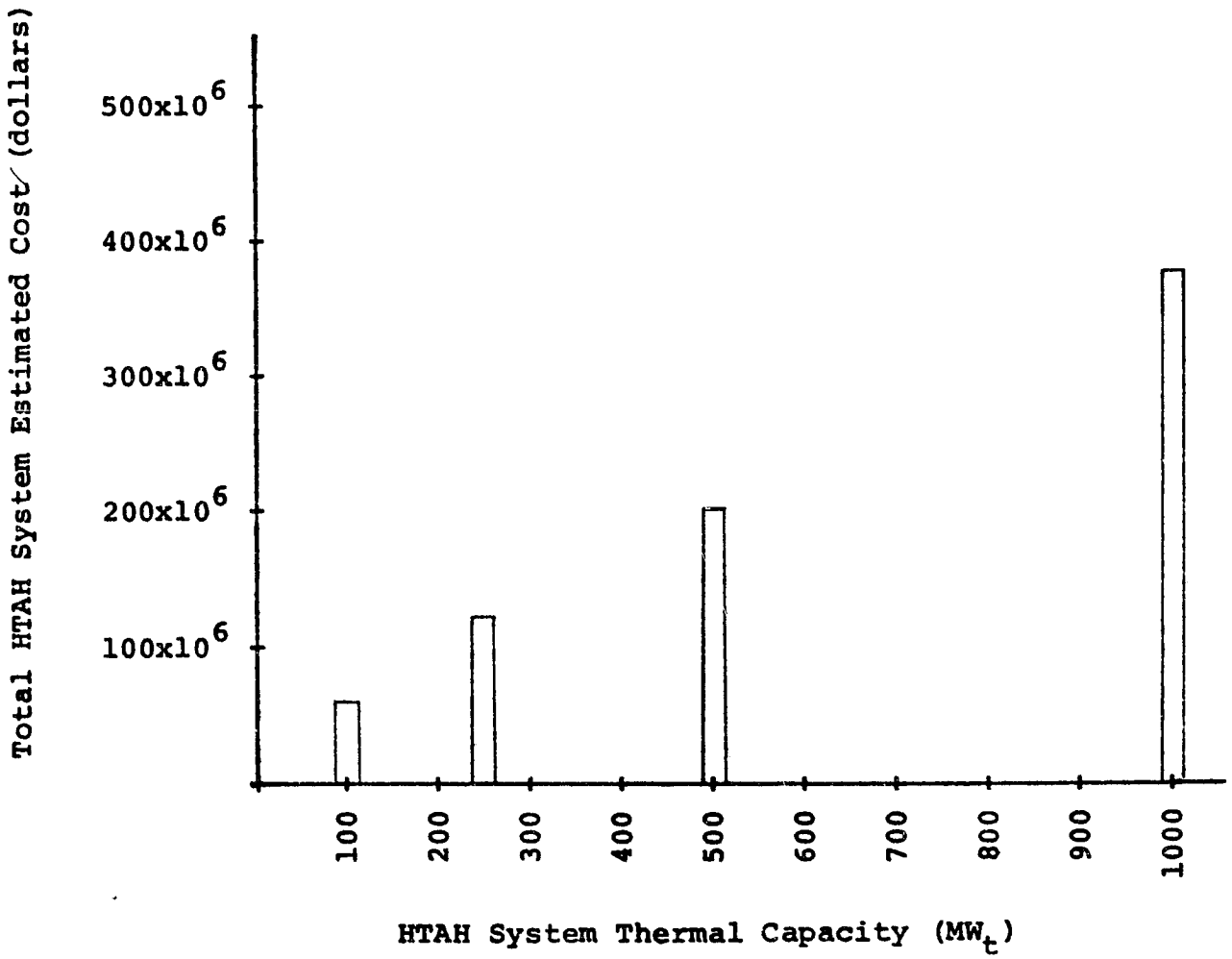

Figure 12. - Total estimated cost for HTAH system for Case D - low Btu gas-fired, 1922° K (3000° F) air preheat, pressurized combustion.

Tables or figures showing a direct comparison of the cost estimates for each of the four HTAH system concepts are not presented in this report because of the strong dependence of the cost estimates upon the assumptions made in references 2-1 and 2-2 for the ETF reference designs. Since there is no assurance that each of the previous investigators employed design bases and assumptions which are consistent with the design bases and assumptions employed by the other investigators, such a direct comparison would not be valid without detailed explanation of the differences in the underlying assumptions.

Several areas are recommended for further investigation to refine and supplement the results of the present investigation. These areas include investigations of

- Differences in designs and underlying assumptions for the various ETF reference designs
- Cost estimates of auxiliary systems and accessories in more detail than in the present investigation
- Alternate types of coal gasification systems
- Heat losses and potential fuel or capital cost savings resulting from reducing the percentage heat loss or reducing insulation material thicknesses on scale-up
- Relationship between number of vessels and system reliability
- Maintenance costs associated with periodic replacement of refractory materials and refurbishment and replacement of valves
- Fluctuations in pressure, temperature and flow rate of preheated MHD air

Such investigations should be conducted for one specified system thermal capacity and the HTAH system matrix configurations for that system thermal capacity should be optimized by employing the detailed heat transfer and stress analysis techniques which were utilized to optimize the matrix configurations for the ETF reference designs.

INTRODUCTION

In an MHD power plant, it is necessary to preheat the MHD combustion air to a high temperature or to enrich it with oxygen to attain the level of combustion flame temperature which is necessary for achieving high electrical conductivity of the seeded products of combustion. Without oxygen enrichment, the air must be preheated to temperatures in the 1644° to 1922° K (2500° to 3000° F) range. These temperatures can be achieved by means of the refractory regenerative type of heater which is used as a blast furnace stove in the steel-making industry. There are two ways in which such preheaters can be used in an MHD power plant. One way is to use the exhaust gas from the MHD generator as a source of heat. Such a preheater is referred to as a directly-fired high temperature air heater (HTAH) system and is an integral part of the steam bottoming plant. The other way is to provide the heat by the combustion of a separate fuel specifically for this purpose. Such a preheater is referred to as an indirectly-fired high temperature air heater (HTAH) system. This report addresses only the indirectly-fired HTAH systems.

Several conceptual designs for indirectly-fired HTAH systems were developed in the MHD Engineering Test Facility (ETF) studies conducted by General Electric Company (ref. 2-1) and Avco Everett Research Laboratory (ref. 2-2) under contract to the Department of Energy. Two conceptual designs were developed under the General Electric Company contract. One was an oil-fired HTAH system prepared (under subcontract to GE) by Arthur G. McKee Co. The other was an oil-fired HTAH system prepared by General Electric Company. A conceptual design of a dual-fuel (oil or low-Btu gas) HTAH system was prepared under the Avco contract. The Avco study also included an investigation of a low-Btu gasifier to provide a coal-derived fuel for the HTAH system.

The objective of this investigation is to develop a method and rationale for scaling indirectly-fired HTAH system designs to larger sizes and obtain cost estimates for several sizes of each of four indirectly-fired HTAH system designs based upon the conceptual designs prepared in the MHD ETF studies. The sizes of the HTAH systems in the MHD ETF studies ranged from 63.3 to 93.8 MW_t, defined in terms of the steady-state average rate of thermal energy transfer to the air between the inlet and exit of the HTAH system. The sizes of the HTAH systems for which cost estimates are developed in this investigation are 100, 250, 500 and 1000 MW_t. Cost estimates are developed for these four sizes for each configuration, resulting in 16 separate sub-cases.

DESCRIPTION OF A TYPICAL SEPARATELY-FIRED HTAH SYSTEM

Figure 13 is a schematic diagram illustrating the basic elements of an indirectly-fired HTAH system. The air which is to be preheated (referred to as MHD combustor air) enters the HTAH system at temperature T_{a1} and pressure p_{a1}; its mass flow rate is m_A. It is preheated to temperature T_{a2} and its pressure is reduced to p_{a2} at the outlet of the HTAH system before entering the MHD combustor. Fuel enters the HTAH combustor system at temperature T_f and pressure p_f; its mass flow rate is m_f. Combustion air for the fuel enters the HTAH combustion system at temperature T_c and pressure p_c; its mass flow rate is m_c. The products of combustion leave the HTAH system at temperature T_p and pressure p_p; its mass flow rate is m_p. A fraction of the products of combustion is reheated to temperature T_r and is recirculated back to the HTAH combustion system at pressure p_r; its mass flow rate is m_r.

A regenerative HTAH system consists of several vessels containing a large number of refractory bricks which are alternately heated by a hot reheat gas and cooled by the MHD combustor air which is being preheated. At any given instant

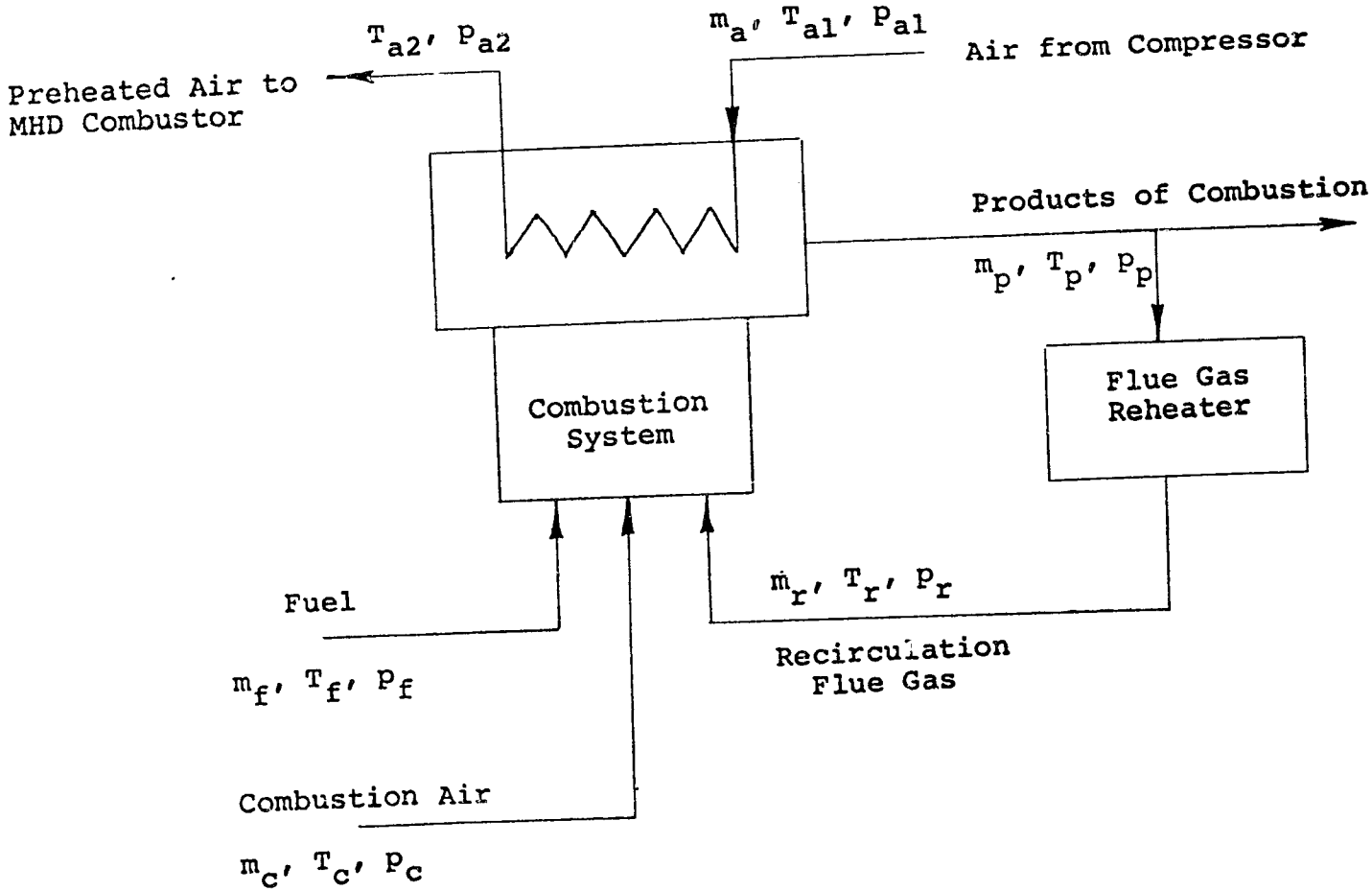

Figure 13.- Basic schematic diagram of indirectly-fired high temperature air heater (HTAH) system.

during operation of the plant, one or more vessels are in the "air blast mode", i.e., the MHD combustor air is passing through the brick matrices within these vessels transferring heat from the bricks to the air. At the same time, the remaining vessels are either in the "reheat mode" or "switching mode", i.e., the bricks are being heated by the reheat gas, or the vessels are being switched from cold blast to reheat, or vice versa. Figure 14 is a diagram showing two vessels, one in the hot blast mode and the other in the reheat mode. Each vessel is periodically switched from one mode to the other to provide a continuous uniform supply of high temperature air to the MHD combustor.

The internal arrangement of the vessel shown in figure 14 is one of several possible configurations. For any configuration, each vessel consists of a steel shell, refractory insulation to protect the shell and reduce heat loss to the surroundings, a refractory-brick matrix and a matrix support structure. The ducting connected to the vessels are made of steel with internal or external insulation and expansion joints. The reheat burner systems may be integral with the heater vessel or may consist of one or more separate combustion chambers with one or more burners per chamber. The combustion chamber is a refractory-lined steel vessel. HTAH system auxiliaries include instruments and controls, vessel and ducting support structure, valves, a valve water-cooling system, fuel supply system and other auxiliaries dependent upon the type of HTAH system. Table VII is a list of the major components and subcomponents of a typical regenerative indirectly-fired HTAH system. More detailed breakdowns of each HTAH system case are presented in Appendices 2A, 2B, 2C and 2D.

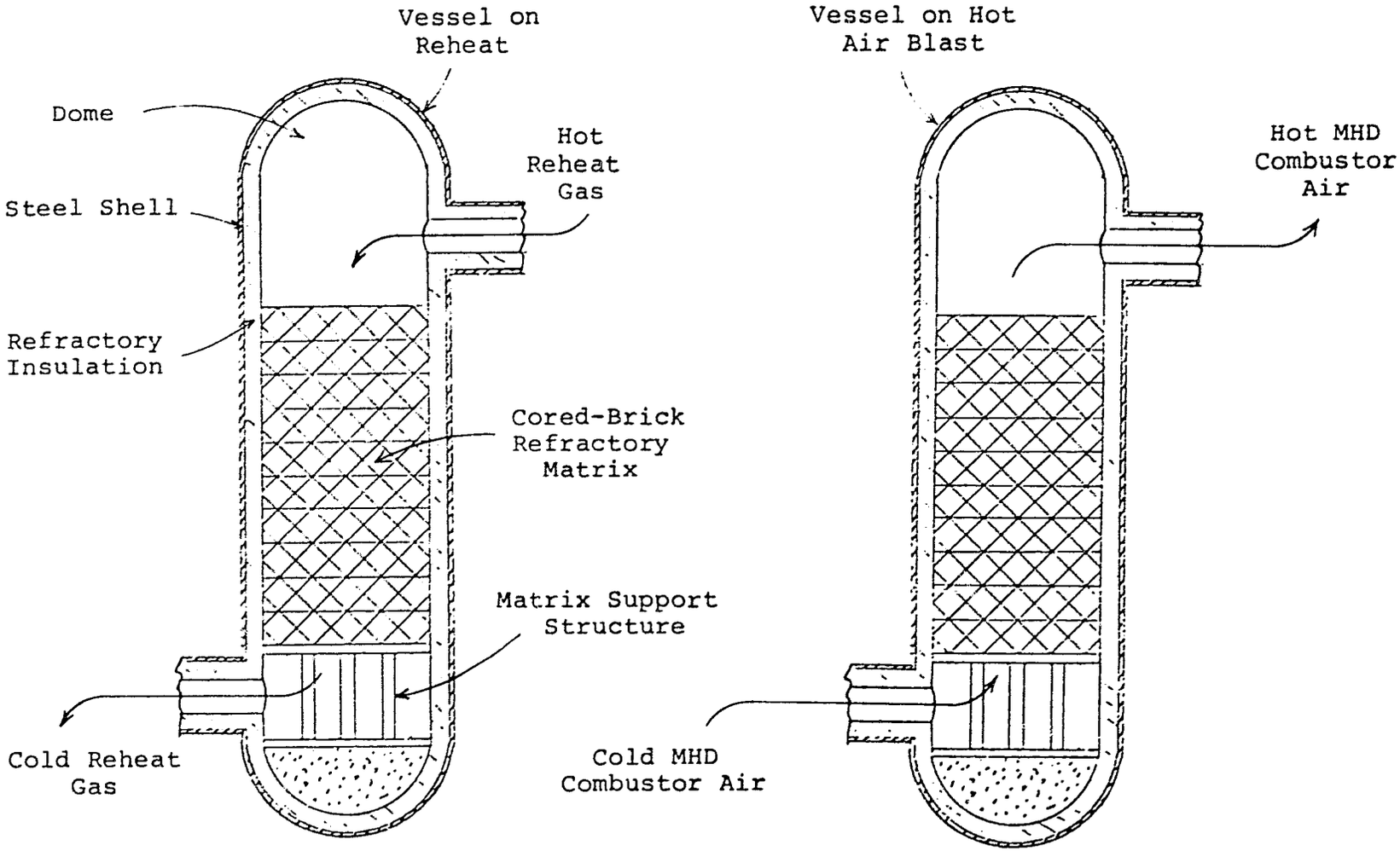

Figure 14. - Diagram of Regenerative HTAH System Showing Two Vessels in Different Phases of Operating Sequence.

TABLE VII. - MAJOR COMPONENTS AND SUBCOMPONENTS OF A REGENERATIVE INDIRECTLY-FIRED HTAH SYSTEM

Air Heater Vessel

- Matrix
- Insulation
- Steel Shell
- Matrix Support

Reheat Burner System

- Combustion Chamber Steel Shell
- Combustion Chamber Insulation

Ducting

- Steel
- Insulation
- Expansion Joints

Auxiliary Systems and Accessories

- Valves
- Burner(s)
- Instruments and Controls
- Vessel Support Structure
- Valve Water-Cooling System
- Fuel Supply System
- Other Auxiliaries Dependent Upon System Configuration and Definition

HTAH SYSTEM SPECIFICATIONS

Table VIII lists the design parameters specified by NASA for the four HTAH system cases considered in this investigation. The configuration for Case A is based upon the conceptual design of the oil-fired HTAH system prepared by Arthur G. McKee under subcontract to General Electric Co. for the DOE MHD ETF study (ref. 2-1). The configuration for Case B is based upon an adaptation of the conceptual design of the dual-fuel HTAH system prepared by AERL for the DOE MHD ETF study (ref. 2-2) to provide for using only oil as a fuel. The configuration for Case C is based upon an adaptation of Case B to provide for using a coal-derived low-Btu gas in place of oil as a fuel. The configuration for Case D is based upon an adaptation of the conceptual design of the oil-fired HTAH system prepared by General Electric Co. for the DOE MHD ETF study (ref. 2-1), modified to utilize a coal-derived low-Btu gas instead of oil as a fuel. Cases C and D are each considered for two types of coal: Illinois No. 6 and Montana Rosebud.

Table IX lists the parameters specified by NASA for the HTAH system for Case A and the parameters specified for the ETF reference HTAH system design upon which the Case A configuration is based. Both systems use oil as a fuel and preheat the air to 1756° K (2700° F). In addition to the differences in sizes (thermal capacity) between the NASA-specified systems and the ETF reference system, there are several differences in the flow conditions, as indicated in table IX. These include the inlet pressure and temperature of the air to be preheated and the temperature of the combustion air. The temperature of the recirculation flue gas is not included in the NASA specifications for Case A and there is no recirculation flue gas in the ETF reference design for this case. However, because of the change in the HTAH combustion air inlet temperature specified by NASA, it is necessary to employ flue gas recirculation as a means of controlling the flame temperature in the HTAH combustion system. It is therefore assumed, in this investigation, that the recirculation

TABLE VIII. - SPECIFIED DESIGN PARAMETERS FOR HTAH CASES

CASE	A	B	C	D
Design Basis	McKee (Oil-Fired)[1]	AVCO (Oil-Fired)[2]	AVCO (LBTU Gas-Fired)[2]	GE (LBTU Gas-Fired)[1]
Air Delivery Temperature, ^{o}K (^{o}F)	1756 (2700)	1922 (3000)	1922 (3000)	1922 (3000)
Inlet Air Temperature, ^{o}K (^{o}F)	533 (500)	533 (500)	533 (500)	533 (500)
Inlet Air Pressure, MPa (psia)	0.69 (100)	0.69 (100)	0.69 (100)	0.83 (120)
Combustion Air Temperature, ^{o}K (^{o}F)	811 $\pm$ 28 (1000 $\pm$ 50)	811 $\pm$ 28 (1000 $\pm$ 50)	811 $\pm$ 28 (1000 $\pm$ 50)	811 $\pm$ 28 (1000 $\pm$ 50)
Combustion Air Pressure, MPa (psia)	0.10 (14.7)	0.10 (14.7)	0.10 (14.7)	0.69 (100)
Recirculated Gas Temperature, ^{o}K (^{o}F)	N.A.	811 (1000)	811 (1000)	811 (1000)

1. Reference 2-1
2. Reference 2-2

TABLE IX. - NASA SPECIFICATIONS AND ETF

REFERENCE DESIGN SPECIFICATIONS

FOR HTAH SYSTEM FOR CASE A

Parameter	NASA Specification	ETF Reference Design Specifications*
Fuel Type	No. 2 Fuel Oil	No. 2 Fuel Oil
System Thermal Capacity, MW_t	100/250/500/1000	72.0
Air Delivery Temperature, ^{o} K(^{o} F)	1756 (2700)	1756 (2700)
Inlet Air Temperature, ^{o} K(^{o} F)	533 (500)	589 (600)
Inlet Air Pressure, MPa (psia)	0.69 (100)	0.81 (118)
Combustion Air Temperature, ^{o} K(^{o} F)	811 ± 28 (1000 ± 50)	ambient
Combustion Air Pressure, MPa (psia)	0.10 (14.7)	0.10 (14.7)
Recirculated Gas Temperature, ^{o} K(^{o} F)	not specified	not applicable

*Based upon MHD Engineering Test Facility separately-fired HTAH system conceptual design prepared by Arthur G. McKee Co. under subcontract to General Electric Co. (ref. 2-1)

flue gas for Case A is reheated to the temperature specified in Cases B, C and D for the recirculation flue gas, which is 811° K (1000° F).

Table X lists the parameters specified by NASA for the HTAH system for Case B and the parameters specified for the ETF reference HTAH system design upon which the Case B configuration is based. Both systems use oil as a fuel and preheat the air from an inlet temperature of 533° K (500° F) to an exit temperature of 1922° K (3000° F). In addition to the differences in sizes (thermal capacity) between the NASA-specified systems and the ETF reference system, there are several differences in the flow conditions as indicated in table X. These include the pressure of the air to be preheated, the temperature of the combustion gas and the temperature of the recirculation flue gas. The pressure of the combustion air is nominally one atmosphere in both instances and can be treated as being essentially the same.

Table XI lists the parameters specified by NASA for the HTAH system for Case C and the parameters specified for the ETF reference design upon which the Case C configuration is based. The conditions specified by NASA for Case C are the same as those specified for Case B except for the use of a coal-derived low-Btu gas as a fuel for the HTAH combustion system in Case C. The ETF reference design for Case C is the same as that for Case B.

Table XII lists the parameters specified by NASA for the HTAH system for Case D and the parameters specified for the ETF reference design upon which the configuration for Case D is based. In both instances, the air is preheated to 1922° K (3000° F). The changes in conditions between the NASA specifications and the ETF reference design specifications include the type of fuel, system sizes, air inlet temperature, air inlet pressure, combustion air temperature, combustion air pressure and the recirculation flue gas temperature.

TABLE X. - NASA SPECIFICATIONS AND ETF

REFERENCE DESIGN SPECIFICATIONS

FOR HTAH SYSTEM FOR CASE B

Parameter	NASA Specification	ETF Reference Design Specifications*
Fuel Type	No. 2 Fuel Oil	Dual Fuel (No. 2 Fuel Oil/Low-Btu Gas)
System Thermal Capacity, MW_t	100/250/500/1000	93.8
Air Delivery Temperature, ^{o} K(^{o} F)	1922 (3000)	1922 (3000)
Inlet Air Temperature, ^{o} K(^{o} F)	533 (500)	533 (500)
Inlet Air Pressure, MPa (psia)	0.69 (100)	0.61 (88.2)
Combustion Air Temperature, ^{o} K(^{o} F)	811 $\pm$ 28 (1000 $\pm$ 50)	967 (1100)
Combustion Air Pressure, MPa (psia)	0.10 (14.7)	0.12 (17.6)
Recirculated Gas Temperature, ^{o} K(^{o} F)	811 (1000)	867 (1100)

*Based upon MHD Engineering Test Facility separately-fired HTAH system conceptual design prepared by Avco-Everett Research Laboratory. (ref. 2-2)

TABLE XI. - NASA SPECIFICATIONS AND ETF

REFERENCE DESIGN SPECIFICATIONS

FOR HTAH SYSTEM FOR CASE C

Parameter	NASA Specification	ETF Reference Design Specifications*
Fuel Type	Coal-Derived Low Btu Gas	Dual Fuel (No. 2 Fuel Oil/Low Btu Gas)
System Thermal Capacity, MW_t	100/250/500/1000	93.8
Air Delivery Temperature, ^{o} K(^{o} F)	1922 (3000)	1922 (3000)
Inlet Air Temperature, ^{o} K(^{o} F)	533 (500)	533 (500)
Inlet Air Pressure, MPa (psia)	0.69 (100)	0.61 (88.2)
Combustion Air Temperature, ^{o} K(^{o} F)	811 ± 28 (1000 ± 50)	867 (1100)
Combustion Air Pressure, MPa (psia)	0.10 (14.7)	0.12 (17.6)
Recirculated Gas Temperature, ^{o} K(^{o} F)	811 (1000)	867 (1100)

*Based upon MHD Engineering Test Facility separately-fired HTAH system conceptual design prepared by Avco-Everett Research Laboratory. (ref. (2-2)

TABLE XII. - NASA SPECIFICATIONS AND ETF

REFERENCE DESIGN SPECIFICATIONS

FOR HTAH SYSTEM FOR CASE D

Parameter	NASA Specification	ETF Reference Design Specifications*
Fuel Type	Coal-Derived Low-Btu Gas	No. 2 Fuel Oil
System Thermal Capacity, MW_t	100/250/500/1000	63.3
Air Delivery Temperature, ^{o} K(^{o} F)	1922 (3000)	1922 (3000)
Inlet Air Temperature, ^{o} K(^{o} F)	533 (500)	583 (589)
Inlet Air Pressure, MPa (psia)	0.83 (120)	0.60 (87)
Combustion Air Temperature, ^{o} K(^{o} F)	811 ± 28 (1000 ± 50)	589 (600)
Combustion Air Pressure, MPa (psia)	0.69 (100)	0.62 (89)
Recirculated Gas Temperature, ^{o} K(^{o} F)	811 (1000)	589 (600)

*Based upon MHD Engineering Test Facility separately-fired HTAH system conceptual design prepared by General Electric Co. (ref. 2-1)

PROCEDURES FOR DESIGN MODIFICATION, SCALE-UP AND COST ESTIMATING

The methodology used to determine the cost estimates of the 100, 250, 500 and 1000 MW_t HTAH systems is illustrated in figures 15 and 16. The first step (as indicated in figure 15) is to modify the reference designs, as reported in the MHD ETF studies (refs. 2-1 and 2-2) to account for the differences in flow conditions between the NASA HTAH design specifications and the corresponding reference ETF HTAH design specifications. These differences are indicated in tables IX through XII. The design modifications in this step include changes (minor in most cases) in system dimensions and are described in detail in a subsequent section of this report.

The second step is to scale up the dimensions of the modified HTAH designs to correspond to increases in system thermal capacity from the original ETF HTAH system capacity to each of the four levels: 100, 250, 500 and 1000 MW_t. Because of the large number of variable physical parameters, there are several ways in which the systems can be scaled up. The selected procedures and discussions of several alternate procedures are presented in a subsequent section of this report.

The methodology for estimating the costs of the scaled-up HTAH system designs is indicated in figure 16. The total quantities (mass or volume) of each of the materials of construction are determined from the dimensions of the scaled-up system designs. Unit costs (dollars per kg or dollars per cubic meter) of each material are obtained from materials suppliers and equipment fabricators based upon the materials specifications defined for the reference ETF system designs reported in references 2-1 and 2-2. Installation costs are also estimated on a unit basis. The total HTAH system cost estimates are determined by multiplying the materials quantities by the unit costs and adding in the costs of any auxiliary components.

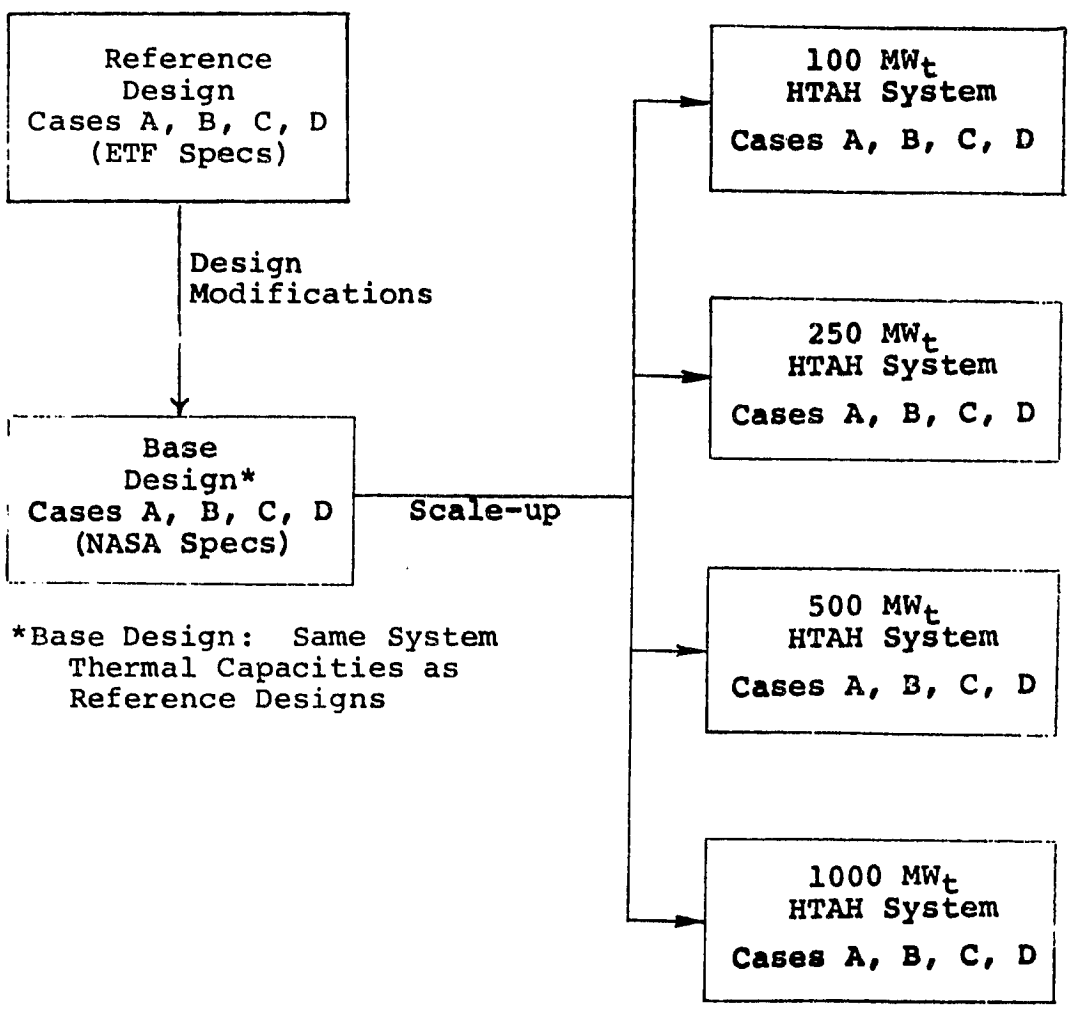

Figure 15. - Diagram Indicating Steps Required in Determining Designs of Scaled-up HTAH Systems.

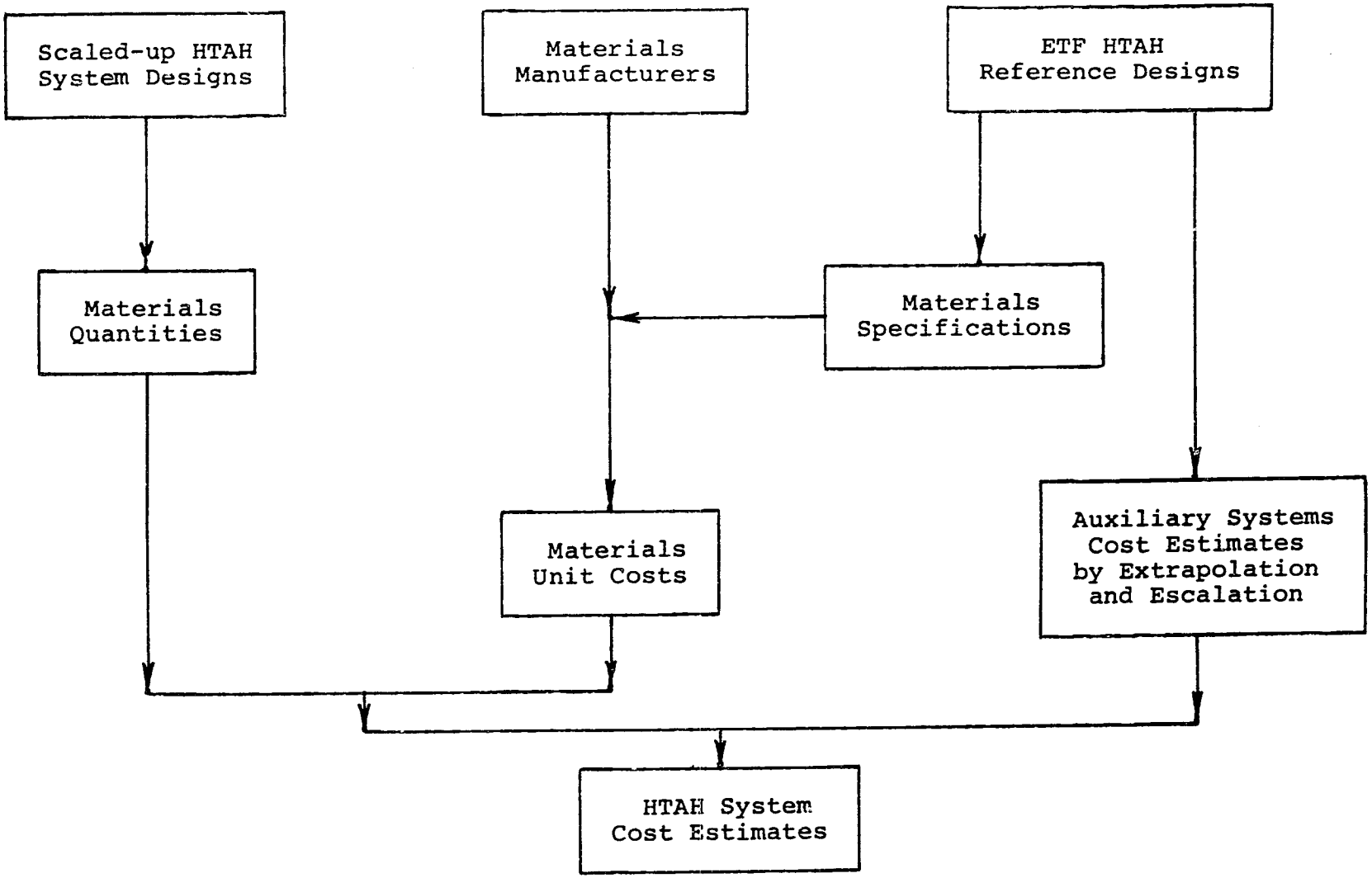

Figure 16. - Diagram indicating procedure for estimation costs of HTAH systems.

GUIDELINES FOR DESIGN ADJUSTMENTS AND SCALING

The MHD ETF reference designs reported in references 2-1 and 2-2 were developed by the application of the principles of heat transfer, fluid mechanics and stress analysis in conjunction with data on materials and fluid properties to attain approximately optimum configurations, dimensions and operating modes to achieve minimum HTAH system cost. The designs are also based to a considerable extent upon industrial experience in the use of steel vessels, refractories and large valves and burners. The ideal way to make design adjustments and to scale up the HTAH systems to meet the NASA specifications would be to re-design each system by employing the same design procedures which were originally used in the MHD ETF conceptual design studies. However, such a procedure is beyond the scope of this investigation and the analytical design tools, such as computer codes, were not available. Therefore, a procedure was developed for adjusting and scaling each of the designs in a simple, yet rational, and consistent manner. There is no assurance that the resulting adjusted and scaled-up designs are optimum designs. However, the procedures attempt to ensure that the design constraints, such as temperature and stress limits, and the heat transfer conditions within the refractory matrix in each case, are nearly the same as in the ETF reference designs.

Several general guidelines were employed in establishing the design-adjustment and scale-up procedure. These guidelines are

- Retain as many of the original ETF reference design features as practical
- Employ the same design codes, constraints and limits as used in the ETF HTAH conceptual design studies
- Retain the same local conditions of heat transfer and stress in the refractory matrix as in the ETF reference designs
- Retain the same local fluid flow conditions in ductwork as in the ETF reference designs

- Adjust the relative flow rates of fuel, combustion air and recirculation gas to retain fixed ratios of system thermal input to thermal energy delivered to the MHD combustor air

Table XIII is a list of the parameters which are considered in the design adjustment and scale-up procedure. The materials selected for the adjusted and scaled-up designs are the same as those in the ETF reference designs except in those cases where cost data on materials could not be obtained. Where necessary, an appropriate substitution was made.

The brick size, hole size and hole spacing of the refractory matrix are kept the same as in the ETF reference designs for all design conditions and system capacities. The overall length of the matrix is adjusted to allow for changes in the rise in specific enthalpy of the air passing through the matrix for those cases in which the MHD air inlet temperature specified by NASA differs from the MHD air inlet temperature specified for the ETF reference designs. The overall diameter of the matrix is adjusted to maintain a fixed ratio of mass flow rate to overall cross-sectional area of the matrix. As a result, the local conditions of heat transfer and stress within the matrix are approximately the same for the adjusted and scaled-up cases as in the ETF reference designs. The equations employed in determining the modified matrix dimensions are developed in Appendix 2E.

The outer dimensions of the air heater vessel are determined from the required dimensions of the matrix and the thicknesses of the layers of insulation between the matrix and the steel shell. Standard steel plate thicknesses are used for the steel shell. These thicknesses depend upon the internal pressure, the vessel diameter and material properties and are determined in accordance with ASME codes. The equations employed for determining the modified dimensions of the vessels are given in Appendix 2F.

TABLE XIII. - DESIGN PARAMETERS FOR ADJUSTMENTS AND SCALING OF HTAH SYSTEMS

Parameters Affecting HTAH System Cost

- Materials Selection
- Refractory Matrix Dimensions
  - Brick Size
  - Hole Size and Spacing
  - Overall Length
  - Overall Diameter
- Vessel and Combustion Chamber Dimensions
  - Length
  - Diameter
  - Shell Thickness
  - Insulation Thickness
- Number of Vessels
- Duct Dimensions
  - Length
  - Diameter
  - Shell Thickness
  - Insulation Thickness
- Equipment Selection
  - Valves
  - Burners

Parameters Affecting HTAH System Performance and Lifetime

- Switching Pattern, Sequencing and Timing
- Amplitude of Fluctuations
  - Delivered Air Flow Rate
  - Delivered Air Temperature
  - Delivered Air Pressure
- Pressure Drop Through System
- Heat Loss from System
- Relative Flow Rates
  - Air
  - Combustion Air
  - Fuel
  - Recirculation Gas

Specifications Subject to Modification

- Fuel Type
- System Thermal Capacity
- Inlet Air Temperature
- Inlet Air Pressure
- Combustion Air Temperature
- Recirculation Gas Temperature

The insulation layers in the ETF reference designs are constructed from standard sizes of refractory brick. Since the increments in dimensions from one standard size to the next are quite large in the refractory brick industry, the procedure for determining the thickness of the insulation layers for the adjusted and scaled-up systems is to employ the same thicknesses as in the ETF reference designs. This results in a change in the system heat loss relative to the system thermal capacity since the scale-up ratio in surface area is not generally the same as the scale-up ratio in system thermal capacity. The effect of the dimension changes on the heat loss is discussed in Appendix 2G.

An alternative approach would be to adjust the insulation layer thicknesses so that the heat loss is the same percentage of the system thermal capacity for the adjusted and scaled-up systems as for the ETF reference designs. This approach would lead to a reduction in insulation material required for the larger sized vessels. However, this alternative was rejected because the reduction in quantity would be offset by the increase in cost and increased risk of delivery delays due to the use of nonstandard brick sizes. The equations which would be used in such an approach are developed in Appendix 2H.

The dimensions of the combustion chambers are adjusted and scaled in accordance with the volumetric requirements of the combustion process. For the cases in which the fuel type and the burner configuration are unaltered from those in the original ETF designs, the combustion chamber cross-sectional areas are modified in proportion to volume flow rate of the products of combustion without changing the combustion chamber length. For cases in which there is a change in fuel type or burner configuration, the combustion chamber dimensions are modified in accordance with recommendations by manufacturers of combustion equipment. For very large combustion chambers, it was considered to be more feasible to use a cluster of several burners of a size which has been previously utilized in industry, than to design a

burner with capabilities beyond the present state of the art. The thickness of the steel shell of the combustion chamber is determined in the same manner as the thickness of the heater vessels. The thicknesses of the insulation layers are the same for the adjusted and scaled-up designs as for the ETF reference designs for the reasons cited previously in conjunction with the heater vessel insulation layers.

The internal diameters of each section of ducting are adjusted and scaled in such a manner that the average velocity of the air or gas flowing through them remain the same as the average velocities in the corresponding duct sections in the ETF reference designs. The scaling ratios of the duct internal diameters therefore depend upon the mass flow rates and fluid densities relative to those in the ETF reference designs. For vessel sizes which would require single ducts which are much larger than the maximum valve sizes, it is necessary to split the flow by using two or more ducts in parallel. The insulation layer thicknesses are the same as the thicknesses in the corresponding duct sections of the ETF reference designs. The wall thicknesses of the ducting steel are determined in accordance with ASME codes. The equations employed in determining the modified duct dimensions are developed in Appendix 2I.

Scaling the HTAH systems from the ETF reference designs to the 100 MW_t level is achieved by keeping the same number of vessels, but increasing the sizes of the vessels, ducting, etc. However, for some cases, as the systems are scaled up to higher thermal capacities, the sizes of various components reach limits imposed by considerations such as present industrial capabilities in fabrication, erection and transportation, so that it becomes necessary to increase the number of vessels and, correspondingly, the number of valves, burners, etc. Selection of the optimum number of vessels involves consideration of capital cost, system reliability and system performance. The procedures employed in determining the optimum number of vessels is given in Appendix

2J. Valves and burners are selected from commercially available equipment. Limitations on the sizes of valves presently available which meet the specifications for MHD HTAH systems were taken into consideration.

The operating modes, switching patterns and time intervals between switchovers are the same for the adjusted and scaled-up systems as for the ETF reference designs for each case, except when the number of vessels is changed in scaling up, as indicated in Appendix 2J. For cases in which the number of vessels is increased, the time intervals for the reheat mode remain the same, but the blowdown periods change and the phasing of the switchovers is changed to achieve more overlap between vessels on blowdown. This has the benefit of reducing the amplitude of the fluctuations in temperature of the air delivered to the MHD generator (or of easing the requirements for utilizing bypass air to achieve uniform temperature of the delivered air).

The pressure drop through the matrix changes only slightly as the systems are adjusted and scaled up because (a) the change in matrix length is small, (b) the mass flow per unit area through the holes in the matrix is constant and (c) the change in density of the fluids is small. The changes in the dimensions and flow conditions in the ductwork as the systems are adjusted and scaled up also lead to a slight change in the pressure drop (usually a decrease). The resulting overall system pressure drops are thus within the allowable pressure drop limits established for the ETF reference designs.

As indicated in tables IX through XII, the inlet temperatures of the combustion air and recirculation gas specified by NASA differ from those specified for the ETF reference designs. This implies that there is also a difference in the flow rates of fuel, combustion air and recirculation gas required to achieve the same thermal input to the HTAH system combustion chamber. For example, if the temperatures of the combustion air and recirculation gas are increased by preheaters, less fuel is

required to provide the same total amount of thermal energy to the HTAH combustion system. In order to maintain the same mass flow rate of combustion products (reheat gas) and the same fuel-to-combustion-air ratio, the mass flow rate of combustion air must decrease and the mass flow rate of recirculation gas must increase. The equations employed in determining the modified flow rates are developed in Appendix 2K.

The ratio of the HTAH system heat loss to the system thermal capacity decreases as the vessel size increases because, under the scale-up approach utilized in this study, the insulation layer thicknesses remain unchanged and the percentage increase in vessel surface area is less than the percentage increase in system thermal capacity. The reduction in heat loss results in a fuel savings and, consequently a re-adjustment in the mass flow rates of combustion air and recirculation gas as explained in the preceding paragraph. Further discussions of the potential fuel savings is presented in Appendix 2L.

HTAH SYSTEM COST ESTIMATES

Because of the large number of cases and the large amount of data for each case, a computer program was developed to determine the costs. Each step in the program is simple and straightforward. The main purpose of the program is to handle the large amount of data. Although the scaled up dimensions were determined with the aid of a computer, these calculations were performed individually and separately from the costing computer program. The costing program is limited to determining the direct materials and installation costs of the vessels and ducting. It does not determine the costs of the valves, burners and other auxiliary equipment. Further information on the computer program and a typical printout is included in Appendix 2M. A discussion of cost estimates of valves, burners and other auxiliary equipment is included in Appendix 2N.

Direct costs for materials include the purchase and delivery costs of the materials. Direct labor costs for installation include wages and fringe benefits. Indirect costs for the vessels and ducting are estimated on the basis of experience in the powerplant construction industry to be 20 percent of the direct materials cost plus 98 percent of the direct labor cost. Indirect costs include craft support labor, insurance on labor, non-craft support labor, small tools, consumables, equipment rentals and the contractors' overhead and profit.

Data are presented in this report on four distinct cases (A, B, C and D) and it may be tempting to make a comparison of the costs of these cases relative to each other. However, all of the results in this study are based upon the concepts developed and assumptions made by the DOE contractors in the ETF studies reported in references 2-1 and 2-2. A comparison of the different concepts would be valid only if the design assumptions made by the original contractors were equivalent and if the same degree of conservatism was employed in areas of uncertainty in the design procedures. Since there is no assurance that these conditions are met, no direct comparison of Cases A, B, C and D is presented in this report.

Case A - Oil-Fired 1756° K (2700° F) HTAH System

Materials prices. - Manufacturers of the refractory materials specified for the ETF reference design for Case A did not respond to Burns and Roe's request for prices. Therefore, costs of materials for which prices were available were used for each of the specified refractory materials based upon the costs of materials with similar property values and temperature limitations. The substitutions are indicated in Appendix 2A in parentheses alongside the originally specified materials. The prices of the refractory materials, which are based upon data obtained from manufacturers, are given in Appendix 2O.

Adjustments. - Because of the differences between the pressures and temperatures specified by NASA for Case A and those specified in the ETF reference design (see table IX), various dimensions were modified prior to scaling up the HTAH system. These adjustments included changes in matrix length, matrix diameter, ducting internal diameters (with corresponding changes in vessel and duct shell and insulation dimensions) and flow rates of fuel, combustion air and recirculation flue gas in accordance with Appendixes 2E, 2F, 2J and 2K.

The matrix length must increase because of the decrease in MHD air inlet temperature. This also results in a reduction in the reheat gas temperature at the exit of the vessel and reduction in the flow rates of air and reheat gas. In accordance with the equations of Appendix 2E the MHD air flow rate and the reheat gas flow rate decrease by 4 percent.

The combustion air inlet temperature specified by NASA is 811° K (1000° F) compared to ambient temperature specified for the ETF reference design. This leads to a reduction in fuel and combustion air flow rates by 12.4 percent each in accordance with the equations of Appendix 2K.

In the ETF reference design, there is no recirculation of the flue gas. However, to compensate for the reduction in fuel and combustion air flow rates, it is necessary to include flue

gas recirculation in Case A. Since no preheat temperature is specified, it is assumed that the recirculation flue gas for Case A is 811° K (1000° F), the same as that which is specified for Cases B, C and D.

The reduction in MHD air inlet temperature and the increase in combustion air inlet temperature lead to the following net adjustments in flow rates

fuel flow rate decreases by 16 percent

combustion air flow rate decreases by 16 percent

recirculation gas flow rate equals 15 percent of the adjusted combustion air flow rate

These adjustments are a first approximation because the equations of Appendix 2K do not account for oxygen present in the recirculation flue gas. In the ETF reference design for Case A, the combustion process takes place with 30 percent excess air so that the recirculation flue gas contains a substantial amount of oxygen. The use of revised equations which account for oxygen in the recirculation flue gas would have a very small effect on the overall HTAH system cost.

Scaling. - The number of vessels for each of the four system thermal capacities were selected on the basis of both economics and practical considerations. The economic factors were determined by means of the data given in table XXXIII of Appendix 2J and an estimate of the relationship between system cost and vessel size. On the basis of several preliminary runs on the cost-estimating computer program, it is estimated that the total system cost, C for vessels and ducting is related to the number of vessels, N and the matrix volume, V per vessel in accordance with the relation

$$C = C_o \frac{N}{N_o} \left(\frac{V}{V_o}\right)^{0.89} \qquad (2\text{-}1)$$

where C_o is the cost of the vessels and ducting for the 100 MW_t system, N_o is the number of vessels (four) for the 100 MW_t system and V_o is the matrix volume per vessel for the 100 MW_t

case. This relationship is utilized only as a part of the procedure for selecting the number of vessels and not for making cost estimates.

The relationship between the matrix volume, the number of vessels and the system thermal capacity can be determined from table XXXIII. An an example, consider scaling up from a four-vessel system with a thermal capacity of 100 MW_t to either a four-vessel or a seven-vessel system with a thermal capacity of 250 MW_t. For scaling up to a 250 MW_t system utilizing four vessels, the volume of matrix in each vessel must be 2.5 times the volume of the matrix in each vessel in the 100 MW_t system. From table XXXIII, it is seen that the thermal capacity of a seven-vessel system of a given vessel size is twice the capacity of a four-vessel system with the same vessel size. Therefore, the matrix volume per vessel of a seven-vessel system is one half the matrix volume per vessel of a four-vessel system of the same thermal capacity. Thus, in scaling up to 250 MW_t using seven vessels, the volume of matrix in each vessel must be 1.25 times the volume of matrix in each of the four vessels of the 100 MW_t system.

The total matrix volume for a 250 MW_t system utilizing four vessels is 2.5 times the total matrix volume of the 100 MW_t system, whereas the total matrix volume of a 250 MW_t utilizing seven vessels is only 7/4(1.25) = 2.1875 times the total matrix volume of the four-vessel 100 MW_t system. Table XIV summarizes these results for systems with various numbers of vessels for a 250 MW_t system. The first line indicates the number of vessels. The second line indicates the matrix volume per vessel relative to the matrix volume per vessel for the 100 MW_t system. The third line indicates the total system matrix volume relative to the total system matrix volume for the 100 MW_t system.

Approximate relative system costs can be estimated by applying equation (2-1) to the values in the third line of table XIV. This indicates, for example, that the cost of a

TABLE XIV. - PARAMETERS UTILIZED IN SELECTING NUMBER OF VESSELS FOR 250 MW_t HTAH SYSTEM - CASE A

Number of Vessels	4	6	7	9	10	11
Relative Matrix Volume Per Vessel	2.50	1.67	1.25	1.00	0.83	0.83
Relative Total Matrix Volume	2.50	2.50	2.19	2.25	2.08	2.29
Approximate Relative System Capital Cost	2.26	2.36	2.13	2.25	2.13	2.34
Vessel Outside Diameter m (ft)	12.0 (39.4)	10.0 (32.9)	8.4 (27.7)	8.0 (26.3)	7.4 (24.2)	7.4 (24.2)
Approximate Relative Vessel Heat Loss	1.50	1.88	1.84	2.25	2.30	2.53
Relative Average Air Flow Rate Through Matrix	1.00	1.00	1.33	1.25	1.50	1.20

four-vessel 250 MW_t system is approximately 2.26 times the cost of a four-vessel 100 MW_t system. The fourth line in table XIV indicates the results of such estimates for systems with various numbers of vessels.

According to the data in line four of table XIV, the optimum number of vessels for the 250 MW_t system appears to be 10, since this number of vessels results in the lowest approximate relative cost. However, several other factors must be considered before selecting the number of vessels. These factors include reliability, heat loss to the surroundings, fluctuations in temperature of delivered air, matrix material and valve lifetime, practical limitations on vessel and valve sizes and costs of auxiliary equipment such as instruments and controls. The major disadvantage of the ten-vessel system is its limited reliability. As indicated in table XXXIII, there is only one more vessel than the minimum required. Although there is no firm basis for establishing reliability, it is the opinion of the investigators that one redundant vessel out of a total of ten vessels is not sufficient for the level of system reliability required in a power generating station. It is assumed herein that two redundant vessels are required for systems utilizing 10 to 20 vessels and that three redundant vessels are required for systems utilizing more than 20 vessels. The numbers of vessels in excess of the minimum are indicated in table XXXIII for each option. This would make a seven vessel system the optimum from the standpoint of minimum capital investment.

Another factor which must be considered is system heat loss. Equations are derived in Appendixes 2G and 2L for estimating the effects of scaling up the dimensions on the system heat loss and fuel consumption. Applying these equations to determine the net economic impact of changes in heat loss is beyond the scope of this investigation. However, the equations reveal that the ratio of heat loss to system thermal capacity decreases as the vessel size increases (for a given number of vessels) and leads to a reduction in fuel cost per unit of system thermal capacity.

A very approximate quantitative indication of the relative magnitudes of heat loss for the various options can be obtained by assuming that the heat loss is proportional to the total surface area of the vessels which is approximately proportional to the product of the number of vessels and the outside diameter of each vessel. The vessel outside diameter is the fifth line of table XIV and the approximate relative heat loss is the sixth line. Thus, in comparing a 250 MW_t system with four, six or seven vessels, table XIV indicates that a seven-vessel system would cost the least, but a four-vessel system would result in the lowest heat loss and, hence, the lowest fuel consumption requirement. Whether the fuel savings would offset the higher capital cost is not determined.

As the number of vessels is increased, the amplitude of the fluctuations in the temperature of the MHD air at the exit of the HTAH system is decreased because of the mixing of air coming from a larger number of vessels. This represents an increase in the system efficiency since less cold by-pass air is required for smoothing the temperature fluctuations.

The designs of the matrices for Cases A, B and C were developed by the original ETF contractors on the basis of the most severe operating conditions. These conditions occur when the HTAH systems are operating in the emergency mode with all redundant vessels out of operation. However, the lifetime of the matrices is dependent to a large extent on the conditions of operation in the normal mode, when all of the vessels are being utilized, since this will be the predominant mode. The seventh line of table XIV indicates the relative average air flow rate through the vessels during blowdown. The precise effect of average flow rate on matrix material lifetime cannot be predicted. However, the general statement can be made that the lower the relative average flow rate, the longer the probable matrix lifetime. Thus, the data in table XIV indicate that the four-vessel or the six-vessel systems provide the longest probable lifetimes of the matrix material. The lifetimes of the

valves are also greater for a lower average flow rate because they operate less frequently.

The final step in determining the number of vessels is to ascertain whether the practical limits on vessel and valve size have been exceeded. As noted in reference 2-2, the practice in the blast furnace stove industry is to limit the vessel diameter to no more than approximately 10.7 meters (35 feet). This rules out the use of four vessels for the 250 MW_t case since this would require a vessel diameter of 12.0 meters (39.4 feet), whereas the use of six vessels would require a vessel diameter of 10.0 meters (32.9 feet).

The practical limit on valve sizes is set by the fact that the upper limit on the internal diameter of water-cooled gate valves is considered to be 168 cm (66 in.). In cases in which the internal diameters of piping requiring water-cooled gate valves are only slightly greater than 168 cm (66 in.), it is assumed that the duct size can be reduced to a 168 cm (66 in.) inside diameter without seriously affecting the system pressure drop. For cases in which the piping diameters require water-cooled gate valves substantially larger than 168 cm (66 in.), the piping is considered to be subdivided into two or more parallel pipes with internal diameters equal to or less than 168 cm (66 in.). In the process of selecting the number of vessels in any given system thermal capacity level, preference was given to limiting valve sizes without resorting to doubling up any pipe sections where it was considered to be impractical to do so.

In summary, six vessels are selected for the 250 MW_t system with the aid of data in table XIV on the basis of a compromise between minimum capital cost, maximum reliability, practical limitations, maximum matrix and valve lifetime, minimum heat loss and minimum temperature fluctuation. The number of vessels for the 500 and 1000 MW_t systems are selected with the aid of data in tables XV and XVI. The selected numbers of vessels for the 100, 250, 500 and 1000 MW_t systems are 4, 6, 11 and 21, respectively. The relative volumes of the refractory matrix for the

C-2

TABLE XV. - PARAMETERS UTILIZED IN SELECTING NUMBER OF VESSELS FOR 500 MW_t HTAH SYSTEM - CASE A

Number of Vessels	7	9	11	13	14
Relative Matrix Volume Per Vessel	2.50	2.00	1.67	1.43	1.25
Relative Total Matrix Volume	4.38	4.50	4.58	4.64	4.38
Approximate Relative System Capital Cost	3.96	4.17	4.33	4.46	4.27
Vessel Outside Diameter m (ft)	12.0 (39.4)	10.9 (35.7)	10.0 (32.9)	9.4 (30.7)	8.4 (27.7)
Approximate Relative Vessel Heat Loss	2.62	3.05	3.44	3.79	3.69
Relative Average Air Flow Rate Through Matrix	1.33	1.25	1.20	1.17	1.33

TABLE XVI. - PARAMETERS UTILIZED IN SELECTING NUMBER OF VESSELS FOR 1000 MW_t HTAH SYSTEM - CASE A

Number of Vessels	21	27
Relative Matrix Volume Per Vessel	1.67	1.25
Relative Total Matrix Volume	8.75	8.44
Approximate Relative System Capital Cost	8.29	8.23
Vessel Outside Diameter m (ft)	10.0 (32.9)	8.4 (27.7)
Approximate Relative Vessel Heat Loss	6.57	7.11
Relative Average Air Flow Rate Through Matrix	1.33	1.45

100, 250, 500 and 1000 MW_t systems are 1.00, 1.67, 1.67 and 1.67, respectively. The selected numbers of combustion chambers are 1, 2, 4 and 8, respectively for the 100, 250, 500 and 1000 MW_t systems.

Estimated costs. - The estimated direct costs for vessels and ducting are determined by means of the cost-estimating computer program. A summary of the breakdown of these direct cost estimates for Case A is presented in table XVII for system thermal capacities of 100, 250, 500 and 1000 MW_t. Table XVIII summarizes the cost estimates for auxiliary equipment (including direct and indirect costs) based upon the data and procedures presented in Appendix 2N. Table XIX is a summary of the total HTAH system cost estimates for Case A, including direct costs, indirect costs and cost estimates for auxiliary equipment.

As indicated in table XIX, the HTAH system cost per unit system thermal capacity decreases as the system thermal capacity increases. This is due to an increase in the number of vessels and to an increase in the sizes of the vessels. Increases in duct lengths as the systems are scaled up are responsible for diminishing the benefits from economy of scale. Decreases in fuel consumption per unit system thermal capacity which occur upon scale-up are not determined in this investigation.

Case B - Oil-Fired 1922° K (3000° F) HTAH System

Materials prices. - The materials specified for Case B are indicated in Appendix 2B. The prices of materials, which are based upon data obtained from manufacturers, are given in Appendix 2O.

Adjustments. - Because of the differences between the pressures and temperatures specified by NASA for Case B and those specified in the ETF reference design (see table X), various dimensions have been modified prior to scaling up the HTAH system. These adjustments include changes in matrix diameter, ducting

TABLE XVII. - BREAKDOWN OF DIRECT COSTS (THOUSANDS OF DOLLARS) OF VESSELS AND DUCTING FOR TOTAL HTAH SYSTEM FOR CASE A

Component		System Thermal Capacity: 100 MWt (4 Vessels)	250 MWt (6 Vessels)	500 MWt (11 Vessels)	1000 MWt (21 Vessels)
Total System					
Matrix	Materials	7,808	19,518	35,783	68,313
	Installation	4,660	11,658	21,374	40,804
Matrix Support Structure	Materials	1,132	2,832	5,192	9,912
	Installation	880	2,202	4,037	7,707
Vessel Shell	Materials	2,448	6,030	11,055	21,105
	Installation	3,672	9,048	16,588	31,668
Vessel Insulation	Materials	7,772	18,414	33,759	64,449
	Installation	3,672	8,538	15,653	29,883
Combustion Chamber Shell	Materials	224	529	1,059	2,117
	Installation	321	761	1,522	3,044
Combustion Chamber Insul.	Materials	456	1,005	2,011	4,021
	Installation	332	730	1,461	2,923
Ducting Steel	Materials	446	901	2,889	5,640
	Installation	493	1,008	3,390	6,627
Ducting Insulation	Materials	807	1,510	5,057	9,868
	Installation	589	1,101	3,834	7,489
Total Cost*	Materials	21,091	50,739	96,804	185,424
	Installation	14,623	35,041	67,847	130,122

*Total costs do not necessarily correspond to column totals due to round-off.

TABLE XVIII. - ESTIMATED COSTS (THOUSANDS OF DOLLARS) OF AUXILIARY SYSTEMS AND ACCESSORIES (INCLUDING DIRECT AND INDIRECT COSTS) - CASE A

Item \ System Thermal Capacity	100 MWt (4 Vessels)	250 MWt (6 Vessels)	500 MWt (11 Vessels)	1000 MWt (21 Vessels)
Valves	2,260	4,610	8,440	16,120
Burners	170	410	810	1,630
Instruments and Controls	420	640	1,180	2,260
Fuel Supply System	500	870	1,310	1,990
Turbocompressor System	Not Applicable	Not Applicable	Not Applicable	Not Applicable
HTAH Building	Not Determined	Not Determined	Not Determined	Not Determined
Total Estimated Cost	3,350	6,530	11,740	22,000

TABLE XIX. - SUMMARY OF HTAH SYSTEM COSTS (THOUSANDS OF DOLLARS) FOR CASE A

Item \ System Thermal Capacity	100 MWt (4 Vessels)	250 MWt (6 Vessels)	500 MWt (11 Vessels)	1000 MWt (21 Vessels)
Vessels and Ducting - Materials	21,090	50,740	96,800	185,420
Vessels and Ducting - Direct Labor	14,620	35,040	67,850	130,120
Indirect Costs (Vessels and Ducting)	18,550	44,490	85,850	164,600
Auxiliary Systems and Accessories	3,350	6,530	11,740	22,000
Total HTAH System	57,610	136,800	262,240	502,140
Total HTAH System Cost per Unit System Thermal Capacity ($/kW)	576	547	524	502

internal diameters (with corresponding changes in vessel and duct shell and insulation dimensions) and flow rates of fuel, combustion air and recirculation flue gas in accordance with Appendixes 2E, 2F, 2I and 2K.

The ETF reference design applies to a dual-fuel system which provides the option to utilize either No. 2 fuel oil or low Btu gas. The combustion chambers are designed to handle combustion of either type of fuel and are larger than would be necessary for Case B which utilizes only No. 2 fuel oil. Therefore the height of the combustion chamber is reduced and the piping required for the low Btu gas are eliminated from the ETF reference design.

The combustion air and recirculation flue gas inlet temperatures specified by NASA are 811° K (1000° F) compared to 867° K (1100° F) specified for the ETF reference design. This leads to an increase in fuel and combustion air flow rates by 3.0 percent each in accordance with the equations shown in Appendix 2K. To compensate for the reduction in fuel and combustion air flow rates, it is necessary to increase the flow rate of the flue gas recirculation by 9.0 percent.

Scaling. - The methodology for selecting the number of vessels for each system thermal capacity for Case B is the same as the methodology used for Case A. Equation (2-1) and tables XXXIV and XXXV can be utilized to develop data for Case B similar to the data in tables XIV, XV and XVI for Case A. The resulting data for Case B is presented in tables XX, XXI and XXII. The number of vessels selected for Case B for the 100, 250, 500 and 1000 MW_t systems are 4, 6, 8 and 15, respectively. There is one combustion chamber for each vessel. The relative volumes of the refractory matrix and combustion chambers for the 100, 250, 500 and 1000 MW_t systems are 1.00, 1.25, 1.67 and 1.67, respectively.

Estimated costs. - The estimated direct costs for vessels and ducting are determined by means of the cost-estimating computer program. A summary of the breakdown of these direct cost

TABLE XX. - PARAMETERS UTILIZED IN SELECTING NUMBER OF VESSELS FOR 250 MW_t HTAH SYSTEM - CASES B AND C

Number of Vessels	4	6	8	9	10	11
Relative Matrix Volume Per Vessel	2.50	1.25	0.83	0.83	0.63	0.63
Relative Total Matrix Volume	2.50	1.88	1.67	1.88	1.56	1.65
Approximate Relative System Capital Cost	2.26	1.83	1.70	1.91	1.72	1.81
Vessel Maximum Outside Diameter m (ft)	10.6 (34.7)	8.0 (26.1)	6.8 (22.3)	6.8 (22.3)	6.1 (20.1)	6.1 (20.1)
Approximate Relative Vessel Heat Loss	1.45	1.64	1.87	2.10	2.10	2.31
Relative Average Air Flow Rate Through Matrix	1.00	1.33	1.50	1.20	1.60	1.33

TABLE XXI. - PARAMETERS UTILIZED IN SELECTING NUMBER OF VESSELS FOR 500 MW_t HTAH SYSTEM - CASES B AND C

Number of Vessels	6	8	9	10	11	13
Relative Matrix Volume Per Vessel	2.50	1.67	1.67	1.25	1.25	1.00
Relative Total Matrix Volume	3.75	3.33	3.75	3.13	3.44	3.25
Approximate Relative System Capital Cost	3.39	3.15	3.55	3.05	3.35	3.25
Vessel Maximum Outside Diameter m (ft)	10.6 (34.7)	8.9 (29.3)	8.9 (29.3)	8.0 (26.1)	8.0 (26.1)	7.3 (23.9)
Approximate Relative Vessel Heat Loss	2.18	2.45	2.76	2.73	3.00	3.25
Relative Average Air Flow Rate Through Matrix	1.33	1.50	1.20	1.60	1.33	1.43

TABLE XXII. - PARAMETERS UTILIZED IN SELECTING NUMBER OF VESSELS FOR 1000 MW_t HTAH SYSTEM - CASES B AND C

Number of Vessels	10	11	13	15	20
Relative Matrix Volume Per Vessel	2.50	2.50	2.00	1.67	1.25
Relative Total Matrix Volume	6.25	6.88	6.50	6.25	6.25
Approximate Relative System Capital Cost	5.65	6.22	6.02	5.91	6.10
Vessel Maximum Outside Diameter m (ft)	10.6 (34.7)	10.6 (34.7)	9.7 (31.7)	8.9 (29.3)	8.0 (26.1)
Approximate Relative Vessel Heat Loss	3.63	3.99	4.31	4.60	5.46
Relative Average Air Flow Rate Through Matrix	1.60	1.33	1.43	1.50	1.45

estimates for Case B is presented in table XXIII for system thermal capacities of 100, 250, 500 and 1000 MW_t. Table XXIV summarizes the cost estimates for auxiliary equipment (including direct and indirect costs) based upon the data and procedures presented in Appendix 2N. Table XXV is a summary of the total HTAH system cost estimates for Case B, including direct costs, indirect costs and cost estimates for auxiliary equipment.

As indicated in table XXV, the HTAH system cost per unit system thermal capacity decreases as the system thermal capacity increases. This is due in part to an increase in the sizes of the vessels, but to a larger extent to an increase in the number of vessels. The number of vessels for Cases B and C has a greater impact upon the HTAH system thermal capacity than it does for Cases A and D, as can be seen from the data in table XXXV of Appendix 2J. Decreases in fuel consumption per unit system thermal capacity which occur upon scale-up are not determined in this investigation.

Case C - Low Btu Gas-Fired 1922° K (3000° F) HTAH System

Materials prices. - The materials specified for Case C are indicated in Appendix 2C. The prices of materials, which are based upon data obtained from manufacturers, are given in Appendix 2O.

Adjustments. - Because of the differences between the pressures and temperatures specified by NASA for Case C and those specified in the ETF reference design (see table XI), various dimensions were modified prior to scaling up the HTAH system. These adjustments included changes in matrix diameter and ducting internal diameters (with corresponding changes in vessel and duct shell and insulation dimensions) in accordance with Appendixes 2E, 2F and 2I.

The ETF reference design applies to a dual-fuel system which provides the option to utilize either No. 2 fuel oil or

TABLE XXIII. - BREAKDOWN OF DIRECT COSTS (THOUSANDS OF DOLLARS) OF VESSELS AND DUCTING FOR TOTAL HTAH SYSTEM FOR CASE B

Component \ System Thermal Capacity		100 MWt (4 Vessels)	250 MWt (6 Vessels)	500 MWt (8 Vessels)	1000 MWt (15 Vessels)
Total System					
Matrix	Materials	8,140	15,264	27,104	50,820
	Installation	3,848	7,218	12,816	24,030
Matrix Support Structure	Materials	268	498	888	1,665
	Installation	108	198	352	660
Vessel Shell	Materials	1,836	3,102	5,408	10,140
	Installation	2,756	4,656	8,112	15,210
Vessel Insulation	Materials	5,688	9,858	15,944	29,895
	Installation	3,368	5,916	9,736	18,255
Combustion Chamber Shell	Materials	612	1,092	1,952	3,560
	Installation	920	1,632	2,928	5,490
Combustion Chamber Insul.	Materials	2,448	4,218	6,832	12,910
	Installation	1,836	3,258	5,400	10,125
Ducting Steel	Materials	675	1,242	1,947	5,036
	Installation	561	1,027	1,633	4,230
Ducting Insulation	Materials	1,052	1,724	2,736	7,125
	Installation	468	756	1,194	2,998
Total Cost*	Materials	20,717	36,999	62,807	121,143
	Installation	13,866	24,662	42,175	81,005

*Total costs do not necessarily correspond to column totals due to round-off.

TABLE XXIV. - ESTIMATED COSTS (THOUSANDS OF DOLLARS) OF AUXILIARY SYSTEMS AND ACCESSORIES (INCLUDING DIRECT AND INDIRECT COSTS) - CASE B

Item \ System Thermal Capacity	100 MWt (4 Vessels)	250 MWt (6 Vessels)	500 MWt (8 Vessels)	1000 MWt (15 Vessels)
Valves	2,260	3,880	6,140	11,510
Burners	700	1,220	2,000	3,740
Instruments and Controls	480	720	960	1,800
Fuel Supply System	500	870	1,310	1,990
Turbocompressor System	Not Applicable	Not Applicable	Not Applicable	Not Applicable
HTAH Building	Not Determined	Not Determined	Not Determined	Not Determined
Total Estimated Cost	3,940	6,690	10,410	18,770

TABLE XXV. - SUMMARY OF HTAH SYSTEM COSTS (THOUSANDS OF DOLLARS) FOR CASE B

Item \ System Thermal Capacity	100 MWt (4 Vessels)	250 MWt (6 Vessels)	500 MWt (8 Vessels)	1000 MWt (15 Vessels)
Vessels and Ducting - Materials	20,720	37,000	62,810	121,140
Vessels and Ducting - Direct Labor	13,870	24,660	42,180	81,010
Indirect Costs (Vessels and Ducting)	17,730	31,570	53,890	103,610
Auxiliary Systems and Accessories	3,940	6,690	10,410	18,770
Total HTAH System	56,260	99,920	169,290	324,530
Total HTAH System Cost per Unit System Thermal Capacity ($/kW)	562	400	339	325

low Btu gas. When the system operates on low Btu fuel gas, no recirculation flue gas is required. Therefore, the piping required for the fuel oil and recirculation flue gas are eliminated from the ETF reference design. The combustion air inlet temperature specified by NASA for Case C is 811° K (1000° F) compared to 867° K (10100° F) specified for the ETF reference design. If recirculation flue gas were available, it would be possible to compensate for the reduction in combustion air inlet temperature by increasing the fuel and combustion air flow rates and decreasing the recirculation flue gas flow rate as indicated in Appendix 2K. However, in the absence of recirculation flue gas, it is necessary to raise the inlet temperature of the low Btu fuel gas from 619° to 702° K (655° to 805° F).

Scaling. - There is very little difference in vessels and ducting between Cases B and C. The HTAH system for Case C has a larger combustion chamber and requires low Btu gas piping but does not include fuel oil piping or recirculation flue gas piping. The heat exchanger matrix and vessel dimensions are the same for both cases. Therefore the basis for determining the optimum number of vessels for each system thermal capacity level is the same, resulting in the selection of 4, 6, 8 and 15 vessels, respectively for the 100, 250, 500 and 1000 MW_t systems. The data in tables XX, XXI and XXII are applicable to both Cases B and C. There is one combustion chamber for each vessel. The relative volumes of the refractory matrix and combustion chambers for the 100, 250, 500 and 1000 MW_t systems are 1.00, 1.25, 1.67 and 1.67, respectively.

Estimated costs. - The estimated direct costs for vessels and ducting are determined by means of the cost-estimating computer program. A summary of the breakdown of these direct cost estimates for Case C is presented in table XXVI for system thermal capacities of 100,250,500 and 1000 MW_t. Table XXVII summarizes the cost estimates for auxiliary equipment (including direct and indirect costs) based upon the data and procedures presented in Appendix 2N. Table XXVIII is a summary of the total HTAH system cost estimates for Case C, including direct cost, indirect costs and cost estimates for auxiliary equipment.

TABLE XXVI. - BREAKDOWN OF DIRECT COSTS (THOUSANDS OF DOLLARS) OF VESSELS AND DUCTING FOR TOTAL HTAH SYSTEM FOR CASE C

Component \ System Thermal Capacity		100 MWt (4 Vessels)	250 MWt (6 Vessels)	500 MWt (8 Vessels)	1000 MWt (15 Vessels)
Total System					
Matrix	Materials	8,140	15,264	27,104	50,820
	Installation	3,848	7,218	12,816	24,030
Matrix Support Structure	Materials	268	498	888	1,665
	Installation	108	198	352	660
Vessel Shell	Materials	1,836	3,102	5,408	10,140
	Installation	2,756	4,656	8,112	15,210
Vessel Insulation	Materials	5,688	9,858	15,944	29,895
	Installation	3,368	5,916	9,736	18,255
Combustion Chamber Shell	Materials	772	1,350	2,384	4,440
	Installation	1,160	2,028	3,576	6,660
Combustion Chamber Insul.	Materials	2,968	5,082	8,136	15,255
	Installation	1,984	3,498	5,776	10,830
Ducting Steel	Materials	702	1,284	2,015	5,175
	Installation	582	1,058	1,683	4,330
Ducting Insulation	Materials	1,091	1,783	2,830	73,120
	Installation	483	778	1,229	3,068
Total Cost*	Materials	21,462	38,222	64,710	124,700
	Installation	14,288	25,351	43,280	83,039

*Total costs do not necessarily correspond to column totals due to round-off.

TABLE XXVII. - ESTIMATED COSTS (THOUSANDS OF DOLLARS) OF AUXILIARY SYSTEMS AND ACCESSORIES (INCLUDING DIRECT AND INDIRECT COSTS) - CASE C

System Thermal Capacity / Item	100 MWt (4 Vessels)	250 MWt (6 Vessels)	500 MWt (8 Vessels)	1000 MWt (15 Vessels)
Valves	2,260	3,880	6,140	11,510
Burners	700	1,220	2,000	3,470
Instruments and Controls	480	720	960	1,800
Fuel Supply System	18,000	35,000	67,000	135,000
Turbocompressor System	Not Applicable	Not Applicable	Not Applicable	Not Applicable
HTAH Building	Not Determined	Not Determined	Not Determined	Not Determined
Total Estimated Cost	21,440	40,820	76,100	151,780

TABLE XXVIII. - SUMMARY OF HTAH SYSTEM COSTS (THOUSANDS OF DOLLARS) FOR CASE C

Item \ System Thermal Capacity	100 MWt (4 Vessels)	250 MWt (6 Vessels)	500 MWt (8 Vessels)	1000 MWt (15 Vessels)
Vessels and Ducting - Materials	21,460	38,220	64,170	124,700
Vessels and Ducting - Direct Labor	14,290	25,350	43,280	83,040
Indirect Costs (Vessels and Ducting)	18,290	32,490	55,360	106,320
Auxiliary Systems and Accessories	21,440	40,820	76,100	151,780
Total HTAH System	75,480	136,880	238,910	465,840
Total HTAH System Cost Per Unit System Thermal Capacity ($/kW)	755	548	478	466

As indicated in table XXVIII, the HTAH system cost per unit system thermal capacity decreases as the system thermal capacity increases. This is due in part to an increase in the sizes of the vessels, but to a larger extent to an increase in the number of vessels. The number of vessels for Cases B and C has a greater impact upon the HTAH system thermal capacity than it does for Cases A and D, as can be seen from the data in table XXXV of Appendix 2J. Decreases in fuel consumption per unit system thermal capacity which occur upon scale-up are not determined in this investigation.

Case D - Low Btu Gas-Fired 1922° K (3000° F) HTAH System With Pressurized Combustion

Materials prices. - Most of the refractory materials required for Case D were specified in the ETF reference design only in terms of their desired properties as compared to Cases A, B and C in which specific materials were identified for the respective ETF reference designs. Materials were therefore selected for each application based upon the specified properties. These materials were selected from a list of materials for which prices had been obtained. The selected materials are indicated in parentheses in Appendix 2D. Prices of the refractory materials are given in Appendix 2O.

Adjustments. - The ETF reference design applies to an oil-fired HTAH system. The modifications to the ETF reference design to accommodate low Btu gas firing are based upon the differences in design between the HTAH systems for Cases B and C. These modifications include increasing the height of the combustion zone, adding low Btu gas piping and deleting fuel oil and atomizing air piping and eliminating the recirculation of flue gas. The fuel gas properties and the ratio of combustion air to fuel gas are taken to be the same as for Case C. The temperatures of the fuel gas and the combustion air are also taken to be the same as the adjusted temperatures for Case C.

Because of the differences between the pressures and temperatures specified by NASA for Case D and those specified in the ETF reference design (see table XII), various dimensions were modified prior to scaling up the HTAH system in accordance with the equations in Appendixes 2E, 2F and 2I. These adjustments include changes in matrix length, matrix diameter and ducting diameters. The matrix length is increased because of the decrease in MHD air inlet temperature. This also results in a reduction in the reheat gas temperature at the exit of the vessel and a reduction in the flow rates of MHD air and reheat gas. The reduction in these flow rates is approximately 3 percent.

Scaling. - The ETF reference design for Case D utilizes 14 vessels. Twelve are on-line at any one time while two are on standby. There is only one mode of operation as compared with Cases A, B and C for which there are a normal operating mode and an emergency operating mode. For this reason, there is a linear relationship between the system thermal capacity and the number of on-line vessels. Scaling is therefore a straightforward procedure of changing vessel and duct sizes and/or changing the number of vessels.

An investigation which involves consideration of economics, reliability, heat losses, material and valving lifetimes and practical limits on vessel and valve sizes may reveal that the optimum number of vessels may be different from fourteen for any given system thermal capacity. However, since determination of fuel savings due to reduction of heat loss is beyond the scope of the present investigation, the number of vessels is kept at fourteen for all system thermal capacities. This is possible because the vessel outside diameter for a 1000 MW_t system is 6.2 meters (20.3 feet), which is well within practical limits. The numbers and arrangements of the burners for each vessel are the same as for the ETF reference designs.

Estimated costs. - The estimated direct costs for vessels and ducting are determined by means of the cost-estimating computer program. A summary of the breakdown of these direct cost estimates for Case D is presented in table XXIX for system thermal capacities of 100, 250, 500 and 1000 MW_t. Table XXX summarizes the cost estimates for auxiliary equipment (including direct and indirect costs) based upon the data and procedures presented in Appendix 2N. Table XXXI is a summary of the total HTAH system cost estimates for Case D, including direct costs, indirect costs and cost estimates for auxiliary equipment.

As indicated in table XXXI, the HTAH system cost per unit system thermal capacity decreases as the system thermal capacity increases. This is due to an increase in the sizes of the vessels since the number of vessels remains fixed. Decreases in fuel consumption per unit system thermal capacity which occur upon scale-up are not determined in this investigation.

RECOMMENDATIONS

The cost estimates developed in this investigation can be utilized, in conjunction with other MHD power plant studies, to determine the economic feasibility of building an MHD power plant with an indirectly-fired HTAH system in comparison with building an MHD power plant which uses oxygen-enriched air. It must be kept in mind, however, that the costs developed herein do not necessarily reflect the costs of fully-optimized systems and that credit has not been taken for fuel savings which can be achieved because of the increase in system efficiency attributable to a reduction in percentage heat loss as the systems are scaled up in thermal capacity. If the results indicate that indirectly-fired HTAH systems may provide economic advantages, further investigations are warranted, even if the advantages appear to be borderline. Future investigations should refine and supplement the present investigation.

TABLE XXIX. - BREAKDOWN OF DIRECT COSTS (THOUSANDS OF DOLLARS) OF VESSELS AND DUCTING FOR TOTAL HTAH SYSTEM FOR CASE D

Component \ System Thermal Capacity		100 MWt (14 Vessels)	250 MWt (14 Vessels)	500 MWt (14 Vessels)	1000 MWt (14 Vessels)
Total System					
Matrix	Materials	5,026	12,460	25,228	49,840
	Installation	770	1,904	3,864	7,644
Matrix Support Structure	Materials	1,750	3,682	6,664	12,278
	Installation	1,358	2,870	5,180	9,548
Vessel Shell	Materials	1,232	1,988	3,052	5,180
	Installation	1,834	2,982	4,578	7,770
Vessel Insulation	Materials	1,050	1,708	2,618	4,200
	Installation	980	1,568	2,394	3,780
Ducting Steel	Materials	642	1,170	2,095	3,699
	Installation	566	1,021	1,855	3,385
Ducting Insulation	Materials	826	1,335	2,325	4,265
	Installation	462	725	1,334	2,657
Total Cost*	Materials	10,512	22,347	41,978	79,465
	Installation	5,978	11,075	19,209	34,788

*Total costs do not necessarily correspond to column totals due to round-off.

TABLE XXX. - ESTIMATED COSTS (THOUSANDS OF DOLLARS) OF AUXILIARY SYSTEMS AND ACCESSORIES (INCLUDING DIRECT AND INDIRECT COSTS) - CASE D

System Thermal Capacity / Item	100 MWt (14 Vessels)	250 MWt (14 Vessels)	500 MWt (14 Vessels)	1000 MWt (14 Vessels)
Valves	1,860	3,220	4,890	7,400
Burners	1,250	2,390	3,900	6,390
Instruments and Controls	860	860	860	860
Fuel Supply System	18,000	35,000	67,000	135,000
Turbocompressor System	9,060	19,380	34,450	61,250
HTAH Building	Not Determined	Not Determined	Not Determined	Not Determined
Total Estimated Cost	31,030	60,850	111,100	210,900

TABLE XXXI. - SUMMARY OF HTAH SYSTEM COSTS (THOUSANDS OF DOLLARS) FOR CASE D

System Thermal Capacity / Item	100 MWt (14 Vessels)	250 MWt (14 Vessels)	500 MWt (14 Vessels)	1000 MWt (14 Vessels)
Vessels and Ducting - Materials	10,510	22,350	41,980	79,460
Vessels and Ducting - Direct Labor	5,980	11,070	19,210	34,790
Indirect Costs (Vessels and Ducting)	7,960	15,320	27,220	49,990
Auxiliary Systems and Accessories	31,030	60,850	111,100	210,900
Total HTAH System	55,480	109,590	199,510	375,140
Total HTAH System Cost per Unit System Thermal Capacity ($/kW)	555	438	399	375

There are several areas of investigation which would provide useful information. These include the following

- Examination of the differences between the ETF reference designs for Cases A, B, C and D to determine whether the differences in estimated costs are due to significant design differences or to differences in underlying assumptions
- A detailed investigation to develop more accurate cost estimates for auxiliary systems and accessories, especially fuel supply systems for Cases C and D, the turbocompressor system for Case D and the HTAH system foundations, support structure and building for all cases
- Consideration of alternate types of coal gasification systems for Cases C and D to determine the optimum type for each level of system thermal capacity
- Determination of the economic effect of the reduction in fuel consumption due to the reduction in percentage heat loss which occurs upon scale-up. Alternatively, determine the reduction in capital cost which can be achieved when insulation layer thicknesses are reduced to maintain constant percentage heat loss upon scale-up
- Investigation of the implications of the number of vessels and the number in excess of the minimum number required with regard to system reliability and powerplant availability
- Investigation of matrix and insulation material lifetimes and valve lifetimes and determination of maintenance costs associated with periodic replacement of materials and refurbishment and replacement of valves and other auxiliary equipment and accessories

- Determination of the fluctuations in pressure, temperature and flow rate of preheated MHD air and investigation of the impact of such fluctuations on the performance and operation of the MHD power plant

Investigations in any of the above areas should be conducted for a specified system thermal capacity rather than for a range of system thermal capacities. This would reduce the effort and time required and the investigations would follow the pattern which is typically followed in the industry. Industrial firms are inclined to be more responsive to inquiries and requests for quotes when the system is well defined and the required conditions and criteria are completely specified for a single set of conditions. Once the system size and functional specifications have been established, the detailed heat transfer and thermal stress analysis techniques which were utilized to size the matrices for the ETF reference designs should be employed to determine the optimum matrix configuration.

REFERENCES

2-1. General Electric Co., MHD-ETF Program Final Report, Volume IVD - Appendices A17 and A18, U.S. Department of Energy Report FE-2613-6, March 1978.

2-2. Avco-Everett Research Laboratory, Inc., Engineering Test Facility Conceptual Design Final Report, Part 1, U.S. Department of Energy Report FE-2614-2 (Part 1), June 1978.

2-3. Whitman, Requardt and Associates, The Handy-Whitman Index of Public Utility Construction Costs, Bulletin No. 110, to July 1, 1979.

2-4. Westinghouse Electric Corp., Open Cycle MHD Systems Analysis, Report No. 79-5E61-SYMHD-R2.

Appendix 2A

HTAH System Component Definition - Case A

The following description pertains to the ETF reference design based upon data presented in reference 2-1. The design modifications which were required to meet the NASA specifications or material price substitutions which were necessary because of limitations on availability of cost data are indicated in parentheses

General System Characteristics

Type of Fuel: No. 2 fuel oil

Number of Vessels: four (number of vessels for scaled-up systems varies with system thermal capacity)

Vessel Configuration: internal non-combustion blast well

Combustion Chamber: single chamber for entire system (number of chambers for scaled-up systems varies with system thermal capacity)

Nominal Combustion Pressure: atmospheric

Temperature Control Method: cold blast modulating valves and cold blast mixing bypass

Pressure Equalization Method: relief valve and bypass of cold blast branch isolation valve

HTAH Vessel

Matrix

Material

Upper section: 90 percent alumina (A.P. Green Greenal 90)

Lower section: 68 percent alumina (A.P. Green Greenal 90)

Checker tile shape: square

Checker tile size: 19 x 19 x 11.4 cm (7½ x 7½ x 4½ inches)

Hole diameter: 2.54 cm (1 inch)

Insulation

Upper dome

Layer 1: 90 percent alumina (A.P. Green 99-AD)

Layer 2: insulating firebrick (A.P. Green G-30/G-33)

Layer 3: Superex insulating block (A.P. Green G-23)

Layer 4: insulating cement (A.P. Green Greencast-94)

Upper cylindrical section

Layer 1: chrome alumina X-11842-J (A.P. Green 99-AD)

Layer 2: J-M 32 insulating brick (A.P. Green G-30/G-33)

Layer 3: Superex block insulation (A.P. Green G-23)

Layer 4: Cerablanket (A.P. Green G-23)

Middle cylindrical section

Layer 1: 90 percent alumina brick (A.P. Green Greenal 90)

Layer 2: J-M 32 insulating brick (A.P. Green G-30/G-33)

Layer 3: Superex block insulation (A.P. Green G-23)

Layer 4: Cerablanket (A.P. Green G-23)

Lower cylindrical section

Layer 1: 68 percent alumina brick (A.P. Green Greenal 90)

Layer 2: J-M 32 insulating brick (A.P. Green G-30/G-33)

Layer 3: Superex block insulation (A.P. Green G-23)

Layer 4: Cerablanket (A.P. Green G-23)

Blast well insulation

Target wall: zirconia (A.P. Green 99-AD)

Layer 2: chrome alumina X-11842-J (A.P. Green 99-AD)

Layer between blast well and matrix: 90 percent alumina (A.P. Green Greenal 90)

Below blast well: 413 Mullite base castable fill (A.P. Green Greencast-94)

Layer 2: 68 percent alumina (A.P. Green Greenal 90)

Bottom cap insulation

Not specified (A.P. Green Greencast-94)

Support structure

Shoes: cast iron alloy (stainless steel)

Grids: cast iron alloy (stainless steel)

Beams: cast iron alloy (stainless steel)

Columns: cast iron alloy (stainless steel)

Base: concrete

Shell: steel (carbon steel)

Combustion Chamber

Configuration: a single horizontal-axis cylinder with burner at one end (multiple chambers for scaled-up HTAH systems)

Insulation

Layer 1: 90 percent alumina (A.P. Green Greenal 90)

Layer 2: J-M 32 insulating firebrick (A.P. Green G-30/G-33)

Layer 3: Superex insulating block (A.P. Green G-26)

Shell: steel (carbon steel)

Burner system: specifications not included in reference 2-1

Burner Main Manifold

Fluid conveyed: hot combustion products

Insulation

Layer 1: 90 percent alumina (A.P. Green Greenal 90)

Layer 2: J-M 32 insulating firebrick (A.P. Green G-30/G-33)

Layer 3: Superex insulating block (A.P. Green G-26)

Shell: steel (carbon steel)

Expansion joints: three low pressure drum type

Valving: one burner backdraft water-cooled gate valve

Burner Main Branch

Number of branches: one per vessel

Fluid conveyed: hot combustion products

Insulation

Layer 1: 90 percent alumina (A.P. Green Greenal 90)

Layer 2: J-M 32 insulating firebrick (A.P. Green G-30/G-33)

Layer 3: Superex insulating block (A.P. Green G-26)

Shell: steel (carbon steel)

Expansion joints: one low pressure drum type

Valving: one water-cooled gate valve per branch

Cold Blast Main

Fluid conveyed: cold MHD air

Insulation: none specified

Shell: steel (carbon steel)

Expansion joints: three stainless steel bellows type

Valving: one swing check valve and one modified snort valve

Cold Blast Branch

Fluid conveyed: cold MHD air

Number of branches: one per vessel

Insulation: none specified

Shell: steel (carbon steel)

Valving: one gate-type isolation valve, one gate-type bypass equalizing valve and one butterfly flow control valve per branch

Cold Blast Bypass Line

Fluid conveyed: cold MHD air

Insulation: none specified

Shell: steel (carbon steel)

Valving: one gate-type shut-off valve and one mixer control butterfly valve

Waste Gas Breeching

Number of branches: one per vessel

Fluid conveyed: cold combustion products

Insulation: one layer of firebrick (A.P. Green G-20)

Shell: steel (stainless steel)

Valving: one positive isolation and control tricentric-type chimney type per branch

Hot Blast Main

Fluid conveyed: hot MHD air

Insulation

Layer 1: 90 percent alumina (A.P. Green Greenal 90)

Layer 2: JM-32 insulating firebrick (A.P. Green G-30/G-33)

Layer 3: Superex insulating block (A.P. Green G-26)

Shell: steel (carbon steel)

Expansion valves: three omega type

Hot Blast Branch

Number of branches: one per vessel

Fluid conveyed: hot MHD air

Insulation

Layer 1: 90 percent alumina (A.P. Green Greenal 90)

Layer 2: JM-32 insulating firebrick (A.P. Green G-30/G-33)

Layer 3: Superex insulating block (A.P. Green G-26)

Shell: steel (carbon steel)

Expansion joint: one omega type

Valving: one water cooled gate type per branch

Atomizing Air Line

Fluid conveyed: cold air

Insulation: none specified

Shell: steel (carbon steel)

Combustion Air Line

Fluid conveyed: HTAH combustion air

Insulation: none specified (Johns-Mansville Thermo-12)

Shell: steel (stainless steel)

Expansion joints: one fan vibration isolation joint

Air handling, metering and control: one burner fan with inlet and outlet louver dampers and one quick-opening positive shut off isolation valve and one venturi meter

Recirculation Flue Gas Main

Not included in reference 2-1

(Fluid conveyed: recirculation flue gas)

(Insulation
External layer: J-M Thermo-12)

(Shell: stainless steel)

Recirculation Flue Gas Branch

Not included in reference 2-1

(Number of branches: one per vessel)

(Fluid conveyed: recirculation flue gas)

(Insulation

External layer: J-M Thermo 12)

(Shell: stainless steel)

(Valving: one isolation valve and one control valve per branch)

Fuel Lines

No. 2 fuel oil line

Natural gas or propane lines for ignition

Appendix 2B

HTAH System Component Definition - Case B

The following description pertains to the ETF reference design based upon data presented in reference 2-2. The design modifications which were required to meet the NASA specifications are indicated in parentheses.

General System Characteristics

Type of Fuel: No. 2 fuel oil or coal-derived low Btu gas (No. 2 fuel oil)

Number of Vessels: four (number of vessels for scaled-up systems varies with system thermal capacity)

Vessel Configuration: vertical-axis vessel without internal combustion

Combustion Chamber: one chamber dedicated to each vessel with cross-over duct between top of combustion chamber and top of vessel

Nominal Combustion Pressure: atmospheric

Temperature Control Method: cold blast mixing bypass

Pressure Equalization Method: separate compressor and relief valves

HTAH Vessel

Matrix

Material: high purity alumina (A.P. Green 99-AD)

Checker tile shape: hexagonal

Checker tile size: 19.4 x 19.4 x 11.4 cm (7.65 x 7.65 x 4.5 inches)

Hole diameter: 2.54 cm (1 inch)

Insulation

Upper dome

Layer 1: A.P. Green 99 AD

Layer 2: A.P. Green G30

Upper cylindrical section

Layer 1: A.P. Green 99 AD

Layer 2: A.P. Green G33

Layer 3: A.P. Green G33

Layer 4: mineral wool

Upper middle cylindrical section

Layer 1: A.P. Green 99 AD

Layer 2: A.P. Green G33

Layer 3: A.P. Green G26

Layer 4: mineral wool

Lower middle cylindrical section

Layer 1: A.P. Green 99 AD

Layer 2: A.P. Green G30

Layer 3: A.P. Green G23

Layer 4: mineral wool

Lower cylindrical section

Layer 1: A.P. Green 99 AD

Layer 2: A.P. Green G28

Layer 3: A.P. Green G23

Layer 4: mineral wool

Support structure

Grate: 304 stainless steel

Cross-flow spacer plate: 304 stainless steel

Support girders: 304 stainless steel

Support columns: 304 stainless steel with insulation

Base: high density castable refractory (A.P. Green Greencast 94)

Shell: carbon steel

Combustion Chamber

Configuration: vertical-axis cylinder with burner at base

Insulation

Dome

Layer 1: A.P. Green 99 AD

Layer 2: A.P. Green G30

Cylindrical section

Layer 1: A.P. Green 99 AD

Layer 2: A.P. Green G30

Layer 3: mineral wool

Shell: carbon steel

Burner system: single dual-fuel burner based upon design by Bloom Engineering Co., Pittsburgh, Pa.

Cold Blast Main

Fluid conveyed: cold MHD air

Insulation

External layer: J-M Thermo 12

Shell: ASTM A53 GR B

Cold Blast Branch

Fluid conveyed: cold MHD air

Number of branches: one per vessel

Insulation

Layer 1: A.P. Green Greencast 94

Shell: ASTM 516 GR 70

Valving: one isolation valve per branch

Cold Blast Bypass Line

Fluid conveyed: cold MHD air

Insulation

Layer 1: A.P. Green Greencast 94

Shell: ASTM 516 GR 70

Valving: one control valve

Crossover Pipe

Number of pipes: one per vessel

Fluid conveyed: hot combustion products and hot MHD air

Insulation

Layer 1: A.P. Green 99 AD

Layer 2: A.P. Green G33

Layer 3: A.P. Green G26

Shell: ASTM SA240 GR 316

Expansion joints: indicated, but type not specified

Combustion Gas Exit Main

Fluid conveyed: cold combustion products

Insulation

External layer: J-M Thermo 12

Shell: ASTM A312 GR TP304

Combustion Gas Exit Branch

Number of branches: one per vessel

Fluid conveyed: warm combustion products

Insulation

Layer 1: A.P. Green Greencast 94

Layer 2: A.P. Green VSL 50

Shell: ASTM 516 GR 70

Valving: one isolation valve per branch

Hot Blast Main

Fluid conveyed: hot MHD air

Insulation

Layer 1: A.P. Green 99 AD

Layer 2: A.P. Green G33

Layer 3: A.P. Green G26

Shell: ASTM 516 GR 70

Valving: one isolation valve and one isolation valve for bypass to stack

Hot Blast Branch

Number of branches: one per vessel

Fluid conveyed: hot MHD air

Insulation

Layer 1: A.P. Green 99 AD

Layer 2: A.P. Green G33

Layer 3: A.P. Green G26

Shell: ASTM 516 GR 70

Valving: one isolation valve per branch

Pressurization/Depressurization Main

Fluid conveyed: intermittently hot and cold air

Insulation

External layer: J-M Thermo 12

Shell: ASTM A53 GR B

Valving: three isolation valves and two control valves

Pressurization/Depressurization Branch

Number of branches: one per vessel

Fluid conveyed: intermittently hot and cold air

Insulation

External layer: J-M Thermo 12

Shell: ASTM A53 GR B

Valving: one isolation valve per branch

Combustion Air Main

Fluid conveyed: HTAH combustion air

Insulation

External layer: J-M Thermo 12

Shell: ASTM A312 GR TP304

Combustion Air Branch

Number of branches: one per vessel

Fluid conveyed: HTAH combustion air

Insulation

External layer: J-M Thermo 12

Shell: ASTM A312 GR TP304

Valving: one isolation valve and one control valve per branch

Recirculation Flue Gas Main

Fluid conveyed: recirculation flue gas

Insulation

External layer: J-M Thermo 12

Shell: ASTM A312 GR TP304

Recirculation Flue Gas Branch

Number of branches: one per vessel

Fluid conveyed: recirculation flue gas

Insulation

External layer: J-M Thermo 12

Shell: ASTM A312 GR TP304

Valving: one isolation valve and one control valve per branch

Fuel Oil Main

Fluid conveyed: No. 2 fuel oil

Insulation: not specified (none)

Shell: not specified (carbon steel)

Fuel Oil Branch

Number of branches: one per vessel

Fluid conveyed: No. 2 fuel oil

Insulation: not specified (none)

Shell: not specified (carbon steel)

Valving: one isolation valve and one control valve per branch

Appendix 2C

HTAH System Component Definition - Case C

The following description pertains to the ETF reference design based upon data presented in reference 2-2. The design modifications which were required to meet the NASA specifications are indicated in parentheses.

General System Characteristics

Type of Fuel: No. 2 fuel oil or coal-derived low Btu gas (coal-derived low Btu gas)

Number of Vessels: four (number of vessels for scaled-up systems varies with system thermal capacity)

Vessel Configuration: vertical-axis vessel without internal combustion

Combustion Chamber: one chamber dedicated to each vessel with cross-over duct between top of combustion chamber and top of vessel

Nominal Combustion Pressure: atmospheric

Temperature Control Method: cold blast mixing bypass

Pressure Equalization Method: separate compressor and relief valves

HTAH Vessel

Matrix

Material: high purity alumina (A.P. Green 99-AD)

Checker tile shape: hexagonal

Checker tile size: 19.4 x 19.4 x 11.4 cm (7.65 x 7.65 x 4.5 inches)

Hole diameter: 2.54 cm (1 inch)

Insulation

Upper dome

Layer 1: A.P. Green 99 AD

Layer 2: A.P. Green G30

Upper cylindrical section

Layer 1: A.P. Green 99 AD

Layer 2: A.P. Green G33

Layer 3: A.P. Green G33

Layer 4: mineral wool

Upper middle cylindrical section

Layer 1: A.P. Green 99 AD

Layer 2: A.P. Green G33

Layer 3: A.P. Green G26

Layer 4: mineral wool

Lower middle cylindrical section

Layer 1: A.P. Green 99 AD

Layer 2: A.P. Green G30

Layer 3: A.P. Green G23

Layer 4: mineral wool

Lower cylindrical section

Layer 1: A.P. Green 99 AD

Layer 2: A.P. Green G28

Layer 3: A.P. Green G23

Layer 4: mineral wool

Support structure

Grate: 304 stainless steel

Cross-flow spacer plate: 304 stainless steel

Support girders: 304 stainless steel

Support columns: 304 stainless steel with insulation

Base: high density castable refractory (A.P. Green Greencast 94)

Shell: carbon steel

Combustion Chamber

Configuration: vertical-axis cylinder with burner at base

Insulation

Dome

Layer 1: A.P. Green 99 AD

Layer 2: A.P. Green G30

Cylindrical section

Layer 1: A.P. Green 99 AD

Layer 2: A.P. Green G30

Layer 3: mineral wool

Shell: carbon steel

Burner system: single dual-fuel burner based upon design by Bloom Engineering Co., Pittsburgh, Pa.

Cold Blast Main

Fluid conveyed: cold MHD air

Insulation

External layer: J-M Thermo 12

Shell: ASTM A53 GR B

Cold Blast Branch

Fluid conveyed: cold MHD air

Number of branches: one per vessel

Insulation

Layer 1: A.P. Green Greencast 94

Shell: ASTM 516 GR 70

Valving: one isolation valve per branch

Cold Blast Bypass Line

Fluid conveyed: cold MHD air

Insulation

Layer 1: A.P. Green Greencast 94

Shell: ASTM 516 GR 70

Valving: one control valve

Crossover Pipe

Number of pipes: one per vessel

Fluid conveyed: hot combustion products and hot MHD air

Insulation

Layer 1: A.P. Green 99 AD

Layer 2: A.P. Green G33

Layer 3: A.P. Green G26

Shell: ASTM SA240 GR 316

Expansion joints: indicated, but type not specified

Combustion Gas Exit Main

Fluid conveyed: cold combustion products

Insulation

External layer: J-M Thermo 12

Shell: ASTM A312 GR TP304

Combustion Gas Exit Branch

Number of branches: one per vessel

Fluid conveyed: warn combustion products

Insulation

Layer 1: A.P. Green Greencast 94

Layer 2: A.P. Green VSL 50

Shell: ASTM 516 GR 70

Valving: one isolation valve per branch

Hot Blast Main

Fluid conveyed: hot MHD air

Insulation

Layer 1: A.P. Green 99 AD

Layer 2: A.P. Green G33

Layer 3: A.P. Green G26

Shell: ASTM 516 GR 70

Valving: one isolation valve and one isolation valve for bypass to stack

Hot Blast Branch

Number of branches: one per vessel

Fluid conveyed: hot MHD air

Insulation

Layer 1: A.P. Green 99 AD

Layer 2: A.P. Green G33

Layer 3: A.P. Green G26

Shell: ASTM 516 GR 70

Valving: one isolation valve per branch

Pressurization/Depressurization Main

Fluid conveyed: intermittently hot and cold air

Insulation

External layer: J-M Thermo 12

Shell: ASTM A53 GR B

Valving: three isolation valves and two control valves

Pressurization/Depressurization Branch

Number of branches: one per vessel

Fluid conveyed: intermittently hot and cold air

Insulation

External layer: J-M Thermo 12

Shell: ASTM A53 GR B

Valving: one isolation valve per branch

Combustion Air Main

Fluid conveyed: HTAH combustion air

Insulation

External layer: J-M Thermo 12

Shell: ASTM A312 GR TP304

Combustion Air Branch

Number of branches: one per vessel

Fluid conveyed: HTAH combustion air

Insulation

External layer: J-M Thermo 12

Shell: ASTM A312 GR TP304

Valving: one isolation valve and one control valve per branch

Low Btu Fuel Gas Main

Fluid conveyed: low Btu fuel gas

Insulation

External layer: J-M Thermo 12

Shell: ASTM A312 GR TP304

Low Btu Fuel Gas Branch

Number of branches: four

Fluid conveyed: Low Btu fuel gas

Insulation

External layer: J-M Thermo 12

Shell: ASTM A312 GR TP304

Valving: two isolation valves, one control valve and one relief valve per branch

Appendix 2D

HTAH System Component Definition - Case D

The following description pertains to the ETF reference design based upon data presented in reference 2-1. The design modifications which were required to meet the NASA specifications or material price substitutions which were necessary because of limitations on availability of cost data are indicated in parentheses.

General System Characteristics

Type of fuel: No. 2 fuel oil (coal-derived low Btu gas)

Number of vessels: twelve on-line vessels and two stand-by vessels

Vessel configuration: vertical-axis vessel with matrix in lower section and combustion chamber in upper section

Nominal combustion pressure: 0.69 MPa (100 psia)

Temperature control method: passive

Pressure equalization method: system designed for nominally-equal reheat gas and blowdown air pressures

HTAH Vessel

Matrix

Material: Norton AH-299A (A.P. Green 99-AD)

Checker tile shape: hexagonal

Checker tile size: 11.5 x 11.5 x 7.8 cm (4.54 x 4.54 x 3-1/16 inches)

Hole diameter: 1.27 cm (0.5 inch)

Insulation

Crown Section

Layer 1: high density alumina, 2089° K (3300° F) maximum (A.P. Green 99-AD)

Layer 2: moderate density fire brick, 1978° K (3100° F) maximum (A.P. Green G-33)

Layer 3: moderate density fire brick, 1700° K (2600° F) maximum (A.P. Green G-26)

Layer 4: light weight fire brick, 1367° K (2000° F) maximum (A.P. Green G-20)

Burner Section.

Layer 1: high density alumina, 2089° K (3300° F) maximum (A.P. Green 99-AD)

Layer 2: moderate density fire brick, 1978° K (3100° F) maximum (A.P. Green G-33)

Layer 3: moderate density fire brick, 1700° K (2600° F) maximum (A.P. Green G-26)

Layer 4: light weight fire brick, 1367° K (2000° F) maximum (A.P. Green G-20)

Upper Cylindrical Section

Layer 1: high density alumina, 2089° K (3300° F) maximum (A.P. Green 99-AD)

Layer 2: moderate density fire brick, 1978° K (3100° F) maximum (A.P. Green G-33)

Layer 3: moderate density fire brick, 1700° K (2600° F) maximum (A.P. Green G-26)

Layer 4: light weight fire brick, 1367° K (2000° F) maximum (A.P. Green G-20)

Upper Middle Cylindrical Section

Layer 1: high density alumina, 2089° K (3300° F) maximum (A.P. Green 99-AD)

Layer 2: moderate density fire brick, 1867° K (2900° F) maximum (A.P. Green G-30)

Layer 3: moderate density fire brick, 1700° K (2600° F) maximum (A.P. Green G-26)

Layer 4: light weight fire brick, 1422° K (2100° F) maximum (A.P. Green G-23)

Lower Middle Cylindrical Section

Layer 1: high density alumina, 2089° K (3300° F) maximum (A.P. Green 99-AD)

Layer 2: moderate density fire brick, 1478° K (2200° F) maximum (A.P. Green G-23)

Layer 3: moderate density fire brick, 1367° K (2000° F) maximum (A.P. Green G-20)

Layer 4: light weight fire brick, 1144° K (1600° F) maximum (A.P. Green G-20)

Lower Cylindrical Section

Layer 1: high density alumina, 2089° K (3300° F) maximum (A.P. Green 99-AD)

Layer 2: moderate density fire brick, 1144° K (1600° F) maximum (A.P. Green G-20)

Layer 3: moderate density fire brick, 922° K (1200° F) maximum (A.P. Green G-20)

Layer 4: light weight fire brick, 811° K (1000° F) maximum (A.P. Green G-20)

Grate section: castable refractory, 1756° K (2700° F) maximum (A.P. Green Greencast 94)

Support Structure

Support grate: material not specified (stainless steel)

Burner system: eight modified Bloom Engineering Co. Model No. 2126-060 burners per vessel (eight burners modified for low Btu gas firing)

Shell: SA 516 GR 70 (carbon steel)

Cold Blast Main

Fluid conveyed: cold MHD air

Insulation: fiberglass (mineral wool)

Shell: ASTM A106 GR B (carbon steel)

Cold Blast Branch

Number of branches: fourteen

Fluid conveyed: cold MHD air

Insulation: mineral wool

Shell: ASTM A355-P22 (stainless steel)

Valving: one isolation valve per branch

Combustion Gas Exit Main

Fluid conveyed: cold combustion products

Insulation: mineral wool

Shell: ASTM A355-P22 (stainless steel)

Combustion Gas Exit Branch

Number of branches: fourteen

Fluid conveyed: cold combustion products

Insulation: mineral wool

Shell: ASTM A355-P22 (stainless steel)

Valving: one isolation valve per branch

Hot Blast Main

Fluid conveyed: hot MHD air

Insulation

Layer 1: high density alumina, 2033° K (3200° F) maximum (A.P. Green 99-AD)

Layer 2: moderate density fire brick, 1922° K (3000° F) maximum (A.P. Green G-33)

Layer 3: moderate density fire brick, 1700° K (2600° F) maximum (A.P. Green G-26)

Layer 4: light weight density fire brick, 1367° K (2000° F) maximum (A.P. Green G-20)

Shell: SA 516 GR 70 (carbon steel)

Hot Blast Branch

Number of branches: fourteen

Fluid conveyed: hot MHD air

Insulation

Layer 1: high density alumina (A.P. Green 99-AD)

Layer 2: moderate density fire brick (A.P. Green G-33)

Layer 3: moderate density fire brick (A.P. Green G-26)

Layer 4: light weight fire brick (A.P. Green G-20)

Shell: SA 516 GR 70 (carbon steel)

Valving: one water-cooled gate valve per branch

Combustion Air Main

Fluid conveyed: HTAH combustion air

Insulation: fiberglass (mineral wool)

Shell: ASTM A106 GR B (stainless steel)

Combustion Air Branch

Number of branches: fourteen with eight sub-branches each

Fluid conveyed: HTAH combustion air

Insulation: fiberglass (mineral wool)

Shell: ASTM 106 GR B (stainless steel)

Valving: two control valves per branch

Low Btu Fuel Gas Main

Not included in reference 1

(Fluid conveyed: low Btu fuel gas)

(Insulation: mineral wool)

(Shell: stainless steel)

Low Btu Fuel Gas Branches

Not included in reference 1

(Number of branches: fourteen with eight sub-branches each)

(Fluid conveyed: low Btu fuel gas)

(Insulation: mineral wool)

(Shell: stainless steel)

(Valving: eight control valves per branch)

Appendix 2E

Basis for Determination of Modified Matrix Dimensions

The capital cost of the refractory matrix represents a significant fraction of the total HTAH system cost. The matrix itself is therefore designed, to a large extent, for minimum cost within the constraints imposed by performance and system lifetime requirements, materials capabilities and fabrication techniques. The interrelationships between the matrix design parameters is quite complex, making the optimization of the matrix design an involved process. The approach which is followed in making design adjustments and scaling the matrix is to retain, as closely as possible, the same conditions locally within the matrix for the adjusted and scaled-up designs as for the ETF reference designs. This means that, although the overall dimensions (length and diameter) of the matrix may change, the hole spacing and hole diameters remain fixed and the temperatures, stresses and heat transfer rates at corresponding locations within the matrix also remain approximately unchanged. In other words, the conditions at a specific location in the adjusted and scaled-up designs are the same as in the corresponding location in the ETF reference designs.

The convective heat transfer coefficient h_c for flow in the cylindrical passages in the matrix is given by the expression

$$h_c = 0.023 \frac{k}{d} Re^{0.8} Pr^{0.33} \qquad (2E\text{-}1)$$

where k is the thermal conductivity of the fluid, d is the passage diameter, Re is the Reynolds number and Pr is the Prandtl number. The Reynolds number can be written in either of the forms

$$Re = \frac{\rho v d}{\mu} \qquad (2E\text{-}2)$$

$$Re = \frac{m_i d}{A_i \mu} \qquad (2E\text{-}3)$$

where ρ is the fluid density, V is the fluid velocity, m_i is the mass flow rate through a single passage, A_i is the cross-sectional area of the passage and μ is the fluid viscosity.

From equations (2E-1) through (2E-3) it is evident that the convective heat transfer coefficient remains constant if the passage diameter, the Reynolds number and the fluid properties, k and Pr remain constant. The Reynolds number remains constant if the product ρV or the quotient m_i/A_i remain constant along with the passage diameter and the viscosity μ. The fluid properties k, Pr and μ depend primarily on the fluid temperature and are relatively insensitive to pressure in the range of pressure variations in the HTAH system. It may be noted that changes in pressure can result in changes in ρ and V separately, but the product ρV remains constant as long as the quotient m_i/A_i remains constant. It is therefore concluded that, at corresponding times in the cycle, the convective heat transfer coefficient is the same at a given location in the adjusted and scaled-up matrix as it is at a location in the ETF matrix with the same fluid temperature if the passage diameters and the quotients m_i/A_i are the same.

The length of the matrix must be modified to take into account a change in the inlet air temperature at the bottom of the matrix (as indicated in tables IX and XII for Cases A and D) from T_{a1} to T_{a1}'. The air outlet temperature T_{a2} at the top of the matrix is unchanged, so that

$$T_{a1}' < T_{a1} \tag{2E-4}$$

and

$$T_{a2}' = T_{a2} \tag{2E-5}$$

The inlet reheat gas temperature also remains unchanged and the reheat gas outlet temperature decreases, as a result of the change in the matrix conditions.

The temperature distribution is expected to vary almost linearly with distance along the vertical axis of the matrix, and the temperature difference between the air and the matrix

is approximately the same all along the length. Therefore, the design adjustment is made by increasing the length of the matrix in proportion to the increase in temperature difference between the air at the inlet and the air at the outlet. Therefore,

$$\frac{L_m'}{L_m} = \frac{T_{a2}' - T_{a1}'}{T_{a2} - T_{a1}} \tag{2E-6}$$

The validity of this approach is based upon the assumptions that the distribution of conditions (e.g. temperature) with respect to radial distance from the centerline of the matrix are not substantially altered by changing the aspect ratio of the matrix (overall length divided by overall diameter). The temperature and stress distributions in the upper regions of the matrix should therefore be approximately unchanged by the modification indicated by equation (2E-6).

The thermal energy input to the air per unit mass of air increases by virtue of the increase in temperature differential between the inlet and the exit. This requires an adjustment in the mass flow rate of the air to achieve a specified rate of thermal energy input to the air. The rate of thermal energy input Q to the air is related to the mass flow rate m of air through the matrix by

$$Q = m\ (h_{a2} - h_{a1}) \tag{2E-7}$$

where h_{a1} and h_{a2} are the values of the specific enthalpy of the air at the inlet and exit of the matrix, respectively. For the modified matrix, the relationship is

$$Q' = m'\ (h_{a2}' - h_{a1}') \tag{2E-8}$$

where the prime symbols denote the parameters for the adjusted and scaled systems. The mass flow rate of air through the modified matrix is related to the mass flow rate of air through the reference system matrix by

$$m' = m \left(\frac{Q'}{Q}\right)\left(\frac{h_{a2} - h_{a1}}{h_{a2}' - h_{a1}'}\right) \tag{2E-9}$$

The enthalpy-change ratio can also be written as

$$\left(\frac{h_{a2} - h_{a1}}{h_{a2}' - h_{a1}'}\right) = \frac{1}{1 + \frac{mc_p(T_{a1} - T_{a1}')}{Q}} \qquad (2E\text{-}10)$$

where c_p is the average specific heat capacity of the air in the temperature range, $T_{a1}' < T < T_{a1}$. Using equations (2E-9) and (2E-10), the expression for the modified mass flow rate can be written

$$m' = \frac{m\left(\frac{Q'}{Q}\right)}{1 + \frac{mc_p(T_{a1} - T_{a1}')}{Q}} \qquad (2E\text{-}11)$$

For cases in which the inlet air temperature is the same as in the ETF reference design (as in Cases B and C), the equation simplifies to

$$m' = m\left(\frac{Q'}{Q}\right) \qquad (2E\text{-}12)$$

This is applicable for a given matrix so long as the number of vessels in the HTAH system remains fixed.

In order to maintain fixed local conditions within the matrix to accommodate changes in mass flow rate through the matrix (due to changing the air inlet temperature and/or thermal energy input to the air) the cross-sectional area of the matrix must change to maintain a fixed ratio of mass flow rate to cross-sectional area A. Thus,

$$\frac{m'}{A'} = \frac{m}{A} \qquad (2E\text{-}13)$$

The overall matrix diameter varies with mass flow rate according to the relation

$$D_m' = D_m\sqrt{\frac{m'}{m}} \qquad (2E\text{-}14)$$

Appendix 2F

Basis for Determination of Modified Vessel Dimensions

The vessel dimensions depend upon the size of the matrix, the thicknesses of the insulation layers and steel shell and the space requirements above and below the matrix. The procedure for determining the matrix dimensions is described in Appendix 2E. The thicknesses of the insulation layers for the adjusted and scaled-up cases are taken to be the same as in the ETF reference designs. The inner diameter D_v of the vessel is thus given by

$$D_v = D_m + 2 \sum_{i=1}^{n} t_i \qquad (2F\text{-}1)$$

where D_m is the diameter of the matrix, t_i is the thickness of the ith layer of insulation and n is the number of layers. The thickness t_s of the cylindrical part of the vessel shell is determined from the relation

$$t_s = \frac{PR}{SE - 0.6P} + t_c \qquad (2F\text{-}2)$$

where P is the design pressure, R is the inside radius of the shell, S is the maximum allowable stress, E is the joint efficiency and t_c is a corrosion allowance. The design pressure is given by

$$P = P_1 + P_2 \qquad (2F\text{-}3)$$

where P_1 is the pressure of the air or gas inside the vessel and P_2 is the additional pressure due to refractory expansion. The values of S and E are taken to be the same values as reported in the ETF final reports for the reference design calculations. The design thicknesses selected for the scaled up cases are the next standard mill size which is greater than the calculated thickness.

The steel shell of the upper dome of the vessel is taken to be the same shape (height-to-diameter ratio) as the steel shell of the upper dome of the ETF reference designs. The shape of the upper dome is assumed to be a segment of a sphere as shown in Figure 17. The segment has base diameter b and height h with radius of curvature a. The base diameter is selected as that which is required to match the diameter of the cylindrical part of the dome. In scaling up the vessels the proportions are maintained the same as in the ETF reference designs, so that

$$\frac{a'}{a} = \frac{b'}{b} = \frac{h'}{h} \qquad (2F\text{-}4)$$

where the primed quantities denote the dimensions of the scaled-up systems. The thickness of the steel shell of the dome is determined from the relation

$$t_d = \frac{PbK}{2SE - 0.2P} + t_c \qquad (2F\text{-}5)$$

where

$$K = \frac{1}{6}\left(2 + \left(\frac{b}{2h}\right)^2\right) \qquad (2F\text{-}6)$$

The thickness of each layer of thermal insulation is taken to be the same as the thickness of the corresponding layer in the ETF reference design.

The bottoms of the vessels are also scaled by maintaining the same shapes and proportions as the bottoms in the ETF reference designs. The thicknesses of the steel shell of the bottoms are determined by equations (2F-5) and (2F-6). However, the design pressure P is given by

$$P = P_1 + P_2 + P_3 \qquad (2F\text{-}7)$$

where P_3 accounts for the dead load due to the weight of the matrix, the insulation and the matrix support structure.

The heights of the matrix support structures for the adjusted and scaled-up conditions are the same as for the ETF reference

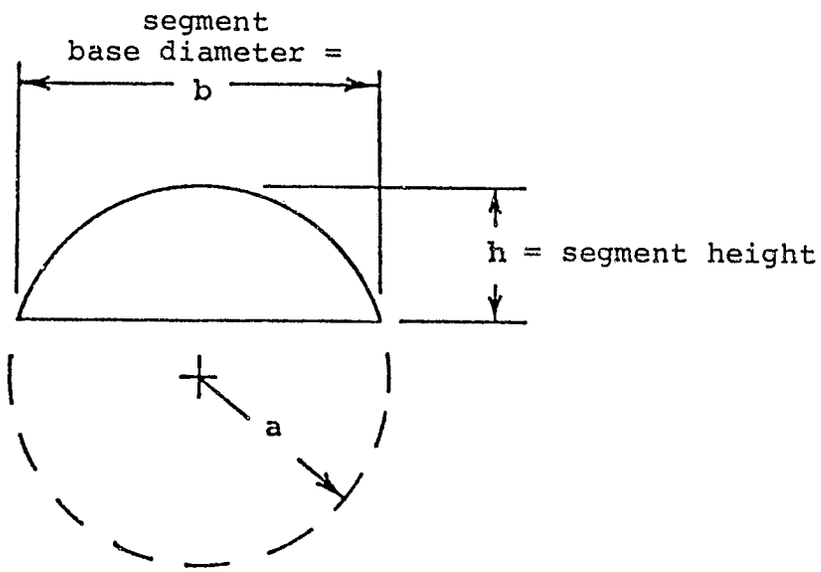

Figure 17. - Spherical segment nomenclature.

designs. The overall support structure cross-sectional area is modified to match the cross-sectional area of the matrix. The number of columns is also changed to allow for the change in cross-sectional area while maintaining approximately the same spacing between the columns.

Appendix 2G

Basis for Determination of Changes in Heat Loss Due to Modifications in System Dimensions

The HTAH system is designed to reduce heat losses to the surroundings by installing insulating materials on the interior walls of the vessels and ductwork and on the exterior of some sections of ducting. The insulation in the regions subjected to very high temperatures is comprised of several layers. The layers in the hottest zones are special refractory materials selected to withstand the maximum temperature. The insulation also serves to protect metal surfaces from reaching high temperatures. The insulation is largely comprised of refractory brick and is built of standard sizes. The use of non-standard sizes would increase the cost as well as the risk of delays in delivery. Since the increments in brick dimensions from one standard size to the next are quite large, the insulating wall thicknesses are not changed as the systems are scaled-up in the procedure used in this investigation.

Figure 18 represents the cross section of a vessel or a duct with two layers of insulation within a steel shell. The innermost layer of insulation has a thermal conductivity k_a, an inner radius r_1 and an outer radius r_2. The outermost layer of insulation has a thermal conductivity k_b and an outer radius r_3. The steel shell has a thermal conductivity k_c and an outer radius r_4. The convective heat transfer coefficients for the interior of the innermost layer and the exterior of the steel shell are h_1 and h_4, respectively. In most cases, the number of layers of insulation is greater than two but this serves to illustrate the behavior and the method of analysis.

The transfer of heat from the vessel interior to the surroundings actually does not occur in a steady-state manner. However, the amplitude of the fluctuations is small relative to the difference between the interior and exterior temperatures and

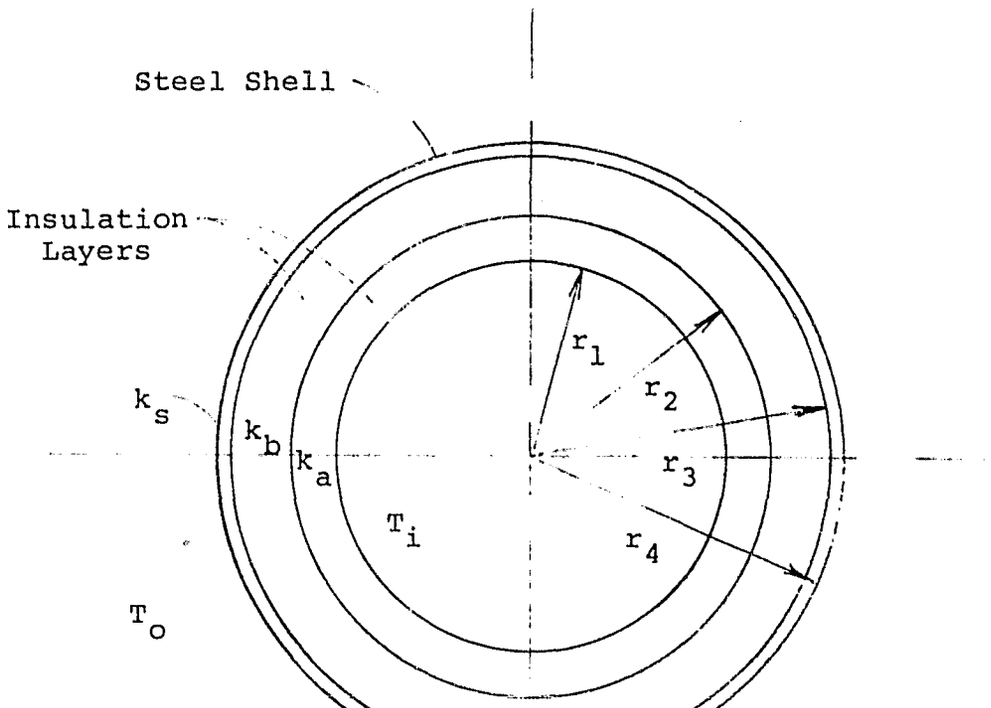

Figure 18. - Cross section of vessel or duct, indicating layers at insulation.

a steady-state analysis is, therefore, a good approximation. The steady-state relation for the rate of heat transfer through the vessel walls is

$$Q_L = \frac{2\pi L\ (T_i - T_o)}{\frac{1}{r_1 h_1} + \frac{1}{k_a} \ln\left(\frac{r_2}{r_1}\right) + \frac{1}{k_b} \ln\left(\frac{r_3}{r_2}\right) + \frac{1}{k_c} \ln\left(\frac{r_4}{r_3}\right) + \frac{1}{r_4 h_4}} \qquad (2G\text{-}1)$$

where T_i is the temperature of the fluid inside the duct or vessel, T_o is the temperature of the air surrounding the vessel or duct and L is the length of the vessel or duct.

As the vessels and ducts are scaled up in size, the temperatures T_i and T_o remain nearly constant. Changes in the convective heat transfer coefficients h_1 and h_4 have a relatively small impact on the overall heat transfer rate and temperature distribution. The length L remains constant for scaling the vessel dimensions, but may change for scaling various sections of ducting.

The mass flow rate of air or reheat gas through the vessel or duct section is proportional to the system capacity (for a fixed system configuration and number of vessels). For scaling the vessels and ducting, the mass flow rate is proportional to the cross-sectional area πr_1^2. Therefore, the ratio of the heat loss to the system thermal capacity is given by

$$\frac{Q_L}{Q_S} = \frac{C}{r_1^2} Q_L \qquad (2G\text{-}2)$$

where C is a constant of proportionality. Combining this relation with equation (2G-1) gives the relation

$$\frac{Q_L}{Q_S} = \frac{C'L}{\frac{r_1}{h_1} + \frac{r_1^2}{k_a} \ln\left(\frac{r_2}{r_1}\right) + \frac{r_1^2}{k_b} \ln\left(\frac{r_3}{r_2}\right) + \frac{r_1^2}{k_c} \ln\left(\frac{r_4}{r_3}\right) + \frac{r_1^2}{r_4 h_4}} \qquad (2G\text{-}3)$$

where C' is a constant of proportionality.

A simplified approximation to this relationship can be derived by taking the limit of this expression as the thicknesses of the insulation layers and the steel shell become very small compared to the radius r_1. The limit is

$$\frac{Q_L}{Q_S} \approx \frac{C'L}{r_1\left(\frac{1}{h_1} + \frac{t_a}{k_a} + \frac{t_b}{k_b} + \frac{t_c}{k_c} + \frac{1}{h_4}\right)} \qquad (2G\text{-}4)$$

where t_a, t_b and t_c are the thicknesses of the innermost and outermost insulation layers and the steel shell, respectively. Since these thicknesses and the heat transfer coefficients are essentially constant, the following approximate relationship holds

$$\frac{Q_L}{Q_S} \approx C''\left(\frac{L}{r_1}\right) \qquad \text{(limiting case)} \qquad (2G\text{-}5)$$

where C'' is a constant of proportionality.

This indicates that the ratio of the heat loss to the system thermal capacity is approximately proportional to the length and inversely proportional to the radius.

The vessels are scaled up (after making adjustments for changes in temperatures relative to those in the ETF reference designs) by increasing the radii of the matrices without changing their lengths. Thus, the ratio of the heat loss from the vessels to the system capacity decreases as the vessels increase in size. For the limiting case, as given by equation (2G-5), the ratio is inversely proportional to the radius. The same qualitative trend holds true for the more precise relation given by equation (2G-3). For a case in which there is a change in the number of vessels, the heat transfer analysis must take into account the increase in number of vessels as well as the change in dimensions.

It is also necessary to determine the impact of scale-up on the distribution of the temperature within the insulation layers, because the materials are selected on the basis of a combination of their cost and thermal properties as well as their ability to

maintain their strength at high temperatures. For the configuration shown in figure 18, the temperature T_2 at radius r_2 (selected as a typical point for purposes of illustration) is given by the expression

$$T_2 = T_i - Q_L \left[\frac{1}{2\pi r_1 L h_1} + \frac{1}{2\pi L k_a} \ln\left(\frac{r_2}{r_1}\right) \right] \qquad (2G\text{-}6)$$

where Q_L can be found from equation (2G-1).

Under the same assumptions as those made in deriving equation (2G-4), an approximate relation for T_2 is given by

$$T_2 \quad T_i - \frac{\left(T_i - T_o\right)\left(\frac{1}{h_1} + \frac{t_a}{k_a}\right)}{\frac{1}{h_1} + \frac{t_a}{k_a} + \frac{t_b}{k_b} + \frac{t_c}{k_c} + \frac{1}{h_4}} \qquad (2G\text{-}7)$$

This equation indicates that the temperature distribution is independent of the radius for the limiting case of very thin layers. Therefore, under these circumstances, the temperature distribution does not change upon scaling to larger sizes. Although the convective heat transfer coefficients h_1 and h_4 may change slightly, their impact on the temperature distribution is small compared to that of the other terms in the equation. For instances in which the layers are not thin relative to the radius, there will be a minor change in the temperature distribution as the systems are scaled up.

Appendix 2H

Alternate Procedure for Scale-up: Modifying Insulation Layer Thicknesses to Retain Constant Percentage Heat Loss

In the scaling procedure employed in this investigation, the thicknesses of the insulation layers remain unchanged as the HTAH system vessels and ducts are increased in size. Equations are given in Appendix 2G which can be used to determine the change in the heat loss as the vessel and duct sizes are increased. These equations indicate that the ratio of the heat loss to the system thermal capacity decreases as the vessel and duct diameters increase, but increases as the vessel and duct lengths increase. For the scaling procedures employed, the decrease in relative heat loss due to increases in the diameter outweighs the increase in relative heat loss due to increases in the lengths, resulting in an increase in the system efficiency upon scaling up.

An alternate procedure is to reduce the thicknesses of the insulation layers as the system is scaled up - thereby resulting in a reduction in capital cost - while retaining the same ratio of heat loss to system thermal capacity for all system sizes. Approximate equations relating the thicknesses of insulation layers for the scaled up systems to the thicknesses of the corresponding insulation layers in the original system can be obtained from a steady state analysis in cylindrical and spherical coordinates.

Figure 19 shows two cross sections of a vessel or duct with several layers of insulation. The smaller cross section represents a part of a HTAH system of thermal capacity Q_c and the larger cross section represents the corresponding part of a larger HTAH system with a thermal capacity Q_c'. Both HTAH systems have the same number of vessels. The lengths of the two vessels or duct sections are L and L', respectively.

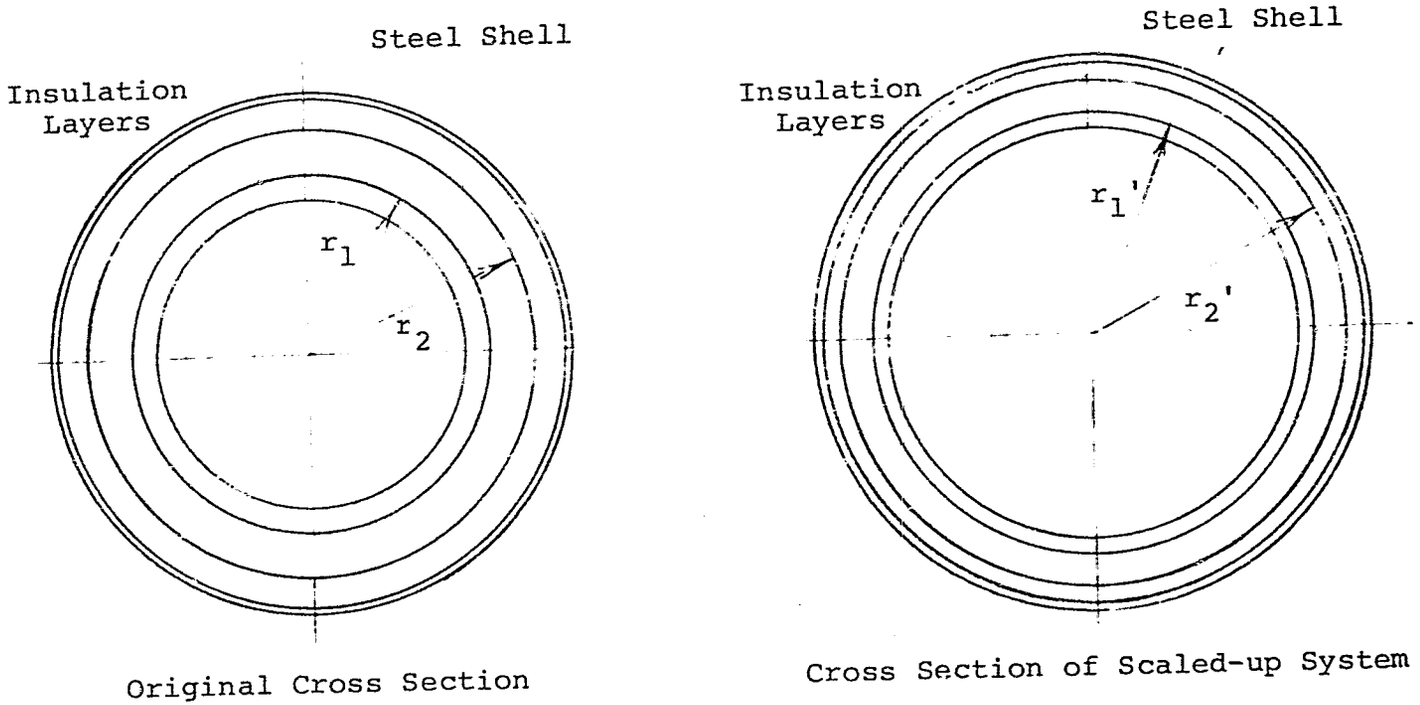

Figure 19. - Cross section of vessel or duct illustrating change in thickness of insulation layers.

The difference between the temperature T_1 at the inner radius r_1 of any layer and the temperature T_2 at the outer radius of the same layer is given by the relation

$$T_1 - T_2 = \frac{Q_L}{2\pi kL} \ln\left(\frac{r_2}{r_1}\right) \qquad \text{(2H-1)}$$

where Q_L is the rate of heat loss from the section of vessel or ducting and k is the thermal conductivity of the layer. The corresponding relation for the scaled up section of vessel or ducting is

$$T_1' - T_2' = \frac{Q_L'}{2\pi kL'} \ln\left(\frac{r_2'}{r_1'}\right) \qquad \text{(2H-2)}$$

where the primes denote parameters for the scaled up system. The thermal conductivity remains unchanged since the material is the same.

As the HTAH system is scaled up, it is necessary to maintain nearly the same temperatures at the interfaces between the layers because the materials in each layer have been selected on the basis of their properties in specified temperature ranges. Deviations from the original temperatures due to scaling of convective heat transfer are small because the temperature drops through the insulation layers are much larger than the temperature drops between the air or reheat gas and the innermost surface and between the vessel shell and the air outside the vessel.

Therefore, the temperature differences $T_1 - T_2$ and $T_1 - T_2'$ will be nearly the same and equations (2H-1) and (2H-2) yield the relation

$$\frac{Q_L}{2\pi kL} \ln\left(\frac{r_2}{r_1}\right) = \frac{Q_L'}{2\pi kL'} \ln\left(\frac{r_2'}{r_1'}\right) \qquad \text{(2H-3)}$$

Solving this equation for r_2'/r_1' yields the relation

$$\frac{r_2'}{r_1'} = \left(\frac{r_2}{r_1}\right)^{\left(\frac{Q_L}{Q_L'}\right)\left(\frac{L'}{L}\right)} \qquad \text{(2H-4)}$$

For the alternate scale up procedure in which the ratio of heat loss to system thermal capacity is held constant,

$$\frac{Q_L}{Q_L'} = \frac{Q_c}{Q_c'} \tag{2H-5}$$

Combining equations (2H-4) and (2H-5) yields the relation

$$\frac{r_2'}{r_1'} = \left(\frac{r_2}{r_1}\right)^{\left(\frac{Q_c}{Q_c'}\right)\left(\frac{L'}{L}\right)} \tag{2H-6}$$

The thicknesses t and t' of the layers are given by the expressions

$$t = r_2 - r_1 \tag{2H-7}$$

$$t' = r_2 - r_1' \tag{2H-8}$$

Equation (2H-6) can thus be written in the form

$$t' = r_1' - r_1'\left(1 - \frac{t}{r_1}\right)^{\left(\frac{Q_c}{Q_c'}\right)\left(\frac{L'}{L}\right)} \tag{2H-9}$$

For the vessels, the lengths L and L' are the same and, since $Q_c' > Q_c$, it follows that

$$t' < t \qquad \text{(for vessels only)} \tag{2H-10}$$

Equation (2H-9) will in general lead to non-standard insulation material thicknesses. An economic analysis would be required to determine whether it is preferable to utilize non-standard thicknesses or to increase the thickness to the nearest standard size.

The refractory thickness of the vessel dome cap scales in a different manner since its shape is approximately that of a partial hemisphere. The radius of curvature, a of a partial hemisphere of height, h and base diameter, b is given by the relation

$$a = \frac{(b/2)^2 + h^2}{2H} \tag{2H-11}$$

The symbols a, b and h are defined in figure 13. The scaling factors for a part of a sphere are the same as that for a complete sphere because of symmetry if the scaling relations are expressed in terms of the radii of the surfaces of the layers.

The heat transfer rate through a spherical layer of inner radius a_1 at temperature T_1 and outer radius a_2 at temperature T_2 is

$$q = 4\pi k \frac{T_1 - T_2}{1/a_1 - 1/a_2} \qquad \text{(2H-12)}$$

Scaling from the initial size to larger sizes in a manner similar to that of a cylinder as given by equations (2H-2) through (2H-9) yields

$$\frac{1}{a_1'} - \frac{1}{a_2'} = \left(\frac{1}{a_1} - \frac{1}{a_2}\right) \frac{Q}{Q'} \qquad \text{(2H-13)}$$

The scaled up thickness of each layer is determined from the relations

$$t' = a_2' - a_1' \qquad \text{(2H-14)}$$

and

$$a_2' = \left(\frac{1}{a_2'} - \left(\frac{1}{a_1} - \frac{1}{a_2}\right) \frac{Q}{Q'}\right)^{-1} \qquad \text{(2H-15)}$$

if a_1' is previously known, or

$$a_1' = \left(\frac{1}{a_2'} + \left(\frac{1}{a_1} - \frac{1}{a_2}\right) \frac{Q}{Q'}\right)^{-1} \qquad \text{(2H-16)}$$

if a_2' is previously known.

Appendix 2I

Basis for Determination of Modified Duct Dimensions

The inside diameter of each segment of ducting is adjusted and scaled up to accommodate differences in mass-flow rates, pressures and temperatures between the adjusted and scaled up HTAH systems and the corresponding ETF reference designs. The internal diameter of ducting in power plants is generally determined on the basis of compromises in which the capital cost advantages of smaller diameter ducting is traded off against the advantages of larger diameter ducting because of reduced pressure drop, leading to reduced operating costs and, possibly, reduced capital cost for fans or compressors. Erosion effects due to high velocities are also taken into consideration. For this investigation, the modifications in ducting inside diameters are determined by maintaining the same average fluid velocities in each section of ducting as in the ETF reference designs. The resulting changes in the system pressure drops are small compared to the total system pressure drops. For duct sections which must handle both the MHD combustor air and the reheat gas, it is the larger of the two velocities which is kept constant.

The mass flow rate m of an ideal gas through a duct section is related to the average gas velocity V by the relation

$$m = \frac{\pi}{4} \frac{pD^2}{RT} V \qquad (2I\text{-}1)$$

where p is the absolute pressure, D is the internal diameter of the duct, R is the ideal gas constant and T is the absolute temperature. The velocity is a constant only if the term

$$\frac{mT}{pD^2} \qquad (2I\text{-}2)$$

is a constant. Therefore, the duct diameter D' for the adjusted and scaled-up HTAH system is related to the duct diameter for the ETF reference design by the expression

$$D' = D\sqrt{\frac{m'T'p}{mTp'}} \qquad (2I\text{-}3)$$

where the primed terms denote the adjusted and scaled up systems, and the non-primed terms denote the ETF reference design.

The length of each duct section is modified in accordance with the HTAH system layout to accommodate increases in size and/or number of vessels. The thicknesses of the insulation layers for each duct section are the same for the adjusted and scaled-up designs as they are for the ETF reference designs. The inner diameter of the ductwork steel D_s is equal to the sum of the modified duct inner diameter and the thicknesses of the internal insulation layers as given by

$$D_s = D_o + 2 \sum_{i=1}^{n} t_i \qquad (2I\text{-}4)$$

where D_o is the diameter of the duct internal to the insulation, t_i is the thickness of the ith layer of insulation and n is the number of layers.

The ductwork steel thickness t_w is determined, in accordance with ASME Power Piping Codes, using the equation

$$t_w = \frac{P_d d_w}{2(SE + Py)} + t_c \qquad (2I\text{-}5)$$

where P_d is the design pressure, d_w is the outer diameter of the steel duct, S is the maximum allowable stress, E is the joint efficiency, y is an adjustment factor which depends upon the metal temperature and t_c is a corrosion allowance. The design pressure is given by

$$P_d = P_1 + P_2 \qquad (2I\text{-}6)$$

where P_1 is the pressure of the air or gas inside the vessel and P_2 is the additional pressure due to refractory expansion. The values of S and E are taken to be the same values as reported in the ETF final reports for the reference design calculations. The design thicknesses selected for the scaled up cases are the next standard mill size which is greater than the calculated thickness.

Appendix 2J

Basis for Determination of the Number of Vessels for Scaled-up HTAH Systems

In scaling up a HTAH system, there is the option of (1) increasing the dimensions of the vessels and ducting without changing the number of vessels or (2) increasing the number of vessels and determining the vessel and duct sizes required to provide the required system capacity with that number of vessels. Since there are practical limits to sizes of vessels, ducting and valves, both options must be employed in order to cover the range of system thermal capacities from 100 MW_t to 1000 MW_t.

The determination of the relationship between vessel (i.e., matrix) size, HTAH system capacity and the number of vessels requires an investigation of the operating modes and the patterns of sequencing, timing and switching for the HTAH systems. The patterns and the basis for selecting the numbers of vessels differs from case to case. Cases B and C have the same pattern, but the patterns for Cases A and D differ from this pattern as well as from each other.

The ETF reference design for Case A is a four-vessel system. Under normal operating conditions, all four vessels are utilized. In the event that one vessel is inoperable due to failure or scheduled maintenance, the remaining three vessels are capable of providing preheated air at full capacity. Under normal operation with four vessels, the system operates in the staggered parallel mode with two vessels on blowdown and two vessels on reheat except during the brief switchover periods when two vessels are on blowdown and one is on reheat. The time period for each vessel on blowdown is 20 minutes. The time period for each vessel on reheat is 20 minutes minus the sum of the periods for switching from blowdown to reheat and from reheat to blowdown.

Under emergency operation with three vessels, the system operates in the single mode with one vessel on blowdown and two

vessels on reheat except during the brief switchover periods when one vessel is on blowdown and one is on reheat. The time period for each vessel on blowdown is 10 minutes. The time period for each vessel on reheat is 20 minutes minus the sum of the periods for switching from blowdown to reheat and from reheat to blowdown. Thus, in converting from four-vessel operation to three-vessel operation, the reheat time period and average reheat gas flow rate per vessel remain the same, but the time period on blowdown is reduced by one half while the average air flow rate per vessel is doubled. These conditions are summarized in table XXXII.

The guiding principle in increasing the number of vessels for Case A is to retain the same time period on reheat as in the ETF reference design and to utilize the minimum number of blowdown vessels consistent with the number of reheat vessels such that the time period for air blowdown is greater than or equal to the minimum air blowdown time for the ETF reference design. That is,

$$t_r = 20_{min} - t_{s1} - t_{s2} \qquad (2J\text{-}1)$$

$$t_b \geq 10_{min} \qquad (2J\text{-}2)$$

where t_r is the reheat time period, t_{s1} is the time period for switching from blowdown to reheat, t_{s2} is the time period for switching from reheat to blowdown and t_b is the blowdown time period. These conditions must apply when a specified number of vessels is inoperable due to failure or scheduled maintenance.

For example, the next smallest number of vessels which would meet these requirements is six, in a system which can operate at full capacity with five vessels when necessary. When operating with only five vessels, three are on reheat at a time (for 20 minutes minus switching time, each) while two are on blowdown at a time (for 13.33 minutes, each). When operating with six vessels, three are on reheat at a time (for 20 minutes minus switching time, each) while three are on blowdown at a time (for 20 minutes each). In comparing a system with six vessels of a given size with a

TABLE XXXII. - OPERATING MODES AND PERIODS OF OPERATION FOR THE ETF REFERENCE DESIGN FOR CASE A

Number of Vessels in HTAH System: 4

Normal Operating Mode

"Staggered-Parallel" with 4 vessels

Number of Vessels on Reheat

2, except during switchover

1 during switchover

Number of Vessels on Blowdown

2

Durations per Vessel

Reheat: 20 minutes minus switching time

Blowdown: 20 minutes

Switching: unspecified

Emergency Operating Mode

"Single" with 3 vessels

Number of Vessels on Reheat

2, except during switchover

1 during switchover

Number of Vessels on Blowdown

1

Duration per Vessel

Reheat: 20 minutes minus switching time

Blowdown: 10 minutes

Switching: unspecified

system of four vessels of the same size, the average flow rate of reheat gas in each vessel would be the same in both cases and the flow rate of air in each vessel for the six-vessel system would not exceed the maximum flow rate of air in each vessel for the four-vessel system. These relations between the flow rates are consistent with the restrictions indicated in equations (2J-1) and (2J-2). Under these conditions, a six-vessel HTAH system provides fifty percent more capacity than a four-vessel system comprised of vessels of the same size.

Table XXXIII is a summary of the operating patterns and time periods for HTAH systems for Case A with various numbers of vessels. In each case the number of vessels is the optimum number which will satisfy equations (2J-1) and (2J-2) and will provide a measure of system reliability by having at least one more vessel than the minimum number capable of providing full capacity. For systems with up to 10 vessels, there is one more vessel than the minimum number required. For systems with more than 10 vessels, an option of operating with either one or two more vessels than the minimum number required is indicated.

The ETF reference design for Case B is a four-vessel system just as in Case A. Under normal operating conditions, all four vessels are utilized. In the event that one vessel is inoperable due to failure or scheduled maintenance, the remaining three vessels are capable of providing preheated air at full capacity. The operation of the system for Case B differs from the operation in Case A for both four-vessel and three-vessel operation. Under normal operation with four vessels, the system operates in the staggered parallel mode with one vessel on reheat, two vessels on blowdown and one vessel always in the process of switching either from reheat to blowdown or from blowdown to reheat. The time period for each vessel on reheat is 20 minutes; the time period for each vessel on blowdown is 40 minutes and the time period for each vessel on switchover (from either reheat to blowdown or vice versa) is 10 minutes.

TABLE XXXIII. - OPERATING-MODE DATA AND RELATIVE SYSTEM THERMAL CAPACITIES FOR HTAH SYSTEMS WITH VARIOUS NUMBERS OF VESSELS OF ONE GIVEN SIZE FOR CASE A

Number of Vessels in HTAH System	4	6	7	9	10	11	12	13	14	21	27
Relative HTAH System Thermal Capacity (Percent)*	100	150	200	250	300	300	350	350	400	600	800
Number of Vessels in Excess of Minimum Required	1	1	1	1	1	2	1	2	2	3	3
Normal Mode Conditions											
Number of Vessels Utilized	4	6	7	9	10	11	12	13	14	21	27
Number on Reheat Except During Switchover	2	3	4	5	6	6	7	7	8	12	16
Number on Reheat During Switchover	1	2	3	4	5	5	6	6	7	11	15
Number on Blowdown	2	3	3	4	4	5	5	6	6	9	11
Period on Reheat (Minutes) and 2 Switchover Periods	20	20	20	20	20	20	20	20	20	20	20
Period on Blowdown (Minutes)	20	20	15	16	13.3	16.7	14.3	17.1	15	15	13.3
Period on Switchover from Blowdown to Reheat (Minutes)	Unspec.	Unspec.	Unspec.	Unspec.	Unspec.	Unspec.	Unspec.	Unspec.	Unspec.	Unspec.	Unspec.
Period on Switchover from Reheat to Blowdown (Minutes)	Unspec.	Unspec.	Unspec.	Unspec.	Unspec.	Unspec.	Unspec.	Unspec.	Unspec.	Unspec.	Unspec.
Relative Average Reheat Gas Flow Rate Per Vessel (Percent)*	100	100	100	100	100	100	100	100	100	100	100
Relative Average Air Flow Rate Per Vessel (Percent)*	50	50	66.7	62.5	75	60	70	58.3	66.7	66.7	72.7
Emergency Mode Conditions											
Number of Vessels Utilized	3	5	6	8	9	9	11	11	12	18	24
Number on Reheat Except During Switchover	2	3	4	5	6	6	7	7	8	12	16
Number on Reheat During Switchover	1	2	3	4	5	5	6	6	7	11	15
Number on Blowdown	1	2	2	3	3	3	4	4	4	6	8
Period on Reheat (Minutes) and 2 Switchover Periods	20	20	20	20	20	20	20	20	20	20	20
Period on Blowdown (Minutes)	10	13.3	10	12	10	10	11.4	11.4	10	10	10
Period on Switchover from Blowdown to Reheat (Minutes)	Unspec.	Unspec.	Unspec.	Unspec.	Unspec.	Unspec.	Unspec.	Unspec.	Unspec.	Unspec.	Unspec.
Period on Switchover from Reheat to Blowdown (Minutes)	Unspec.	Unspec.	Unspec.	Unspec.	Unspec.	Unspec.	Unspec.	Unspec.	Unspec.	Unspec.	Unspec.
Relative Average Reheat Gas Flow Rate Per Vessel (Percent)*	100	100	100	100	100	100	100	100	100	100	100
Relative Average Air Flow Rate Per Vessel (Percent)*	100	75	100	83.3	100	100	87.5	87.5	100	100	100

*System thermal capacities and flow rates as measured relative to a 4-vessel HTAH system with vessels of same size (blowdown flow rate measured relative to that of blowdown flow rate in 3-vessel emergency mode)

Under emergency operation with three vessels, the system operates in the series mode with one vessel on reheat, one vessel on blowdown and one vessel on switchover. The time periods for each vessel on reheat, blowdown and switchover are 20 minutes, 20 minutes and 10 minutes, respectively. Thus, in converting from four-vessel operation to three-vessel operation, the number of vessels on reheat and their time periods remain unchanged, while the number of vessels on blowdown is reduced from two to one with a reduction in the blowdown time period by 50 percent. The average air flow rate per vessel is, therefore, doubled. These conditions are summarized in table XXXIV.

There are two major characteristics which distinguish Case B from Case A. One is the utilization of one vessel at a time on reheat for Case B. This means that each vessel in Case B is sized for handling the entire reheat gas flow rate. Furthermore, since each vessel is connected to its own combustion chamber and burner system, the HTAH requires four full-size combustion systems. Another unique characteristic of the Case B HTAH system is that there is always one vessel in the switchover mode, so that the full flow capacity is being carried by the remaining vessels. These distinguishing characteristics play a significant role in determining the manner of selecting the number of vessels. The HTAH system for Case B tends to benefit from increasing the number of vessels to a greater extent than does the HTAH system for Case A, since the larger the number of vessels, the more there are to share the total reheat gas flow capacity and the shorter the durations of the switchover periods.

The guiding principle in increasing the number of vessels for Case B is to retain the same time period on reheat as in the ETF reference design and to make the number of blowdown vessels a specified number greater than the number of reheat vessels. The specified number will be one more than the difference between the number of vessels operating in the normal mode

TABLE XXXIV. - OPERATING MODES AND PERIODS OF OPERATION FOR THE ETF REFERENCE DESIGN FOR CASES B AND C

Number of Vessels in HTAH System: 4

Normal Operating Mode

"Staggered-Parallel" with 4 vessels

Number of Vessels on Reheat: 1

Number of Vessels on Blowdown: 2

Number of Vessels on Switchover: 1

Duration per Vessel

Reheat: 20 minutes

Blowdown: 40 minutes

Switchover: 10 minutes

Emergency Operating Mode

"Series" with 3 vessels

Number of Vessels on Reheat: 1

Number of Vessels on Blowdown: 1

Number of Vessels on Switchover: 1

Duration per Vessel

Reheat: 20 minutes

Blowdown: 20 minutes

Switchover: 10 minutes

and the number operating in the emergency mode. By this procedure, the number of blowdown vessels in the emergency mode will be the same as the number of reheat vessels and the time period on blowdown (for emergency operation) will be the same as in the ETF reference design. During the normal operating mode, the duration of operation of each vessel on blowdown is greater than the time period on blowdown during emergency operation. The switchover time period decreases as the number of vessels in the HTAH system increases. Thus, for a HTAH system with any number of vessels greater than four,

$$t_r = 20 \text{ minutes} \tag{2J-3}$$

$$t_b = 20 \text{ minutes in emergency mode} \tag{2J-4}$$

$$t_b > 20 \text{ minutes in normal mode} \tag{2J-5}$$

$$t_s < 10 \text{ minutes} \tag{2J-6}$$

For example, the next smallest number of vessels which meets these requirements is six, in a system which can operate at full capacity with five vessels when necessary. When operating with only five vessels, there are two on reheat, two on blowdown and one switching at a time. The time durations on reheat, blowdown and switchover are, respectively, 20 minutes, 20 minutes and 5 minutes. When operating with six vessels, there are two on reheat, three on blowdown and one switching at a time. The time durations on reheat, blowdown and switchover are, respectively, 20 minutes, 30 minutes and 5 minutes. In comparing a system with six vessels of a given size with a system of four vessels of the same size, the average flow rate of reheat gas in each vessel would be the same in both cases and the flow rate of air in each vessel for the six-vessel system would not exceed the maximum flow rate of air in each vessel for the four-vessel system. These relations between the flow rates are consistent with the restrictions indicated in equations (2J-3) through (2J-6). Under these conditions, a six-vessel HTAH system provides 100 percent more capacity than a four-vessel system comprised of vessels of the same size. This dramatically illustrates the greater sensitivity to the number of

vessels for Case B than for Case A, in which there is only a 50 percent increase in total system capacity due to increasing the number of vessels from four to six.

Table XXXV is a summary of the operating patterns for HTAH systems for Case B with various numbers of vessels. In each case, the number of vessels is the optimum number which will satisfy equations (2J-3) through (2J-6) and will provide a measure of system reliability by having at least one more vessel than the minimum number capable of providing full capacity. For systems with up to 8 vessels, there is one more vessel than the minimum required. For systems with more than 8 vessels, the table shows the option of operating with either one or two more vessels than the minimum number required.

The ETF reference design for Case C differs from that of Case B only in the combustion system (i.e. combustion chamber and burners), the fuel supply system and the ducting which provides air and fuel to the combustion system. The air heater vessels and the remainder of the system are identical with that of Case B. Therefore, the rationale for selecting the number of vessels for Case C is the same as the rationale which has been described for Case B. Tables XXXIV and XXXV are applicable to both Cases B and C.

The ETF reference design for Case D is a fourteen-vessel system. There is only one mode of operation and it utilizes twelve of the fourteen vessels. The other two are spares which are not utilized in the operating sequence. Over the lifetime of the HTAH system, all fourteen vessels can be fully utilized by alternating which vessels are designated as spares. Because of the large number of vessels the sizes of the vessels for Case D are much smaller than the vessels in the ETF reference designs for Cases A, B and C. Therefore it is feasible to scale the HTAH system for Case D up to a thermal capacity of 1000 MW_t without increasing the number of vessels since the sizes of the vessels and the valves for the 1000 MW_t thermal capacity level are within the limits which are considered to be practical.

TABLE XXXV. - OPERATING-MODE DATA AND RELATIVE SYSTEM THERMAL CAPACITIES FOR HTAH SYSTEMS WITH VARIOUS NUMBERS OF VESSELS OF ONE GIVEN SIZE FOR CASES B AND C

Number of Vessels in HTAH System	4	6	8	9	10	11	12	13	15	20
Relative HTAH System Thermal Capacity (Percent)*	100	200	300	300	400	400	500	500	600	800
Number of Vessels in Excess of Minimum Required	1	1	1	2	1	2	1	2	2	3
Normal Mode Conditions										
Number of Vessels Utilized	4	6	8	9	10	11	12	13	15	20
Number on Reheat	1	2	3	3	4	4	5	5	6	8
Number on Blowdown	2	3	4	5	5	6	6	7	8	11
Period on Reheat (Minutes)	20	20	20	20	20	20	20	20	20	20
Period on Blowdown (Minutes)	40	30	26.7	33.3	25	30	24	28	26.7	27.5
Period on Switchover from Blowdown to Reheat (Minutes)	10	5	3.33	3.33	2.5	2.5	2	2	1.67	1.25
Period on Switchover from Reheat to Blowdown (Minutes)	10	5	3.33	3.33	2.5	2.5	2	2	1.67	1.25
Relative Average Reheat Gas Flow Rate Per Vessel (Percent)*	100	100	100	100	100	100	100	100	100	100
Relative Average Air Flow Rate Per Vessel (Percent)*	50	66.7	75	60	80	66.7	83.3	71.4	75	72.7
Emergency Mode Conditions										
Number of Vessels Utilized	3	5	7	7	9	9	11	11	13	17
Number on Reheat	1	2	3	3	4	4	5	5	6	8
Number on Blowdown	1	2	3	3	4	4	5	5	6	8
Period on Reheat (Minutes)	20	20	20	20	20	20	20	20	20	20
Period on Blowdown (Minutes)	20	20	20	20	20	20	20	20	20	20
Period on Switchover from Blowdown to Reheat (Minutes)	10	5	3.33	3.33	2.5	2.5	2	2	1.67	1.25
Period on Switchover from Reheat to Blowdown (Minutes)	10	5	3.33	3.33	2.5	2.5	2	2	1.67	1.25
Relative Average Reheat Gas Flow Rate Per Vessel (Percent)*	100	100	100	100	100	100	100	100	100	100
Relative Average Air Flow Rate Per Vessel (Percent)*	100	100	100	100	100	100	100	100	100	100

*System thermal capacities and flow rates as measured relative to a 4-vessel HTAH system with vessels of same size (blowdown flow rate measured relative to that of blowdown flow rate in 3-vessel emergency mode)

The determination of the optimum number of vessels to achieve a specified overall system thermal capacity is basically a matter of the comparative economics of the available options. However, there are several factors which are significant but which do not have a direct impact on the capital cost of the HTAH system. One of these factors is the amplitude of the fluctuations in delivered preheated air temperature. As the number of vessels is increased, the amplitude of the temperature fluctuations decreases because of the more frequent switching. This reduces the penalty in performance or the cost of employing other means (such as a by-pass) to minimize the fluctuations.

Another factor is the lifetimes of the refractory matrix materials and the valves. In Cases A, B and C, the lifetimes of the matrix materials are reduced as the relative flow rates of air through the matrices increases in accordance with the data given in tables XXXIII and XXXV. The valve lifetimes also decrease with greater frequency of operation which can be determined from the durations of operation which are also indicated in tables XXXIII and XXV.

The reliability and availability of the HTAH system depends upon the number of vessels in excess of the minimum number required relative to the minimum number of vessels. In a four-vessel system, the redundancy is one vessel out of three (33 percent), while in a six-vessel system, the redundancy is one out of five (20 percent). Due to lack of data and experience on the use of HTAH systems in MHD power plants, it is not possible to judge, with any specific degree of assurance, the relative merits of these two cases in terms of a reliability/cost tradeoff.

Appendix 2K

Basis for Determination of Modified Fuel, Combustion Air and Recirculation Flue Gas Flow Rates

Figure 20 is a schematic diagram showing the flow stream conditions associated with the HTAH system combustion process. This figure serves as a basis for developing the combustor mass and energy balance equations. Thermal energy is provided from three sources: (a) the fuel, (b) prehe ting the combustion air and (c) reheating the recirculation flue gas. The purpose of recirculating some flue gas back to the combustor is to provide a means for controlling the combustion gas temperature T_g for protection of the refractory materials in the HTAH system.

As indicated in tables IX through XII, the combustion air temperature T_c and the recirculation flue gas temperature T_r for the NASA HTAH system specifications are different from the corresponding temperatures for the ETF reference designs. This difference represents a change in relative rates of thermal energy input from the three sources. For the case in which the temperatures specified by NASA are higher than those specified for the ETF reference designs, it is necessary to reduce the fuel flow rate to achieve the same total thermal energy input to the combustion system. For the opposite case, the fuel flow rate must be increased. It is also necessary to modify the combustion air flow rate m_c and the recirculation gas flow rate m_r to maintain the same total flow rate m_g and the same fuel-to-combustion-air ratio.

The adjustments in the three flow rates m_f, m_c and m_r to accommodate changes in the temperatures T_c and T_r are made on the basis of (a) constant mass flow rate of combustion gas m_g, (b) constant enthalpy of the combustion gas and (c) constant fuel-to-combustion-air ratio. The assumption is also made that the heat loss Q_{LC} from the combustion system is constant. Thus the relations which form the basis of the adjustments are

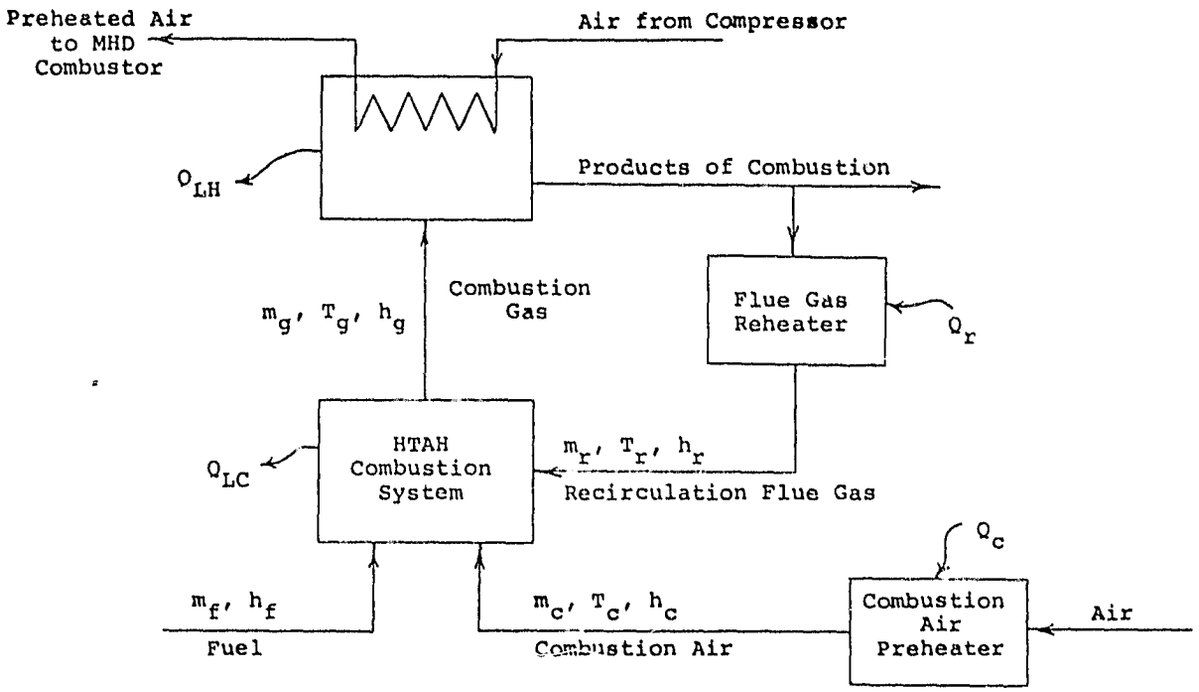

Figure 20. - Schematic Diagram of Indirectly-Fired HTAH System Combustion System Flow Rates and Flow Conditions

$$m_{g2} = m_{g1} \tag{2K-1}$$

$$h_{g2} = h_{g1} \tag{2K-2}$$

$$\frac{m_{f2}}{m_{c2}} = \frac{m_{f1}}{m_{c1}} = f \tag{2K-3}$$

$$Q_{LC1} = Q_{LC2} \tag{2K-4}$$

where the subscript 1 denotes the values of the parameters under ETF reference design conditions, the subscript 2 denotes the values of the parameters under the NASA specifications and f is the fuel-to-air mass ratio.

The equation expressing the mass balance for the combustion system is

$$m_g = m_f + m_c + m_r \tag{2K-5}$$

The equation expressing the energy balance for the combustion system is

$$m_g h_g + Q_{LC} = m_f h_f + m_c h_c + m_r h_r \qquad (2K\text{-}6)$$

Combining equations (2K-5) and (2K-6) with equations (2K-1), (2K-2) and (2K-4) and introducing subscripts to denote the two different sets of specifications yields the relations

$$m_{f2} + m_{c2} + m_{r2} = m_{f1} + m_{c1} + m_{r1} \qquad (2K\text{-}7)$$

and

$$m_{f2}h_{f2} + m_{c2}h_{c2} + m_{r2}h_{r2} = m_{f1}h_{f1} + m_{c1}h_{c1} + m_{r1}h_{r1} \qquad (2K\text{-}8)$$

The parameters m_{f1} and m_{f2} can be eliminated from these two equations by employing equation (2K-3), resulting in the relations

$$(1 + f)m_{c2} + m_{r2} = (1 + f)m_{c1} + m_{r1} \qquad (2K\text{-}9)$$

and

$$(h_{c2} + fh_{f2})m_{c2} + h_{r2}m_{r2} = (h_{c1} + fh_{f1})m_{c1} + h_{r1}m_{r1} \qquad (2K\text{-}10)$$

These two equations can be solved simultaneously to provide an expression for the adjusted combustion air flow rate and equations (2K-3) and (2K-7) can be employed to provide expressions for determining the adjusted fuel and recirculation gas flow rates as follows

$$m_{c2} = \frac{\left[(1 + f)m_{c1} + m_{r1}\right]h_{r2} - (h_{c1} + fh_{f1})m_{c1} - h_{r1}m_{r1}}{(1 + f)h_{r2} - (h_{c2} + fh_{f2})} \qquad (2K\text{-}11)$$

$$m_{f2} = fm_{c2} \qquad (2K\text{-}12)$$

$$m_{r2} = m_{f1} - m_{f2} + m_{c1} - m_{c2} + m_{r1} \qquad (2K\text{-}13)$$

Appendix 2L

Basis for Determination of Fuel Savings Due to Reduction in Percentage Heat Loss

Equations were derived in Appendix 2G for determining changes in heat loss due to modifications of system dimensions on the basis of retaining the same thickness of insulation layers as the equipment is scaled up. A reduction in heat loss increases the efficiency of the HTAH system. This can lead to either an increase in the air preheat temperature or a reduction in the amount of fuel required to preheat a given amount of air to the specified temperature. Since the maximum air preheat temperature is determined primarily by materials limitations, a reduction of heat loss is considered to result in a fuel savings.

An energy balance for the heat exchanger vessels and ducting can be developed with the aid of figures 13 and 20. The heat loss Q_{LC} from the combustion system can be combined with the heat loss Q_{LH} from the heat exchanger vessels and ducting and denoted as the total system heat loss Q_L.

$$Q_L = Q_{LC} + Q_{LH} \tag{2L-1}$$

The thermal energy Q_A delivered to the air is

$$Q_A = m_a(h_{a2} - h_{a1}) \tag{2L-2}$$

where m_a is the flow rate of the MHD air, h_{a1} is the enthalpy of the MHD air at the inlet to the HTAH system and h_{a2} is the enthalpy of the MHD air at the outlet.

The energy balance across the HTAH system is

$$m_f h_f + m_c h_c + m_r h_r - m_p h_p = m_a(h_{a2} - h_{a1}) + Q_L \tag{2L-3}$$

where m_f, m_c, m_r and m_p are the flow rates of the fuel, combustion air, recirculation flue gas and products of combustion, respectively and h_f, h_c, h_r and h_p are the fuel inlet enthalpy, combustion air inlet enthalpy, recirculation flue gas inlet enthalpy and the combustion products exit enthalpy, respectively.

The left-hand side of equation (2L-3) can be rearranged by factoring out the fuel flow rate and equation (2L-2) can be introduced, yielding the expresssion

$$m_f\left(h_f + \frac{m_c}{m_f} h_c + \frac{m_r}{m_f} h_r - \frac{m_p}{m_f}\right) = Q_A + Q_L \qquad (2L\text{-}4)$$

As the HTAH system is scaled up in size without alteration of any of the flow conditions, the expression in parentheses remains constant. Therefore, in scaling up the high temperature air heater system from a thermal capacity of Q_A to a thermal capacity of Q_A',

$$\frac{m_f'}{Q_A' + Q_L'} = \frac{m_f}{Q_A + Q_L} \qquad (2L\text{-}5)$$

where the primed quantities correspond to the scaled up system and the un-primed quantities correspond to the original system with identical inlet and exit flow conditions.

From equation (2L-5), it follows that the fuel requirement scales according to the relation

$$\frac{m_f'}{m_f} = \frac{1 + q'}{1 + q}\left(\frac{Q_A'}{Q_A}\right) \qquad (2L\text{-}6)$$

where q and q' are the fractional heat losses for the original system and the scaled up system, respectively, as defined by the equations

$$q = \frac{Q_L}{Q_A} \qquad (2L\text{-}7)$$

$$q' = \frac{Q_L'}{Q_A'} \qquad (2L\text{-}8)$$

Appendix 2M

Cost Estimating Computer Program

A computer program was developed for this investigation for handling the large amount of data required. The input to the program includes unit materials prices (dollars per pound or dollars per cubic foot), unit installation costs (dollars per cubic foot) and all the required dimensions of the system components. The program determines the quantities of each type of material specified and multiplies the quantities by the corresponding unit costs. The program prints out the direct cost for each major item in the system as indicated in table XXXVI as well as the total system direct cost for materials and installation.

Table XXXVII is a listing of the program and table XXXVIII is a printout of the estimated costs for the 100 MW_t HTAH system for Case B, selected as a typical example. The calculations of the scaled up dimensions for each system size and the costing of auxiliary equipment are not incorporated into this computer program.

TABLE XXXVI. - COST ESTIMATING COMPUTER PROGRAM TYPICAL DATA PRINTOUT FORMAT

Heat Exchanger/Combustion Chamber (One Unit)	
Checkerbrick Matrix	- Material Cost - Installation Cost
Matrix Support	- Material Cost - Installation Cost
Heat Exchanger Shell	- Material Cost - Installation Cost
Heat Exchanger Insulation	- Material Cost - Installation Cost
Reheat Combustion Chamber Shell	- Material Cost - Installation Cost
Reheat Combustion Chamber Insulation	- Material Cost - Installation Cost
Total Heat Exchanger/Combustor	
Chamber Cost (One Unit)	- Material Cost - Installation Cost
Total Heat Exchanger/Combustor	
Chamber Cost (All Units)	- Material Cost - Installation Cost
Ducting	
Burner Air Inlet Manifold	
Shell	- Material Cost - Installation Cost
Insulation	- Material Cost - Installation Cost
Burner Fuel Oil Pipe	- Material Cost - Installation Cost
Burner Recycle Gas Inlet Manifold	
Shell	- Material Cost - Installation Cost
Insulation	- Material Cost - Installation Cost
Burner-Checker Chamber Crossover	
Shell	- Material Cost - Installation Cost
Insulation	- Material Cost - Installation Cost
Combustion Gas Exit Manifold	
Shell	- Material Cost - Installation Cost
Insulation	- Material Cost - Installation Cost
Air Blowdown Inlet Manifold	
Shell	- Material Cost - Installation Cost
Insulation	- Material Cost - Installation Cost
High Temperature Air Outlet Manifold	
Shell	- Material Cost - Installation Cost
Insulation	- Material Cost - Installation Cost
Pressurization/Depressurization Manifold	
Shell	- Material Cost - Installation Cost
Insulation	- Material Cost - Installation Cost
Total Ducting Cost	
Shell	- Material Cost - Installation Cost
Insulation	- Material Cost - Installation Cost
Total HTAH System Cost	- Material Cost - Installation Cost - Total Direct Cost

TABLE XXXVII. - COST ESTIMATING COMPUTER PROGRAM LISTING

```
PROGRAM HTAH        74/74    OPT=0 TRACE                 FTN 4.6+423F                  10.14.00        PAGE     1

          PROGRAM HTAH(INPUT,OUTPUT,TAPE5=INPUT,TAPE6=OUTPUT)
    C
          REAL MC,MH,MP,MA,MW,NUNIT(1),NUNITMC,NUNITIC
          REAL MMLC,MILC,MMC,MIC
          DIMENSION CIT(5), CIH(5), CIF(5), CIIA(5), CIIH(5), CIIP(5)
          DIMENSION CIMLC(5),CIILC(5),CIMC(5),CIIC(5)
          DIMENSION CIIN(8),CIIMLC(8),CIIILC(8),CIIMC(8),CIIIC(8)
          DIMENSION CIN(5), CIIC(5), DIT(5), DIP(5), DIN(5), DICD(5), DIH(5)
          DIMENSION DIMLC(5),DIILC(5),DIMC(5),DIIC(5)
          DIMENSION RICIC(5), RICT(5), RICH(5), RICP(5), RICW(5)
          DIMENSION RIDT(5), RIDH(5), RIDP(5), RIDCD(5), RIDN(5)
          DIMENSION RICMLC(5),RICILC(5),RICMC(5),RICIC(5)
          DIMENSION RIDMLC(5),RIDILC(5),RIDMC(5),RIDIC(5)
          DIMENSION RID(10), RT(10), RP(10), PL(10), PW(10),INS(10),NINS(10)
          DIMENSION PICD(10,5), PIT(10,5), PIP(10,5), PIN(10,5),PPUC(10)
          DIMENSION PILC(10),PIMLC(10,5),PIILC(10,5),PIMC(10,5),PIIC(10,5)
          DIMENSION PMC(10),PIC(10),FIFNAME(4),TITLE(6),TITLE2(6)
          INTEGER CIN, CII, DIN, RICN, RIDN
          LOGICAL A,PC,D
    C
          READ(5,50) NCASE
       50 FORMAT(I3)
          DO 1000 N=1,NCASE
          PI=3.14159
          NPAGE=1
          DAY=DATE(A)
          READ(5,75) (TITLE(J),J=1,6),(TITLE2(J),J=1,6)
       75 FORMAT(6A10,/,6A10)
          READ(5,100)  A,PC,D
      100 FORMAT(3L1)
          WRITE(6,110) NPAGE,DAY
      110 FORMAT(1H1,//    ,10X,*W.O. #3473-02*,10X,*NASA-LEWIS*
         1 * HIGH TEMPERATURE AIR HEATER COST SUMMARY*,
         1 T105,*PAGE *,I3,/,T104,A10)
          WRITE(6,112) TITLE,TITLE2
      112 FORMAT(40X,6A10,///,30X,6A10)
    C
    C    CHECKERBRICK MATRIX
    C     MC - DIAMETER
    C     MH - HEIGHT
    C     MP - DENSITY
    C     MA - CROSS-SECTIONAL AREA
    C     MW - TOTAL WEIGHT
    C
          READ(5,200) MC,MH,MP,MA,MMLC,MIUC
      200 FORMAT(6F10.0)
          IF(A) GO TO 210
          MA=PI*MC**2/4
      210 MW=MA*MH*MP
          MMC=MMLC*MW/1000.
          MIC=MILC*MW/1000.
    C
          WRITE(6,220)
      220 FORMAT(/,20X,*CHECKERBRICK MATRIX*)
          IF(A) GO TO 224
          WRITE(6,222) MC
      222 FORMAT(/,25X,*DIAMETER - *,F4.1,* FT.*)
```

```
      224 WRITE(6,225) PA
      225 FORMAT(/,25X,*CROSS SECTIONAL AREA = *,F5.1,* S.F.*)
          WRITE(6,228) PH,PP,PMLC,PILC,PW,PMC,PIC
      228 FORMAT(/25X,*HEIGHT = *,F4.1,* FT.*,/,
     1 25X,*DENSITY = *,F5.1,* LB/CU.FT.*,/,
     1 25X,*UNIT MAT'L. COST = $*,F4.2,* /LB.*,/,
     1 25X,*UNIT INST'L. COST = $*,F4.2,* /LB.*,/,
     1 T40,*MATRIX WEIGHT = *,FE.0,* LB.*,/,
     1 T7*,*MATRIX MAT'L. COST = $ *,FE.0,T100,*00C.*,/,
     1 T72,*MATRIX INST'L. COST = $ *,FE.0,T100,*00C.*)
C
C
C
C
C
C     MATRIX SUPPORT
C       SCN - # OF COLUMNS
C       SCW - WEIGHT PER COLUMN
C       SGL - TOTAL GIRDER LENGTH
C       SGW - WEIGHT PER FT. OF GIRDER
C       SGRW - WEIGHT PER S.F. OF GRATE
C       SCTOTW - TOTAL COLUMN WEIGHT
C       SGTOTW - TOTAL GIRDER WEIGHT
C       SGRTOTW - TOTAL GRATE WEIGHT
C       STOTW - TOTAL SUPPORT WEIGHT
C
        READ(5,255) SCN,SCW,SGL,SGW,SGRW,SMUC,SILC
      255 FORMAT(7F10.0)
          SCTOTW=SCN*SCW
          SGTOTW=SGL*SGW
          SGRTOTW=SGRW*PA
          STOTW=SCTOTW+SGTOTW+SGRTOTW
          SMC=STOTW*SMUC/1000.
          SIC=STOTW*SILC/1000.
C
          WRITE(6,260) SCN,SCW,SGL,SGW,SGRW,SMUC,SILC,
     1 SCTOTW,SGTOTW,SGRTOTW,STOTW,SMC,SIC
      260 FORMAT(20X,*MATRIX SUPPORT*,//,
     1 25X,*NO. OF COLUMNS = *,F3.0,/,
     1 25X,*WEIGHT PER COLUMN = *,F6.0,* LB.*,/,
     1 25X,*TOTAL GIRDER LENGTH = *,F4.0,* FT.*,/,
     1 25X,*WEIGHT PER FT. OF GIRDER = *,F4.0,* LB./FT.*,/,
     1 25X,*WEIGHT PER S.F. OF GRATE = *,F3.0,* LB./S.F.*,/,
     1 25X,*UNIT MAT'L. COST = $*,F4.2,* /LB.*,/,
     1 25X,*UNIT INST'L. COST = $*,F4.2,* /LB.*,/,
     1T40,*TOTAL COLUMN WEIGHT = *,F6.0,* LB.*,/,
     1 T40,*TOTAL GIRDER WEIGHT = *,F6.0,* LB.*,/,
     1 T40,*TOTAL GRATE WEIGHT  = *,F6.0,* LB.*,//,
     1 T39,*TOTAL SUPPORT WEIGHT= *,F7.0,* LB.*,/,
     1 T72,*SUPPORT MAT'L. COST = $*,F5.0,T99,*00C.*,/,
     1 T71,*SUPPORT INST'L. COST = $*,F5.0,T99,*00C.*)
C
C
C
C     SHELL
C      A. CYLINDER
C       CID - I.D.
C       CH - HEIGHT
```

```
C       CT - WALL THICKNESS
C       CD - DENSITY
C       CW - TOTAL WEIGHT
C
        READ(5,305) CID,CH,CT,CD,CMLC,CILC
  305 FORMAT(6F10.0)
        CW=PI/4*((CID+2*CT)**2-CID**2)*CH*CD
        CMC=CMLC*CW
        CIC=CILC*CW
C
        WRITE(6,375) CID,CH,CT,CD,CMLC,CILC,CW
  375 FORMAT(22X,*SHELL CYLINDER*,//,
     1 25X,*I.D. = *,F4.1,* FT.*,/,
     1 25X,*HEIGHT = *,F4.1,* FT.*,/,
     1 25X,*WALL THICKNESS = *,F6.4,* FT.*,/,
     1 25X,*DENSITY = *,F4.3,* LB./CU.FT.*,/,
     1 25X,*UNIT MATL. COST = $*,F4.2,* /LB.*,/,
     1 25X,*UNIT INST'L. COST = $*,F4.2,* /LB.*,/,
     1 T40,*CYLINDER WEIGHT = *,F8.0,* LB.*)
C
C    B.  DOME
C    SDT - THICKNESS
C    CRSID - DIAMETER OF CONNECTING PIPING TO REHEAT CHAMBER
C    SDW - WEIGHT
C
        READ(5,360) SDT,SDCID
  360 FORMAT(2F10.0)
        C2=1.0
        C3=1.02
        IF(A) C1=.346
        IF(BC) C1=.459
        IF(C) C1=.5
        IF(EC) C2=1.205
        SDW=PI*(C2*CID)**2/4*(C1*CID)**2)*SDT*CD
        IF(EC) SDW=SDW + PI/4*((C2*CID+2*SDT)**2-(C2*CID)**2)*
     1 C2*CID*CD - PI/4*CRSID**2*SDT*CD
        SDMC=CMLC*SDW
        SDIC=CILC*SDW
C
        WRITE(6,375) SDT,SDW
  375 FORMAT (22X,*SHELL DOME*,//,
     1 25X,*THICKNESS = *,F5.3* FT.*,/,
     1 T40,*DOME WEIGHT = *,F8.0,* LB.*)
C
C   C.  BOTTOM CAP
C    BCT - THICKNESS
C    BCW - WEIGHT
C
        READ(5,380)BCT
  380 FORMAT(F10.0)
        IF(A) C4=.5
        IF(BC) C4=.25
        IF(C) C4=.5
        BCW=PI*(CID**2/4+(C4*CID)**2)*BCT*CD
        BCMC=CMLC*BCW
        BCIC=CILC*BCW
        TCW=SDW+BCW
```

```
      STCTMC=(CMC+SCMC+ECMC)/1000.
      STCTIC=(CIC+SCIC+ECIC)/1000.
C
      WRITE(6,385) PCT,BCW,TSW,STCTMC,STOTIC
  385 FORMAT(20X,*SHELL BOTTOM CAP*,//,
     1 25X,*THICKNESS = *,F5.3,* FT.*,/,
     1 T4C,*BOTTOM CAP WEIGHT = *,F7.0,* LB.*,//,
     1 T4C,*TOTAL SHELL WEIGHT = *,F7.0,* LB.*,/,
     1 T74,*SHELL MAT'L. COST = $*,F6.0,T100,*000.*,/,
     1 T73,*SHELL INST'L. COST = $*,F6.0,T100,*000.*)
C
C
C   INSULATION
C
C
C  A. CYLINDER INSULATION
C    CIN - # OF LAYERS
C    CIID(J)=I.D. OF EACH LAYER
C    CIT(J) - THICKNESS OF EACH LAYER
C    CIH(J) - HEIGHT OF EACH LAYER
C    CIP(J) - DENSITY OF EACH LAYER
C    CIW(J) - WEIGHT OF EACH LAYER
C    CILTOTW - TOTAL WEIGHT OF ALL LINING INSULATION
C    CII - # OF INTERIOR ZONES
C    CIIA(J) - X-SECTIONAL AREA OF EACH ZONE
C    CIIH(J) - HEIGHT OF EACH ZONE
C    CIIP(J) - DENSITY OF EACH ZONE
C    CIIW(J) - WEIGHT OF EACH ZONE
C    CIITOTW - TOTAL WEIGHT OF ALL INTERIOR INSULATION
C    CITOTW - TOTAL WEIGHT OF ALL CYLINDER INSULATION
C
      NPAGE=2
      WRITE(6,110)NPAGE,DAY
      WRITE(6,398) TITLE
  398 FORMAT(40X,6A10)
      WRITE(6,400) TITLE2
  400 FORMAT(///,10X,6A10,//,20X,*CYLINDER WALL INSULATION*,/,
     1 57X,*MAT'L    INST'L*,/,
     1 25X,*LAYER     I.D.   THICKNESS   HEIGHT   DENSITY    WEIGHT*,
     1 *   MAT'L INST'L   COST     COST*,/,
     1 27X,*#        (FT.)     (FT.)      (FT.)  (LB./CU.FT.)  (LB.)*,
     1 *   $/LB. $/LB.     $          $*,/,
     1 26X,*----*,4X,5(10H  -----   ),2(8H ---  ),2(10H  -----   ))
      READ(5,405) CIN
  405 FORMAT(I1)
      DO 410 J=1,CIN
        READ(5,406) CIID(J),CIT(J),CIH(J),CIP(J),CIMLC(J),CIILC(J)
  406   FORMAT(6F10.0)
        CIW(J)=PI/4*((CIID(J)+2*CIT(J))**2-CIID(J)**2)*CIH(J)*CIP(J)
        CIMC(J)=CIMLC(J)*CIW(J)
        CIIC(J)=CIILC(J)*CIW(J)
      WRITE(6,408) J,CIID(J),CIT(J),CIH(J),CIP(J),CIW(J),
     1 CIMLC(J),CIILC(J),CIMC(J),CIIC(J)
  408 FORMAT(27X,I1,F11.2,F10.3,F10.2,F10.1,F12.0,2F8.2,2F10.0)
      CITOTMC=CITOTMC+CIMC(J)
  410 CITOTIC=CITOTIC+CIIC(J)
C
```

```
      IF(.NOT.A) GO TO 449
      WRITE(6,414)
  414 FORMAT(//,20X,*INTERIOR INSULATION*,/,
     1 8BX,*MAT'L    INST'L*,/,
     1 25X,*ZONE  X-SECT. AREA  HEIGHT   DENSITY    WEIGHT*,
     1 *   MAT'L INST'L   COST      COST*,/,
     1 27X,*#       (S.F.)     (FT.)  (LB./CU.FT.)  (LB.)*,
     1 *   $/LF. $/LB.     $          $*,/,
     1 26X,*----*,4X,4(10H -----   ),2(6H ---  ),3(10H -----   ))
      READ(5,415)CII
  415 FORMAT(I1)
      DO 420 J=1,CII
        READ(5,416) CIIA(J),CIIH(J),CIIP(J),CIIMUC(J),CIIIUC(J)
  416   FORMAT(5F10.0)
        CIIW(J)=CIIA(J)*CIIH(J)*CIIP(J)
        CIIMC(J)=CIIMUC(J)*CIIW(J)
        CIIIC(J)=CIIIUC(J)*CIIW(J)
        CIIMCT=CIIMCT+CIIMC(J)
        CIIICT=CIIICT+CIIIC(J)
      WRITE(6,419) J,CIIA(J),CIIH(J),CIIP(J),CIIW(J),
     1 CIIMUC(J),CIIIUC(J),CIIMC(J),CIIIC(J)
  419 FORMAT(/27X,I1,F11.1,F10.2,F10.1,F12.0,2F6.2,2F10.0)
  420 CIITOTW=CIITOTW+CIIW(J)
  449 CONTINUE
C
C   B. DOME INSULATION
C    DIN - # OF INSULATION LAYERS
C    DIT(J) - THICKNESS OF EACH LAYER
C    DIP(J) - DENSITY OF EACH LAYER
C    DIW(J) - WEIGHT OF EACH LAYER
C    DICC(J) - C.C. OF EACH LAYER
C    DIH(J) - HEIGHT OF EACH LAYER
C    DITOTW - TOTAL WEIGHT OF ALL LAYERS
C
      WRITE(6,452)
  452 FORMAT(//,20X,*DOME INSULATION*,/,
     1 97X,*MAT'L    INST'L*,/,
     1 25X,*LAYER     C.C.   THICKNESS   HEIGHT   DENSITY    WEIGHT*,
     1 *   MAT'L INST'L   COST      COST*,/,
     1 27X,*#       (FT.)     (FT.)     (FT.)  (LB./CU.FT.)  (LB.)*,
     1 *   $/LF. $/LB.     $          $*,/,
     1 26X,*----*,4X,5(10H -----   ),2(6H ---  ),2(10H -----   ))
      READ(5,453) DIN,DICC(1),DIT(1)
  453 FORMAT(I1,9X,2F10.2)
      DO 490 J=1,DIN
        READ(5,460) DIT(J),DIP(J),DIMUC(J),DIIUC(J)
  460   FORMAT(4F10.0)
        DIW(J)=PI*(DICC(J)**2/4-DIH(J)**2)*DIT(J)*DIP(J)
        IF(J.GT.1) DIW(J)=DIW(J)+PI/4*(DICC(J)**2-(DICC(J)-2*DIT(J))**2)*
     1   .03*DID*DIP(J) - PI/4*CRSID**2*DIT(J)*DIP(J)
        DIMC(J)=DIMUC(J)*DIW(J)
        DIIC(J)=DIIUC(J)*DIW(J)
      WRITE(6,468)J,DICC(J),DIT(J),DIH(J),DIP(J),DIW(J),
     1 DIMUC(J),DIIUC(J),DIMC(J),DIIC(J)
        DITOTMC=DITOTMC+DIMC(J)
        DITOTIC=DITOTIC+DIIC(J)
        DICC(J+1)=DICC(J)-2*DIT(J)
```

```
      450    CIP(J+1)=CIP(J)-DIT(J)
            C
            C   C. BOTTOM CAP INSULATION
            C    BIP - DENSITY
      250   C    BIW - WEIGHT
            C
                 READ(5,502) BIP,BIMUC,BIIUC
            502  FORMAT(3F10.0)
                 BIW=2/3.*PI*((CID/2)**3.*BIP
      290        IF(J) BIW=BIW/2
                 BIMC=BIMUC*BIW
                 BIIC=BIILC*BIW
                 WRITE(6,498) BIP,BIMUC,BIILC,BIW,BIMC,BIIC
            498  FORMAT(/,20X,'BOTTOM CAP INSULATION',//,
      300       1 25X,'DENSITY = ',F4.0,' LB.'/,
                1 25X,'UNIT MAT'L. COST = $',F4.2,' /LB.'/,
                2 25X,'UNIT INST'L. COST = $',F4.2,' /LB.'/,
                1 T40,'CAP INSULATION WEIGHT = ',F8.0,' LB.'/,
                1 T41,'MAT'L. COST = $',F8.0,/,
      305       1 T40,'INST'L. COST = $',F8.0)
                 TOTIMC=(CITCTMC+CIIMCT+CITCTMC+BIMC)/1000
                 TOTIIC=(CITCTIC+CIIICT+CITCTIC+BIIC)/1000
                 WRITE(6,505) TOTIMC,TOTIIC
            505  FORMAT(/,T35,'TOTAL HEAT EXCHANGER INSULATION MAT'L.',
      310       1 ' COST = $',F7.0,
                1 T108,'000.'/,
                1 T34,'TOTAL HEAT EXCHANGER INSULATION INST'L. COST = $',
                1 F7.0,T108,'000.')
            C
      315   C
            C
            C
            C   REHEAT COMBUSTION CHAMBER (CASE BC ONLY)
            C
      320        IF(.NOT.BC) GO TO 750
            C
            C    SHELL CYLINDER
            C     RCID - I.D.
            C     RCH - HEIGHT
      325   C     RCT - THICKNESS
            C     RCP - DENSITY
            C     RCW - TOTAL WEIGHT
            C
                 READ(5,605) RCID,RCH,RCT,RCP
      330       FORMAT(4F10.0)
                 RCW=PI/4*((RCID+2*RCT)**2-RCID**2)*RCH*RCP
                 RCMC=CMLC*RCW
                 RCIC=CILC*RCW
            C
      335   C    SHELL DOME
            C     RCT - THICKNESS
            C     RCW - WEIGHT
            C
                 READ(5,610) RCT
      340       FORMAT(F10.0)
                 C6=.535
                 C7=1.25
```

```
                C8=1.23
                RCL=PI*((C7*RCID)**2/4+(C8*RCID)**2)*RCT*RCP+
      345      1 PI/4*((C7*RCID+2*RCT)**2-(C7*RCID)**2)*C8*RCIC*RCP+
               1 PI/4*CRSID**2*RCT*RCP
                RCMC=CMLC*RCL
                RCIC=CIUC*RCL
              C
      350       NPAGE=NPAGE+1
                WRITE(6,110) NPAGE,DAY
                WRITE(6,298)TITLE
                RSMC=(RCMC+RCMC)/1000
                RSIC=(RCIC+RCIC)/1000
      355       WRITE(6,615) RCID,RCH,RCT,RCP,RCL,RCT,RCL,RSMC,RSIC
             615 FORMAT(///,20X,'REHEAT COMBUSTION CHAMBER',//,
                1 25X,'SHELL CYLINDER',/,
                1 30X,'I.D. = ',F4.1,' FT.',/,
                1 30X,'HEIGHT = ',F4.1,' FT.',/,
      360       1 30X,'WALL THICKNESS = ',F6.4,' FT.',/,
                1 30X,'DENSITY = ',F4.0,' LB./S.F.',/,
                1 30X,'CYLINDER WEIGHT = ',F8.0,' LB.',/,
                1 25X,'SHELL DOME',/,
                1 30X,'THICKNESS = ',F6.4,' FT.',/,
      365       1 30X,'DOME WEIGHT = ',F8.0,' LB.',//,
                1 30X,'SHELL MAT'L. COST = $',F6.0,T100,'000.',/,
                1 30X,'SHELL INST'L. COST = $',F6.0,T100,'000.')
              C
              C   REHEAT CHAMBER  CYLINDER INSULLATION
      370     C
              C     RICN = # OF INSULLATION LAYERS
              C     RICID(J) = I.D. OF EACH LAYER
              C     RICT(J) = THICKNESS OF EACH LAYER
              C     RICH(J) = HEIGHT OF EACH LAYER
      375     C     RICP(J) = DENSITY OF EACH LAYER
              C     RICW(J) = WEIGHT OF EACH LAYER
              C     RICTCTW = TOTAL WEIGHT OF ALL LAYERS
              C
                WRITE(6,620)
      380     620 FORMAT(/,25X,'CYLINDER WALL INSULLATION',/,
                1 97X,'MAT'L    INST'L',/,
                1 25X,'LAYER     I.D.   THICKNESS   HEIGHT   DENSITY    WEIGHT',
                1 '   MAT'L INST'L   COST     COST',/,
                1 27X,'#        (FT.)    (FT.)     (FT.)  (LB./CU.FT.)  (LB.)',
      385       1 '   $/LB. $/LB.     $          $',/,
                1 26X,'-----',4X,5(10H  -----   ),2(6H ---  ),2(10H  -----   ))
                READ(5,660) RICN
              660 FORMAT(I1)
                DO 690 J=1,RICN
      390         READ(5,670) RICID(J),RICT(J),RICH(J),RICP(J),RICMLC(J),RICILC(J)
              670   FORMAT(6F10.0)
                    RICW(J)=PI/4*((RICID(J)+2*RICT(J))**2-RICID(J)**2)*
                1   RICH(J)*RICP(J)
                    RICMC(J)=RICMLC(J)*RICW(J)
      395           RICIC(J)=RICILC(J)*RICW(J)
                  WRITE(6,408) J,RICID(J),RICT(J),RICH(J),RICP(J),RICW(J),
                1 RICMLC(J),RICILC(J),RICMC(J),RICIC(J)
                  RICTMC=RICTMC+RICMC(J)
              690 RICTIC=RICTIC+RICIC(J)
```

```
      C
      C   REPEAT CHAMBER CONE INSULATION
      C
      C     RICN - # OF LAYERS
      C     RICT(J) - THICKNESS OF EACH LAYER
      C     RICH(J) - HEIGHT OF EACH LAYER
      C     RICD(J) - DENSITY OF EACH LAYER
      C     RICOD(J) - O.D. OF EACH LAYER
      C     RICW(J) - WEIGHT OF EACH LAYER
      C     RICTOTW - TOTAL WEIGHT OF ALL LAYERS
      C
            WRITE(6,700)
        700 FORMAT(/,25X,*CONE INSULATION*,/,
           1 97X,*MAT*L    INST*L*,/,
           1 25X,*LAYER     O.D.   THICKNESS   HEIGHT   DENSITY    WEIGHT*,
           1 *   MAT*L INST*L   COST      COST*,/,
           1 33X,*(FT.)      (FT.)      (FT.)  (LB./CU.FT.)  (LB.)*,
           1 *   $/LB. $/LB.      $          $*,/,
           1 26X,*-----*,4X,5(10H -----    ),2(6H ---  ),2(10H -----    ))
            READ(5,710) RICN,RICOD(1),RICH(1)
        710 FORMAT(I1,9X,2F10.0)
            DO 740 J=1,RICN
              READ(5,720) RICT(J),RICD(J),RICMUC(J),RICILC(J)
        720   FORMAT(4F10.0)
              RICW(J)=PI*(RICOD(J)**2/4+RICH(J)**2)*RICT(J)*RICD(J)+
           1   PI/4*(RICOD(J)**2-(RICOD(J)-2*RICT(J))**2)*SR*RCID*RICD(J)-
           1   PI/4*RCID**2*RICT(J)*RICD(J)
              RICMC(J)=RICMUC(J)*RICW(J)
              RICIC(J)=RICILC(J)*RICW(J)
              RICTMC=RICTMC+RICMC(J)
              RICTIC=RICTIC+RICIC(J)
            WRITE(6,730) J,RICOD(J),RICT(J),RICH(J),RICD(J),RICW(J),
           1 RICMUC(J),RICILC(J),RICMC(J),RICIC(J)
              RICOD(J+1)=RICOD(J)-2*RICT(J)
        740   RICH(J+1)=RICH(J)-RICT(J)
            RITMC=(RICTMC+RICTMC)/1000
            RITIC=(RICTIC+RICTIC)/1000
            RCCTMC=RCMC+RITMC
            RCCTIC=RCIC+RITIC
            WRITE(6,741) RCCTMC,RCCTIC
        741 FORMAT(/,T40,*TOTAL REPEAT COMBUSTION CHAMBER*,
           1 * MAT*L. COST = $*,F7.3,T53,*000.*,/,
           1 T25,*TOTAL REPEAT COMBUSTION CHAMBER INST*L.*,
           1 * COST = $*,F7.3,T53,*000.*)
      C
        750 GO TO 753
            NPAGE=NPAGE+1
            WRITE(6,110) NPAGE,DAY
            WRITE(6,398) TITLE
            WRITE(6,755)
        755 FORMAT(5(/))
        753 READ(5,751)NU,NUNIT
        751 FORMAT(I1,A10)
            UNITMC=MMC+SMC+STOTMC+TOTIMC
            IF(NU) UNITMC=UNITMC+RCCTMC
            UNITIC=MIC+SIC+STOTIC+TOTIIC
            IF(NU) UNITIC=UNITIC+RCCTIC
```

```
      NUNITMC=UNITMC*NL
      NUNITIC=UNITIC*NL
      WRITE(6,752) UNITMC,UNITIC,NUNIT,NUNITMC,NUNIT,NUNITIC
  752 FORMAT(20X,55(1H-),/,
     1 25X,*TOTAL MATL. COSTS FOR ONE HEAT EXCHANGER*,
     1 * AND COMBUSTION CHAMBER (HXC) UNIT      = $*,F8.0,
     1 T113,*000.*,/,
     1 25X,*TOTAL INSTL. COSTS FOR ONE HEAT EXCHANGER*,
     1 * AND COMBUSTION CHAMBER (HXC) UNIT      = $*,F8.0,
     1 T113,*000.*,//,
     1 25X,*TOTAL MATL. COSTS FOR *,I3,* HEAT EXCHANGER*,
     1 * AND COMBUSTION CHAMBER (HXC) UNITS   = $*,F8.0,
     1 T113,*000.*,/,
     1 25X,*TOTAL INSTL. COSTS FOR *,I3,* HEAT EXCHANGER*,
     1 * AND COMBUSTION CHAMBER (HXC) UNITS   = $*,F8.0,
     1 T113,*000.*)
C
C
C
C   DUCTING
C
C    NP - # OF DUCTING GROUPS
C    PID(J) - DUCT I.D.
C    PT(J) - DUCT WALL THICKNESS
C    PP(J) - DUCT DENSITY
C    PL(J) - DUCT LENGTH
C    PW(J) - DUCT WEIGHT
C    INS(J) - 1)INSIDE, 2)OUTSIDE,
C             OR 3)NO INSULATION
C    NINS(J) - # OF INSULATION LAYERS
C    PIOD(J,K) - O.D. OF EACH LAYER
C    PIT(J,K) - THICKNESS OF EACH LAYER
C    PIP(J,K) - DENSITY OF EACH LAYER
C    PIW(J,K) - WEIGHT OF EACH LAYER
C
      NPAGE=NPAGE+1
      WRITE(6,110) NPAGE,DAY
      WRITE(6,398)TITLE
      WRITE(6,800)
  800 FORMAT(//,10X,*DUCTING*)
      READ(5,805) NP
  805 FORMAT(I2)
      DO 850 J=1,NP
      IF(J.GT.1) GO TO 804
        IF(     J.EQ.3.OR.J.EQ.6.OR.J.EQ.9) GO TO 806
      GO TO 807
  804   IF(J.EQ.4.OR.J.EQ.7.OR.J.EQ.10) GO TO 806
        GO TO 807
  806   NPAGE=NPAGE+1
        WRITE(6,110) NPAGE,DAY
        WRITE(6,398)TITLE
  807   READ(5,808) (PIPNAME(L),L=1,4)
  808   FORMAT(4A10)
        READ(5,810) PID(J),PT(J),PP(J),PL(J),PMLT(J),PILT(J),INS(J)
  810   FORMAT(6F10.0,I1)
        PW(J)=3.1416/4*((PID(J)+2*PT(J))**2-PID(J)**2)*PL(J)*PP(J)
        PMC(J)=PMLT(J)*PW(J)/2000
```

```
      PIC(J)=PILC(J)*PW(J)/1000
      PTOTW=PTOTW+PW(J)
      PTOTMC=PTOTMC+PMC(J)
      PTOTIC=PTOTIC+PIC(J)
    WRITE(6,812) PIPNAME
812 FORMAT(/,22X,4A10)
    WRITE(6,815)PID(J),PT(J),PP(J),PL(J),PMUC(J),PIUC(J),PW(J),PMC(J),
   1 PIC(J)
815 FORMAT(/,30X,*I.D. - *,F5.2,* FT.*,/,
   1 30X,*WALL THICKNESS - *,F7.5,* FT.*,/,
   1 30X,*DENSITY - *,F4.0,* LB./CU.FT.*,/,
   1 30X,*LENGTH - *,F5.0,* FT.*,/,
   1 30X,*MAT'L. UNIT COST - $*,F6.2,*/LB.*,/,
   1 30X,*INST'L. UNIT COST - $*,F6.2,*/LB.*,/,
   1 T60,*DUCT WEIGHT = *,F8.0,* LB.*,/,
   1 T65,*MAT'L. COST  = $*,F5.0,T85,*000.*,/,
   1 T65,*INST'L. COST = $*,F5.0,T85,*000.*)
      IF(INS(J).EQ.0) GO TO 855
    WRITE(6,818)
818 FORMAT(2/X,*INSULATION*,
   1 51X,*MAT'L     INST'L*,/,
   1 25X,*LAYER     O.D.    THICKNESS  DENSITY   WEIGHT*,
   1 *   MAT'L INST'L   COST     COST*,/,
   1 27X,*#        (FT.)      (FT.)  (LB./CU.FT.) (LB.)*,
   1 *   $/LB. $/LB.      $        $*,/,
   1 26X,*----*,4X,4(10H -----   ),2(8H ---  ),2(10H -----   ))
      READ(5,820) NINS(J)
820   FORMAT(I1)
      IF(INS(J).EQ.1) PIOD(J,1)=PID(J)
      NIN=NINS(J)
      DO 840 K=1,NIN
        READ(5,845) PIT(J,K), PIP(J,K),PIMUC(J,K),PIILC(J,K)
845     FORMAT(4F10.0)
        IF(INS(J).EQ.2.AND.K.EQ.1) PIOD(J,1)=PID(J)+2*PT(J)+2*PIT(J,1)
        IF(INS(J).EQ.2.AND.K.GT.1) PIOD(J,K)=PIOD(J,K-1)+2*PIT(J,K)
        PIW(J,K)=PI/4*(PIOD(J,K)**2-(PIOD(J,K)-2*PIT(J,K))**2)*
   1     PL(J)*PIP(J,K)
        PIMC(J,K)=PIMUC(J,K)*PIW(J,K)/1000
        PIIC(J,K)=PIIUC(J,K)*PIW(J,K)/1000
        PITOTMC=PITOTMC+PIMC(J,K)
        PITOTIC=PITOTIC+PIIC(J,K)
    WRITE(6,846) K,PIOD(J,K),PIT(J,K),PIP(J,K),PIW(J,K),
   1 PIMUC(J,K),PIIUC(J,K),PIMC(J,K),PIIC(J,K)
846 FORMAT(27X,I1,F11.1,F10.3,F11.1,F11.0,2F6.2,F7.0,F10.0,
   1 T90,*000.*,T100,*000.*)
849     IF(INS(J).EQ.1) PIOD(J,K+1)=PIOD(J,K)-2*PIT(J,K)
850     CONTINUE
      PMTOT=PTOTMC+PITOTMC
      PICTOT=PTOTIC+PITOTIC
      TOTMC=ALNITMC+PMCTOT
      TOTIC=ALNITIC+PICTOT
      TOTCOST=TOTMC+TOTIC
      WRITE(6,870) PTOTMC,PITOTMC,PTOTIC,PITOTIC,TOTMC,TOTIC,TOTCOST
870 FORMAT(/////,25X,65(1H-),//,
   1 30X,*TOTAL DUCTING MAT'L. COSTS  = $*,F6.0,T67,*000.*,/,
   1 30X,*TOTAL DUCTING INSULATION MAT'L. COSTS  = $*,F6.0,T78,
   1 *000.*,/,
```

```
     1 70X,*TOTAL ELCTING INST'L. COSTS = $*,F6.0,T67,*000.*,/,
     1 30X,*TOTAL ELCTING INSULATION INST'L. COSTS = $*,F6.0,T78,
     1 *000.*,////,
     1 25X,*TOTAL HEAT EXCHANGER/COMBUSTION CHAMBER (H&C) AND ELCTING*,
575  1 * H/I'L. COSTS  = $*,F8.0,T108,*000.*,/,
     1 25X,*TOTAL HEAT EXCHANGER/COMBUSTION CHAMBER (B&C) AND ELCTING*,
     1 * INST'L. COSTS = $*,F8.0,T108,*000.*,/,
     1 25X,82('=')/,
     1 25X,*TOTAL HEAT EXCHANGER/COMBUSTION CHAMBER (B&C) AND ELCTING*,
580  1 * COST'          = $*,F8.0,T108,*000.*)
  1000 CONTINUE
       END
```

TABLE XXXVIII. - COMPUTER-PRINTED OUTPUT OF COST ESTIMATING COMPUTER PROGRAM FOR 100 MW_t HTAH SYSTEM FOR CASE B (TYPICAL CASE)

```
W.O. #3473-02          NASA-LEWIS HIGH TEMPERATURE AIR HEATER COST SUMMARY                PAGE  1

                              CASE B - AVCO 4 VESSEL HTAH 100 MW. OIL FIRED

HEAT EXCHANGER/COMBUSTION CHAMBER (ONE UNIT)

          CHECKERBRICK MATRIX

               DIAMETER - 15.5 FT.

               CROSS SECTIONAL AREA - 188.7 S.F.
               HEIGHT - 85.0 FT.
               DENSITY - 114.3 LB/CU.FT.
               UNIT MAT'L. COST - $1.11 /LB.
               UNIT INST'L. COST - $ .53 /LB.
                              MATRIX WEIGHT = 1833235. LB.
                                                    MATRIX MAT'L. COST = $ 2033000.
                                                   MATRIX INST'L. COST = $  962003.
          MATRIX SUPPORT

               NO. OF COLUMNS - 23.
               WEIGHT PER COLUMN -   513. LB.
               TOTAL GIRDER LENGTH -  85. FT.
               WEIGHT PER FT. OF GIRDER - 134. LB./FT.
               WEIGHT PER S.F. OF GRATE - 80. LB./S.F.
               UNIT MAT'L. COST - $1.75 /LB.
               UNIT INST'L. COST - $ .70 /LB.
                              TOTAL COLUMN WEIGHT = 11799. LB.
                              TOTAL GIRDER WEIGHT = 11444. LB.
                              TOTAL GRATE WEIGHT  = 15020. LB.

                             TOTAL SUPPORT WEIGHT=  38262. LB.
                                                    SUPPORT MAT'L. COST = $  67000.
                                                   SUPPORT INST'L. COST = $  27000.
          SHELL CYLINDER

               I.D. - 15.7 FT.
               HEIGHT - 90.0 FT.
               WALL THICKNESS -  .0938 FT.
               DENSITY - 490. LB./CU.FT.
               UNIT MAT'L. COST - $1.20 /LB.
               UNIT INST'L. COST - $1.80 /LB.
                              CYLINDER WEIGHT =  256442. LB.
          SHELL DOME

               THICKNESS -  .083 FT.
                              DOME WEIGHT =   91323. LB.
          SHELL BOTTOM CAP

               THICKNESS -  .198 FT.
                              BOTTOM CAP WEIGHT =  34827. LB.

                              TOTAL SHELL WEIGHT = 382592. LB.
                                                    SHELL MAT'L. COST = $  459000.
                                                   SHELL INST'L. COST = $  689000.
```

CASE B - AVCO 4 VESSEL RTAP 100 MW. OIL FIRED

HEAT EXCHANGER/COMBUSTION CHAMBER (ONE UNIT)

CYLINDER WALL INSULATION

LAYER #	I.D. (FT.)	THICKNESS (FT.)	HEIGHT (FT.)	DENSITY (LB./CU.FT.)	WEIGHT (LB.)	MAT'L $/LB.	INST'L $/LB.	MAT'L COST $	INST'L COST $
1	19.42	.125	94.00	1.5	721.	12.44	30.00	9687.	21622.
2	19.69	.375	67.00	46.0	69078.	.24	.65	16579.	45039.
3	19.69	.375	17.00	50.5	19242.	.30	.59	5772.	11436.
4	18.69	.375	10.00	80.5	18743.	.76	.37	13712.	6730.
5	17.50	.375	37.00	48.5	76237.	.35	.63	13383.	23858.
6	17.50	.375	30.00	58.5	37725.	.44	.51	16625.	19238.
7	17.50	.375	27.00	80.5	46795.	.76	.37	35564.	17454.
8	15.69	1.125	94.00	196.5	1061685.	.70	.16	743165.	166681.

CONE INSULATION

LAYER #	I.D. (FT.)	THICKNESS (FT.)	HEIGHT (FT.)	DENSITY (LB./CU.FT.)	WEIGHT (LB.)	MAT'L $/LB.	INST'L $/LB.	MAT'L COST $	INST'L COST $
1	23.83	.375	9.78	58.5	46775.	.40	2.65	18510.	59990.
2	23.08	1.500	9.41	196.5	587240.	.68	.63	399323.	369961.

BOTTOM CAP INSULATION

DENSITY = 166. LB.
UNIT MAT'L. COST = $ .45 /LB.
UNIT INST'L. COST = $ .18 /LB.
CAP INSULATION WEIGHT = 329734. LB.
MAT'L. COST = $ 148380.
INST'L. COST = $ 59682.

TOTAL HEAT EXCHANGER INSULATION MAT'L. COST = $ 1422000.
TOTAL HEAT EXCHANGER INSULATION INST'L. COST = $ 842000.

CASE B - AVCO 4 VESSEL HTAH 100 MW. OIL FIRED

REHEAT COMBUSTION CHAMBER

SHELL CYLINDER
I.D. = 16.3 FT.
HEIGHT = 28.0 FT.
WALL THICKNESS = .0938 FT.
DENSITY = 490. LB./C.F.
CYLINDER WEIGHT = 66285. LB.

SHELL DOME
THICKNESS = .0677 FT.
DOME WEIGHT = 61530. LB.

SHELL MAT'L. COST = $ 153000.
SHELL INST'L. COST = $ 230000.

CYLINDER WALL INSULATION

LAYER #	I.D. (FT.)	THICKNESS (FT.)	HEIGHT (FT.)	DENSITY (LB./CU.FT.)	WEIGHT (LB.)	MAT'L $/LB.	INST'L $/LB.	MAT'L COST $	INST'L COST $
1	16.15	.083	28.00	1.0	119.	13.44	30.00	1595.	3568.
2	15.46	.375	28.00	58.5	35441.	.44	.51	12394.	15616.
3	12.46	1.500	28.00	150.5	349388.	.70	.16	244572.	54454.

DOME INSULATION

LAYER #	I.D. (FT.)	THICKNESS (FT.)	HEIGHT (FT.)	DENSITY (LB./CU.FT.)	WEIGHT (LB.)	MAT'L $/LB.	INST'L $/LB.	MAT'L COST $	INST'L COST $
1	20.83	.375	8.78	58.5	40435.	.40	2.05	16162.	82830.
2	19.78	1.500	8.38	150.5	479581.	.70	.63	335987.	302296.

TOTAL REHEAT COMBUSTION CHAMBER MAT'L. COST = $ 765000.
TOTAL REHEAT COMBUSTION CHAMBER INST'L. COST = $ 685000.

TOTAL MAT'L. COSTS FOR ONE HEAT EXCHANGER AND COMBUSTION CHAMBER (E&C) UNIT = $ 4748000.
TOTAL INST'L. COSTS FOR ONE HEAT EXCHANGER AND COMBUSTION CHAMBER (E&C) UNIT = $ 3209000.

TOTAL MAT'L. COSTS FOR FOUR HEAT EXCHANGER AND COMBUSTION CHAMBER (E&C) UNITS = $ 18991000.
TOTAL INST'L. COSTS FOR FOUR HEAT EXCHANGER AND COMBUSTION CHAMBER (E&C) UNITS = $ 12836000.

CASE 8 - AVCO 4 VESSEL HTAH 100 MW. OIL FIRED

DUCTING

BURNER AIR INLET MANIFOLD

I.D. = 4.77 FT.
WALL THICKNESS = .03125 FT.
DENSITY = 490. LB./CU.FT.
LENGTH = 153. FT.
MAT'L. UNIT COST = $ 2.00/LB.
INST'L. UNIT COST = $ 2.25/LB.
DUCT WEIGHT = 35345. LB.
MAT'L. COST = $ 106000.
INST'L. COST = $ 80000.

INSULATION LAYER #	O.D. (FT.)	THICKNESS (FT.)	DENSITY (LB./CU.FT.)	WEIGHT (LB.)	MAT'L $/LB.	INST'L $/LB.	MAT'L COST $	INST'L COST $
1	6.3	.750	13.0	26167.	6.15	2.31	161000.	60000.

BURNER FUEL OIL PIPE

I.D. = .13 FT.
WALL THICKNESS = .01208 FT.
DENSITY = 490. LB./CU.FT.
LENGTH = 173. FT.
MAT'L. UNIT COST = $ .80/LB.
INST'L. UNIT COST = $ 1.15/LB.
DUCT WEIGHT = 470. LB.
MAT'L. COST = $ 0000.
INST'L. COST = $ 1000.

BURNER RECYCLE GAS INLET MANIFOLD

I.D. = 2.27 FT.
WALL THICKNESS = .03125 FT.
DENSITY = 490. LB./CU.FT.
LENGTH = 153. FT.
MAT'L. UNIT COST = $ 2.00/LB.
INST'L. UNIT COST = $ 2.25/LB.
DUCT WEIGHT = 16545. LB.
MAT'L. COST = $ 51000.
INST'L. COST = $ 38000.

INSULATION LAYER #	O.D. (FT.)	THICKNESS (FT.)	DENSITY (LB./CU.FT.)	WEIGHT (LB.)	MAT'L $/LB.	INST'L $/LB.	MAT'L COST $	INST'L COST $
1	3.8	.750	13.0	14451.	6.15	2.31	89000.	33000.

CASE B - AVCO 4 VESSEL HTAH 100 MW. OIL FIRED

BURNER-CHECKER CHAMBER CROSSOVER

I.D. = 11.48 FT.
WALL THICKNESS = .09375 FT.
DENSITY = 490. LB./CU.FT.
LENGTH = 54. FT.
MAT'L. UNIT COST = $ 3.00/LB.
INST'L. UNIT COST = $ 2.25/LB.
DUCT WEIGHT = 90195. LB.
MAT'L. COST = $ 271000.
INST'L. COST = $ 203000.

INSULATION LAYER #	O.D. (FT.)	THICKNESS (FT.)	DENSITY (LB./CU.FT.)	WEIGHT (LB.)	MAT'L $/LB.	INST'L $/LB.	MAT'L COST $	INST'L COST $
1	11.5	.250	50.5	24052.	.30	1.19	7000.	29000.
2	11.0	.250	80.5	36674.	.86	.75	32000.	27000.
3	10.5	1.125	190.5	349122.	.71	.32	241000.	107000.

COMBUSTER GAS EXIT MANIFOLD

I.D. = 4.94 FT.
WALL THICKNESS = .03125 FT.
DENSITY = 490. LB./CU.FT.
LENGTH = 233. FT.
MAT'L. UNIT COST = $ 3.00/LB.
INST'L. UNIT COST = $ 2.25/LB.
DUCT WEIGHT = 55693. LB.
MAT'L. COST = $ 167000.
INST'L. COST = $ 125000.

INSULATION LAYER #	O.D. (FT.)	THICKNESS (FT.)	DENSITY (LB./CU.FT.)	WEIGHT (LB.)	MAT'L $/LB.	INST'L $/LB.	MAT'L COST $	INST'L COST $
1	6.2	.667	12.0	35969.	6.15	2.31	221000.	83000.

AIR ELECTRODE INLET MANIFOLD

I.D. = 1.77 FT.
WALL THICKNESS = .03125 FT.
DENSITY = 490. LB./CU.FT.
LENGTH = 233. FT.
MAT'L. UNIT COST = $ .80/LB.
INST'L. UNIT COST = $ 1.15/LB.
DUCT WEIGHT = 20201. LB.
MAT'L. COST = $ 16000.
INST'L. COST = $ 23000.

INSULATION LAYER #	O.D. (FT.)	THICKNESS (FT.)	DENSITY (LB./CU.FT.)	WEIGHT (LB.)	MAT'L $/LB.	INST'L $/LB.	MAT'L COST $	INST'L COST $
1	2.5	.333	12.0	6865.	6.15	2.31	42000.	16000.

CASE 6 - AVCO 4 VESSEL HTAH 100 MW. OIL FIRED

HIGH TEMPERATURE AIR OUTLET MANIFOLD

I.D. = 6.22 FT.
WALL THICKNESS = .05729 FT.
DENSITY = 490. LB./CU.FT.
LENGTH = 123. FT.
MAT'L. UNIT COST = $ .60/LB.
INST'L. UNIT COST = $ 1.10/LB.
DUCT WEIGHT = 66022. LB.
MAT'L. COST = $ 54000.
INST'L. COST = $ 78000.

INSULATION LAYER #	C.L. (FT.)	THICKNESS (FT.)	DENSITY (LB./CU.FT.)	WEIGHT (LB.)	MAT'L $/LB.	INST'L $/LB.	MAT'L COST $	INST'L COST $
1	6.2	.250	50.5	39190.	.30	.75	12000.	27000.
2	5.7	.375	81.5	62333.	.76	.50	47100.	31000.
3	5.1	.750	130.5	232097.	.76	.51	177100.	46000.

PRESSURIZATION-DEPRESSURIZATION MANIFOLD

I.D. = 1.44 FT.
WALL THICKNESS = .03125 FT.
DENSITY = 490. LB./CU.FT.
LENGTH = 123. FT.
MAT'L. UNIT COST = $ .60/LB.
INST'L. UNIT COST = $ 1.10/LB.
DUCT WEIGHT = 11517. LB.
MAT'L. COST = $ 5000.
INST'L. COST = $ 13000.

INSULATION LAYER #	C.L. (FT.)	THICKNESS (FT.)	DENSITY (LB./CU.FT.)	WEIGHT (LB.)	MAT'L $/LB.	INST'L $/LB.	MAT'L COST $	INST'L COST $
1	2.2	.333	13.0	4063.	6.15	2.21	25000.	9000.

TOTAL CLOTHING MAT'L. COSTS = $ 675000.
TOTAL CLOTHING INSULATION MAT'L. COSTS = $ 1052000.
TOTAL CLOTHING INST'L. COSTS = $ 561000.
TOTAL CLOTHING INSULATION INST'L. COSTS = $ 468000.

TOTAL HEAT EXCHANGER/COMBUSTION CHAMBER (HXC) AND CLOTHING MAT'L. COSTS = $ 20717000.
TOTAL HEAT EXCHANGER/COMBUSTION CHAMBER (HXC) AND CLOTHING INST'L. COSTS = $ 13864000.

TOTAL HEAT EXCHANGER/COMBUSTION CHAMBER (HXC) AND CLOTHING COSTS = $ 34581000.

Appendix 2N

Auxiliary Systems and Accessories

The major auxiliary systems and accessories include valves, burners, instruments and controls, fuel supply systems, the HTAH system building and, for Case D, a turbocompressor system. The cost estimates for these auxiliary systems and accessories are given in tables XVIII, XXIV, XXVII and XXX for Cases A, B, C and D, respectively. The cost estimates are based upon extrapolations of the cost estimates for auxiliary systems and accessories reported in references 2-1 and 2-2 for the ETF reference designs. The costs in references 2-1 and 2-2 are given in mid-1977 dollars. According to reference 2-3, the costs for miscellaneous power plant equipment in North Central United States in mid-1979 dollars is approximately 1.20 times the costs in mid-1977 dollars.

Some of the cost estimates in references 2-1 and 2-2 are reported in terms of direct materials costs and direct labor costs and some cost estimates are reported only in terms of total installed costs with indirect costs included. Therefore all costs for auxiliary systems and components are expressed in terms of total installed costs (including indirect costs) to establish a consistent basis for extrapolation. Based upon experience in the power plant construction industry, indirect costs are assumed to be 20 percent of direct materials costs plus 98 percent of direct labor costs.

Valves. - A separate investigation was conducted on hot blast valves since limitations on the operating conditions and available sizes of hot blast valves may have an impact on the design and scale-up of the HTAH systems. Weights and prices of water-cooled hot blast gate valves manufactured by S.P. Kinney Engineers, Inc. are given in table XXXIX for valve inside diameters ranging from 40.6 cm (16 in.) to 168 cm (66 in.). These valves are capable of continuous operation at temperatures up to 1922° K (3000° F) and

TABLE XXXIX. - WATER-COOLED HOT BLAST GATE VALVE WEIGHTS AND PRICES

Inside Diameter, cm (in.)	Dry Weight, kg (1000 lb.)	Cost*, $	Direct Labor Cost for Installation, $
40.6 (16)	-	28,000	2,500
50.8 (20)	-	32,000	2,750
61.0 (24)	4,080 (9.0)	35,750	3,000
76.2 (30)	4,760 (10.5)	42,000	3,500
91.4 (36)	6,260 (13.8)	50,000	3,750
107 (42)	7,710 (17.0)	55,000	4,000
122 (48)	9,070 (20.0)	67,000	4,250
137 (54)	10,890 (24.0)	73,000	4,500
152 (60)	15,420 (34.0)	82,000	4,750
168 (66)	18,140 (40.0)	95,000	5,000

*Cost includes valve operator.

intermittently at temperatures up to 2033° K (3200° F), under pressures up to 0.34 MPa (50 psi). At the present time, this firm manufactures hot blast valves up to 152 cm (60 in.) in diameter and considers 168 cm(66 in.) to be the upper limit of the state of the art. It is uncertain as to whether a program to develop larger size water-cooled gate valves which can operate under these conditions would be successful. Cost estimates for valves larger than 168 cm (66 in.) would be very difficult to predict.

Typical cooling water requirements for these valves are in the range of 15.8 kg/sec (250 gallons per minute) for a 122-cm (48-in.) valve. They can be opened or closed in 10 to 15 seconds. However, the valves are designed to seal only when there is a significant pressure differential across the gate and will open only when this pressure differential is relieved.

For industrial application of these valves it is common to provide spare valves on the site so that valves which fail can be replaced and returned to the factory to be rebuilt. Blast furnace stoves and valves are typically operated initially for a six-year period, refurbished, and then operated for ly one additional six-year period. Therefore, capital investments for a plant should include spares of each major type of valve and the operating and maintenance cost of the plant should include periodic refurbishing and replacement of valving as well as the refractory materials of the HTAH system.

Valve costs are not reported in reference 2-1 for Case A. The cost estimate for the valving for Cases B and C is reported in reference 2-2 (in mid-1977 dollars) as $1,812,000 installed (including indirect costs) for a system thermal capacity of 93.8 MW_t. According to escalation indices reported in reference 2-3, this cost is equivalent to $2,174,000 in mid-1979 dollars. The cost estimate for the valving for Case D is reported in reference 2-1 to be $787,000 for materials and $118,000 for direct labor in mid-1977 dollars. Assuming indirect costs to be 20 percent of the materials costs and 98 percent of the direct labor cost, the

total installed cost (including indirects) is $1,178,000 for a system thermal capacity of 63.3 MW_t. According to escalation indices reported in reference 2-3, this cost is equivalent to $1,414,000 in mid-1979 dollars.

The total HTAH system valve costs are assumed to scale according to the equation

$$\frac{C}{C_o} = \frac{N}{N_o}\left(\frac{MAV}{MAV_o}\right)^{0.6} \qquad (2N\text{-}1)$$

where C is the total valve cost, C_o is the total valve cost for the ETF reference design, N is the number of vessels, N_o is the number of vessels in the ETF reference design, MAV is the matrix cross-sectional area per vessel and MAV_o is the matrix cross-sectional area per vessel for the ETF reference designs. Since no valve costs are reported for the ETF reference design for Case A, the cost of valves for Case A is assumed to be the same as that for Cases B and C at the 100 MW_t system thermal capacity level.

Burners. - The burners required for Cases A, B, C and D cover a wide range of sizes, since the reference design for Case A requires one burner for the entire system, the reference designs for Cases B and C require four burners (each capable of providing full system capacity), and the reference design for Case D requires 112 burners, 48 of which must provide full system capacity. The burner cost for Case A is not reported in reference 2-1. The total cost for four burner assemblies for Cases B and C is reported in reference 2-2 (in mid-1977 dollars) as $560,000 or $140,000 per burner. According to escalation indices reported in reference 2-3, this cost is equivalent to $168,000 per burner in mid-1979 dollars. Each burner must be capable of providing the full thermal capacity of 93.8 MW_t (delivered to the MHD air). The thermal capacity in terms of fuel consumption is larger than 93.8 MW_t due to system losses. The cost reported for Case D in reference 2-1 for 112 burner assemblies is $560,000 for materials and $40,000 for direct labor. Assuming indirect

costs to be 20 percent of the materials costs and 98 percent of the direct labor costs, the total installed cost (including indirects) is $751,000. This is equivalent to a cost of $6,700 per burner. According to escalation indices reported in reference 2-3, this cost is equivalent to $8,040 per burner in mid-1979 dollars. The full system thermal capacity (in terms of energy delivered to the air) is 63.3 MW_t. Since this must be provided at any given instant of time by 48 burners, the capacity per burner is 1.32 MW_t (delivered to the MHD air).

It is assumed in this investigation that the burner costs scale in accordance with the relationship

$$\frac{C_B}{C_{Bo}} = \left(\frac{M_B}{M_{Bo}}\right)^k \qquad (2N\text{-}2)$$

where C_B is the cost for a single burner, C_{Bo} is the cost for a single burner for the ETF reference design, M_B is the burner thermal capacity (in terms of thermal energy per burner delivered to the MHD air) and M_{Bo} is the corresponding burner thermal capacity for the ETF reference designs. Equation (2N-2) can be utilized to determine the value of the exponent k by inserting the ETF reference design costs and burner capacities, resulting in a value of 0.71 for k. Thus, for all cases, the cost for each burner is assumed to be given by

$$C_B = 8040 \left(\frac{M_B}{1.32}\right)^{0.71} \qquad (2N\text{-}3)$$

Instruments and controls. - Costs for instruments and controls are not reported for Case A in reference 2-1. The estimated costs (in mid-1977 dollars) for instruments and controls for Cases B and C are reported in reference 2-2 to be $400,000 installed (including indirect costs). The estimated costs (in mid-1977 dollars) for instruments and controls for Case D are reported in reference 2-2 to be $514,000 for materials and $49,000 for direct labor. Assuming the indirect costs to be 20 percent of the materials cost and 98 percent of the direct labor cost, the total

costs for instruments and controls for Case D are estimated to be $713,000 in mid-1977 dollars. The cost of instruments and controls is more dependent upon the number of vessels than upon the system power level. For Cases B and C the cost per vessel is $100,000 and for Case D it is $51,000. This difference may be accounted for by differences in interpretation in the definition of the part of the instrument and control equipment which is considered to be part of the HTAH system and the part which is considered to be part of the plant as a whole. Since the cost of instruments and controls is a relatively minor part of the cost of the HTAH system, it is deemed unnecessary to conduct an investigation to establish a firmer basis for estimating the instruments and controls costs for all four cases. Therefore, the same costs per vessel will be employed in this investigation as were reported in references 2-1 and 2-2. In accordance with indices reported in reference 2-3, escalation to mid-1979 dollars raises the cost for Cases B and C to $120,000 per vessel and to $61,000 per vessel for Case D. For Case A, the combustion chambers and burners are separate from the heat exchanger vessels. The cost of instruments and controls for Case A is estimated on the basis of $100,000 per vessel and $20,000 per combustion chamber/burner.

Pressurization/depressurization systems. - For Cases A, B and C, the vessels are pressurized prior to switching to blowdown and depressurized prior to switching to reheat for the purposes of equalizing the pressures across the valves and to minimize pressure and mass flow fluctuations in the MHD air and reheat gas streams. This is not necessary for Case D since both the MHD air and the reheat gas are nominally at the same pressure. The method for achieving pressurization and depressurization for Case A is to utilize pressure relief valves for depressurizing the vessels and by-pass valves around the cold blast isolation valves to pressurize the vessels. The costs of these valves are considered to be included in the costs for valving for Case A. For Cases B and C, a small air compressor

and air accumulator dedicated to the HTAH system are utilized for pressurization. The piping for the pressurization system is included in the cost estimates for piping for the HTAH system for Cases B and C and pressure relief valves are considered to be included in the costs for valving. Therefore, the only component not previously accounted for is the compressor/accumulator for Cases B and C. The specifications and estimated cost of this equipment are not indicated in reference 2-2. Since the cost of the compressor/accumulator is a very small fraction of the total HTAH system cost, an investigation, to estimate this cost, is deemed unnecessary.

Combustion pressurization system for Case D. - In the ETF reference design for Case D, the compression of the combustion air for the HTAH system is accomplished by a turbocompressor system in which part of the flue gas from the HTAH system expands through a turbine which drives the air compressor. The cost of this system (in mid-1977 dollars) is reported in reference 2-1 to be $2,340,000 for materials and $750,000 for direct labor for an oil-fired HTAH system with a system thermal capacity of 63.3 MW_t. Assuming indirect costs to be 20 percent of the materials cost and 98 percent of the labor cost, the total cost of the turbocompressor system is estimated to be $4,290,000. Escalation to mid-1979 dollars by cost indices reported in reference 2-3 leads to an estimate of $5,150,000.

If the HTAH system is fired with a low Btu gas which is also pressurized by a compressor driven by the expansion turbine, the turbocompressor system must handle approximately 25 percent more flow than it does for an oil-fired system. The establishment of a procedure for scaling up the costs of the turbocompressor system would require determining the cost scale-up factor for a single turbocompressor unit and determining the extent to which the system capacity should be increased by increasing the number of turbocompressor units. Such a determination has not been conducted in this investigation and the scaling will be assumed to follow the relationship

$$\frac{C_{Tc}}{C_{Tco}} = \left(1.25\ \frac{STC}{63.3}\right)^{0.83} \qquad (2N\text{-}4)$$

where C_{Tc} is the cost of the turbocompressor system, C_{Tco} is the cost of the turbocompressor system for the ETF reference design, STC is the system thermal capacity in MW_t and the exponent 0.83 is determined by assuming that the turbocompressor system cost scales according to the same exponent as the cost of the vessels and ducting for Case D.

It is suggested that a more detailed investigation be conducted to determine the appropriate scale factor for the turbocompressor system. Another factor which should be investigated further is the stack gas clean-up requirement for the products of combustion of the low Btu gas which is dictated by the need to protect the expansion turbine from excessive erosion and corrosion.

Building, foundation and support structure. - The only data available on the cost of the HTAH building for the ETF reference designs are the costs reported in reference 2-2 for Cases B and C. The HTAH building for these Cases houses the HTAH system, low temperature heat recovery equipment, the coal crusher and miscellaneous support equipment. Therefore, the entire cost of the building cannot be attributed solely to the HTAH system. The building is enclosed and also houses a bridge crane and a railroad spur to facilitate installation and maintenance of equipment. The total installed cost (including indirects) of this building is reported to be $12,450,000 (excluding contingency) in mid-1977 dollars for a HTAH system with a system thermal capacity of 93.8 MW_t. This represents approximately 40 percent of the cost of the HTAH system itself (excluding contingency). The fact that this percentage is so high indicates that further investigation of the cost of the building, foundation and support structure for the HTAH system is warranted. The investigation would be necessary so that the complete cost of the HTAH system can be determined in order to make a valid comparison between indirectly-fired high temperature air heating and the alternative approach

of utilizing oxygen enrichment, as well as a comparison of alternate HTAH system concepts with one another.

Fuel supply system. - The fuel required for Cases A and B is No. 2 fuel oil and the fuel required for Cases C and D is a low Btu gas produced in an on-site coal gasification plant. No cost estimates are given in reference 2-1 for the oil supply system for Case A. The cost estimate given in reference 2-2 for the oil supply system for Case B is $290,000 (not including contingency) in mid-1977 dollars for a 93.3 MW_t HTAH system. Escalation by means of cost indices reported in reference 2-3 gives a cost estimate of $350,000. This fuel supply system provides fuel oil for other MHD power plant subsystems, but the major fuel oil requirement is for the HTAH system. The storage capacity specified for the ETF reference design is less than would be required for a commercial plant because the duration of operation of a test facility is considerably less than that for a commercial power plant. However, this difference would be insignificant in comparison to the overall cost of the HTAH system and to the cost of the coal gasification plant required for Cases C and D.

Although Case D is a low Btu gas-fired HTAH system, the ETF reference design for Case D is an oil-fired system. The oil supply system cost estimate for this case is given in reference 2-1 as $236,000 for materials and $62,000 for direct labor. Assuming the indirect costs to be 20 percent of the material costs plus 98 percent of the labor cost yields a total cost of $460,000 in mid-1977 dollars for a 63.3 MW_t system. This escalates to $490,000 in accordance with price indices reported in reference 2-3.

An average cost for the oil supply system which reflects the data in references 2-1 and 2-2 would be approximately $500,000 for a 100 MW_t HTAH system. The costs for the larger HTAH systems can be considered to scale according to the equation

$$C_{os} = \$500{,}000\left(\frac{STC}{100}\right)^{0.6} \qquad (2N\text{-}5)$$

where C_{os} is the cost of the oil supply system and STC is the system thermal capacity in MW_t.

The reference design for Case C calls for a Wellman-Galusha coal gasification plant. The costs determined for this investigation are also based upon a Wellman-Galusha gasifier. However, it is highly recommended that further investigations be conducted to determine the types of coal gasification plant which are optimum for HTAH systems at each of the four thermal power levels under consideration. Cost estimates were obtained for the Wellman-Galusha gasification plant utilizing Illinois No. 6 coal from Dravo Corporation and are presented in table XL. The Wellman-Galusha gasifier unit has a production capability of from 17.6 to 19.0 MW_t (60 to 65 million Btu/hr). A 100 MW_t HTAH system would require the equivalent of approximately 117 MW_t (400 million Btu/hr) of fuel gas, thus requiring 7 gasifier units. Table XL also indicates the number of gasifier units required for each HTAH system thermal capacity level.

TABLE XL. - COST ESTIMATES FOR WELLMAN-GALUSHA
COAL GASIFICATION PLANTS UTILIZING
ILLINOIS NO. 6 COAL

HTAH System Thermal Capacity (MW_t)	Number of Gasifier Units	Estimated Plant Cost
100	7	18,000,000
250	16	35,000,000
500	32	67,000,000
1000	64	135,000,000

Appendix 20

Refractory Materials Costs

The costs of the refractory materials used for the cored-brick matrices and for the insulation for the vessels and ducting are indicated in table XLI. The materials costs are reported in dollars per unit mass of material except for mineral wool, which is reported in terms of dollars per unit volume. These unit prices are based upon data obtained from manufacturers of the indicated materials. The cost data for each material were obtained by submitting, to the manufacturers, specifications on quantity, sizes and configurations of the equipment in which the materials are to be installed. The tabulated data represent average prices determined from the data received and were utilized for estimating the HTAH system.

The large difference in unit price between the 99-AD matrix brick for Case D and for Cases B and C is due primarily to the difference in the size of the brick, rather than the difference in the hole size. The brick for Case D are smaller than the brick for Cases B and C. It is recommended that an investigation be conducted to determine the cost savings which can be derived from an increase in brick size for Case D.

The direct costs of installation of the refractory materials are indicated in table XLII. The installation costs are reported in dollars per unit volume of installed material. These unit costs are based upon data presented in reference 2-4.

TABLE XLI. - ESTIMATED COSTS OF REFRACTORY MATERIALS AND INSULATION

DESCRIPTION	UNIT PRICE ($ per lb)
Matrix Brick	
Greenal 90 (A.P. Green) - Case A	1.59 (0.72)
99-AD (A.P. Green) - Cases B and C	2.45 (1.11)
99-AD (A.P. Green) - Case D	5.75 (2.61)
Vessel Wall Insulation	
99-AD (A.P. Green)	1.54 (0.70)
Greenal 90 (A.P. Green)	1.01 (0.46)
G-33 (A.P. Green)	1.68 (0.76)
G-30 (A.P. Green)	0.97 (0.44)
G-28 (A.P. Green)	0.77 (0.35)
G-26 (A.P. Green)	0.66 (0.30)
G-23 (A.P. Green)	0.53 (0.24)
G-20 (A.P. Green)	0.46 (0.21)
Mineral Wool (Babcock & Wilcox)	475 $/m^3 (13.44 $/ft^3)
Greencast 94 (A.P. Green)	0.99 (0.45)
Lumnite Concrete (Universal-Atlas Co.)	0.11 (0.048)
Vessel Dome Insulation	
99-AD (A.P. Green)	1.50-1.57 (0.68-0.71)
G-33 (A.P. Green)	1.68 (0.76)
G-30 (A.P. Green)	0.88 (0.40)
G-23 (A.P. Green)	0.53 (0.24)
Greencast 94 (A.P. Green)	0.99 (0.45)
Vessel Bottom Cap Insulation	
Greencast 94 (A.P. Green)	0.99 (0.45)
Duct Wall Insulation	
Greenal 90 (A.P. Green)	1.01 (0.46)
G-33 (A.P. Green)	1.68 (0.76)
G-30 (A.P. Green)	0.97 (0.44)
G-26 (A.P. Green)	0.66 (0.30)
G-20 (A.P. Green)	0.46 (0.21)
Greencast 94 (A.P. Green)	0.99 (0.45)
VSL 50 (A.P. Green)	0.51 (0.23)
Thermo-12 (Johns-Manville)	13.56 (6.15)

TABLE XLII. - ESTIMATED COSTS OF INSTALLATION OF REFRACTORY MATERIALS AND INSULATION

DESCRIPTION	UNIT COST $/m^3$ ($/ft)^3
Matrix Material	2119 (60)
Vessel Walls	1059 (30)
Vessel Domes	4238 (120)
Heater Bottom Cap	1059 (30)
Crossover Duct Interior Insulation (Short With 2 Junctions)	2119 (60)
Other Ducting Interior Insulation (Including Junctions)	1413 (40)
Duct Exterior Insulation	1059 (30)

3. ENGINEERING SURVEY OF COAL HANDLING AND PROCESSING EQUIPMENT FOR MHD POWER PLANT APPLICATION

INVESTIGATION DEFINITION

The objective of this investigation is to present technical and cost data that can be used in the evaluation and selection of coal preparation equipment applicable to an MHD power plant and to identify those parameters relating to coal properties and preparation requirements which impact on either equipment cost or performance. The work reviews data associated with 250, 500 and 1000 MW_t plant sizes and emphasizes the pulverizing, classifying and drying aspects of coal preparation. The investigation considers two coals - a high sulfur, low moisture Illinois No. 6 coal and a low sulfur, high moisture Montana Rosebud coal - pulverized to three particle sizes - 70 percent -200 mesh, 80 percent -270 mesh and 100 percent -325 mesh. A wide range of equipment is reviewed for the various preparation functions with current and near term availability.

SUMMARY AND CONCLUSIONS

The report discusses the purposes of the pulverizing, sizing and drying processes in coal preparation for combustion, the type of equipment used in each category and the technical factors which affect selection of each type. Based on proposals and budget cost estimates received in response to a letter inquiry, the magnitude of the capital investment, power requirements, and estimated annual operation and maintenance costs for two types of pulverizers for the three plant sizes are presented and evaluated.

Coal preparation is practiced in all central power stations. Pulverizing and size classification are necessary, first for maximum combustion efficiency, and second to minimize fouling of heat absorbing surfaces. Drying is essential for efficient grinding and to achieve proper air-coal mixture temperatures prior to the

combustor and/or bunkers. All these elements are usually provided as a system in which drying, classification by size and grinding are integrated both physically and by controls.

The degrees to which fuel are pulverized and dried are determined by the technical requirements and economic factors associated with its end use. Because the benefits of coal preparation are realized throughout the thermodynamic cycle, a cost-benefit analysis, which would evaluate all these treatments and costs, is beyond the scope of this investigation.

To obtain reliable performance and up-to-date cost information on present day commercially available equipment for pulverizing the designated coals, a short performance specification was prepared and issued to potential suppliers. This is included as Appendix 3A.

Three levels of grinding are specified in the investigation: 70 percent through -200 mesh; 80 percent through -270 mesh; and 100 percent through -325 mesh.

A survey indicated that a wide selection of coal processing equipment is available - most have been developed to meet the needs of specific applications in present day power plants. In view of the lack of extensive experience with MHD cycles and combustors, their applicability can be based on only analogous needs and requirements.

From the two full responses to the inquiry (ref. 3-1 and 3-2), the relative costs of ball or tube mill and roller mill systems are determined. The ball mill is the lower cost type, even with a separate classifier, but for the fineness of 100 percent through -325 screen, the manufacturer would not quote information. A ball mill may require an external dryer to improve grinding efficiency.

On the other hand, the roller mill offered can realize close to 100 percent through -325 mesh. This type is generally more effective in drying moist coal than the ball mill, but is limited in capacity/unit and more mills may be required for a particular size plant.

A classifier is required to separate oversized particles and return them to the mill. The classifier is integral in a roller mill. The ball mill, on the other hand, does not have an integral classifier which must therefore be purchased as a separate item.

The particle size distribution achieved by commercial screening and classifying systems is normally fixed by system design. It is not a guaranteed parameter. The achievement of a range that is narrower requires special methods or power adjustment and is not required for today's powerplant design.

Drying, for both ball and roller mills, is accomplished within the mill by flue gases which also serve as a pneumatic conveying medium. Drying systems associated with pulverizers are direct-fired and semidirect systems. Alternative systems such as flash, steam and spray drying are used in special applications but have not secured a niche in coal-fired power plant applications.

Table XLIII shows the comparative results obtained from proposals for pulverizing systems. Investment and O&M costs and power requirements increase as the degree of fineness of the product increases (ref. 3-1 and 3-2).

INTRODUCTION

Magnetohydrodynamics (MHD) is a process of generating electricity from coal by feeding the combustion gases into a channel between the poles of a superconducting magnet. The combustion gases, which are seeded with a potassium salt to increase their conductivity, interact with the magnetic field and produce a direct current drawn off through the channel wall.

The efficiency of the process is closely associated with the properties of the coal as it is fed into the combustor, particularly with respect to fineness and moisture content. The selected fineness for the MHD power plant will be dependent upon allowable residence time in the combustor and the coal

TABLE XLIII. - EFFECT OF FINENESS OF GRIND ON COSTS AND PERFORMANCE

Plant Size	Percent Difference		
	70 percent -200 mesh (-74u)	80 percent -270 mesh (-53u)	100 percent -325 mesh (-44u)
A. 250 MW_t			
Equipment Costs (Adj)	Base	+46	+129
O&M Costs	Base	+45	+ 92
Power Consumption	Base	+53	+ 84
B. 500 MW_t			
Equipment Costs (Adj)	Base	+22	+ 92
O&M Costs	Base	+45	+ 92
Power Consumption	Base	+46	+ 81
C. 1000 MW_t			
Equipment Cost (Adj)	Base	+46	+108
O&M Costs	Base	+45	+ 92
Power Consumption	Base	+44	+ 59

volatility. As in all coal combustion processes, it is necessary in the MHD application to completely burn the coal particles within a prescribed volume or time span. Otherwise, the particles are carried out of the furnace before the total heat available from the coal is released. The same considerations apply to the MHD process whereby it is desirable for the combustion to be completed within the combustor. The optimum combustion gas temperature can be achieved before the gas enters the channel. There is, therefore, an optimum size to which the coal should be ground, not only to assure complete combustion before entering the channel, but also to preclude carryover of unburnt carbon into the channel.

The effect of moisture content of the coal-oxidant on MHD cycle efficiency is more pronounced. The presence of water in the as-fired coal reduces the enthalpy of the combustion gas, thus decreasing the gas temperature and reducing the gas conductivity and thence the generator power output. Tests have been conducted at the Pittsburgh Energy Technology Center to determine the effects of moisture content on combustion gas temperature and conductivity and the results are shown in figures 20 and 21 for a Montana Rosebud coal. The reduction in combustion gas enthalpy is due to a portion of the heating value of the coal being used to evaporate the moisture; this amounts to about 2.57×10^6 J/kg (1104 Btu/lb) of moisture. For a 40 percent efficient plant, such as the MHD plant, this could represent a loss of one to two efficiency points. The loss of conductivity of the combustion gases is due to the loss of potassium atoms in the formation of KOH, absorption of electrons by the OH radical and the increased number of KOH and H_2O molecules.

It is evident, therefore, that the fineness and moisture content of the as-fired coal require considerable attention to ensure that the maximum cycle efficiencies can be achieved.

For the purposes of this investigation, the coal type, fineness and "required as-fired moisture contents" have been selected by NASA and form the basis of the investigation. The effects that these parameters have on the selection of equipment and their

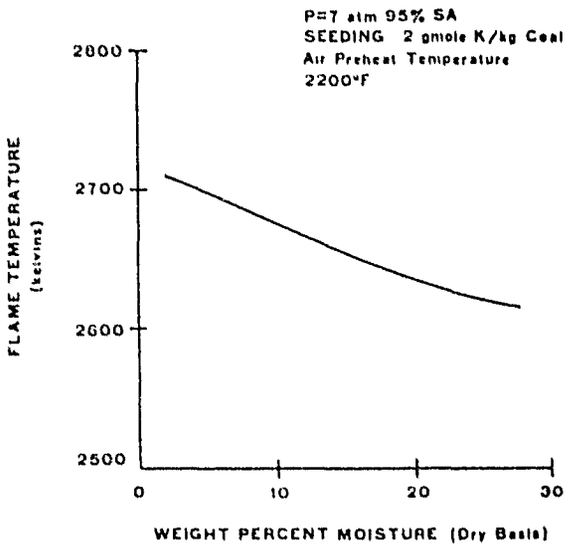

Figure 20. - Theoretical flame temperature as a function of moisture for Montana coal from the Rosebud seam (ref. 3-3).

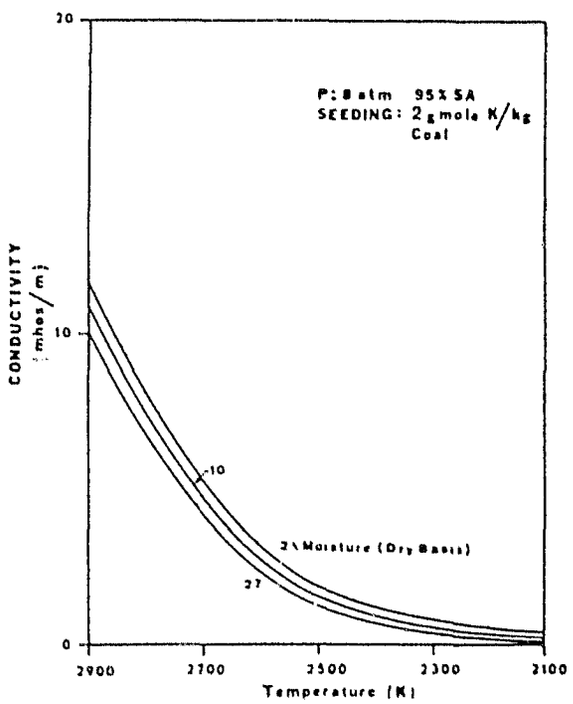

Figure 21. - Electrical conductivity of MHD combustion plasma vs. temperature for Montana Rosebud coal (ref. 3-3).

performance are reviewed, the applicability of equipment design to the operating conditions is evaluated and recommendations on equipment type selection are given.

BACKGROUND

Methodology

The methodology used to complete this investigation required two parallel activities. The first activity covered a review of in-house published data on coal preparation which included such publications as vendor catalogs, technical books, papers and articles from trade magazines, and discussions with in-house personnel actively engaged in coal plant design activities. This phase resulted in the accumulation of data relating to equipment design and performance and the effects of the coal properties and preparation requirements on the overall coal preparation system. Data relating to commercially available equipment are established based upon significant experience, but the far-term technologies have not acquired such a record. However, as a case in point, the use of fluidized bed technology for drying is well recognized in the ore mining industry and has been used for many years, thus accumulating a significant record in what may be termed a related service. The development required, therefore, is not necessarily technical but rather one of application, a significantly lower risk.

The second activity included obtaining quotations from equipment manufacturers for a coal preparation system covering specific plant sizes, coal types and coal finenesses. The request for quotation was sent to seven manufacturers, two of whom responded with the requested information. The request contained a letter specification of the system performance requirements and a listing of performance and cost data to be provided by the manufacturer. A copy of the request is included in this report as Appendix 3A and the responses are tabulated in tablex XLIV, XLV and XLVI. The

TABLE XLIV. - MANUFACTURER'S AS-REPORTED PERFORMANCE AND COST DATA FOR 250 MW_t PLANT USING ILLINOIS AND MONTANA COALS (ref. 3-1 and 3-2)

Coal Type	Illinois No. 6						Montana Rosebud					
Particle Size	-200		-270		-325		-200		-270		-325	
Manufacturer	A	B	A	B	A	B	A	B	A	B	A	B
Mill Type	Roller	Ball	Roller	Ball	Roller	Ball	Roller	Ball	Roller	Ball	Roller	Ball
Number of Mills	3	3	3	3	3	No Quote	3	3	3	3	3	No Quote
Outlet Moisture Content, %	2.0	1.4	2.0	1.0	2.0	-	5.0	5.0	5.0	4.7	5.0	-
Coal Feed Per Mill, kg/sec (t/hr)	4.8 (19)	4.8 (19)	4.8 (19)	5.3 (21)	4.8 (19)	-	6.0 (23.9)	6.0 (23.9)	6.0 (23.9)	6.2 (24.5)	6.0 (23.9)	-
Power Consumption, kJ/kg (kwh/ton)	46 (11.6)	62 (15.6)	70 (17.7)	85 (21.4)	114 (28.7)	-	48 (12.2)	62 (15.5)	71 (17.9)	85 (21.4)	121 (30.4)	-
Gas Temperature to Mill, °K (°F)	439 (330)	422 (300)	432 (318)	422 (300)	422 (300)	-	589 (600)	561 (550)	589 (600)	561 (550)	589 (600)	-
Gas Flow Per Mill, kg/sec (1000 acfm)	8.6 (23)	9.3 (24)	10.8 (28)	9.3 (24)	19.4 (50)	-	8.6 (30)	12.1 (41)	10.3 (36)	12.1 (41)	18.6 (66.5)	-
Mill Outlet Temperature, °K (°F)	356 (180)	344 (160)	356 (180)	344 (160)	356 (180)	-	356 (180)	344 (160)	356 (180)	344 (160)	356 (180)	-
Mill Pressure Drop, kPa (ins H_2O)	5.0 (20)	0.5 (2)	4.1 (16.5)	0.5 (2)	4.9 (19.5)	-	5.2 (21)	0.5 (2)	4.5 (18)	0.5 (2)	5.2 (21)	-
Estimated O&M Cost, ¢/kg ($/ton)	.012 (0.105)	.020 (0.18)	.017 (0.152)	.016 (0.142)	.022 (0.202)	-	.010 (0.088)	.020 (0.179)	.014 (0.130)	.027 (0.242)	.019 (0.170)	-
Equipment Cost, $ FOB	1,369,810	1,020,000	1,999,916	1,350,000	3,135,585	-	1,738,981	1,215,000	2,560,324	1,395,000	4,059,761	-
Adjusted Costs, $ FOB	1,369,810	1,100,000	1,999,916	1,450,000	3,135,585	-	1,738,981	1,325,000	2,560,324	1,525,000	4,059,761	-

TABLE XLV. - MANUFACTURER'S AS-REPORTED PERFORMANCE AND COST DATA FOR 500 MW_t PLANT USING ILLINOIS AND MONTANA COALS (ref. 3-1 and 3-2)

Coal Type	Illinois No. 6						Montana Rosebud					
Particle Size	-200		-270		-325		-200		-270		-325	
Manufacturer	A	B	A	B	A	B	A	B	A	B	A	B
Mill Type	Roller	Ball	Roller	Ball	Roller	Ball	Roller	Ball	Roller	Ball	Roller	Ball
Number of Mills	3	3	4	3	4	No Quote	4	3	4	3	5	No Quote
Outlet Moisture Content, %	2.0	1.5	2.0	1.0	2.0	-	5.0	5.0	5.0	4.7	5.0	-
Coal Feed Per Mill, kg/sec (t/hr)	9.6 (38)	9.6 (38)	6.3 (25)	11.0 (43.7)	6.3 (25)	-	8.0 (31.9)	12.0 (47.6)	8.0 (31.9)	13.2 (52.4)	6.0 (23.9)	-
Power Consumption, kJ/kg (kwh/ton)	47 (11.8)	62 (15.6)	68 (17.2)	85 (21.4)	123 (31.1)	-	50 (12.7)	62 (15.5)	73 (18.4)	85 (21.4)	121 (30.4)	-
Gas Temperature to Mill, $^{\circ}$ K ($^{\circ}$ F)	439 (330)	422 (300)	432 (317)	422 (300)	423 (301)	-	589 (600)	561 (550)	589 (600)	561 (550)	589 (600)	-
Gas Flow Per Mill, kg/sec (1000 acfm)	17.9 (45)	18.6 (48)	14.4 (36.5)	18.6 (48)	26.2 (66.5)	-	11.6 (41)	23.9 (81)	14.1 (50)	23.9 (81)	18.9 (66.5)	-
Mill Outlet Temperature, $^{\circ}$ K ($^{\circ}$ F)	356 (180)	344 (160)	356 (180)	344 (160)	356 (180)	-	356 (180)	344 (160)	356 (180)	344 (160)	356 (180)	-
Mill Pressure Drop, kPa (ins H_2O)	6.2 (25)	0.5 (2)	4.5 (18)	0.6 (2.5)	0.5 (2.15)	-	5.7 (23)	0.5 (2)	4.9 (19.5)	0.6 (2.5)	5.2 (21)	-
Estimated O&M Cost, c/kg ($/ton)	.012 (0.105)	-	.017 (0.152)	-	.022 (0.202)	-	.010 (0.088)	.019 (0.174)	.014 (0.130)	.026 (0.235)	.019 (0.170)	-
Equipment Cost, $ FOB	2,817,882	1,425,000	3,426,408	2,040,000	5,399,108	-	3,047,772	1,620,000	4,375,038	2,340,000	6,721,300	-
Adjusted Costs, $ FOB	2,817,882	1,600,000	3,426,408	2,250,000	5,399,108	-	3,047,772	1,850,000	4,375,038	2,600,000	6,721,300	-

TABLE XLVI. - MANUFACTURER'S AS-REPORTED PERFORMANCE AND COST DATA FOR 1000 MW_t PLANT USING ILLINOIS AND MONTANA COALS (ref. 3-1 and 3-2)

Coal Type	Illinois No. 6						Montana Rosebud					
Particle Size	-200		-270		-325		-200		-270		-325	
Manufacturer	A	B	A	B	A	B	A	B	A	B	A	B
Mill Type	Roller	Ball	Roller	Ball	Roller	Ball	Roller	Ball	Roller	Ball	Roller	Ball
Number of Mills	3	3	4	3	6	No Quote	3	3	5	3	8	No Quote
Outlet Moisture Content, %	2	1.4	2	1.0	2	-	5.0	5.0	5.0	4.7	5.0	-
Coal Feed Per Mill, kg/sec (t/hr)	19.0 (75.75)	21.0 (83.3)	12.7 (50.5)	19.8 (78.7)	7.6 (30.3)	-	24.1 (95.7)	24.1 (95.7)	12.0 (47.8)	24.2 (96.1)	6.9 (27.3)	-
Power Consumption, kJ/kg (kwh/ton)	54 (13.5)	62 (15.6)	77 (19.4)	85 (21.4)	122 (30.7)	-	58 (14.5)	62 (15.5)	79 (19.9)	85 (21.4)	128 (32.2)	-
Gas Temperature to Mill, $^{\circ}$ K ($^{\circ}$ F)	439 (330)	422 (300)	432 (317)	422 (300)	422 (300)	-	589 (600)	561 (550)	589 (600)	561 (550)	589 (600)	-
Gas Flow Per Mill, kg/sec (1000 acfm)	35.8 (90.5)	38.1 (97)	32.3 (81.5)	38.1 (97)	32.3 (81.5)	-	34.8 (122.5)	49.1 (167)	23.2 (81.5)	49.1 (167)	22.2 (81.5)	-
Mill Outlet Temperature, $^{\circ}$ K ($^{\circ}$ F)	356 (180)	344 (160)	356 (180)	344 (160)	356 (180)	-	356 (180)	344 (160)	356 (180)	344 (160)	356 (180)	-
Mill Pressure Drop, kPa (ins H_2O)	7.3 (29.5)	0.6 (2.5)	5.6 (22.5)	0.7 (3.0)	5.6 (22.5)	-	7.8 (31.5)	0.7 (3)	5.6 (22.5)	0.9 (3.5)	5.6 (22.5)	-
Estimated O&M Cost, c/kg ($/ton)	.012 (0.105)	.009 (0.08)	.017 (0.152)	.020 (0.18)	.022 (0.202)	-	.010 (0.088)	.019 (0.170)	.015 (0.132)	.020 (0.182)	.019 (0.172)	-
Equipment Cost, $ FOB	4,927,312	2,760,000	7,200,182	3,600,000	10,256,541	-	6,435,354	3,150,000	8,943,681	3,900,000	13,529,648	-
Adjusted Costs, $ FOB	4,927,312	3,200,000	7,200,182	4,000,000	10,256,541	-	6,435,354	3,600,000	8,943,681	4,400,000	13,529,648	-

responses were reviewed and, after discussions with the respective manufacturers, it was apparent that the respective scopes of supply differed. Thus the costs of one manufacturer were adjusted to include allowances for omitted components as follows

- Fan costs calculated at $1322 per kg/sec (75¢/scfm)
- Baghouse costs calculated at 18.6 ¢/m^2 ($2/$ft^2$) of filtering area
- Fan and mill motor costs at $54/kW ($40/HP)

These adjustment factors were derived from in-house cost estimating data used for similarly sized equipment on existing projects. It should be noted that the adjustments affect only the ball mill system and increase the costs by 10 to 20 percent.

Comparison of the results of these two activities (the technical review and the vendor solicitation) provides a correlation of the theoretical and practical effects of coal properties, coal throughput capacities and fineness requirements. Furthermore, the latter activity provides an indication of the cost driven factors related to coal preparation and the relative cost impact of each for the various designs considered. Data from each activity provides the bases for engineering judgements in the selection of coal preparation system equipment (pulverizing, drying and classifying) for the MHD plants specified. This report does not address the partial removal of ash and sulfur from the coal prior to combustion by either physical coal cleaning (via gravity, flotation, or electrical methods) or chemical coal cleaning (via acid treatment, alkaline treatment, or oxidation reaction). Such an assessment is beyond the scope of this investigation, but should certainly be considered in future programs. Only coal washing, as currently practiced at the mines, has been assumed to have occurred for the purposes of this investigation.

Pulverizing

Need for pulverizing. - The coal particle size range established for this investigation requires size reduction beyond that

accomplished in crushing. Following the mining of the coal, crushing is the first, and for some applications the only, stage of size reduction and results in coal sizes ranging up to a nominal 5.1 cm (2 in.) diameter. For pulverized coal facilities it is not uncommon to specify coal size, as delivered, less than 1.9 cm (3/4 in.). This would include the use of "slack" which, prior to the advent of pulverized coal systems, was rejected as being too fine. Table XLVII provides a comparison of sieve, micron and mesh sizes and indicates that for the 1.9 cm (3/4 in.) size coal a significant further size reduction is required. This is accomplished in a pulverizer or mill, the various types of which are described in greater detail in a later section of this report.

Pulverizing offers further advantages in the drying and firing aspects of the coal since pulverizing increases the effective surface area of the coal particles. This promotes combustibility and assists in the efficient drying of the particles as it exposes the inherent moisture to the drying process. Other advantages attributable to pulverizing coal are

- Increase in thermal efficiency due to lower excess air requirements and lower carbon losses when compared with stoker fired systems
- Use of pneumatic transport systems
- Increase in reliability and decrease in maintenance requirements compared with conveyor systems

The design of a mill will depend upon the following operating parameters

- Grindability
- Fineness or classification
- Moisture content
- Mill outlet and inlet temperatures
- Throughput

Grindability. - The grindability of coal is a measure of the relative hardness of that coal compared with a standard coal

TABLE XLVII. - COMPARISON OF FINENESS SIZING METHODS (ref. 3-4)

U.S.S. A.S.T.M. Designations		Mesh Equiv.	Sieve Opening	
Sieve Size or Number	Micron		Milli-Meters	Inches
4 in.	—	—	101.6	4.00
3½ in	—	—	88.9	3.50
3 in.	—	—	76.2	3.00
2½	—	—	63.5	2.50
2 in.	—	—	50.8	2.00
1¾	—	—	44.4	1.75
1½ in.	—	—	38.1	1.50
1¼ in.	—	—	31.7	1.25
1 in.	—	—	25.4	1.00
⅞ in.	—	—	22.2	0.875
¾ in.	—	—	19.1	0.750
⅝ in.	—	—	15.9	0.625
½	—	—	12.7	0.500
7/16 in.	—	—	11.1	0.438
⅜ in.	—	—	9.52	0.375
5/16 in.	—	—	7.93	0.312
¼ in.	—	3	6.35	0.250
3½	5660	3½	5.66	0.223
4	4760	4	4.76	0.187
5	4000	5	4.00	0.157
6	3360	6	3.36	0.132
7	2830	7	2.83	0.111
8	2380	8	2.38	0.0937
10	2000	9	2.00	0.0787
12	1680	10	1.68	0.0661
14	1410	12	1.41	0.0555
16	1190	14	1.19	0.0469
18	1000	16	1.00	0.0394
20	840	20	0.84	0.0331
25	710	24	0.71	0.0280
30	590	28	0.59	0.0232
35	500	32	0.50	0.0197
40	420	35	0.42	0.0165
45	350	42	0.35	0.0138
50	297	48	0.297	0.0117
60	250	60	0.250	0.0098
70	210	65	0.210	0.0083
80	177	80	0.177	0.0070
100	149	100	0.149	0.0059
120	125	115	0.125	0.0049
140	105	150	0.105	0.0041
170	88	170	0.088	0.0035
200	74	200	0.074	0.0029
230	62	250	0.062	0.0024
270	53	270	0.053	0.0021
325	44	325	0.044	0.0017
400	37	400	0.037	0.0015

chosen with an index of 100 grindability. Thus, a coal is harder to grind if the index is lower and vice versa. The testing method used is based on the premise that the work done in pulverizing is proportional to the new surface produced. The most common method is the Hardgrove Method which uses a small amount of the coal (50 grams) and conducts the test in accordance with ASTM D409. The amount of coal passing through a 200 mesh screen after 60 seconds of grinding is used to determine the index. The grindability indices of the two coals investigated are 56 and 57, and are well within the normal range. Figures 22 and 23 show the effect of grindability on mill capacity as given by two different manufacturers. Although the curves are different, the net results are similar. Figure 23 indicates that for a 70 percent -200 mesh fineness there is a loss of mill capacity in the ratio of 1.6:1.0 for grindability indices of 100:50. Alternatively, this indicates that 60 percent more power is required to grind the harder coal with the same throughput. With the increase of power input to a pulverizer it is reasonable to expect the equipment cost to increase accordingly; not only due to the increase in motor size but also the requirement for a more rugged design.

Fineness. - The fineness to which the coal must be ground is dependent upon, primarily, the volatility of the coal. High-volatile coals do not need to be as finely ground as low-volatile coals as they are more readily ignited. The high-volatile coals are normally found in the bituminous and subbituminous groups with a volatile matter content greater than 30 percent. This classification includes a coal such as the reference Illinois No. 6, but would exclude the reference Montana Rosebud coal. Thus the latter coal could be expected to require grinding to a finer degree to achieve the same combustibility as the former. Figures 22 and 23 also show the effect of fineness on mill capacity for given grindability indices and indicate significant increases in power requirement or decreases in capacity, as the fineness requirements become smaller. For the two coals under consideration, figure 22 indicates a 20 percent reduction in mill capacity

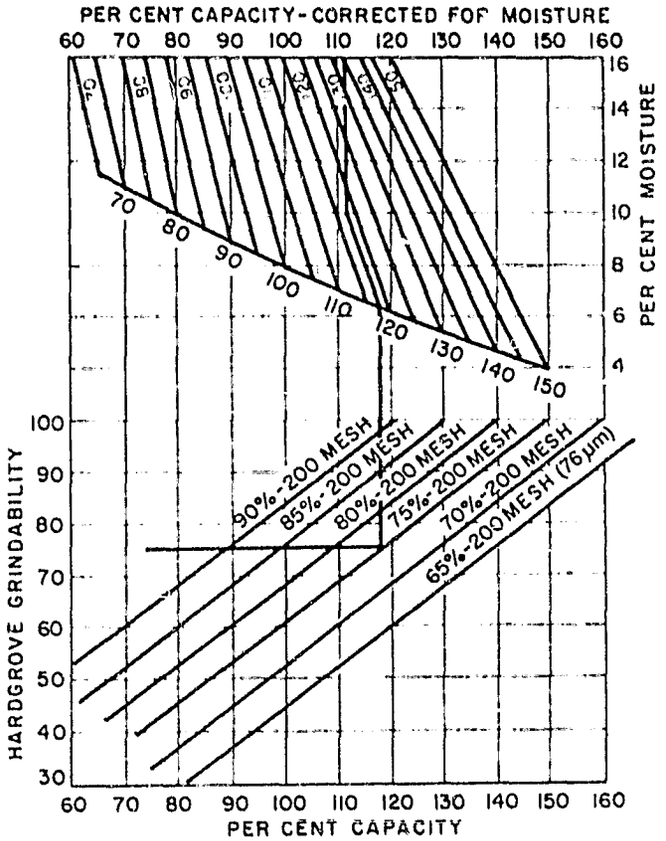

Figure 22. - Effects of grindability, fineness and moisture content on mill capacity (ref. 3-5).

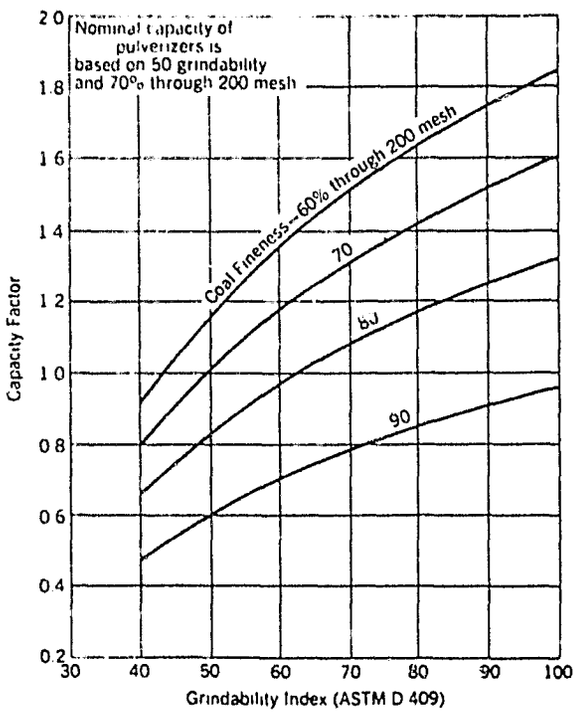

Figure 23. - Effects of grindability and fineness on mill capacity (ref. 3-6).

(from 1.05 to 0.85) can be expected if the fineness requirements are changed from 70 percent -200 mesh to 80 percent -200 mesh.

It is apparent, therefore, that there is an optimum range of fineness for each coal which is not too large to preclude suspension in the transport air nor too small to result in the waste of grinding power as very fine particles tend to agglomerate, thus defeating the purpose of pulverizing. The selection of particle size is ultimately dependent upon its end use and must be consistent with the burner requirements, furnace design, operating conditions and the coal's volatility.

Table XLVIII presents the coal particle size distribution for the three levels of fineness specified: 70 percent through -200 mesh; 80 percent through -270 mesh; and 100 percent through -325 mesh. These particle size distributions are obtained from figure 24 for an angle setting of 56° (ref. 3-7), the setting recommended by the manufacturer for the two coals specified. It should be noted that obtaining a narrower coal size distribution, as could be achieved by double screening or process adjustment, would be a very costly and wasteful operation and is therefore not a design parameter that is addressed in commercial power plant design.

Moisture content. - High moisture content of the coal has a detrimental effect on the mill capacity. This is due to the fact that, for in-the-mill drying, increased drying capability must be accommodated which normally results in higher drying gas flows and/or temperatures and an increase in mill power requirements. It should be noted that the milling action itself provides some drying power. Thus, a drying gas flow must be selected that will minimize the effect of milling action drying so that the mill power is used specifically for grinding. Figure 22 shows a dramatic decrease in mill capacity as the coal moisture content is increased above the nominal design parameters.

Mill inlet and outlet temperatures. - For in-the-mill drying the inlet and outlet air temperatures are important. If, due to fineness, it is necessary to have low air flow through the mill, wet coal cannot be handled without a reduction in mill capacity. Thus the construction of the mill should allow the

TABLE XLVIII. - COAL PARTICLE SIZE DISTRIBUTION*

%	Levels of Fineness		
	70 percent -200 mesh (-74 μ)	80 percent - 270 mesh (-53 μ)	100 percent -325 mesh (-44 μ)
10	13	8	3
20	22	14	5
30	30	18	7
40	38	24	9
50	48	30	11
60	60	38	13
70	74	43	15
80	90	53	18
90	105	74	26
95	130	90	30
99	170	120	43

*The table indicates the percents by weight of coal particles less than the indicated particle size (ref. 3-7). For example, for the first level of fineness, 70 percent of the coal is in particles that are 74 μ or less, 80 percent of the coal is in particles that are 90 μ or less, etc.

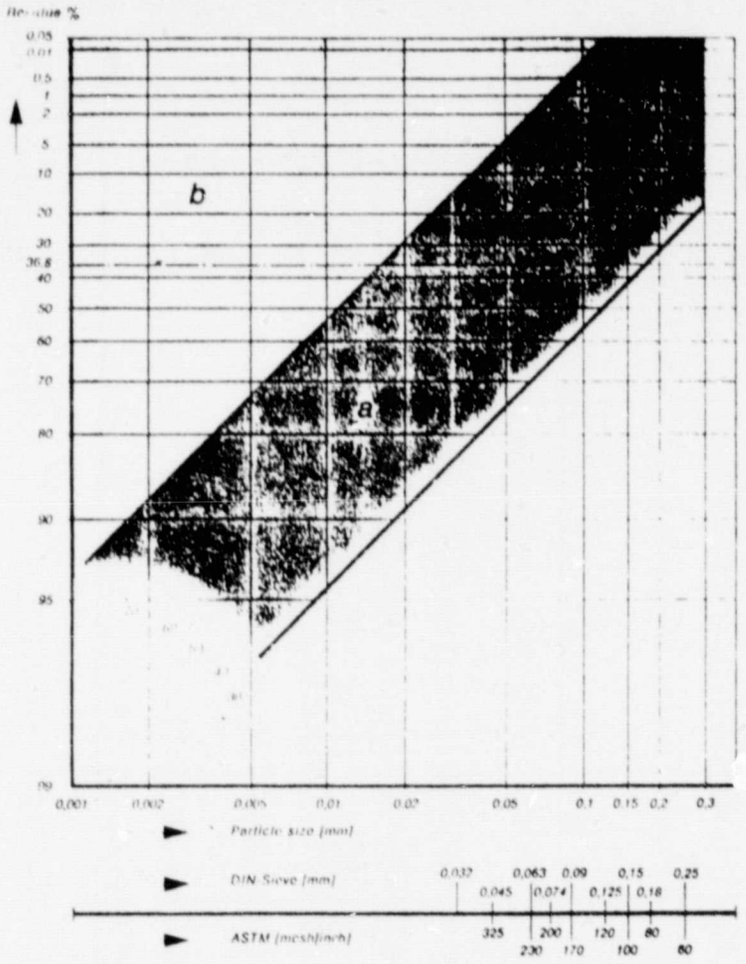

Ranges of Product Fineness

a) Normal range controllable by classifier speed and gas volume through mill.
b) By process adjustment.

Figure 24. - Working chart to determine ranges of product fineness based on mill angle and fineness specification (ref. 3-7).

use of high temperature gas in sufficient volume to maintain a condition of relative humidity below the saturation at the mill outlet. This normally dictates the use of air temperatures greater than 533° K (500° F) for pulverized coal fired boilers which have mill outlet temperatures about 356° K (180° F). Because the MHD combustor requires bunkering of the fines, the fines must either be stored at temperatures below approximately 328° K (130° F) or an inert gas such as N_2 must be utilized to preclude spontaneous combustion in the bunker. The availability of N_2 in an MHD plant makes this second approach particularly attractive, especially since storing the fines at low temperatures may recondense the moisture driven off during the drying process and could present a corrosion problem due to the formation of sulfurous and sulfuric acids. This condition is not prevalent with pulverized coal fired power plants as the pulverized coal and air mixture is swept directly into the boiler where it is combusted. However, this problem is experienced in outdoor coal handling facilities particularly at receiving and reclaim hoppers handling wet (from rain) high sulfur content coal.

Figure 25 shows a typical comparison of air quantity vs. air temperature for various drying requirements for eastern and western coals. These curves are not specifically related to any of the cases discussed in this report but show the relative effect of increasing moisture content. The two manufacturers who responded to the inquiry have indicated gas temperatures are required to be greater than 422° K (300° F) for the Illinois coal and greater than 533° K (500° F) for the Montana coal. The weight ratio of air flow to coal flow for the Illinois coal is approximately 2:1 for the 70 percent -200 mesh and 80 percent -270 mesh, whereas for the 100 percent -325 mesh the ratio is given as 4:1. For the Montana coal the ratios given are between 1.5 to 2.0 for the -200 mesh and 3.0 for the -325 mesh. The higher air temperatures noted for the Montana coal are to be expected as the moisture content of the coal is higher, thus requiring greater drying.

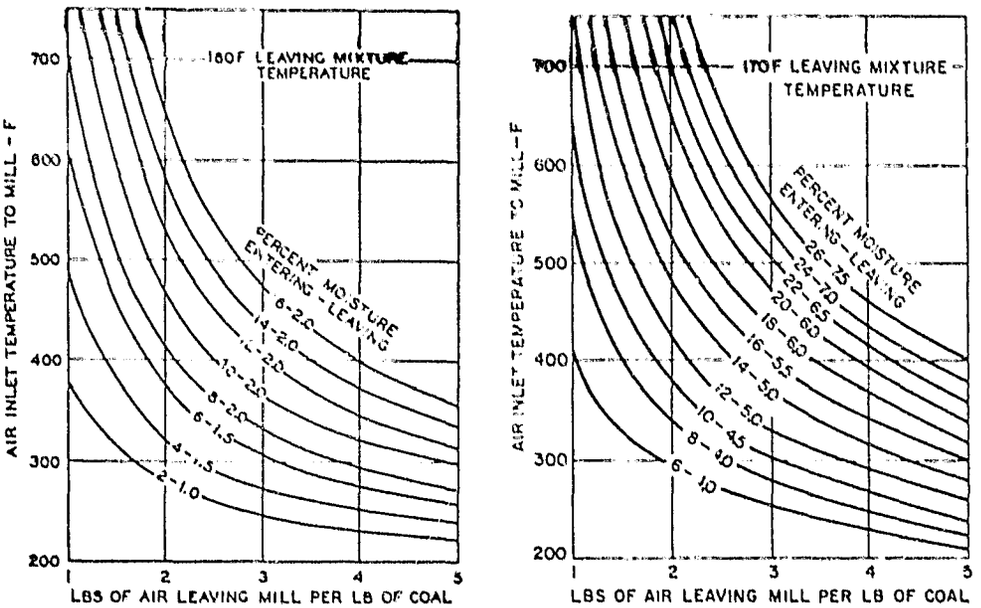

Eastern Coal Western Coal

Figure 25. - Air quantity vs. air temperature for different drying conditions (ref. 3-5).

Throughput. - Throughput relates directly to the rate at which the coal must be processed. Inevitably, as the throughput increases the mill capacity and power input increase. For certain types of mills this size increase reaches a maximum practical limit after which further increases in throughput must be accommodated by increasing the number of mills. Throughput is not the only parameter which impacts size; the combination of the effects of grindability, fineness and moisture content also must be considered in the size selection process. Although the use of multiple mills may increase the overall availability of the pulverizing system it has a significant effect on costs as the benefits of scaling cannot be realized to the maximum extent. Furthermore, the use of multiple units also increases the investment in supporting systems and controls.

Classifiers

Need for classifiers. - During the pulverizing process the suspended coal particles are transported out of the pulverizing

area by the motive air. Although these particles are small enough to be suspended in the air some will not meet the specified fineness and must be returned to the pulverizing section for further size reduction. At the same time there is no need to return the correctly sized particles and thus a classifier is incorporated into the system to drop out the largest particles.

Technical features. - Although classifiers are available in various shapes and sizes, they rely, predominately, on expansion and/or centrifugal action to accomplish separation. With the exception of the ball mill, the classifier is normally incorporated as an integral part of the mill design and is situated immediately before the mill outlet facilitating the return of the larger particles to the pulverizing section. The ball mill does not provide this capability within the mill itself. The classifier must be installed downstream of the mill outlet with the larger particles being returned to the feed end of the mill. External classifiers take various forms, the most usual being the cyclone. These are readily available in sizes up to 229 cm (90 in.) in diameter and can be used in various unit combinations. For particles -200 to -325 mesh in size, cyclone efficiency approaching 98 percent can be expected. Vendor data indicate optimum air velocity is 18.3 m/sec (3600 ft/min) and design pressure drops are in the range of 1000 to 1250 Pa (4 to 5 inches w.g.).

Drying

Need for drying. - The need for drying the coal is dictated by the detrimental effect of wet coal on the MHD cycle efficiency previously discussed in the Introduction. Furthermore the detrimental effect that moisture content has on the mill design supports the requirement for drying. There are a variety of means to accomplish drying the most common of which are

- In-the-mill drying
- Direct steam drying

- Fluidized bed drying
- Louvre and rotating drum drying
- Flash drying
- Indirect drying

Technical features. - Most of the coal drying systems available rely upon direct contact between the coal and the drying medium to achieve drying. Although this is the most efficient method it does result, in the gaseous systems, with the problem of carryover of the smaller particles requiring gas/particle separation equipment. The systems available, with the exception of in-the-mill drying, accomplish the drying upstream of the pulverizer and are capable of handling coal sizes from about 3.8 cm (1-1/2 in.) down to 0.

The concerns relating to in-the-mill drying and mill inlet and outlet temperatures have been covered in the previous discussion on pulverizers. This approach has been incorporated in power plant designs for many years and has accumulated a significant experience record. The use of a pulverizer will require transport air and particulate separation equipment which is independent of the external drying system selected.

The direct drying systems require an intimate mixing of the coal and drying medium to be effective. The steam drying process takes advantage of the improved drainage quality of water at elevated temperatures. The fluidized bed dryers suspend the coal in an active fluid bed by the passage of hot air. This hot air is normally generated by an independently oil- or coal-fired air heater as the air temperatures required are greater than may be available from an existing boiler system. The louvre and rotating drum dryers operate by passing hot air through moving louvres which support the coal to be dried. The flash dryer relies on contact of the coal with gas at a temperature of approximately 922^{o} K (1200^{o} F), accomplishing drying almost instantly (about 1/2 second). The high inlet temperature is possible due to the nature of the flash drying and does not result in any change in coal characteristics.

The indirect dryers overcome the problem of carryover by eliminating the gas from the coal drying space. This is accomplished either by the use of hot steel balls, hollow screw feeders containing the drying medium or rotating hollow discs filled with the drying medium through the coal bed.

INVESTIGATIONS AND FINDINGS

Pulverizers

To affect the particle size reduction of coal as specified will require the use of pulverizers or mills to grind the coal. The pulverizers use one or more of the basic principles of size reduction, namely impact, attrition and crushing. The machines are normally classified by speeds, low, medium and high and the four most common are the ball, roller, ball-and-race and impact types. Table XLIX compares speed classification with pulverizer type (ref. 3-5).

TABLE XLIX. - COMPARISON OF SPEED CLASSIFICATION WITH PULVERIZER TYPE

Mill Type	Speed (RPM)
Ball	18-35
Roller and Ball-and Race	75-225
Impact Attrition	> 200

These mills are normally designed for coal sizes 70 percent -200 mesh to 90 percent -200 mesh, but can meet 80 percent -270 mesh without difficulty. Our contact with manufacturers during this investigation has indicated that meeting 100 percent -325 mesh is more difficult. In fact, one vendor who submitted data on a ball mill did not quote on this option.

Ball mills. - The ball mill (also known as the tube mill) is shown in figure 26. The ball mill consists of a hollow horizontal cylinder fitted with heavy case liners filled to less than half with varying sized steel balls. The drum is rotated at a speed in the range of 18 to 35 rpm and coal is fed into the cylinder through hollow trunnions. Pulverizing is accomplished through the continual cascading of the mixture as a result of

- Impact of the falling balls
- Attrition as particles slide over each other and the liners
- Crushing as the balls roll over the particles

The larger pieces of coal are broken by impact and the smaller particles are produced by the attrition and crushing actions. Drying can be accomplished in the mill by the passage of hot air through the mill. The mill design does not incorporate an integral classifier which must therefore be installed externally. The larger particles removed from the classifier, now dried, are returned to the feed cycle of the mill for reinjection. The required fineness is achieved by judicious selection of different sizes for the ball charge and drum rotational speed. Fineness of the product varies with ball life as the small balls are efficient for breaking small particles and the large balls are efficient for breaking large particles.

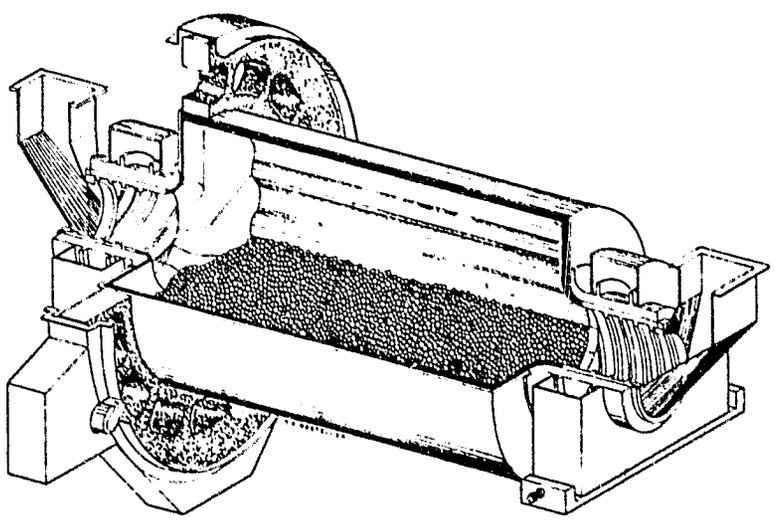

Figure 26. - Ball mill (ref. 3-4).

Due to its simplistic design, this mill is noted for low maintenance and high reliability. However, due to its size and weight, it inevitably uses more power per ton of coal pulverized than the lighter, higher speed mills. This mill also exhibits a less efficient mixing of the drying air with the pulverized fuel, thus requiring a higher drying air flow. This becomes particularly noticeable with high moisture coals. Data received from the manufacturers indicate higher drying air flows for the ball mill compared to the roller mill.

Roller and ball-and-race mills. - The roller and ball-and-race mills represent the largest number of mills used for coal grinding and are shown in figures 27 and 28. These mills are of medium speed (75 to 225 rpm) and utilize, primarily, crushing and attrition for size reduction. The grinding action takes place between two surfaces, one rolling over the other. The rolling element is either a roller or a ball. For the roller mill there are normally two roller/ring arrangements, one with the roller being driven (figure 29) and the other with the ring being driven (figure 30). The required grinding pressure is applied by adjusting the external springs attached to the roller shaft. In the ball-and-race mill the balls are confined between upper and lower races either of which can be the rotating member. The grinding pressure is applied by forcing the races together using springs, pneumatic or hydraulic systems.

Maintenance of the roller and ball-and-race mills is about equal with the ball mill. Due to its relative complexity, the roller mill is more expensive for a given capacity. However, the roller mill is compact and occupies a smaller area. Manufacturers' data show that there is a practical limit to the roller mill capacity which is significantly less than that of the ball mill. Hence for high capacities multiple roller mills are required utilizing more space and effectively being even more expensive.

Impact mill. - The impact mill, shown in figure 31, consists primarily of a series of hinged or fixed hammers or lugs revolving

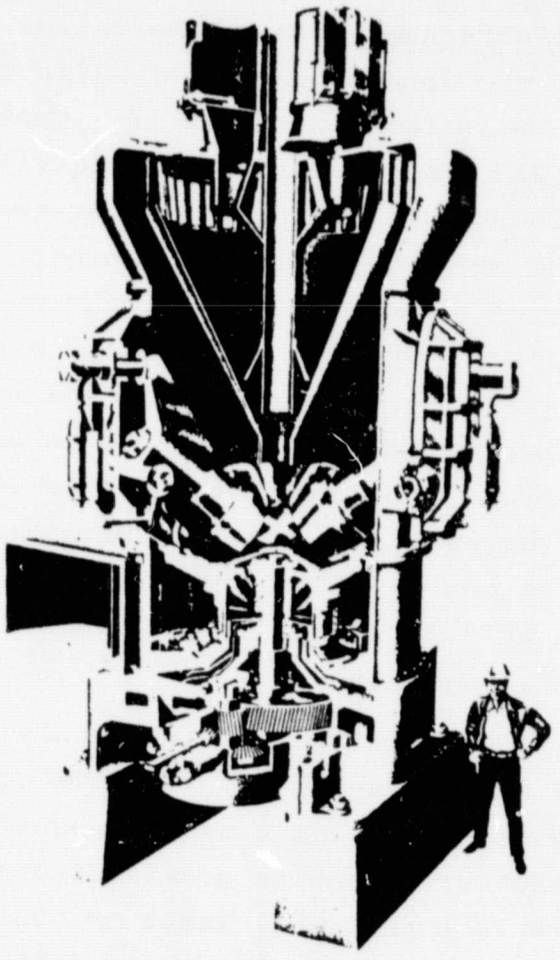

Figure 27 . - Roller mill (ref. 3-7).

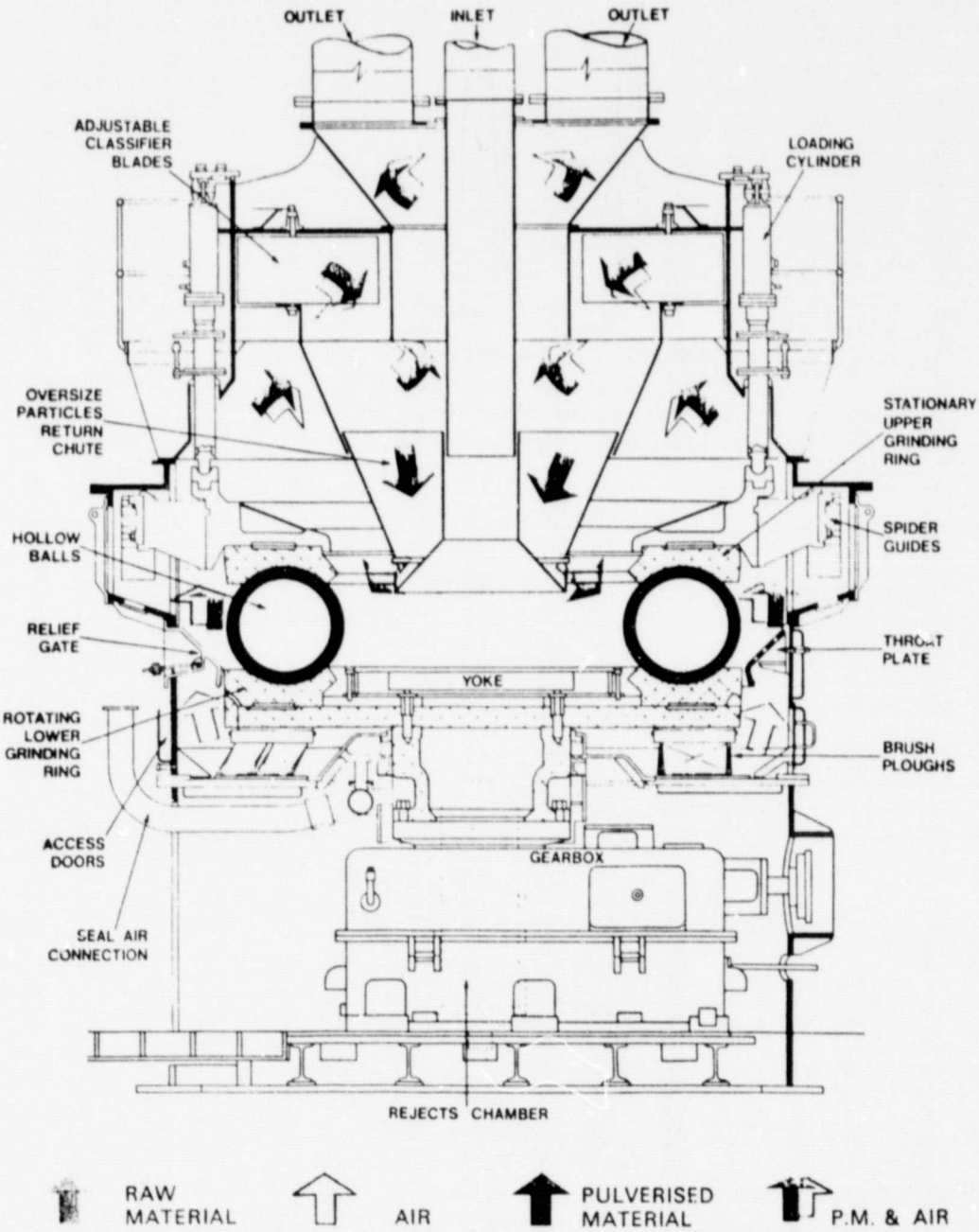

Figure 28. - Ball and race mill (ref. 3-9).

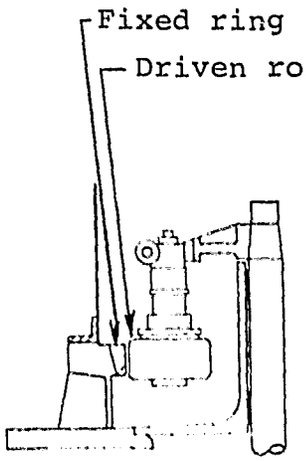

Figure 29. - Roller mill with stationary ring and driven roller (ref. 3-5).

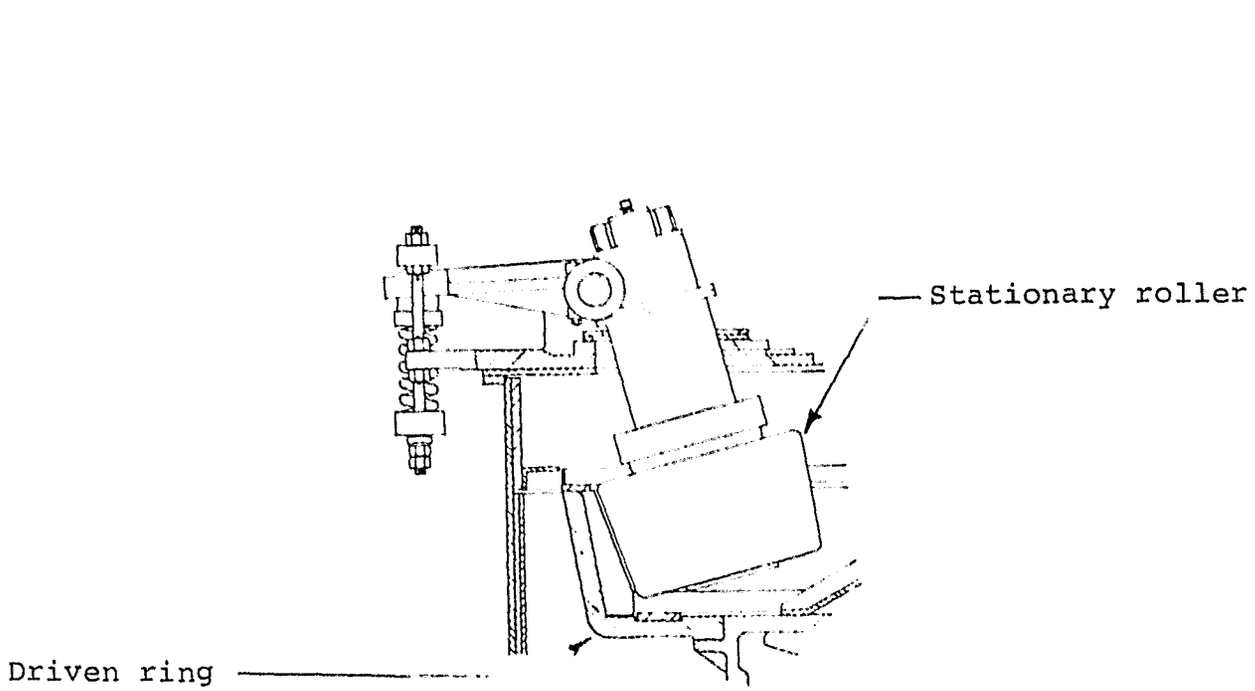

Figure 30. - Roller mill with stationary roller and driven ring (ref. 3-5).

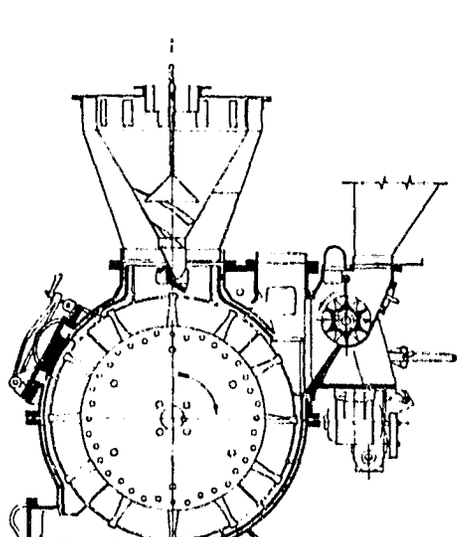

Figure 31. - Impact mill (ref. 3-5).

in an enclosed chamber. These mills rely on the principle of impact, crushing and, unlike the previous mills described, shear between the hammer and casing. In some impact mill designs the shearing action is confined to a first separated stage from where the coal is passed through a grid to the impact/crushing section (figure 32). This shearing action affects all coal which is too large to pass through the gap between the hammer and the case. The hammers are hinged to accommodate material that is too tough to be broken and open up allowing the material to pass without jamming. As the particles become smaller they break by direct impact with the hammers, by being thrown against the casing or by shearing action with larger lumps.

The high speed of the impact mill, normally greater than 200 rpm, results in high maintenance and power consumption for fine grinding such as that specified. The progressive wear of the grinding elements results in an effective increase in particle size and thus it is difficult or nearly impossible to maintain

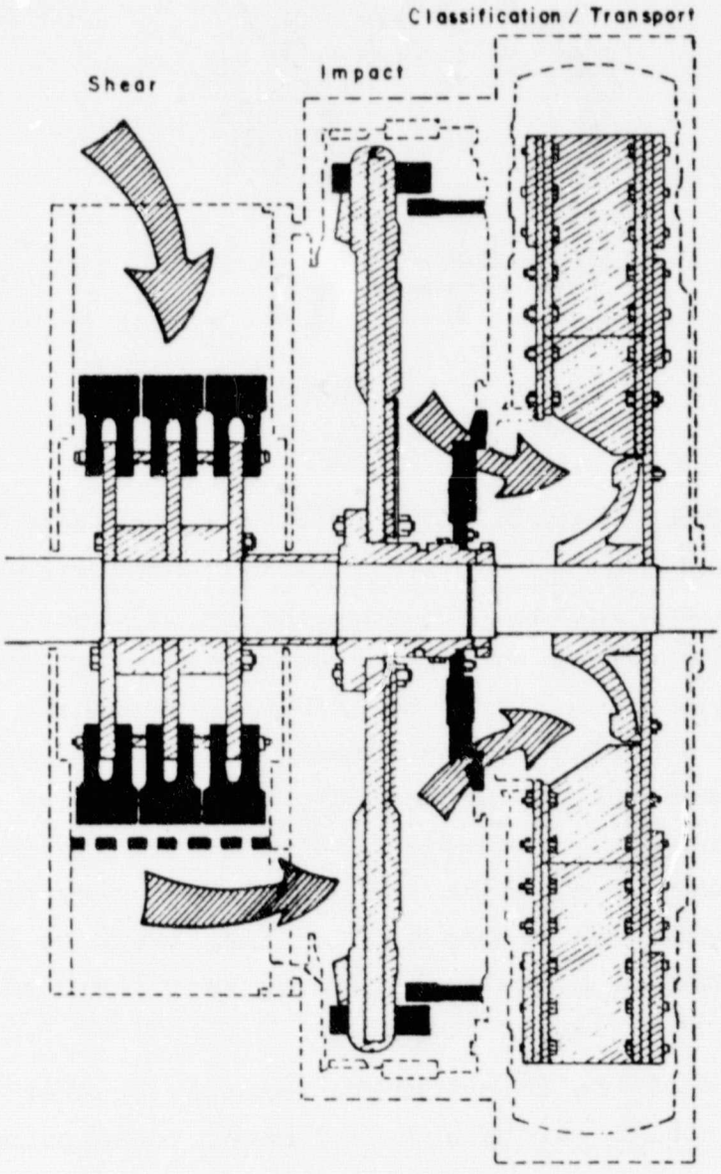

Figure 32. - Staged grinding in an impact mill (ref. 3-4).

fineness during the life of the mill. The use of a classifier can ensure return of oversized particles, but at the expense of a reduction in capacity as the parts wear.

Ultrafine pulverizers. - In addition to the standard type mills discussed above, another commercially available pulverizer is the Pulvajet milling system. The -200 mesh size specified for this report corresponds to 74 microns in the ASTM B214 designation and -325 mesh corresponds to 45 microns. The Pulvajet system introduces a high pressure fluid - usually air or steam - into the mill which entrains the coal particles into sonic and supersonic velocities. The resulting high speed collisions pulverizes the particles. This mill, shown diagramatically in figure 33, can produce particle sizes in the 0.2 to 2.5 micron range as well as coarser particles to 150 mesh size. However, the largest size of mill has about a 1.5 kg/sec (6 tons/hr) capacity and requires air in a weight ratio of 2:1 at around 790 kPa (100 psig). Multiplicity of units is necessary for the required coal throughput. The attendant high air pressure will result in considerably higher cost than the standard type mills. For these reasons, this steam jet system was not given further consideration in this report. However, since this process is being applied experimentally for other purposes, such as coal-oil mixtures, larger and more economical sizes may become available in the near future.

Dryers

Mechanical dryers such as screens, centrifuges and filters are used to reduce the moisture content of as-mined coals. This equipment is suitable for large coal particles but is inappropriate for the -200 mesh and smaller fines specified in this report. The use of mechanical methods would not be able to produce moisture contents to the range of 2 to 5 percent as specified. It is, therefore, necessary to use another method, thermal drying, which is available as in-the-mill drying, direct or indirect fired dryers.

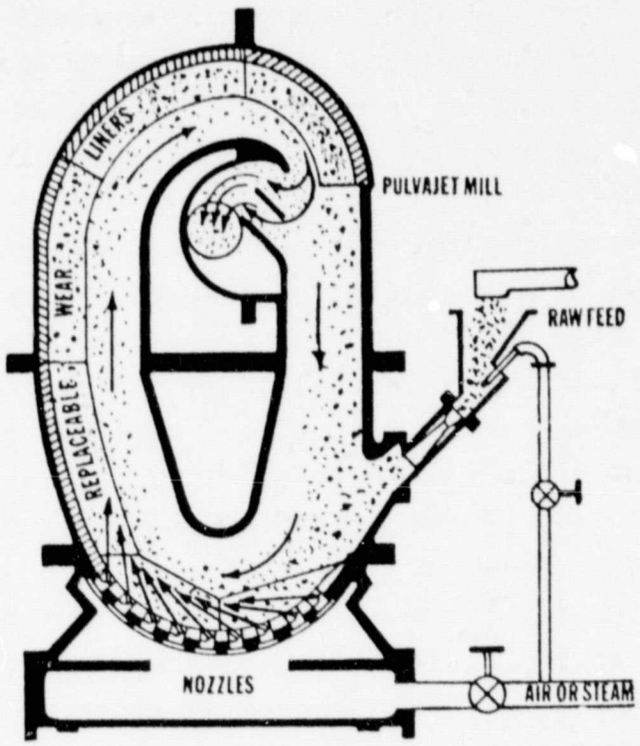

Figure 33. - Ultra fine pulverizer (ref. 3-10).

In-the-mill drying. This drying is accomplished in the mill simultaneously with the grinding. Hot air or diluted flue gas is used as the drying medium and supplied to the pulverizer where it provides heat for drying the coal and transport power for moving the coal around and out of the mill. In power plant direct fired systems this drying air is also used to support combustion in the furnace (known as primary air). Thus the oxygen content must not be too low or combustion stability will be affected. In the MHD power plant, however, the oxygen content in the dryer is not a consideration as the pulverized fuel will be fed to an intermediate bunker and the drying gas is discharged. Thus flue gas can be readily used. Storage temperatures for the reference bituminous coals must not exceed 328° K (130° F) to preclude spontaneous combustion unless the stored coal is blanketed with an inert atmosphere such as N_2, as indicated earlier, and a low oxygen concentration conveying medium is used thereafter. This mill outlet temperature will dictate the allowable mill inlet temperature and thus the dilution required of the reference 644° K (700° F) flue gas.

If the direct use of hot flue gases is unavailable for this drying either a regenerative or tubular air heater can be used for indirect heating of ambient air.

Direct coal drying. - The direct drying methods available are

- Steam filters
- Fluidized bed
- Flash drying
- Louvre drying

Steam filters operate on the basis of improved drainage rather than evaporation to remove water. When water is heated to 363° K (194° F) its viscosity is 0.3 centipoise compared with 1.0 centipoise at 296° K (72° F). Thus when atmospheric steam is passed through a filter cake condensation occurs immediately and the steam gives up

its heat to the cake. Greatly improved drainage results in a substantially reduced moisture content. The moisture content can be further reduced by passing room temperature air or hot gas through the cake reducing the temperature to 344° K (160° F). The steam filter cannot be applied to coal sizes greater than about 0.64 cm (1/4 in.) x 0 in size as a filter cake must be formed. For this reason it may not be applicable to the MHD plant if the coal is delivered as 1.9 cm (3/4 in.) x 0. For the 0.64 cm (1/4 in.) x 0 size the filter uses a horizontal belt whereas for the smaller sizes a rotary drum is utilized.

Fluidized bed drying has been used for many years in the mineral and ore industries. This process dries the coal as it is suspended in a hot gas stream (see figure 34). During operation, air at 756° to 922° K (900° to 1200° F) is passed at a prescribed velocity through a distribution plate beneath the coal to be dried. The air stream suspends the coal above the distribution plate ensuring that maximum surface area is presented for drying. The small coal particles are carried over by the air stream and are removed by cyclone separators or dust collectors. The larger particles are removed from the bed through a lock hopper and conveyed via the cyclone discharge to the next phase of preparation. The entrained bed fluidized bed dryer is designed to carry-over all the coal to be dried. This requires a heavier load to be removed by the cyclone separators. The fluidized bed dryer normally requires a dedicated air heater to provide the hot gas. This can be coal-, oil- or gas-fired and can also be supplemented by flue gas from the main plant. The fluidized bed is very efficient, but requires a significant investment in both cost and space.

Flash drying is a variation of the fluidized bed (see figure 35). Wet coal is introduced continuously into a column of high temperature gases and moisture removal is practically instantaneous. A dedicated furnace produces flue gases with temperatures around 922° K (1200° F). The gases are routed to a drying column where the gases rise at high velocity. Coal is injected at the bottom

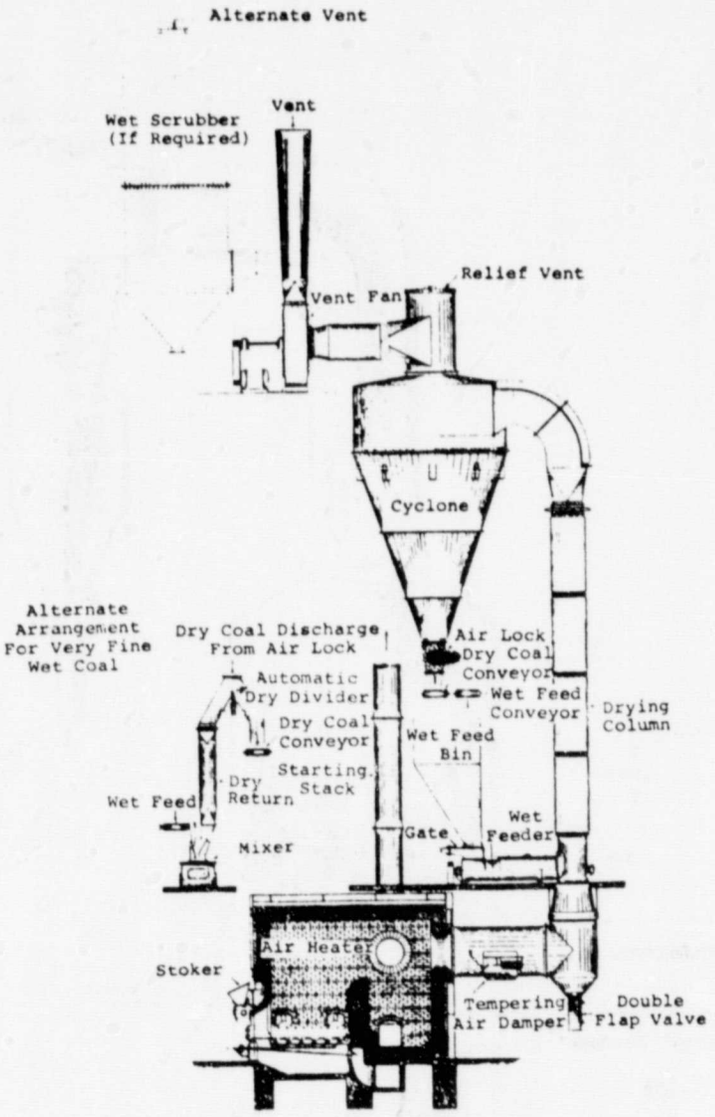

Figure 35. - Flash drying system (ref. 3-7).

of the column and rises in the turbulent gas stream where the drying takes place. At the top of the column, the dried particles are removed from the gas stream by a cyclone separator. This system relies on complete suspension of coal in the gas stream, consequently the coal size is limited to about 1 cm (3/8 in.) x 0. It may have limited application for the MHD plant if coal is delivered 1.9 cm (3/4 in.) x 0.

Louvre drying takes on two forms; belt type and rotary drum type (see figures 36 and 37). The belt type consists of a specially designed moving flight of louvres. Coal moves up in the flight and then flows downward in a shallow bed over the ascending flights. Hot air is passed through the flights from the underside. The rotary drum type consists of a solid outer cylindrical shell and an inner shell composed of full length louvres The inner shell is slightly conically shaped so that its rotation will move the feed from the narrow end to the broader end where it is discharged. Hot air is fed around the inner shell at the narrow end passing through the louvres where it dries the coal and exits vertically upward at the dried material discharge end.

Indirect coal drying. - Indirect coal dryers were introduced in an effort to overcome the disadvantage of removing particulates from an air stream associated with air drying methods. One method for accomplishing this uses hot steel balls. Here a rotating cylinder is supported at each end in such a way that one end can be raised or lowered to control the slope. The wet material is fed into the upper end where it is joined by hot steel balls. As the fine material moves down the cylinder they are broken by impact with the balls and dried by intimate contact with them. A trommel at the end of the cylinder separates the dried material from the balls. The balls are returned by a scoop to a central tube section through which flows hot gases which in turn heat the balls. The central tube contains a perforated or slotted screw conveyor to permit flow of the gas and to convey the balls to the upper end of the cylinder where they drop into the wet material.

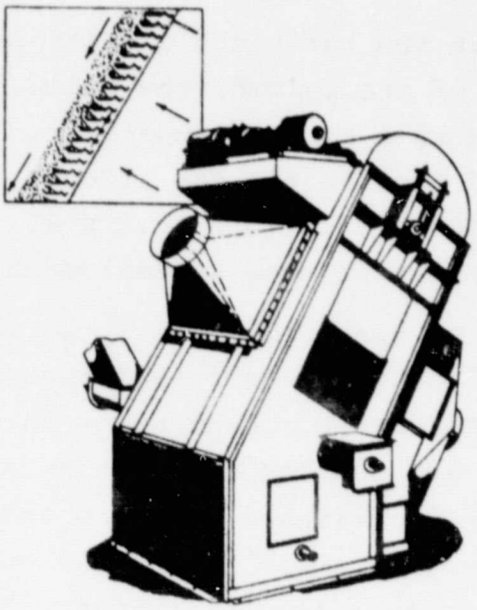

Figure 36. - Louvre type dryer (ref. 3-7).

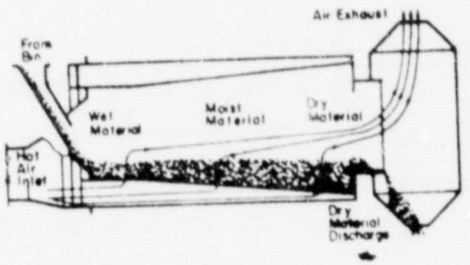

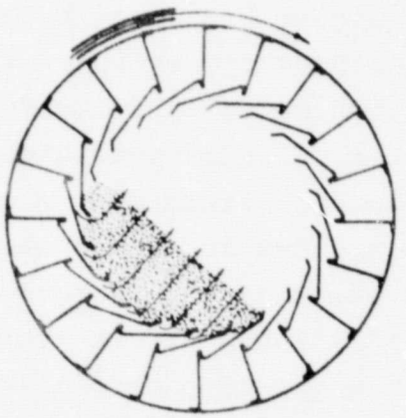

Figure 37. - Rotary louvre dryer (ref. 3-7).

A second method uses a hollow screw conveyor. The wet material is introduced into the feed end of a screw conveyor and conveyed to the discharge end in the normal manner. A hot liquid is introduced into the hollow vanes of the screw conveyor and the conveyor jacket resulting in dry material being discharged. Vapors given off during the drying are vented through vapor ports in the casing. The liquid used in the process must be heated externally in a dedicated furnace.

A third method utilizes a series of vertical, parallel, hollow discs mounted on a common shaft and rotating within a jacket covered trough. Wet material is fed into the trough and the rotating discs pass through the material. The discs and jacket utilize steam or hot oil at 589° K (600° F) as the heating medium. The dryer operates at low speed, 5-8 rpm, and conveys the material through the trough by a combination of gravity (an inclined trough) and the use of conveying vanes installed at the periphery of the discs.

Classifiers

Classification of the mill outlet flow is required to ensure recirculation of oversized particles. This can be accomplished in the mill or externally. Generally speaking, in-the-mill classifying is included in the design of the roller and ball-and-race type mills, whereas the ball mill requires external classification.

In-the-mill classifiers. - The roller and ball-and-race mills are designed such that, once ground, the pulverized coal is carried by the drying air upwards around the periphery of the mill then horizontally into a multi-inlet cyclone. Here, the larger particles are dropped out of the air stream and returned to the pulverizing section and the correctly sized particles leave the mill through the top outlet. The cyclone can be adjusted by positioning the vanes which determines the degree of centrifuge action and thus the coarseness of the rejected material. The material returned to the milling section is already dried and may be three to five times the raw feed input. Thus, the mixing in the milling zone

with the wet incoming feed provides a lower average moisture content for the material being milled. The vane setting is affected by a number of factors

- Required fineness
- Coal grindability
- Pressure on roller or balls
- Wear of the grinding elements
- Effectiveness of the drying process
- Volume and velocity of drying gas

It is possible to adjust the classifier to compensate for these aspects, but the adjustments are limited to fineness changes of about 20 to 30 percent on a -200 mesh product.

External classifiers. - External classifiers take on many forms but generally employ the following basic design principles

- Small particles fall at a slower rate than large particles
- Small particles can change direction more easily than large particles
- Large particles exhibit higher centrifugal forces than small particles when in cyclonic flow
- Large particles require a higher conveying velocity than small particles

The most commonly used classifiers are expansion and cyclonic types. For the expansion type (typical unit shown in figure 38) the solids are conveyed into the classifier in the air stream through a central pipe. As the mixture exits the pipe into the classifying chamber, the expansion causes a large reduction in conveying velocity. Thus, the coarser particles cannot be conveyed and drop to the bottom of the chamber. As the gas stream continues upward the chamber volume continually increases, reducing the velocity even more and dropping out the middling particles. Finally,

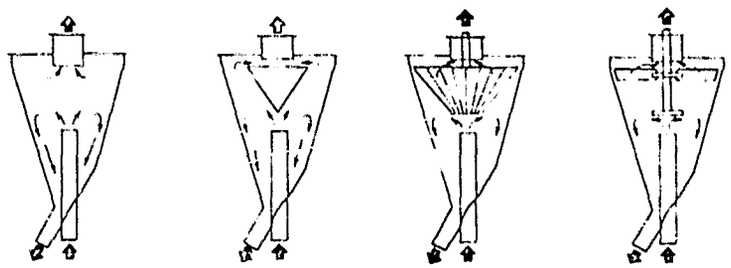

Figure 38. - Typical expansion classifiers (ref. 3-4).

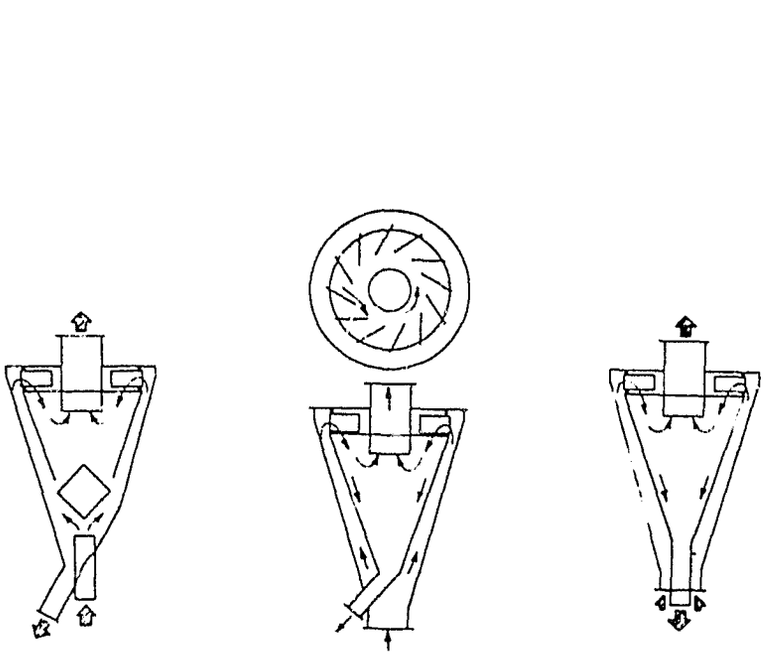

Figure 39. - Twin cone classifier (ref. 3-4).

the air steam exits the classifier with only fine particles and the velocity is once again increased. Variations of the expansion classifier include the incorporation of devices to impose radial flow on the air stream to further improve the separation characteristics (also shown in figure 38).

The twin cone classifier is another variation of the expansion classifier and is shown in figure 39. The classifier consists of two concentric cones. The coal/air stream is fed into the space between the two cones and the coarse particles drop out as the air stream rises. At the top of the annulus the flow is reversed and fed downwards into an expansion chamber where the remaining large particles are removed. Some designs incorporate vanes at the top of the annulus which can be adjusted to induce cyclonic flow further improving the separation characteristics.

The cyclone or centrifugal separator is shown in figure 40. The coal laden air stream enters the cyclone tangentially. The resulting cyclonic flow induces centrifugal forces on the particles throwing them against the side of the cyclone where they lose their momentum and fall to the bottom of the cyclone. The air stream spirals to an inner vortex before exiting as a clean air stream. As the centrifugal force imposed is proportional to the velocity squared, the higher the velocity the better the separation. However, high velocities require more power as the system pressure drop increases. Furthermore, the centrifugal force is inversely proportional to the radius of the cyclone suggesting the use of small sized cyclones for improved separation. For these reasons, therefore, it is preferred to limit the air stream velocities, but at the same time use multiple small cyclones, which tends to increase the costs.

RECOMMENDATIONS

Pulverizers

Illinois coal. - Our investigation has shown that for coal sizes to 80 percent -270 mesh most common pulverizers are suitable.

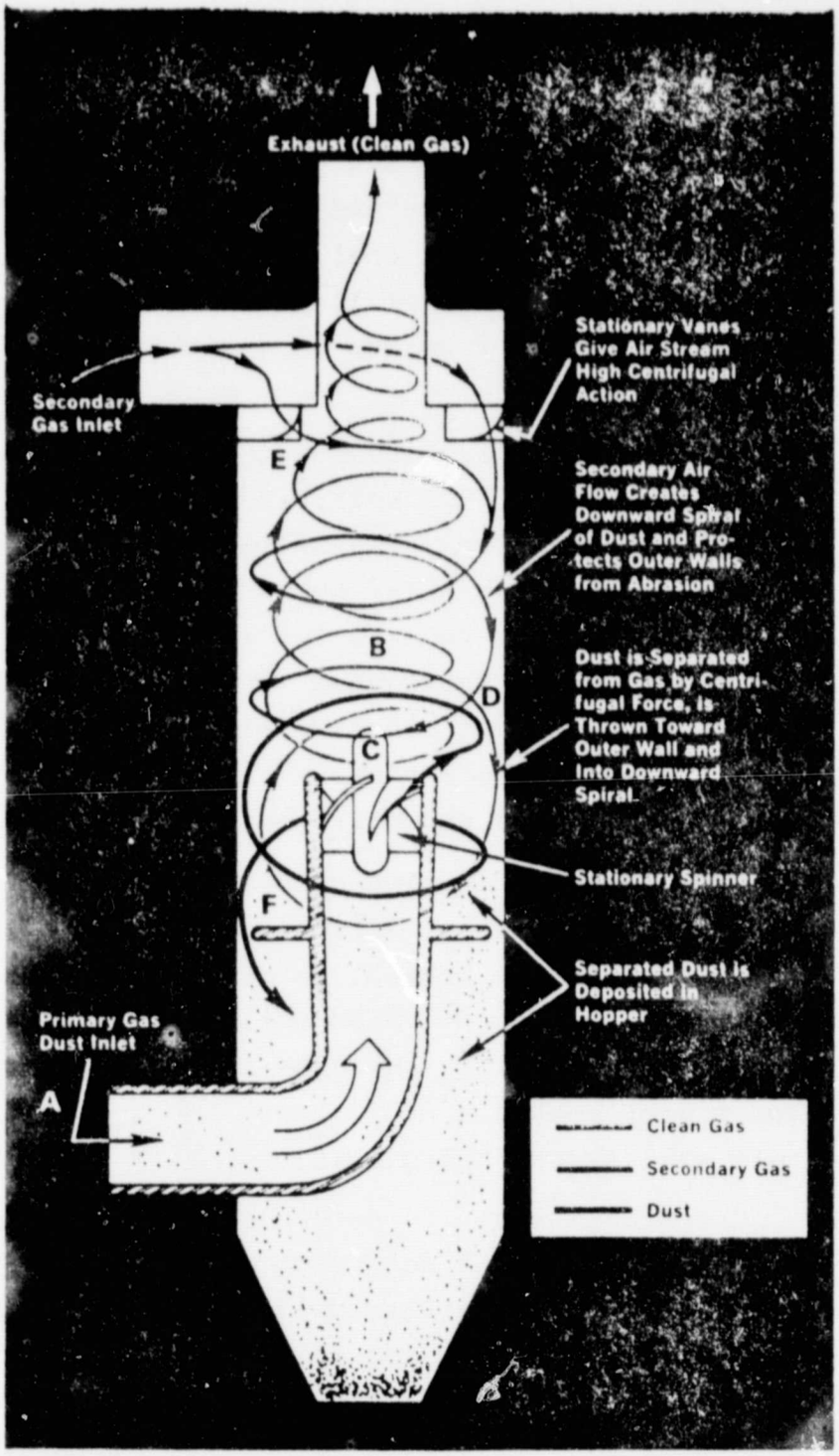

PRINCIPLE OF OPERATION

The dirty gas stream (A) enters the collector chamber (B), past a stationary turning vane (C), which imparts a rotary motion to the flow (D). Centrifugal force directs the dust toward the outer wall of the collector where it is engaged by a secondary gas stream of superior energy (E) and directed spirally downward (F).

Figure 40. - Two configurations for a cyclone separator (ref. 3-12).

The use of the ball mill or tube mill, for this application is recommended primarily due to its dependability resulting from the relatively simple design and low speed. However, the ball mill is larger in size and heavier in construction and will use more power per ton of coal input. Vendors indicate that the ball mill uses an average of 11,900 J/kg (3 KWh/ton) more power than the roller mill, requires more air for drying but its capital cost is less.

The ball mill, however, would not be suitable for the coal size 100 percent -325 mesh, whereas the roller mill would be. Due to the fineness, the roller mill uses more than twice the power and drying air for pulverizing to 100 percent -325 mesh than required for pulverizing to 70 percent -200 mesh. Vendor information also shows that the roller mill pressure drop is higher than that of a ball mill, thus significantly increasing the fan power requirements. Thus, for coal size 100 percent -325 mesh, a more expensive pulverizing system will be required.

Montana coal. - The recommendations for Montana coal are the same as those for Illinois coal. In this instance, however, the coal moisture content is relatively high which results in a much higher air flow through the ball mill compared with the Illinois coal. This increase in air flow is still outweighed by the higher pressure drop across the roller mill resulting in the ball mill system being less expensive.

For coal size 100 percent -325 mesh the ball mill is unsuitable, requiring the selection of the roller mill. As with the Illinois coal the roller mill uses more than twice the power and drying air than required for pulverizing to 70 percent -200 mesh, with an attendant increase in fan power.

For this coal the preferred air temperature is around 589^{o} K (600^{o} F). It should be noted that the vendor information received is based upon 344 to 356^{o} K (160 to 180^{o} F) mill outlet temperature. This is too high if the coal is to be bunkered for any period, in

which case the inlet air temperature must be reduced so that mill outlet temperatures of 317 to 328° K (110 to 130° F) is achieved.

Drying

According to the data received by the responding manufacturers, the required drying can be accomplished in the mill by the introduction of a hot gas stream. This approach precludes the use of external drying equipment with its attendant capital, operating and maintenance costs and use of space. Even with external drying it is still necessary to have pulverizers with the supporting pneumatic coal conveying and particulate separation systems. Thus, there is no benefit gained by substitution of equipment; rather, the preparation system becomes more complex and expensive.

The required mill inlet temperatures for the Illinois and Montana coals are different due to the respective moisture contents of 8.9 and 22.7 percent. The Illinois coal requires a temperature of about 422° K (300° F), whereas the Montana coal requires a temperature of about 589° K (600° F). The use of the recirculated gas at 644° K (700° F) will, thus, require tempering. It is recommended that this tempering air stream be drawn from the gas normally vented to atmosphere after having conveyed the pulverized coal to the bunkers.

Classifiers

For the roller mill application the classifier is included as part of the mill and thus an external unit is not required. The ball mill on the other hand requires an external classifier which we recommend to be of the cyclone type. Vendor data indicate that cyclones are available in sizes up to 118 m^3/sec (250,000 acfm). This suggests that the combined mill outlet flow for a 250 or 500 MW_t Illinois and Montana coal plant could be accommodated by one cyclone. Other MHD plants, rated at 1000 MW_t, may require multiple parallel paths. The removed material should be returned to the feed end of the mill for regrinding. With no moving parts the cyclone separator is a very dependable piece of equipment. There will be some wear

at the air stream entrance and around the periphery of the cyclone in that section. This is probably the only maintenance requirement of the unit.

Bunkering and Venting

The system components discussed above are required to provide an air stream with suspended coal particles of the size required. It is necessary in the MHD system to deliver the coal fines to a bunker and vent the air stream to atmosphere. Thus coal fines separating and last stage particulate clean-up will be required to complete the overall preparation system.

For coal fines separation the cyclone type separator is recommended. This device shows efficient removal characteristics down to the 10 micron size (the ASTM Standards do not classify lower than 37 microns which is equivalent to 400 mesh).

For final clean-up prior to releasing the conveyor gas to the atmosphere, it may be necessary to install a baghouse filter to ensure that EPA emission standards are not violated. The normal temperature limitation for baghouse filters is 408^{o} K (275^{o} F) although more expensive high temperature materials are now available for service up to 519^{o} K (475^{o} F) (ref. 3-13).

COSTS

In an effort to obtain credible cost data, a letter requesting performance and cost data was sent to six coal preparation system manufacturers. Two manufacturers responded and their data are shown on tables XLIV, XLV and XLVI. The data from the Fuller Company (ref. 3-2), identified as A on the tables, were based on a roller mill and the data from Kennedy Van Saun Corp. (ref. 3-1), identified as B on the tables, were based on a ball mill.

Equipment Costs

It is apparent from the as-reported data that the roller mill system is more expensive. This observation resulted in discussions with the manufacturers and it was ascertained that manufacturer B did not include costs for fans, fan and mill motors or a baghouse. The costs were then revised to include allowances for these items and are given under Adjusted Costs.

As would be expected, the equipment costs for the Montana coal-fired plant are higher than those costs for the Illinois coal-fired plant for similar plant ratings. This is due to two factors

- The higher moisture content of the Montana coal
- The lower heating value of the Montana coal

The higher moisture content coal requires a higher Btu input to the mill in the form of heated gas to accomplish the drying. Although part of this can be accommodated using a higher gas temperature, it is generally limited to 589° K (600° F). Thus, the remaining heating requirements are met by increasing the flow. This effect can be readily noted by comparing the drying gas requirements for the -270 mesh, 1000 MW plant as shown in table L. This in turn increases the volumetric size of the mill to ensure that internal recirculation is optimized and particle carryover is minimized.

The lower heating value of the Montana coal requires a higher feed rate, also increasing the mill size. This is particularly noticeable in the roller mill which ranges in size from a 1.3 meter diameter table with two rollers for the 250 MW_t plant using -200 mesh coal to a 2.4 meter diameter table with three rollers for the 1000 MW_t -200 mesh coal. If a single mill size were to be selected for all cases, it would be necessary to increase the number of mills to provide the total equivalent table area. From the manufacturers' data it appears that the roller mill is at a disadvantage in this respect as a total of 4 operating mills are

required for the 1000 MW_t plant using -270 mesh Montana coal vs. two for the ball mill. This limit on size does not permit the roller mill to take full advantage of scaling.

TABLE L. - DRYING GAS REQUIREMENTS FOR 1000 MW_t PLANTS

Coal Type	Illinois No. 6		Montana Rosebud	
Mill Type	Ball	Roller	Ball	Roller
Mills Operating	2	3	2	4
m^3/sec (ACFM) Per Mill	46 (97,000)	38 (81,500)	79 (167,000)	38 (81,500)
m^3/sec (ACFM) Total	92 (194,000)	115 (244,500)	158 (334,000)	154 (326,000)

The fineness requirement also affects the size of the mill and is compensated in the roller mill design by increasing the number of mills. Again, the roller mill cannot take full benefit of scaling.

It is, primarily, the effect of scaling which benefits the ball mill design. In all cases the ball mill requires only two units to meet the required coal throughput thus holding costs to a minimum. In addition, the pressure drop through the ball mill, plus classifier, is about a factor of two less than that required for the roller mill. This requires less fan horsepower reducing the cost of the fan and offsetting the higher input power required for the ball mill.

Operating and Maintenance Costs

The two manufacturers have provided cost data for operating and maintenance of the respective mill designs in $/ton coal pulverized. This cost relates directly to the mill and covers such materials as rollers or balls, liners, springs, etc. It does not include manpower or auxiliary power costs.

A review of the mill maintenance costs shows that the roller mill exhibits the lower unit cost in all Montana coal cases whereas for the Illinois coal cases, the costs are comparable. Table LI shows the results of converting these costs to a dollar/year basis, assuming a 70 percent load factor. It is evident that the annual maintenance costs for Illinois coal are comparable but the roller mill costs on Montana coal show savings ranging from 20 to 50 percent. It would, however, require many years for this differential to compensate for the capital cost differences. The actual number is dependent on the financial factors used to evaluate alternative systems.

The labor costs were not provided by the manufacturers, but it is reasonable to expect that the manpower differential will be small. For the 12 cases where both manufacturers provided data, four show the roller mill requiring an extra mill, and in one case, the roller mill requires two extra mills. For the -325 mesh cases only the roller mill is practical, precluding any comparison in manpower costs.

The fan horsepowers required are greater for the roller mill systems as the pressure drop through the whole system exceeds that for the ball mill systems by 2490 to 3735 Pa (10 to 15 in. of water). Thus, the roller mill system's additional auxiliary power requirements range from about 112 kW (150 HP) for the Illinois coal 250 MW plant to 597 kW (800 HP) for the Montana coal 1000 MW plant (or 700 MWh/year to 3700 MWh/year).

Similarly, the mill power consumption must be considered in the evaluation. It is evident from the manufacturers' data that the ball mill uses more energy. This is due to the heavy weight of equipment it has to drive. On an average, the ball mill uses about 11,900 J/kg (3 KWh/ton) additional power which converts to a range of 700 MWh/year for Illinois coal 250 MW plant to 3500 MWh/year for 1000 MW plant.

These calculations of estimated auxiliary power requirements indicate that the additional fan power required by the roller mill

TABLE LI. - ANNUAL MILL MAINTENANCE COSTS (ref. 3-1 and 3-2)

	Estimated O&M Cost $/Ton		Coal Processed Ton/Yr	Annual O&M Cost $	
Manufacturer	A	B		A	B
Mill Type	Roller	Ball		Roller	Ball
Illinois Coal					
250 MW Plant					
-200 Mesh	0.105	0.18		24,360	41,760
-270 Mesh	0.152	0.142	232,000	35,264	32,944
-325 Mesh	0.202	-		46,864	-
500 MW Plant					
-200 Mesh	0.105	-		48,720	-
-270 Mesh	0.152	-	464,000	70,528	-
-325 Mesh	0.202	-		93,728	-
1000 MW Plant					
-200 Mesh	0.105	0.08		97,440	74,240
-270 Mesh	0.152	0.13	928,000	141,056	120,640
-325 Mesh	0.202	-		187,456	-
Montana Coal					
250 MW Plant					
-200 Mesh	0.088	0.179		25,784	52,447
-270 Mesh	0.130	0.242	293,000	38,090	70,906
-325 Mesh	0.170	-		49,810	-
500 MW Plant					
-200 Mesh	0.088	0.174		51,568	101,964
-270 Mesh	0.130	0.235	586,000	76,180	137,710
-325 Mesh	0.170	-		99,620	-
1000 MW Plant					
-200 Mesh	0.088	0.170		103,136	199,240
-270 Mesh	0.132	0.182	1,172,000	154,704	213,304
-325 Mesh	0.172	-		201,584	-

system is essentially offset by the additional mill power required by the ball mill system. However, for a specific design this may not be the case and it is necessary to include these factors in the evaluation of a particular installation.

REFERENCES

3-1. Kennedy Van Saun Corp. quotation to Burns and Roe, Inc., dated September 18, 1979.

3-2. Fuller Co. quotation to Burns and Roe, Inc., dated January 4, 1980.

3-3. Bergman, P.D., and Bienstock, D., "Utilization of Western Coal for MHD Energy Conversion," Proceedings of the 15th Symposium on Engineering Aspects of Magnetohydrodynamics, May 1976.

3-4. Luchie, P.T., and Austin, L.G., "Coal Grinding Technology," U.S. ERDA Contract EX-76-C-01-2475, 1976.

3-5. Fryling, G.R., Combustion Engineering, Combustion Engineering Inc., 1966.

3-6. Steam, Its Generation and Use, The Babcock and Wilcox Co., Thirty-eighth Edition, 1972.

3-7. "Fuller Roller Mills," Fuller Co. Bulletin M-6.

3-9. "E Mills Grinding and Pulverizing," Babcock Publication 2008.

3-10. Aljet Equipment Co., Pulva Jet Milling Systems, Bulletin 1000.

3-11. "Fuller Fluidized Bed Systems," Fuller Co. Bulletin FB-1B.

3-12. "Buell Mechanical Collectors," Envirotech Corp. Bulletin, 1974.

3-13. "Fuller Plenum-Pulse High-Ratio Compressed Air Cleaning Dust Collector," Fuller Co. Bulletin DCB-325B.

APPENDIX 3A

Burns and Roe, Inc.

185 Crossways Park Drive Woodbury New York 11797 Telephone (516) 777-4200
TWX 510-221-1853 Cable Burnsroe Woodbury

Subject: NASA-Lewis Research Center,
Cleveland, Ohio
Coal Processing Equipment for
Magnetohydrodynamic (MHD)
Power Plant Applications
W. O. 3473-04

August 1, 1979

Gentlemen:

Burns and Roe is currently investigating coal processing equipment for MHD power plant applications for the NASA-Lewis Research Center. The objectives of the study are to provide technical and cost data to be used to select coal processing equipment for commercial sized coal-fired MHD power plants.

Two coals are being considered for this application - Montana Rosebud and Illinois No. 6. The purpose of the coal processing system is to accept the coal under the conditions specified in Attachment 1, for Montana Rosebud and Illinois No. 6, respectively, and to provide a dry, pulverized product which meets the requirements specified in Attachment 2. Three plant sizes are being considered for each coal - 250 MWt, 500 MWt and 1000 MWt. For each size system, three sizes of pulverized coal are of interest: 70 percent through 200 mesh, 80 percent through 270 mesh and 100 percent through 325 mesh.

Attachment 3 is a schematic of a possible coal processing system for which data on in-the-mill drying pulverizers are requested. Flue gas at the composition and conditions specified in Attachment 4 is available and would be the preferred drying medium.

The data requested are stated in Attachment 5. We particularly would like to obtain an estimate of the particle size distribution for each size requested and are also interested in the effect of varying the narrowness of the particle size distribution on equipment cost and performance.

We request a response not later than August 20, 1979.

Please contact me at 516-677-2223, Mr. Dennis Shikar at 516-677-2225 or Dr. A. Carlson at 516-677-2234 if you have any questions.

Your cooperation is greatly appreciated.

Very truly yours,

Irving L. Chait
Project Manager

Attachments

LIST OF COAL HANDLING EQUIPMENT
MANUFACTURERS TO WHOM A REQUEST
FOR QUOTATION WAS SENT

Foster Wheeler Corp.
110 S. Orange Avenue
Livingston, NJ 07039

Williams Patent Crusher and Pulverizer Co.
2701 Broadway
St. Louis, NO 63102

C-E Power Systems
Combustion Engineering, Inc.
277 Park Avenue
New York, NY 10017

GATX Corporation/Fuller Company
P.O. Box 29
Catasauqua, PA 18032

Denier Equipment Company
600 Broadway
Denver, CO 80233

Pennsylvania Crusher Corp.
P.O. Box 100
Broomall, PA 19008

Kennedy Van Saun Corp.
Panville, PA 17821

ATTACHMENT 1

COAL FEED TO PROCESSING SYSTEM

AS RECEIVED

	Illinois No. 6	Montana Rosebud
Coal Rank	HVCB	Subbit B
Feed size *	———	———
Hardgrove Grindability	56	57
Proximate Analysis, %		
Ash	11.4	8.7
Volatile Matter	38.0	29.4
Fixed Carbon	41.7	39.2
Surface Moisture	0	0
Inherent Moisture	8.9	22.7
Ultimate Analysis, %		
Hydrogen	5.4	6.0
Carbon	62.4	52.1
Nitrogen	1.2	0.79
Oxygen	16.3	31.5
Sulfur	3.3	0.85
Ash Analysis, %		
SiO_2	41.4	37.6
Al_2O_3	19.3	17.3
Fe_2O_3	22.3	5.1
TiO_2	0.9	0.7
P_2O_5	0.12	0.4
CaO	5.4	11.0
MgO	1.7	4.0
Na_2O	0.6	3.1
K_2O	2.1	0.5
SO_3	7.5	17.5

*Please state and base your response on the most suitable coal feed size for your equipment.

ATTACHMENT 2

PROPERTIES OF COAL OUT OF COAL PROCESSING SYSTEM

	Illinois No. 6	Montana Rosebud
Total moisture content, %	2	5
Product Sizes		
Alternative 1	70% through 200 mesh	70% through 200 mesh
Alternative 2	80% through 270 mesh	80% through 270 mesh
Alternative 3	100% through 325 mesh	100% through 325 mesh

ATTACHMENT 3

SCHEMATIC OF A POSSIBLE COAL PROCESSING SYSTEM

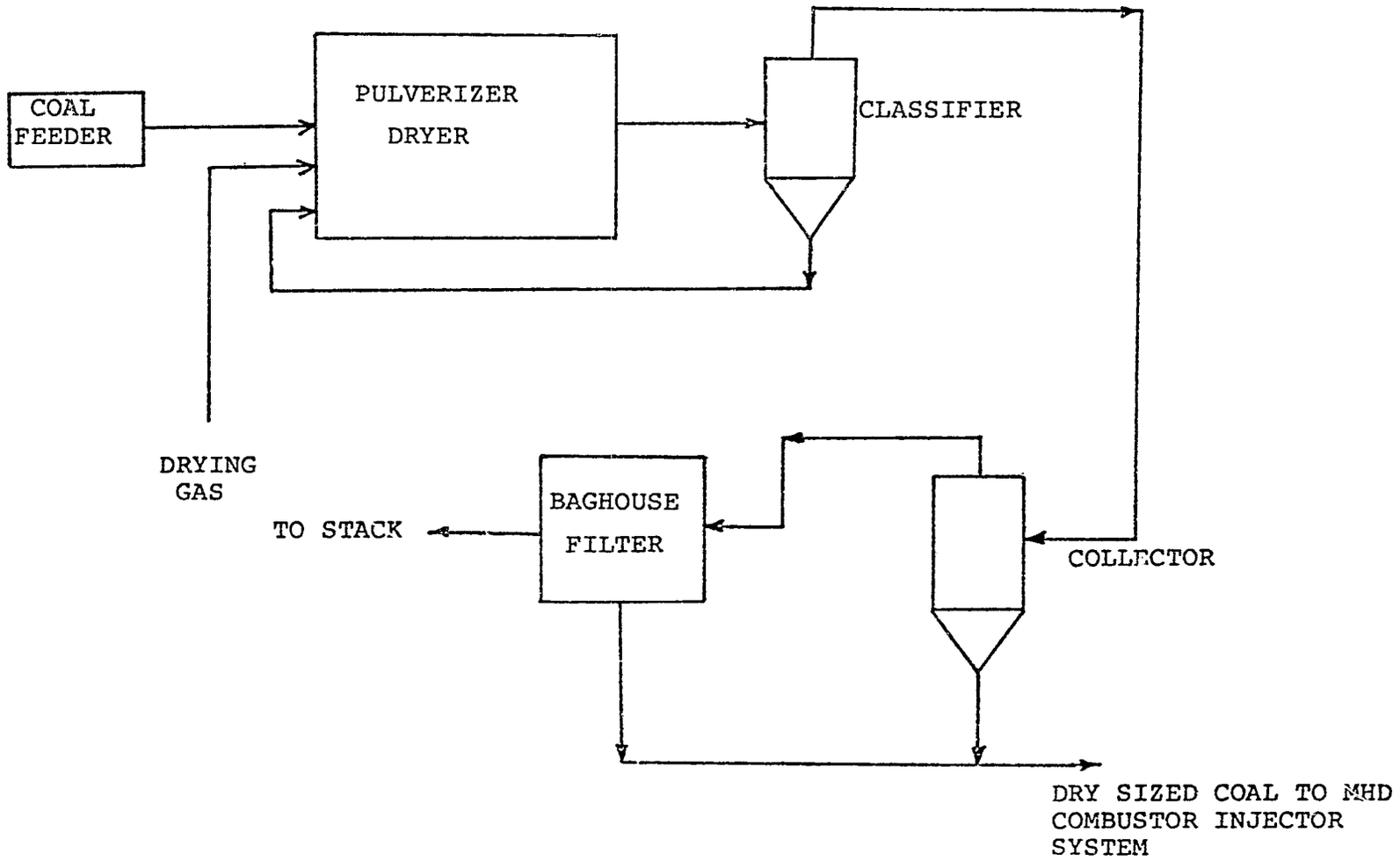

ATTACHMENT 4

DRYING MEDIUM DATA

Gas Temperature, ^{o}F	700
Max. Flow Rate Available, SCFM	
Composition, % by weight	
CO_2	18.82
SO_2	0.04
N_2	71.35
O_2	1.86
H_2O	7.83

ATTACHMENT 5

INFORMATION REQUESTED - ILLINOIS NO. 6 COAL

General Data

Manufacturer and Location _____

Mill type and model* _____

Classification type (internal, external) _____

Operating condition (pressurized, vacuum) _____

Maintenance requirements _____

_____ _____

Indicate scope of equipment to be supplied _____

_____

_____

Technical Data

Thermal level, MW_t 250

Coal Throughput, ton/hour 37.9 (as received)

	70%-200 mesh	80%-270 mesh	100%-325 mesh
Particle size - out			
Particle size dist.			
No. of mills req'd. (minimum 2 units plus 1 spare)			
Moisture content of coal, out, %			
Coal throughput per mill as received, ton/hr			
Power consumption, KWH/Ton			

Drying Medium (see attachment 4)

Recommended Temperature into mill, °F			
Minimum & maximum pressure into mill, inch H_2O			
Flow rate, SCFM			

* Attach pertinent arrangement drawings, dimensions, weight, list of codes and standards to which manufactured and other technical data

Technical Data

Thermal level, MW_t 500

Coal Throughput, ton/hour 75.7 (as received)

Particle size - out	70%-200 mesh	80%-270 mesh	100%-325 mesh
Particle size dist.			
No. of mills req'd. (minimum 2 units plus 1 spare)			
Moisture content of coal, out, %			
Coal throughput per mill as received, ton/hr			
Power consumption, KWH/Ton			

Drying Medium
(see attachment 4)

Recommended Temperature into mill, ^oF			
Minimum & maximum pressure into mill, inch H_2O			
Flow rate, SCFM			
Temperature out of mill, ^oF			
Pressure drop in mill, in. H_2O			

Cost Data

Estimated O&M Cost (excluding power), $/Ton			
Equipment Cost (present day $) F.O.B. manufacturing site			

Temperature out of mill, ^{o}F	_____	_____	_____
Pressure drop in mill, in. H_2O	_____	_____	_____

Cost Data

Estimated O&M Cost (excluding power), $/Ton	_____	_____	_____
Equipment Cost (present day $) F.O.B. manufacturing site	_____	_____	_____

Technical Data

Thermal level, MW_t 1000

Coal Throughput, ton/hour 151.5 (as received)

	70%-200 mesh	80%-270 mesh	100%-325 mesh
Particle size - out			
Particle size dist.			
No. of mills req'd. (minimum 2 units plus 1 spare)			
Moisture content of coal, out, %			
Coal throughput per mill as received, ton/hr			
Power consumption, KWH/Ton			

Drying Medium
(see attachment 4)

Recommended Temperature into mill, ^oF			
Minimum & maximum pressure into mill, inch H_2O			
Flow rate, SCFM			
Temperature out of mill, ^oF			
Pressure drop in mill, in. H_2O			

Cost Data

Estimated O&M Cost (excluding power), $/Ton			
Equipment Cost (present day $) F.O.B. manufacturing site			

Please indicate the effect on cost and performance of narrowing the particle size distribution

ATTACHMENT 5

INFORMATION REQUESTED - MONTANA ROSEBUD COAL

General Data

Manufacturer and Location _____

Mill type and model* _____

Classification type (internal, external) _____

Operating condition (pressurized, vacuum) _____

Maintenance requirements _____

_____

Indicate scope of equipment to be supplied _____

_____

_____

Technical Data

Thermal level, MW_t 250

Coal Throughput, ton/hour 47.8 (as received)

Particle size - out	70%-200 mesh	80%-270 mesh	100%-325 mesh
Particle size dist.			
No. of mills req'd. (minimum 2 units plus 1 spare)			
Moisture content of coal, out, %			
Coal throughput per mill as received, ton/hr			
Power consumption, KWH/Ton			

Drying Medium
(see attachment 4)

Recommended Temperature into mill, ^oF			
Minimum & maximum pressure into mill, inch H_2O			
Flow rate, SCFM			

* Attach pertinent arrangement drawings, dimensions, weight, list of codes and standards to which manufactured and other technical data

Temperature out of mill, ^{o}F			
Pressure drop in mill, in. H_2O			
Cost Data			
Estimated O&M Cost (excluding power), $/Ton			
Equipment Cost (present day $) F.O.B. manufacturing site			

Technical Data

Thermal level, MW_t 500

Coal Throughput, ton/hour 95.7 (as-received)

Particle size - out	70%-200 mesh	80%-270 mesh	100%-325 mesh
Particle size dist.			
No. of mills req'd. (minimum 2 units plus 1 spare)			
Moisture content of coal, out, %			
Coal throughput per mill as received, ton/hr			
Power consumption, KWH/Ton			

Drying Medium
(see attachment 4)

Recommended Temperature into mill, ^oF			
Minimum & maximum pressure into mill, inch H_2O			
Flow rate, SCFM			
Temperature out of mill, ^oF			
Pressure drop in mill, in. H_2O			

Cost Data

Estimated O&M Cost (excluding power), $/Ton			
Equipment Cost (present day $) F.O.B. manufacturing site			

Technical Data

Thermal level, MW_t 1000

Coal Throughput, ton/hour 191.3 (as received)

Particle size - out	70%-200 mesh	80%-270 mesh	100%-325 mesh
Particle size dist.			
No. of mills req'd. (minimum 2 units plus 1 spare)			
Moisture content of coal, out, %			
Coal throughput per mill as received, ton/hr			
Power consumption, KWh/Ton			

Drying Medium
(see attachment 4)

Recommended Temperature into mill, ^oF			
Minimum & maximum pressure into mill, inch H_2O			
Flow rate, SCFM			
Temperature out of mill, in. H_2O			
Pressure drop in mill, in. H_2O			

Cost Data

Estimated O&M Cost (excluding power), $/Ton			
Equipment Cost (present day $) F.O.B. manufacturing site			

Please indicate the effect on cost and performance of narrowing the particle size distribution